

NDOT Research Report

Report No. 122-12-803



**Post-Earthquake Assessment of Nevada
Bridges Using ShakeMap/ShakeCast**



January 2016

**Nevada Department of Transportation
1263 South Stewart Street
Carson City, NV 89712**



Disclaimer

This work was sponsored by the Nevada Department of Transportation. The contents of this report reflect the views of the authors, who are responsible for the facts and the accuracy of the data presented herein. The contents do not necessarily reflect the official views or policies of the State of Nevada at the time of publication. This report does not constitute a standard, specification, or regulation.

Post-Earthquake Assessment of Nevada Bridges Using ShakeMap/ShakeCast

Mohammed Saeed Mohammed

Graduate Research Assistant
Civil and Environmental Engineering

Glenn Biasi

Research Associate Professor
Seismology

David H. Sanders

Professor
Civil and Environmental Engineering

CCEER-16-04

A Report for the
Nevada Department of Transportation
Carson City, NV
2016



Center for Earthquake Engineering Research
Department of Civil and Environmental Engineering
University of Nevada
Reno, Nevada 89557-0258

Abstract

Post-earthquake capacity of Nevada highway bridges is examined through a combination of engineering study and scenario earthquake evaluation. The study was undertaken by the University of Nevada Reno Department of Civil and Environmental Engineering with the collaboration of the Nevada Seismological Laboratory under project funding from the Nevada Department of Transportation, with technical engagement through the NDOT Bridge Division. The vulnerability of Nevada bridges relative to earthquake hazard is evaluated using two different methods. First, a distributed set of 112 realistic earthquake scenarios were processed with USGS program ShakeMap, and USGS program ShakeCast was used to extract site-specific ground motion levels for the 1831 Nevada bridges in the Federal Highway Administration National Bridge Inventory. Second, using hazard curves underlying the 2014 USGS National Seismic Hazard Map (NSHM), return periods for earthquakes causing extensive damage to bridges were extracted and compared to the 1000-year design level adopted by the AASHTO. For both methods, demand vs. capacity comparisons were restricted to spectral acceleration at 1 Hz. Initial bridge capacities for ShakeCast were adopted from corresponding HAZUS estimates on the basis of bridge design type. HAZUS capacities were found to be too high for five bridge design types: HWB10-205 and HWB11-205, Continuous Concrete Box Girder, non-seismically and seismically designed, respectively; HWB15-402, Continuous Steel Bridge; and HWB22-605 and HWB23-605, non-seismic and seismic Continuous Prestressed Concrete Box Girder. HAZUS capacities for these bridge types considered only columns and not the broader suite of potential failure modes recognized in subsequent studies. Revised capacity values were proposed in consultation with NDOT engineers using a combination of literature review, Nevada bridge plans, and Nevada bridge design spectra. The two evaluation approaches provide complimentary views of bridge performance. Scenarios from ShakeMap provide points in a deterministic seismic hazard approach. The occurrence of the earthquake is assumed, and bridge response is interpreted independent of the probability of the demand. The probability aspect of strong ground shaking enters the analysis through the NSHM hazard curves, which are based on a probabilistic approach. A graphical method is presented to unite the two approaches. A list of potentially vulnerable bridges was developed for use by the Nevada Department of Transportation (NDOT) in bridge retrofit planning. As a continuing benefit, ShakeCast now operates in Nevada to provide near-real-time inspection priorities in the event of a serious earthquake. In addition a damage assessment and repair manual has been developed, presented in an appendix. The manual initially describes the typical damage that would be observed as a result of an earthquake and then describes methods for repairing this damage.

Acknowledgments

The research described in this report was funded by the Nevada Department of Transportation (NDOT). Conclusions and recommendations of this report are those of the authors only, and should not be construed to be endorsed by NDOT. The authors would like to thank Dr. Hisham Nada who assisted in developing the report, and Lisa Bryant who helped in collecting the material for Appendix D.

Table of Contents

ABSTRACT	I
ACKNOWLEDGMENTS	II
LIST OF FIGURES	VI
CHAPTER 1: INTRODUCTION.....	1
CHAPTER 2: SHAKEMAP/SHAKECAST - PATH FROM EARTHQUAKE TO BRIDGE EVALUATION	3
2.1 EARTHQUAKES IN NEVADA.....	3
2.1.1 <i>Tectonic Context</i>	3
2.1.2 <i>Nevada History</i>	3
2.1.3 <i>Earthquake Locations and Magnitudes</i>	4
2.2 SHAKEMAP: MAP BASED VIEW OF GROUND SHAKING.....	4
2.2.1 <i>Overview</i>	4
2.2.2 <i>ShakeMap and Seismic Demand</i>	5
2.2.3 <i>ShakeMap Scenarios</i>	7
2.3 SHAKECAST – APPLYING SHAKEMAP GROUND MOTIONS TO NEVADA BRIDGES	8
2.3.1 <i>Overview</i>	8
2.3.2 <i>National Bridge Inventory and ShakeCast</i>	8
2.3.3 <i>Implementation of ShakeCast</i>	9
CHAPTER 3: BRIDGE FRAGILITIES.....	26
3.1 SEISMIC RISK ASSESSMENT	26
3.2 FRAGILITY FUNCTIONS	26
3.2.1 <i>Fragility Functions Based on Expert Opinion</i>	27
3.2.2 <i>Empirical Fragility Functions</i>	27
3.2.3 <i>Analytical Fragility Functions</i>	27
3.2.3.1 <i>Elastic Response Spectrum Analysis</i>	28
3.3 SHAKECAST FRAGILITY FUNCTIONS.....	28
3.3.1 <i>Bridge Classification Based on National Bridge Inventory (NBI) and HAZUS</i>	29
3.3.2 <i>Bridge fragilities in HAZUS</i>	29
3.3.3 <i>Main steps for damage algorithm for bridges</i>	29
3.4 SHAKECAST FOR NEVADA BRIDGES	30
3.4.1 <i>Limitations in the HAZUS fragility curves</i>	30
3.4.2 <i>Nevada bridge inventory</i>	30
3.4.3 <i>Modifications in ShakeCast fragility functions</i>	31
CHAPTER 4: SHAKECAST RESULTS.....	51
4.1. SHAKECAST PREDICTIONS FOR NEVADA BRIDGES FROM SCENARIO EARTHQUAKES	51
4.2 DEVELOPING SITE CLASS ESTIMATES FOR BRIDGES IN SHAKECAST SCENARIOS	51
4.3 GROUND MOTION PREDICTIONS FOR BRIDGE SITES	52
4.3.1 <i>U.S. Geological Survey (USGS) National Seismic Hazard Map (NSHM) Hazard Curves</i>	52
4.3.2 <i>Adjusting NSHM Hazard Curves for Bridge Site Conditions</i>	53
CHAPTER 5: RECOMMENDATIONS AND FUTURE WORK.....	62
5.1 RECOMMENDATIONS.....	62
5.2 FUTURE RESEARCH	63
REFERENCES	64
APPENDIX A: DEMAND VS. CAPACITY	68
APPENDIX B: HAZARD CURVES AND SHAKECAST PREDICTED DEMAND FOR SELECTED BRIDGE TYPES ..	85

B.1 HWB10 -205 BRIDGES	87
B.2 HWB11 -205 BRIDGES	125
B.3 HWB15 -402 BRIDGES	129
APPENDIX C: RETURN PERIODS CORRESPONDING TO DIFFERENT DAMAGE STATES.....	174
APPENDIX D: DAMAGE ASSESSMENT AND REPAIR MANUAL	180
<i>D.1 Introduction</i>	<i>180</i>
<i>D.2 Damage States of Columns.....</i>	<i>181</i>
<i>D.3 Shear Keys Damage States</i>	<i>186</i>
<i>D.4 Abutments Damage States.....</i>	<i>189</i>
<i>D.5 Repair Literature Review</i>	<i>192</i>
<i>D.6 Repair Design for Columns</i>	<i>198</i>
<i>D.7 Repair Design for Shear Keys</i>	<i>200</i>
<i>D.8 Repair Design for Abutments.....</i>	<i>206</i>
REFERENCES	209

List of Tables

Table 2.1 List of Scenarios, with fault lengths, time since the most recent event (tMRE), and slip rate bounds. Fault slip rate data and time since the most recent event from the USGS Quaternary Fault and Fold database (http://earthquake.usgs.gov/hazards/qfaults/).	13
Table 2.2 Names, locations, physical descriptions, and damage state levels for four example bridges.	17
Table 3.1 Damage matrix for highway concrete bridges in Los Angeles area (Basoz and Kiremidjian, 1997)	33
Table 3.2 Damage matrix for concrete bridges after Kobe earthquake (Yamazaki et al. 1999)	33
Table 3.3 Definition of bridge damage states (Turner et al. 2009)	33
Table 3.4 Bridge material classes in NBI (NBI, 1995)	34
Table 3.5 Bridge types in NBI (NBI, 1995)	34
Table 3.6 HAZUS bridge classification scheme (HAZUS-MH)	35
Table 3.7 Median of the HAZUS fragility functions (HAZUS-MH)	38
Table 3.8 K_{3D} equations (HAZUS-MH).....	38
Table 3.9 Drift limits used by the HAZUS fragility curves (Mander and Basoz, 1999)	39
Table 3.10 MSCC-BG bridge fragilities (Ramanathan, 2012).....	39
Table 3.11 Most vulnerable component for MSCC-BG bridge class with seat abutments (Ramanathan, 2012).....	40
Table 3.12 Comparison between Nielson (2005) fragility curves and HAZUS (Nielson, 2005).....	41
Table 3.13 Predominant bridge classes in Nevada	42
Table 3.14 Medians for the proposed fragility functions (S_a at 1 sec.) (g)	43
Table 4.1 Top 12 bridges of type HWB10-205, with scenario names (attenuation model indicated by “BA” or “CY”), and scenario demands in PGA, PGV, and SA(1).....	56
Table 4.2 Amplitude-dependent site corrections for SA(1 sec).	57
Table 4.3 Return periods corresponding to different damage states for 28 example bridges	57
Table A.1 Bridges of type HWB10-205 (Demand vs Capacity)	68
Table A.2 Bridges of type HWB11-205 (Demand vs Capacity)	77
Table A.3 Bridges of type HWB15-402 (Demand vs Capacity)	77
Table A.4 Bridges of type HWB22-605 (Demand vs Capacity)	79
Table A.5 Bridges of type HWB23-605 (Demand vs Capacity)	80
Table C.1 Bridges of type HWB10-205 (Return periods for different damage states)	174
Table C.2 Bridges of type HWB11-205 (Return periods for different damage states)	176
Table C.3 Bridges of type HWB15-402 (Return periods for different damage states)	176
Table C.4 Bridges of type HWB22-605 (Return periods for different damage states)	177
Table C.5 Bridges of type HWB23-605 (Return periods for different damage states)	178
Table D.1 Ductility Demand, μ , for Damage States (Saini et al, 2013)	199
Table D.2 Damage States v. Required CFRP Thickness- Example Column	200

List of Figures

Figure 1.1 ShakeCast flow chart from ShakeCast users manual (Wald et al., 2005).....	2
Figure 2.1 Southern Pacific water tank in Lovelock, Nevada, damaged by ground motions of the 1915 Pleasant Valley M7.3 earthquake.....	18
Figure 2.2 Map of ShakeMap fault scenarios used for bridge evaluation. Surface traces of fault rupture shown as heavy blue lines. Finer red lines are other known faults, generally having lower slip rates. Shaded areas of western and southern Nevada are the Reno-Carson City and the greater Las Vegas urban areas, respectively.....	19
Figure 2.3 USGS National Seismic Hazard Map for spectral acceleration 1 Hz and return probability of 2% in 50 years (2475 year return time). Ground motions at 1000-year return will be lower (Peterson et al., 2014).	20
Figure 2.4 Virtual machine instances are administered via a web interface at Amazon Web Services (AWS).	20
Figure 2.5 Bridges from the Nevada inventory located using a Search capability on the Facilities tab of ShakeCast 3.....	21
Figure 2.6 Screen capture from the ShakeCast 3 Facilities tab for bridge 32_I1291 on Highway 395 north of Reno near the California state line.	21
Figure 2.7 Summary level page in the ShakeCast 3 web interface for bridge assessment.	22
Figure 2.8 ShakeCast view showing bridges and damage states from the Mount Rose M6.9 scenario earthquake.....	23
Figure 2.9 Detailed map view showing many individual bridges along and just south of I-80 in Reno.	23
Figure 2.10 Facility Inspection Report generated by ShakeCast using as input a scenario M6.9 earthquake on the Mount Rose fault.	24
Figure 2.11 Excerpt from the M6.9 earthquake on the Mount Rose fault report of additional facilities likely or possibly having damage.	24
Figure 2.12 ShakeMap of a small real earthquake in northwest Nevada. Bridges are all grey because none reach the lowest green level at 0.1 g SA(1).	25
Figure 3.1 Before and after earthquake events (Basoz and Kiremidjian 1997)	44
Figure 3.2 Basic steps in seismic risk assessment (King and Kiremidjian 1994).....	45
Figure 3.3 Fragility curve trend.....	46
Figure 3.4 Empirical fragility curves for multi-span bridges (Basoz and Kiremidjian, 1997)	46
Figure 3.5 Demand and capacity response spectra (Mander and Basoz,1999).....	47
Figure 3.6 Generating of fragility curves using nonlinear time history analysis (Nielson, 2005)	47
Figure 3.7 Incremental dynamic analysis procedure to develop PSDM's (Ramanathan, 2012)	48
Figure 3.8 ShakeCast stores only the 50% probability of exceedance value (Turner et al. 2009)....	49
Figure 3.9 Comparison of analytical and HAZUS fragility curves for non-seismically designed bridges LS: limit state, IM: intensity measure, and DS: damage state (AmiriHormozaki, 2013).49	49
Figure 3.10 Comparison of analytical and HAZUS fragility curves for seismically designed bridges (AmiriHormozaki, 2013).....	50
Figure 3.11 High (a) and medium (b) seismic design spectra for 1000-year return periods (AASHTO-site class D). Spectra represent the Reno and Las Vegas areas, respectively. HAZUS SA(1) values are seen to be much higher in both cases than actual Nevada bridge design. Proposed alternative values for seismically (S) and non-seismic (NS) are also shown...50	50

Figure 4.1 Schematic diagram showing how to get the return period corresponding to a specific damage state for a specific bridge.....	58
Figure 4.2 Illustration of an NSHM grid point configuration (red “X”) for extrapolating gridded SA(1) to bridge 32_G_863W (blue circle). In this case the four nearest points do not form a rectangle around the bridge. For scale, 0.01 degrees latitude is 900 meters.	58
Figure 4.3 Net site amplifications for non-linear corrections and three NEHRP site classes.....	59
Figure B-1.1 HWB 10, 32_B_839S SA(1 Hz) hazard curve and capacity estimates, southeast Nevada and not near any high activity faults.	87
Figure B-1.2 HWB 10, 32_B_954N SA(1 Hz) hazard curve and capacity estimates	87
Figure B-1.3 HWB 10, 32_B_954S SA(1 Hz) hazard curve and capacity estimates.....	88
Figure B-1.4 HWB 10, 32_B1544N SA(1 Hz) hazard curve and capacity estimates.....	88
Figure B-1.5 HWB 10, 32_B1544S SA(1 Hz) hazard curve and capacity estimates.....	89
Figure B-1.6 HWB 10, 32_G_925E SA(1 Hz) hazard curve and capacity estimates.....	89
Figure B-1.7 HWB 10, 32_G_925W SA(1 Hz) hazard curve and capacity estimates.....	90
Figure B-1.8 HWB 10, 32_G_941 SA(1 Hz) hazard curve and capacity estimates.....	90
Figure B-1.9 HWB 10, 32_G_947 SA(1 Hz) hazard curve and capacity estimates.....	91
Figure B-1.10 HWB 10, 32_G_953 SA(1 Hz) hazard curve and capacity estimates.....	91
Figure B-1.11 HWB 10, 32_G_961N SA(1 Hz) hazard curve and capacity estimates.....	92
Figure B-1.12 HWB 10, 32_G_961S SA(1 Hz) hazard curve and capacity estimates.....	92
Figure B-1.13 HWB 10, 32_G1153 SA(1 Hz) hazard curve and capacity estimates.....	93
Figure B-1.15 HWB 10, 32_H_788 SA(1 Hz) hazard curve and capacity estimates.....	94
Figure B-1.16 HWB 10, 32_H_856 SA(1 Hz) hazard curve and capacity estimates.....	94
Figure B-1.17 HWB 10, 32_H_866E SA(1 Hz) hazard curve and capacity estimates.....	95
Figure B-1.18 HWB 10, 32_H_866W SA(1 Hz) hazard curve and capacity estimates.....	95
Figure B-1.19 HWB 10, 32_H_918W SA(1 Hz) hazard curve and capacity estimates.....	96
Figure B-1.20 HWB 10, 32_H_918W SA(1 Hz) hazard curve and capacity estimates.....	96
Figure B-1.21 HWB 10, 32_H_933 SA(1 Hz) hazard curve and capacity estimates.....	97
Figure B-1.22 HWB 10, 32_H_935 SA(1 Hz) hazard curve and capacity estimates.....	97
Figure B-1.23 HWB 10, 32_H_936 SA(1 Hz) hazard curve and capacity estimates.....	98
Figure B-1.24 HWB 10, 32_H_946 SA(1 Hz) hazard curve and capacity estimates.....	98
Figure B-1.25 HWB 10, 32_H_970 SA(1 Hz) hazard curve and capacity estimates.....	99
Figure B-1.26 HWB 10, 32_H_990 SA(1 Hz) hazard curve and capacity estimates.....	99
Figure B-1.27 HWB 10, 32_H_991 SA(1 Hz) hazard curve and capacity estimates.....	100
Figure B-1.28 HWB 10, 32_H_993 SA(1 Hz) hazard curve and capacity estimates.....	100
Figure B-1.29 HWB 10, 32_H_995 SA(1 Hz) hazard curve and capacity estimates.....	101
Figure B-1.30 HWB 10, 32_H_997 SA(1 Hz) hazard curve and capacity estimates.....	101
Figure B-1.31 HWB 10, 32_H1003 SA(1 Hz) hazard curve and capacity estimates.....	102
Figure B-1.32 HWB 10, 32_H1042 SA(1 Hz) hazard curve and capacity estimates.....	102
Figure B-1.33 HWB 10, 32_I_754 SA(1 Hz) hazard curve and capacity estimates.....	103
Figure B-1.34 HWB 10, 32_I_770 SA(1 Hz) hazard curve and capacity estimates.....	103
Figure B-1.35 HWB 10, 32_I_796 SA(1 Hz) hazard curve and capacity estimates.....	104
Figure B-1.36 HWB 10, 32_I_862 SA(1 Hz) hazard curve and capacity estimates.....	104
Figure B-1.37 HWB 10, 32_I_889 SA(1 Hz) hazard curve and capacity estimates.....	105
Figure B-1.38 HWB 10, 32_I_892 SA(1 Hz) hazard curve and capacity estimates.....	105
Figure B-1.39 HWB 10, 32_I_908 SA(1 Hz) hazard curve and capacity estimates.....	106
Figure B-1.40 HWB 10, 32_I_915 SA(1 Hz) hazard curve and capacity estimates.....	106

Figure B-1.41 HWB 10, 32_I_924E SA(1 Hz) hazard curve and capacity estimates.	107
Figure B-1.42 HWB 10, 32_I_924W SA(1 Hz) hazard curve and capacity estimates.	107
Figure B-1.43 HWB 10, 32_I_934 SA(1 Hz) hazard curve and capacity estimates.	108
Figure B-1.44 HWB 10, 32_I_937 SA(1 Hz) hazard curve and capacity estimates.	108
Figure B-1.45 HWB 10, 32_I_938 SA(1 Hz) hazard curve and capacity estimates.	109
Figure B-1.46 HWB 10, 32_I_947L SA(1 Hz) hazard curve and capacity estimates.	109
Figure B-1.47 HWB 10, 32_I_947M SA(1 Hz) hazard curve and capacity estimates.	110
Figure B-1.48 HWB 10, 32_I_947R SA(1 Hz) hazard curve and capacity estimates.	110
Figure B-1.49 HWB 10, 32_I_969N SA(1 Hz) hazard curve and capacity estimates.	111
Figure B-1.50 HWB 10, 32_I_969S SA(1 Hz) hazard curve and capacity estimates.	111
Figure B-1.51 HWB 10, 32_I_992 SA(1 Hz) hazard curve and capacity estimates.	112
Figure B-1.52 HWB 10, 32_I_994 SA(1 Hz) hazard curve and capacity estimates.	112
Figure B-1.53 HWB 10, 32_I1000 SA(1 Hz) hazard curve and capacity estimates.	113
Figure B-1.54 HWB 10, 32_I1001 SA(1 Hz) hazard curve and capacity estimates.	113
Figure B-1.55 HWB 10, 32_I1002 SA(1 Hz) hazard curve and capacity estimates.	114
Figure B-1.56 HWB 10, 32_I1005E SA(1 Hz) hazard curve and capacity estimates.	114
Figure B-1.57 HWB 10, 32_I1005W SA(1 Hz) hazard curve and capacity estimates.	115
Figure B-1.58 HWB 10, 32_I1007E SA(1 Hz) hazard curve and capacity estimates.	115
Figure B-1.59 HWB 10, 32_I1007W SA(1 Hz) hazard curve and capacity estimates.	116
Figure B-1.60 HWB 10, 32_I1010 SA(1 Hz) hazard curve and capacity estimates.	116
Figure B-1.61 HWB 10, 32_I1075N SA(1 Hz) hazard curve and capacity estimates.	117
Figure B-1.62 HWB 10, 32_I1075S SA(1 Hz) hazard curve and capacity estimates.	117
Figure B-1.63 HWB 10, 32_I1086 SA(1 Hz) hazard curve and capacity estimates.	118
Figure B-1.64 HWB 10, 32_I1087 SA(1 Hz) hazard curve and capacity estimates.	118
Figure B-1.65 HWB 10, 32_I1088 SA(1 Hz) hazard curve and capacity estimates.	119
Figure B-1.66 HWB 10, 32_I1089 SA(1 Hz) hazard curve and capacity estimates.	119
Figure B-1.67 HWB 10, 32_I1093N SA(1 Hz) hazard curve and capacity estimates.	120
Figure B-1.68 HWB 10, 32_I1093S SA(1 Hz) hazard curve and capacity estimates.	120
Figure B-1.69 HWB 10, 32_I1149 SA(1 Hz) hazard curve and capacity estimates.	121
Figure B-1.70 HWB 10, 32_I1159E SA(1 Hz) hazard curve and capacity estimates.	121
Figure B-1.71 HWB 10, 32_I1159W SA(1 Hz) hazard curve and capacity estimates.	122
Figure B-1.72 HWB 10, 32_I1171 SA(1 Hz) hazard curve and capacity estimates.	122
Figure B-1.73 HWB 10, 32_I1172 SA(1 Hz) hazard curve and capacity estimates.	123
Figure B-1.74 HWB 10, 32_I1173 SA(1 Hz) hazard curve and capacity estimates.	123
Figure B-1.75 HWB 10, 32_I1250 SA(1 Hz) hazard curve and capacity estimates.	124
Figure B-2.1 HWB 11, 32_H1815 SA(1 Hz) hazard curve and capacity estimates.	125
Figure B-2.2 HWB 11, 32_H1816 SA(1 Hz) hazard curve and capacity estimates.	125
Figure B-2.4 HWB 11, 32_I_947 SA(1 Hz) hazard curve and capacity estimates.	126
Figure B-2.5 HWB 11, 32_I_947E SA(1 Hz) hazard curve and capacity estimates.	127
Figure B-2.6 HWB 11, 32_I_947W SA(1 Hz) hazard curve and capacity estimates.	127
Figure B-2.7 HWB 11, 32_I1126 SA(1 Hz) hazard curve and capacity estimates.	128
Figure B-2.8 HWB 11, 32_I1452 SA(1 Hz) hazard curve and capacity estimates.	128
Figure B-3.1 HWB 15, 32_B_303 SA(1 Hz) hazard curve and capacity estimates.	129
Figure B-3.2 HWB 15, 32_B_433N SA(1 Hz) hazard curve and capacity estimates.	129
Figure B-3.3 HWB 15, 32_B1327W SA(1 Hz) hazard curve and capacity estimates.	130
Figure B-3.4 HWB 15, 32_B1489 SA(1 Hz) hazard curve and capacity estimates.	130

Figure B-3.5 HWB 15, 32_G_387 SA(1 Hz) hazard curve and capacity estimates.....	131
Figure B-3.6 HWB 15, 32_G_863E SA(1 Hz) hazard curve and capacity estimates.	131
Figure B-3.7 HWB 15, 32_G_863W SA(1 Hz) hazard curve and capacity estimates.	132
Figure B-3.8 HWB 15, 32_G_872E SA(1 Hz) hazard curve and capacity estimates.	132
Figure B-3.9 HWB 15, 32_G_872R SA(1 Hz) hazard curve and capacity estimates.	133
Figure B-3.10 HWB 15, 32_G_872W SA(1 Hz) hazard curve and capacity estimates.	133
Figure B-3.11 HWB 15, 32_G_913E SA(1 Hz) hazard curve and capacity estimates.	134
Figure B-3.12 HWB 15, 32_G_913W SA(1 Hz) hazard curve and capacity estimates.	134
Figure B-3.13 HWB 15, 32_G_919E SA(1 Hz) hazard curve and capacity estimates.	135
Figure B-3.14 HWB 15, 32_G_919W SA(1 Hz) hazard curve and capacity estimates.	135
Figure B-3.15 HWB 15, 32_G1233 SA(1 Hz) hazard curve and capacity estimates.....	136
Figure B-3.16 HWB 15, 32_G1233L SA(1 Hz) hazard curve and capacity estimates.	136
Figure B-3.17 HWB 15, 32_G1233R SA(1 Hz) hazard curve and capacity estimates.	137
Figure B-3.18 HWB 15, 32_G1296 SA(1 Hz) hazard curve and capacity estimates.....	137
Figure B-3.19 HWB 15, 32_H1234 SA(1 Hz) hazard curve and capacity estimates.....	138
Figure B-3.20 HWB 15, 32_H1443 SA(1 Hz) hazard curve and capacity estimates.....	138
Figure B-3.21 HWB 15, 32_I_868 SA(1 Hz) hazard curve and capacity estimates.	139
Figure B-3.22 HWB 15, 32_I1255 SA(1 Hz) hazard curve and capacity estimates.	139
Figure B-3.23 HWB 15, 32_I1290 SA(1 Hz) hazard curve and capacity estimates.	140
Figure B-4.1 HWB 22, 32_B1526 SA(1 Hz) hazard curve and capacity estimates.....	141
Figure B-4.2 HWB 22, 32_G1414 SA(1 Hz) hazard curve and capacity estimates.....	141
Figure B-4.3 HWB 22, 32_H_869E SA(1 Hz) hazard curve and capacity estimates.	142
Figure B-4.4 HWB 22, 32_H_869W SA(1 Hz) hazard curve and capacity estimates.	142
Figure B-4.5 HWB 22, 32_H1205 SA(1 Hz) hazard curve and capacity estimates.....	143
Figure B-4.6 HWB 22, 32_I_871E SA(1 Hz) hazard curve and capacity estimates.....	143
Figure B-4.7 HWB 22, 32_I_871W SA(1 Hz) hazard curve and capacity estimates.....	144
Figure B-4.8 HWB 22, 32_I_873 SA(1 Hz) hazard curve and capacity estimates.	144
Figure B-4.9 HWB 22, 32_I_878 SA(1 Hz) hazard curve and capacity estimates.	145
Figure B-4.10 HWB 22, 32_I_879 SA(1 Hz) hazard curve and capacity estimates.	145
Figure B-4.11 HWB 22, 32_I_882 SA(1 Hz) hazard curve and capacity estimates.	146
Figure B-4.12 HWB 22, 32_I_896 SA(1 Hz) hazard curve and capacity estimates.	146
Figure B-4.13 HWB 22, 32_I1261 SA(1 Hz) hazard curve and capacity estimates.	147
Figure B-4.14 HWB 22, 32_I1977 SA(1 Hz) hazard curve and capacity estimates.	147
Figure B-5.1 HWB 23, 32_B_455 SA(1 Hz) hazard curve and capacity estimates.....	148
Figure B-5.2 HWB 23, 32_B1014 SA(1 Hz) hazard curve and capacity estimates.....	148
Figure B-5.3 HWB 23, 32_B1533 SA(1 Hz) hazard curve and capacity estimates.	149
Figure B-5.4 HWB 23, 32_G_805R SA(1 Hz) hazard curve and capacity estimates.	149
Figure B-5.5 HWB 23, 32_G_941L SA(1 Hz) hazard curve and capacity estimates.	150
Figure B-5.6 HWB 23, 32_G_961R SA(1 Hz) hazard curve and capacity estimates.	150
Figure B-5.7 HWB 23, 32_G1748N SA(1 Hz) hazard curve and capacity estimates.....	151
Figure B-5.8 HWB 23, 32_G1748S SA(1 Hz) hazard curve and capacity estimates.....	151
Figure B-5.9 HWB 23, 32_G2012 SA(1 Hz) hazard curve and capacity estimates.....	152
Figure B-5.10 HWB 23, 32_G2014 SA(1 Hz) hazard curve and capacity estimates.....	152
Figure B-5.11 HWB 23, 32_G2014R SA(1 Hz) hazard curve and capacity estimates.	153
Figure B-5.12 HWB 23, 32_H_936R SA(1 Hz) hazard curve and capacity estimates.	153
Figure B-5.13 HWB 23, 32_H1212 SA(1 Hz) hazard curve and capacity estimates.....	154

Figure B-5.14 HWB 23, 32_H1214 SA(1 Hz) hazard curve and capacity estimates.....	154
Figure B-5.15 HWB 23, 32_H1446 SA(1 Hz) hazard curve and capacity estimates.....	155
Figure B-5.16 HWB 23, 32_H1458 SA(1 Hz) hazard curve and capacity estimates.....	155
Figure B-5.17 HWB 23, 32_H1460 SA(1 Hz) hazard curve and capacity estimates.....	156
Figure B-5.18 HWB 23, 32_H1804 SA(1 Hz) hazard curve and capacity estimates.....	156
Figure B-5.19 HWB 23, 32_H2013 SA(1 Hz) hazard curve and capacity estimates.....	157
Figure B-5.20 HWB 23, 32_H2013W SA(1 Hz) hazard curve and capacity estimates.....	157
Figure B-5.21 HWB 23, 32_H2290 SA(1 Hz) hazard curve and capacity estimates.....	158
Figure B-5.22 HWB 23, 32_H2331 SA(1 Hz) hazard curve and capacity estimates.....	158
Figure B-5.23 HWB 23, 32_H2348 SA(1 Hz) hazard curve and capacity estimates.....	159
Figure B-5.24 HWB 23, 32_H2349 SA(1 Hz) hazard curve and capacity estimates.....	159
Figure B-5.25 HWB 23, 32_H2350 SA(1 Hz) hazard curve and capacity estimates.....	160
Figure B-5.26 HWB 23, 32_H2486 SA(1 Hz) hazard curve and capacity estimates.....	160
Figure B-5.27 HWB 23, 32_H2710 SA(1 Hz) hazard curve and capacity estimates.....	161
Figure B-5.28 HWB 23, 32_H2711 SA(1 Hz) hazard curve and capacity estimates.....	161
Figure B-5.29 HWB 23, 32_I_806N SA(1 Hz) hazard curve and capacity estimates.....	162
Figure B-5.30 HWB 23, 32_I_806S SA(1 Hz) hazard curve and capacity estimates.....	162
Figure B-5.31 HWB 23, 32_I_944N SA(1 Hz) hazard curve and capacity estimates.....	163
Figure B-5.32 HWB 23, 32_I_944S SA(1 Hz) hazard curve and capacity estimates.....	163
Figure B-5.33 HWB 23, 32_I_950 SA(1 Hz) hazard curve and capacity estimates.....	164
Figure B-5.34 HWB 23, 32_I1091N SA(1 Hz) hazard curve and capacity estimates.....	164
Figure B-5.35 HWB 23, 32_I1091S SA(1 Hz) hazard curve and capacity estimates.....	165
Figure B-5.36 HWB 23, 32_I1219 SA(1 Hz) hazard curve and capacity estimates.....	165
Figure B-5.37 HWB 23, 32_I1456 SA(1 Hz) hazard curve and capacity estimates.....	166
Figure B-5.38 HWB 23, 32_I1949 SA(1 Hz) hazard curve and capacity estimates.....	166
Figure B-5.39 HWB 23, 32_I1950 SA(1 Hz) hazard curve and capacity estimates.....	167
Figure B-5.40 HWB 23, 32_I1952 SA(1 Hz) hazard curve and capacity estimates.....	167
Figure B-5.41 HWB 23, 32_I2139 SA(1 Hz) hazard curve and capacity estimates.....	168
Figure B-5.42 HWB 23, 32_I2139R SA(1 Hz) hazard curve and capacity estimates.....	168
Figure B-5.43 HWB 23, 32_I2140 SA(1 Hz) hazard curve and capacity estimates.....	169
Figure B-5.44 HWB 23, 32_I2141R SA(1 Hz) hazard curve and capacity estimates.....	169
Figure B-5.45 HWB 23, 32_I2288 SA(1 Hz) hazard curve and capacity estimates.....	170
Figure B-5.46 HWB 23, 32_I2293N SA(1 Hz) hazard curve and capacity estimates.....	170
Figure B-5.47 HWB 23, 32_I2293S SA(1 Hz) hazard curve and capacity estimates.....	171
Figure B-5.48 HWB 23, 32_I2296N SA(1 Hz) hazard curve and capacity estimates.....	171
Figure B-5.49 HWB 23, 32_I2296S SA(1 Hz) hazard curve and capacity estimates.....	172
Figure B-5.50 HWB 23, 32_I2339 SA(1 Hz) hazard curve and capacity estimates.....	172
Figure B-5.51 HWB 23, 32_I2499 SA(1 Hz) hazard curve and capacity estimates.....	173
Figure D.1 damage state 2, spalling of corner cover concrete (Kaminosono et al, 2002).....	181
Figure D.2 Damage state 3, spalling and reinforcement exposure- no cracks in core concrete (Kaminosono et al, 2002).....	182
Figure D.3 Damage state 3, wider shear cracking and local crush at top corner (Kaminosono et al, 2002.....	182
Figure D.4 Damage state 4, extensive cracking and spalling, some minor reinforcement buckling (Kaminosono et al, 2002).....	183

Figure D.5 Damage state 4, extensive spalling and reinforcement exposure, but no buckling. (Kaminosono et al, 2002)	183
Figure D.6 Damage state 4, massive spalling and exposure of reinforcement and minor buckling (Kaminosono et al, 2002)	184
Figure D.7 Damage state 5, fracture and buckling of reinforcement and collapse (Kaminosono et al, 2002)	185
Figure D.8 Angled stem wall failure of specimen (Bozorgzadeh et. al. 2004)	186
Figure D.9 Failure of specimens 5 A and B (Bozorgzadeh et. al, 2004)	187
Figure D.10 Damage State 2 (Bozorgzadeh et al, 2004).....	188
Figure B.11 Damage State 5 (Saini et al, 2013)	188
Figure D.12 Damage State 6 (Saini et al, 2013).....	189
Figure D.13 Abutment Damage State 2 (Saini et al, 2013)	190
Figure D.14 Abutment Damage State 3 (Saini et al, 2013)	191
Figure D.15 Abutment Damage State 4 (Saini et al, 2013)	191
Figure D.16 Abutment Damage State 6 (Saini et al, 2013)	192
Figure D.17 Failure of columns (Saadatmanesh et al, 1997)	193
Figure D.18 Repair process for columns (Saadatmanesh et al, 1997).....	193
Figure D.19 Shear damaged bridge Column (Li et al, 2003)	194
Figure D.20: Repair of damaged column (Li at al, 2003).....	194
Figure D.21 Restoration process for damaged column (Belarbi el al, 2008).....	195
Figure D.22 Damaged bars and coupler repair (Saini et al, 2013)	196
Figure D.23 CFRP wrapping (Saini et al, 2013)	196
Figure D.24 Increasing damage states (He et al, 2013)	197
Figure D.25 Failed reinforcement prior to repair (Rutledge et al, 2013).....	198
Figure D.30 Repair process (Rutledge et al, 2013)	198
Figure D.31 Damage state v. required Cfrp thickness- Example column.....	200
Figure D.31 Repair for DS2 and DS5 (Saini et al, 2013)	202
Figure D.32 DS6 repair step 1 (Saini et al, 2013)	203
Figure D.33 DS6 repair step 2 (Saini et al, 2013)	204
Figure D.34 DS6 repair step 3 (Saini et al, 2013)	204
Figure D.35 DS6 repair step 4 (Saini et al, 2013)	205
Figure D.36 DS6 repair step 5 (Saini et al, 2013)	205
Figure D.37 DS6 repair step 6 (Saini et al, 2013)	206

Chapter 1: Introduction

The damage caused by earthquakes to the infrastructure impacts the traveling public immediately. Timely post-earthquake evaluation of transportation structures is critical to both drivers' safety and the state's economy. Many bridges in Nevada are either on highly congested or on isolated highways where detours can be very long. Therefore, after an earthquake, it is essential to obtain a quick estimate of the damage level, identify the appropriate repair method, assess if the bridge can carry the load necessary to maintain traffic, and assure that the bridge still has reserved lateral load capacity to withstand another earthquake. The time required to discover damaged elements and assess its level of damage requires great effort especially in a state like Nevada where bridges can be very distributed. The time required to survey and evaluate the condition of every bridge after a certain limit of earthquake activities could be substantial. High earthquake risk requires preparedness and fast response to the unpredictable event.

In preparedness to the pre and post-earthquake event, authorities like Nevada Department of Transportation (NDOT) require an alert system that enables decision makers to focus on bridges in the state that could be damaged. Earthquake vulnerability of a bridge is based on: bridge location to the earthquake fault, soil data, bridge type and year of design. The spread of earthquake acceleration to the areas close to earthquake fault depends on the geological formation while the design of a bridge and its type play another part in defining whether the bridge is vulnerable or not. In another words, the bridge could be vulnerable in some events while in another event it might not, depending on these factors combined together. In order to study all bridges in Nevada versus the possible scenarios of earthquakes based on the fault distribution in the state, a joint effort between seismologists and structural engineers at the University of Nevada, Reno was carried out.

The USGS has a tool called ShakeMap that can be used to estimate the level of shaking at any given bridge site given the earthquake location and magnitude. Using this tool with the Nevada Bridge Inventory provide inspectors, engineers, and decision makers an instant indication of the possible damage and the necessary response. Another tool developed by USGS called ShakeCast has already been utilized in California to estimate post-earthquake damage levels at bridges and other types of infrastructure.

ShakeMap/ShakeCast has been used to facilitate the post-earthquake decision-making and response within Caltrans. ShakeMap is available in Nevada, and through this project, it is adapted for NDOT use. The impact of different earthquakes can be seen on the USGS website. It provides near-real-time maps of ground motion and shaking intensity following significant earthquakes. These maps are used by federal, state, and local organizations, both public and private, for post-earthquake response and recovery, public and scientific information, as well as for preparedness exercises and disaster planning. From USGS, "ShakeCast is a freely available, post-earthquake situational awareness application that automatically retrieves earthquake shaking data from ShakeMap, compares intensity measures against users' facilities, and generates potential damage assessment notifications, facility damage maps, and other Web-based products for emergency managers and responders." With ShakeCast, a user can automatically determine the shaking values at a given site. Users can then be notified of the potential consequences (see **Figure 1.1**). Biasi et al. (in press) summarize the application developed here of ShakeMap and ShakeCast for bridge evaluation.

As post-earthquake decision making, it will be important for field investigators and engineers to be aware of the type of damage that will be encountered as well as methods that could be used to repair this damage. Appendix D provides summary of the types of damage that could be observed as well as methods for assessing and repairing the damage.

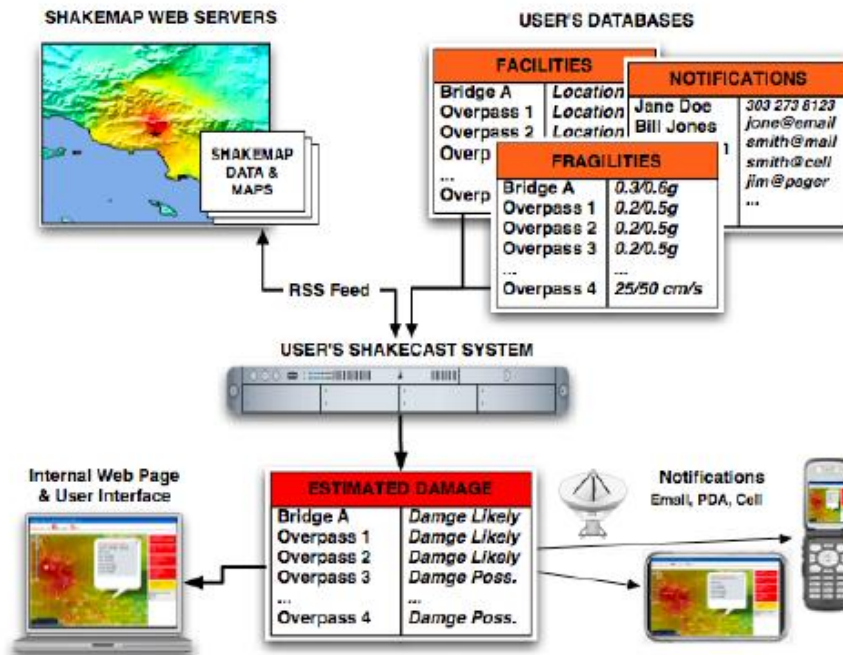


Figure 1.1 ShakeCast flow chart from ShakeCast users manual (Wald et al., 2005)

Chapter 2: ShakeMap/ShakeCast - Path from Earthquake to Bridge Evaluation

2.1 Earthquakes in Nevada

2.1.1 Tectonic Context

Earthquakes in Nevada are the response of the brittle crust to west- and northwest-directed strike-slip and extensional motion of western Nevada relative to stable North America. On the west side of the state, north-west motion of the Sierra Nevada block relative to central Nevada has focused onto well-developed strike-slip faults including Owens, Chalfant, Panamint, Saline, Death and Fish Lake Valleys in eastern California. These faults coalesce near the north end of the White Mountains, before diverging into an interconnected system of strike-slip and normal faults in western Nevada. Strike-slip motion continues on faults through Mina, Hawthorne, Pyramid Lake, and Warm Springs. Normal faulting, with some strike-slip component continues on a nearly N-S trend at least as far as Battle Mountain. Normal faulting and regional dilation thins the crust and creates broad internal drainages of the Carson Sink and Black Rock Desert. This opening reduces the relative strike-slip motion across faults of the northern Sierra Nevada, such that strike-slip essentially dies out as it crosses NE California.

On the east side of Nevada, fault earthquakes occur because the central part of the state roughly from the Nevada-Utah border west to the east side of Dixie Valley is moving in a quasi-block-like fashion west at 1-2 mm/yr relative to the Colorado Plateau and highlands of western Utah. Motion is expressed as extension concentrated on faults of western Utah, and in crustal dilation in depressions including the Great Salt Lake. Between these zones is a more rigid region of limited internal deformation and limited seismic activity. To the south, just north of the Las Vegas Valley, motion on the order of 1 mm/yr concentrates in the left-lateral faults of a broad shear zone. In NE Nevada relative motions are slower and extension occurs in a distributed system of N-S striking very low slip-rate normal faults.

2.1.2 Nevada History

Significant earthquakes in northwest Nevada are reviewed by DePolo (2012), Depolo and Depolo (2012), Pancha et al. (2006), and DePolo et al. (1997). The earliest damaging earthquakes reported in Nevada occurred in 1869. Two events, about 8 hours apart with magnitudes of 6.4 and 6.2, caused considerable damage in Virginia City, Steamboat Springs, and Washoe Valley. Initially this event was thought to have occurred on the NE-trending Olinghouse fault east of Reno and associated with ground rupture observed in an airborne LiDAR survey, but it now appears that a different source acted in 1869. Carson Valley was shaken in 1887 by an earthquake with a magnitude of 6.5 that was widely felt including in the Sacramento Valley. Structures including the State Capitol in Carson City were damaged, and chimneys and brick walls suffered severe damage in Genoa. Another pair of earthquakes of about M 6 and M 6.4 occurred in February and April 1914, probably just east of Reno. This earthquake caused damage to unreinforced masonry buildings including on the campus of the University of Nevada in Reno and in Virginia City. The larger of these events awakened people from their sleep as far away as the Sacramento Valley. The largest earthquake in Nevada history was the M7.3 Pleasant Valley rupture, about 40 km west

of Battle Mountain. This rupture had a total length of 61 km and involved four disjointed segments of range-bounding normal faults. Structures were damaged in the towns of Battle Mountain, Winnemucca, Lovelock and Fallon. Damage in Lovelock included a collapsed water tower (**Figure 2.1**). The 1915 earthquake was the first of a series that included 1932 Cedar Mountain (M7.2), 1954 Fairview Peak (M7.1), 1954 Dixie Valley (M6.8) and several other damaging earthquakes in 1954 through 1959 east of Fallon and west of the southern Humboldt Range. No surface-rupturing earthquakes have occurred in Nevada since that time. The largest event in western Nevada since 1954 occurred in 1994 south of Gardnerville in Double Springs Flat, with a magnitude of 5.9. Minor ground cracking was reported with this event, but no confirmed ground rupture. Notable earthquakes elsewhere in Nevada include the 1992 M5.8 Little Skull Mountain and the 2008 M6.0 Wells earthquakes; both caused ground motions strong enough that they could have damaged bridges had they occurred in more densely populated areas.

2.1.3 Earthquake Locations and Magnitudes

Earthquakes in Nevada are located by the Western Great Basin Seismic Network, a system of real-time seismographs, communications, and recording computers operated by Nevada Seismological Laboratory (NSL) at the University of Nevada Reno. The network is operated under a cooperative agreement with the U. S. Geological Survey (USGS). Data recorded during state-wide monitoring is forwarded by the NSL to the USGS and several other cooperating agencies. The seismic network is a joint funding effort between USGS, State of Nevada, and special projects including experiments on the Nevada Nuclear Safety Site. The seismic network includes strong-motion accelerograph stations in the major urban areas of Nevada including the Reno-Carson City urban corridor and the Las Vegas Valley.

Earthquake locations and magnitudes are determined at NSL initially by an automatic system. The system “listens” to real-time signals from all stations for above-background signals. Noise and local activity may trigger stations individually, but only earthquakes and significant man-made events (e.g., quarry blasts) have sufficient energy to trigger several stations in a short period of time. The system back-projects candidate activity in time and space, and an earthquake is inferred if the trigger times can be explained within some uncertainty by an event at a single point. Events with energy enough to damage structures trigger typically 40-60 stations or more in western Nevada and 30-50 stations in eastern Nevada. Earthquakes with automatic magnitude estimates of 3.0 and larger trigger automatic notifications to NSL review staff, and the event will be confirmed as seismic and relocated within 10-20 minutes. Normally a moment magnitude is reviewed and released if the event has a magnitude greater than about 3.5. The automatic system also sends a notification to the USGS, which reformats the message and posts the event on their web and notification pages. Reviewed locations developed at NSL are also forwarded to the USGS and used to update their information. Aspects of the receiving and revision systems are still under development at the USGS.

2.2 ShakeMap: Map Based View of Ground Shaking

2.2.1 Overview

ShakeMap is a software package developed by the USGS to provide a map-based spatial representation of expected ground shaking from significant earthquakes. The core functionality

of ShakeMap is to take an earthquake location and magnitude and to project in map view expected ground shaking amplitudes using a ground motion prediction equation (GMPE, also known as an attenuation relation). Five ground motion metrics are projected – peak ground acceleration (PGA), peak ground velocity (PGV), and spectral acceleration at 0.3, 1.0, and 3.0 second periods (SA(0.3), SA(1), and SA(3), respectively). While five ground motion metrics are available, SA(1) is the value to be focused on as most relevant to bridges performance. Significant earthquakes automatically trigger the ShakeMap system. The actual lower magnitude at which ShakeMaps are triggered is set by seismic network policy, below where damage is expected. At these lower magnitudes, ShakeMaps are primarily produced to confirm that the system is running and occasionally exercised. ShakeMaps are normally revised for significant events when a new magnitude or materially different location is developed. ShakeMap can also be run in scenario mode. In this case the earthquake location and magnitude are provided in an external file. Scenario ground shaking maps are normally used for planning and evaluation purposes. ShakeMap is used in this research in scenario mode to develop realistic estimates of potential demands on Nevada bridges.

2.2.2 ShakeMap and Seismic Demand

Several aspects of the ShakeMap system affect how it projects ground motion in map view. The earthquake source model controls how the energy release is distributed, normally as either a point or on a surface. Ground motion prediction equations control how shaking intensity extends from the source to points on the surface, especially depending on distance. ShakeMap also includes an approximate site condition correction. Site conditions generally amplify predicted ground motions. Sources and interpretations of uncertainty in ShakeMaps are also discussed, especially as they affect expectations for bridges performance.

2.2.2.1 ShakeMap Earthquake Source Models

Automatically generated ShakeMaps estimate ground motion assuming a point source at the location and depth provided by the seismic network. Point-source ShakeMaps are easily identified by the circular pattern of ground motion contours. Point source ShakeMaps will be, by far, the most frequently developed in routine Nevada operations. For earthquakes larger than ~M6.0 ground motions projections can be improved by modeling the moment release as having occurred on the plane of the active fault. If parameters describing the rupture area on the fault are provided manually to the ShakeMap system, moment is spread over the effective area, and ground motions estimated as the sum of many small areal contributions. An earthquake source modeled this way is called a “finite-source” mechanism. NSL operators may provide these parameters to ShakeMap for use in a reviewed map set. To date, no earthquakes have occurred large enough to exercise this capability. Finite-fault sources are, however, routinely used in ShakeMap scenario mode.

2.2.2.2 Ground Motion Prediction Equations

ShakeMap can be configured with a choice of Ground Motion Prediction Models (GMPEs). The choice of GMPEs within ShakeMap is limited to those for which the GMPE has been reprogrammed into a Perl language module compatible the ShakeMap interface. Adapting a GMPE for use in ShakeMap is somewhat complicated because ShakeMap reports five ground

motion intensity measures, and many available regressions only provide some or other subset. In addition, only a few GMPE's are available suitable for use with normal faulting events. Of the few candidates, after some experimentation, two GMPE relations were found suitable for project use. These GMPEs were developed by Boore and Atkinson (2008; BA08) and by Chiou and Youngs (2008; CY08). Both were released in 2008 as part of the Next Generation Attenuation project (N. Abrahamson, et al. 2008). Another GMPE based on work by Boore et al. (1997) called HAZUS-PGV is available within ShakeMap (Wald et al., 2005). HAZUS-PGV model was initially considered, but predicted larger than expected ground motions for Nevada geological conditions. In addition, after the Boore et al. (1997) regressions were developed, a series of well-recorded international earthquakes provided better data to constrain the GMPEs at near distances and large magnitudes. These new data showed that the HAZUS-PGV model over-predicts ground motion especially at short source-to-site distances. As a result, the HAZUS-PGV relations are no longer considered best for ShakeMap operations in the western U.S.

For automatic and reviewed network operations ShakeMaps, the Nevada Seismological Laboratory currently uses the BA08 regression to estimate ground motion versus distance. The BA08 GMPEs have shown good performance in California ShakeMaps and have a favorable recommendation from within the ShakeMap development team.

2.2.2.3 Site Condition Estimates in ShakeMap

By default ShakeMap calculates ground motions for a nominal 760 m/s shear wave velocity, but can correct ground motion predictions for other Vs30 site conditions. In general, measured site corrections are scarce and too incomplete to apply on the scale needed for ShakeMap. Instead, ShakeMap uses a local slope-based adjustment as a proxy for the actual shallow shear-wave velocity. The Vs30 proxy is based on the generalization that steeper slopes can be geologically sustained primarily by more rock-like materials, while lower Vs30s are expected in flatter-lying areas such as valley bottoms and alluvial plains. A description of the basis for using slope as a Vs30 proxy and its calibration in California are given by D. J. Wald and T. I. Allen (2007). The average Vs30 in Nevada from this slope method is 523 m/s, with a standard deviation of 188 m/s. Vs30 estimates were calibrated against local slopes using a continuous Vs30 survey conducted along the Truckee River by J. B. Scott, et al. (2004). ShakeMap applies slope-based Vs30 amplifications on a kilometer-scale grid designed for regional display of ground shaking. This means that site conditions at a given bridge site are represented in the ShakeMap only by a coarse average Vs30 over the grid cell, and cannot reflect any site-specific knowledge.

2.2.2.4 Uncertainties in ShakeMaps

ShakeMaps are intended to quickly summarize the potential extent of ground motion following an earthquake. Where available, they will incorporate actual strong motion measurements from the earthquake. Nevertheless, there are several fundamental sources of uncertainty in maps that are relevant to their interpretation, especially in the early time following an earthquake. Uncertainty contributions from earthquake location, magnitude, stress drop, and directivity are discussed in the following section.

Uncertainty in location affects the region projected to include strongest ground motions. Automatic locations of significant earthquakes in western Nevada will normally be accurate to 1-2 km, and reviewed locations accurate to 0.5 to 1.0 km. For applications including ShakeCast,

location accuracy is not expected to strongly affect inspection recommendations. A possible exception would be mislocation perpendicular to the strike of a normal fault where the location determines which areas are calculated using the hanging wall amplification term in the GMPE.

Uncertainty in magnitude is potentially more significant, as it determines both the area affected by strong ground motion as well as its maximum amplitude. Earthquake energy is given by seismic moment $M_o = \mu AD$, where μ is the rock shear modulus ($\sim 3 \times 10^{10}$ N-m), A is the area of the rupture surface (m^2), and D is average displacement on the surface (m). The seismic moment magnitude, is given by $M_w = 2/3(\log_{10} M_o - 16.1)$ (Hanks and Kanamori, 1979), so uncertainty of half a magnitude unit difference corresponds to nearly a factor of 6 uncertainty in energy release. Normally uncertainty in moment magnitude will be smaller than this because M_w is based on more stable, long-period measurements of earthquake ground motion.

Earthquake stress drop is a measure of the energy density released on the fault. Nominal GMPE predictions will be reasonable for stress drops in the range of 10-30 bars (1 bar = 14.5 psi = 100 kPa). Earthquakes with significantly lower stress drops generally produce smaller than predicted ground motions, especially at high frequencies. This type of prediction failure is perhaps least unfavorable, since it means an inspector mobilized to look at bridges will find less damage in the field than expected. Higher stress drops are not as likely for large magnitude events in the Basin and Range Province, but can occur on local patches within the rupture.

Directivity refers to the focusing of strong ground shaking by the actual propagation of the rupture front (Lay and Wallace, 1995, p. 368). Directivity is the ground motion analog of the Doppler effect, which is better known from the frequency change in acoustics depending on whether a source is moving toward or away from the observer. In general ground motions are higher ahead of a rupture front in the compressional quadrant (ground rushes toward the point), and lower at the same distance if the ground is physically moving away. In California these effects have been observed in peak ground acceleration data in ShakeMaps for events as small as M3.5 (L. C. Seekins and J. Boatwright 2010). At larger distances directivity is less important and less likely to affect bridge inspection outcomes.

2.2.2.5 Benchmarking the NSL ShakeMap Implementation

As a step in confirming the ground motion predictions from the NSL instance of ShakeMap, a scenario was jointly run on the NSL installation and by USGS personnel using their installation and settings for ShakeMap. At first the NSL predicted peak ground accelerations were substantially smaller than expected. The difference traced primarily to a difference in a setting affecting how the shallow site conditions were being incorporated. Nevada Seismological Laboratory staff installed a clean version of ShakeMap (still v3.5) to ensure that incremental changes in ShakeMap code were picked up and that the site condition setting has been changed to use the Vs30 corrections built into the GMPEs. After these changes, a benchmark scenario was then run by Bruce Worden (lead ShakeMap developer) and by UNR using the same Vs30 layer. Results of the two agreed exactly. Scenario results following these changes look more reasonable than initial versions, and lead to a more realistic set of estimated bridge damage states.

2.2.3 ShakeMap Scenarios

An important application for ShakeMap, as briefly mentioned above, is to develop spatial predictions of ground shaking from hypothetical ruptures on known faults. This “what-if”

application is useful for planning earthquake response, estimating potential consequences, and evaluating preparedness. ShakeMap scenario earthquakes are used to project ground motions to Nevada bridge sites.

For this project, 112 scenario earthquakes were selected for processing with ShakeMap (**Figure 2.2**). ShakeMap scenario input files were provided by USGS collaborators (D. Wald, pers. comm). These scenarios are based on the ruptures used to estimate ground motions for the USGS National Seismic Hazard Maps (**Figure 2.3**). That is, the USGS used the same fault locations and geometries, including complexity in the surface trace and fault dip where applicable. Scenario events are not located according to earthquake probability, but rather were distributed to sample the primary active faults in the state. Scenario coverage ensured that most bridges in Nevada would be included in ShakeCast evaluations. Scenario names, magnitudes, fault slip rates are listed in **Table 2.1**. Likelihoods of individual scenarios vary with the fault activity rate. As a characterization, faults in the western part of the state slip 1-2 orders of magnitude faster than in the central and eastern regions.

Each scenario consists of an earthquake magnitude and a set of latitudes and longitudes defining the spatial extent of a fault rupture. The rupture surface is expressed as one or a small number of linear panels with constant dip that model the slipping portion of the fault. Moment release is assumed to be uniformly distributed on the rupture surface.

2.3 ShakeCast – Applying ShakeMap Ground Motions to Nevada Bridges

2.3.1 Overview

ShakeCast is a USGS application designed to work with ShakeMap to evaluate the consequences of shaking for a building or structure inventory. More information can be obtained at <http://earthquake.usgs.gov/research/software/shakecast/>. Functionally, the basic roles of ShakeCast are to extract ground motion amplitudes at sites of interest from a map developed by ShakeMap, to compare predicted demand to a statistical description of facility capacity, and to report on the comparison. Bridge locations and the metadata necessary to estimate bridge capacities are obtained from the National Bridge Inventory (NBI). Bridge fragility refers to a set of curves that define the probability that a various damage states will be realized given an input ground motion intensity. A more detailed discussion on bridge fragilities is provided in Chapter 3. The report generated by ShakeCast lists potentially affected bridges, reported in order of inspection priority, with first entries in the list being bridges with the greatest exceedance of estimated capacity. Inspection reports are distributed to registered clients and users of the information, but not provided by ShakeCast to the public. ShakeCast runs automatically, including reporting, on detection of a new or revised ShakeMap in or near Nevada.

2.3.2 National Bridge Inventory and ShakeCast

The National Bridge Inventory (NBI) summarizes metadata about bridges in the United States in a standardized database maintained by the Federal Highway Administration (FHWA). Data in the NBI is provided to the FHWA primarily by the individual states. Metadata relevant to ShakeCast evaluation and post-earthquake capacity include the bridge location, length, construction type, construction year, number of spans, column and bents, and details of bridge geometry. A Perl software module, *nbi2sc.pl*, is provided with ShakeCast to parse the metadata

and to set inspection priority levels as a function of SA(1) demand. Nominal values for these relationships were developed by Caltrans engineers based on their own research, particularly on California bridges (Turner et al., 2009). Caltrans periodically revises these relations in cooperation with USGS ShakeCast personnel to incorporate new research. Cities and other non-bridge facilities can also be included in the inventory evaluated by ShakeCast. All damage estimates are probabilistic, and intended as median expectations for the structure.

Bridge capacity assessments depend on the seismic design of the bridge. Construction detailing for seismic design first advanced significantly in California with bridges constructed in and after 1975. California detailing became a national standard in 1990. Nevada adopted the California detailing standards in 1983, several years before it was required by federal standards. For ShakeCast implementation, capacities assume California detailing for Nevada bridges constructed in 1983 or later. This standard is applied in a conversion script provided with ShakeCast, *nbi2sc.pl*, by calling it with a flag “*seismic_year=1983*”. Given the bridge build year and other metadata, program *nbi2sc.pl* associates input ground motion intensity, SA(1), to expected damage associated with labels “Green”, “Yellow”, “Orange”, and “Red”. A detailed discussion of probabilistic bridge capacity is provided in Chapter 3 of this report. Example metadata rows of four Nevada bridges are shown in **Table 2.2** with their capacity bounds.

2.3.3 Implementation of ShakeCast

2.3.3.1 ShakeCast Version 2

ShakeCast 2 was the version available for most of this project. ShakeCast 2 is designed to run on computers running Linux or Windows and maintained at user’s site. This operating mode requires significant user-side participation by computer and networking staff to install and configure the computer, and to ensure connectivity to USGS ShakeMap servers and outbound notifications via email or other end-user communication modes. Users would also need to maintain patches and security for the ShakeCast host.

On the recommendation of ShakeCast developers and with instrumental help by Dr. K-W Lin of the USGS, ShakeCast 2 was implemented in an Oracle Virtual Box environment under Windows 7-64. Virtual Box is a virtual machine implementation that allows an administrator or operator to separate platform system administration issues from ShakeCast operations. Virtual machines are a relatively new technology designed to simplify computer configuration especially for “on-demand” computer services and cloud computing. Virtual Box itself runs as an application on most popular operating system (OS) platforms. Within the virtual machine application, a completely separate computer instance can be configured from the OS upward. ShakeCast developers use this technology to configure and run ShakeCast 2 as virtual machine instance running versions of Windows. The advantage of virtual machine implementations is that only one instance needs to be configured from scratch with the OS and actual ShakeCast software. That software includes Perl and PHP libraries and modules, an Apache web server, shell script executors, and a MySQL database. Once configured, the virtual machine is saved as a file that can be opened and run on other virtual machines and can be cloned as desired. This way two instances of ShakeCast are almost as easy as one to operate (e.g., a primary and backup). Normally the operator will also save the initial configuration in case an operational case crashes beyond repair. In a few minutes a fresh instance can be put in its place. The initial ShakeCast installation was actually done on a MacBook Pro portable computer, then copied to an Oracle Virtual Box host physically

running on a Mac Pro workstation running OS-X 10.6.8. Internally the ShakeCast code itself runs in a Windows 7-64 context. This implementation was used to process all scenarios and develop database results reported in this project.

Implementation of notifications proved to be difficult. ShakeCast 2 is limited to simple email (unencrypted SMTP) transfers, while UNR campus email requires secure socket layer (SSL) protocols. Attempts to update ShakeCast to work over SSL were unsuccessful. In addition, ShakeCast hard-coded the SMTP port in the implementing PHP code. Eventually a successful combination was discovered involving a temporary email capability using a non-UNR email host. These efforts have clarified what would be required for operational implementation for NDOT and why ShakeCast 3 is a preferred solution. Problems uploading some scenarios were also found. After some investigation, the problem was isolated a field overflow condition in the scenario name length database field.

Initial VirtualBox instance with the Windows 7-64 system developed problems with disk space over time as well. The initial disk partition of 25 Gb was overrun by a growing cache (19 Gb) of operating system files apparently added during updates and perhaps as internal save points. As a result, there was not sufficient space to add the new scenarios. After exploring some options, a partition of 80 Gb provided enough space for scenarios, real-time operations, the code base and Windows 7. Code runs slowly in the VirtualBox environment, but the VirtualBox implementation itself has been robust and trouble-free.

2.3.3.2 ShakeCast Version 3

ShakeCast 3 uses a similar virtual machine technology, but has been designed to run as a “cloud-based” service. In terms of calculations performed and results developed, ShakeCast 2 and ShakeCast 3 are identical. The two differ primarily in the user interface and the host operating environment. Cloud-based implementation of ShakeCast V3 means that it runs as a virtual machine, but on a remote host over which the user has administrative control but never any physical contact. ShakeCast V3 as distributed by the ShakeCast development group uses a CentOS Linux operating system over which all the ShakeCast V3 software is installed and ready to configure and use. CentOS Linux is more secure than Windows and better suited for dedicated applications such as ShakeCast.

The hosting platform for ShakeCast V3 is maintained by Amazon Web Services (AWS) at a facility in northern Virginia. Cloud hosting is an advantageous solution for many organizations because the physical hardware is watched by a third party, and can be maintained in a high-availability, intrinsically reliable installation. Access for starting or stopping an instance, editing security settings, and reviewing performance is web-based, so the only required local software at UNR or NDOT is a browser (**Figure 2.4**). The figure shows a page, refers to instance “shakecast2”, and the image was taken when the instance was stopped. The virtual machine is assigned a publicly routed IP address when it is set up, in this case 52.4.53.109.. Various notifications and alarms can be set to alert on status changes. Security and communication settings can be adjusted through the configuration interface. Secure shell methods can be used if necessary for additional administrative access. The current Nevada ShakeCast virtual machine environment was originally installed on an Amazon Web Services promotional account, but maintenance now involves a small monthly fee.

2.3.3.2.1 ShakeCast 3 Configuration

Configuration of ShakeCast 3 is done primarily through the ShakeCast 3 web interface. The primary configuration tasks include setting users and notifications, and inputting the NBI. The current instance of ShakeCast for Nevada may be accessed at <https://ec2-54-172-233-96.compute-1.amazonaws.com>. This number could change. Distribution of the NDOT ShakeCast system URL should be managed; unrestricted public use of it following an earthquake could make the server inaccessible to NDOT users.

Users consist of two types: administrators and ShakeCast report clients. Report users receive notifications when a new ShakeMap is detected, and Inspection Priority Reports when ground shaking levels meet criteria set for the report. Administrative users have control over the ShakeCast instance, including to add or change users, facilities, or notifications. Administrative users can also receive daily “heartbeat” messages that signal the system is alive and on duty. Levels of reporting are distinguished by Group membership. For example, a group for management level might only get notifications when bridge damage is considered likely. Others may wish to see reports whenever bridges are evaluated.

The NBI and capacity level estimates must be uploaded in XML format. An example bridge detail page is shown in **Figure 2.5**. Bridge capacity is expressed as the SA(1) range for Green (Low), Yellow (Moderate), Orange (Extensive), or Red (Complete) damage state conditions, as applied in conversion script *nbi2sc.pl*. Damage levels are assigned by NBI Class (discussed in section 3.3.1 below). A damage level example from the ShakeCast web interface for Bridge I1291 in northwest Nevada is shown in **Figure 2.6**. Values under the “Low Limit” and “High Limit” are in percent g for SA(1). SA(1) levels of 1% will generally be felt and reported by the public but not be associated with damage. Users may elect the Damage Level at which to include a bridge in automatic reporting. Limits for 32_I1291 were developed under this project for continuous steel girder construction bridges of HAZUS type HWB15. Custom capacity levels identified under this project for some bridge types were applied by hand to the XML file before uploading (more details are included in Chapter 3). The most convenient method for obtaining the initial XML version is to use a current Windows-based Excel program with capability to output in XML format. The information used for this report were obtained from Dr. K. Lin of the USGS ShakeCast team. For minor updates such as correcting a bridge location, a text editor is more convenient. As part of the upload process, new records are matched to old ones in the ShakeCast database. New records that match one already in the system become replacements for what was there. The 2012 bridge inventory is the latest for which the NBI was available to us in a usable format. Currently 1885 bridges are included. An attempt to use the 2013 inventory had to be abandoned when a formatting error in the input NBI was discovered that rendered it unusable.

2.3.3.2.2 ShakeCast 3 Displays

Scenarios are managed on a tab of the Processed Earthquakes page, **Figure 2.7**. The colored image is from a M6.9 dip-slip earthquake on the Mount Rose fault. The rupture extends from downtown Reno south through Washoe Valley. The epicenter is shown with a red star, and listed in the blue metadata bar at the bottom of the image. Ground motions are amplified in valley bottoms. This variation is produced by the site-condition layer in ShakeMap. At the bottom of the relief map are numbers in gray, green, yellow, orange, and red rectangles. These are the number of bridges affected at these respective damage states. Below is the delivery status and

groups receiving some level of notification that this scenario event has been processed. The effect of the site condition layer is seen in map view by higher shaking levels in valleys. A total of 364 bridges would be shaken at $SA(1) \geq 0.1$ g (green or higher). **Figure 2.8** shows at overview scale the bridges affected by the Mount Rose scenario earthquake with larger circles summarize the indicated number of individual bridges; the summary is used to reduce mapping clutter. Summary colors are keyed to the highest color among summarized bridges. The top few individual Red level bridges are listed on the left side. The map interface permits zooming in to the individual bridge level (see **Figure 2.9**). **Figure 2.9** shows a more detailed view from just south of I-80 in Reno with many individual bridges.

The top portion of the Facility Inspection Priority Report is shown in **Figures 2.10 and 2.11**. Only the top five facilities are shown in this excerpt, but a total of 364 facilities were evaluated. Earthquake event time and report generation time are listed in the upper text block. A total of 23 bridges were considered likely, given this scenario, to have damage (Orange and Red damage states), and damage was considered possible for 24 others (damage state Yellow).

The scenario earthquake magnitude, location, and time are listed at the top. The Damage Summary lists the total number of bridges exposed to 0.1 g or greater accelerations, the number of red and orange level (Likely Damage) and yellow state bridges. Below are the top few of 364 lines in the report listing potentially damaged bridges by name and exposure.

Figure 2.12 shows an actual ShakeMap, in this case for an M3.3 earthquake in northwest Nevada near the Sheldon Wildlife Preserve. The circular intensity pattern is typical of point source ShakeMaps. The geotechnical layer adjustments to ground motion are visible mainly as deamplifications (bleached regions) in areas of steepest slopes. Bridges in northern Nevada are shown along I-80 and distributed on highways north, as grey circles. The color reflects accelerations smaller than 10% g.

Table 2.1 List of Scenarios, with fault lengths, time since the most recent event (tMRE), and slip rate bounds. Fault slip rate data and time since the most recent event from the USGS Quaternary Fault and Fold database (<http://earthquake.usgs.gov/hazards/qfaults/>).

Scenario Name**	Length (km)	tMRE more recent than:	Slip Rate Lower Limit (mm/yr)(*1)	Slip Rate Upper Limit (mm/yr)
Antelope_Kingsley_M7.2_se	65	130000	0	0.2
Antelope_Valley_M7.0_se	12	15000	0.2	1
Bare_Mountain_fault_M6.6_se	18	130000	0	0.2
Battle_Mountain_fault_M6.7_se	26	130000	0	0.2
Beowawe_fault_M7.0_se	44	750000	0	0.2
Black_Hills_fault_corrected_M6.2_se	9	15000	0	0.2
Black_Rock_fault_zone_M7.3_se	69	15000	0	0.2
Bloody_Run_Hills_fault_M6.7_se	26	750000	0	0.2
Bonham_Ranch_fault_zone_M7.1_se	54	15000	0.2	1
Buena_Vista_Valley_fault_zone_M7.4_se	76	130000	0	0.2
Buffalo_Creek_fault_zone_M6.8_se	27	130000	0	0.2
Buffalo_Mountain_fault_M6.5_se	18	130000	0	0.2
Buffalo_Valley_fault_zone_M7.0_se	38	15000	0	0.2
Butte_Mountains_fault_zone_M7.2_se	73	1600000	0	0.2
California_Wash_fault_M6.9_se	32	15000	0.2	1
Carico_Lake_Valley_fault_zone_M7.0_se	42	15000	0	0.2
Carson_City_fault_M6.5_se	16	15000	0	0.2
Carson_Range_fault_M7.1_se (*2)	16	15000	0.2	1
Carson_Range-Kings_Canyon_faults_M7.2_se	16	15000	0.2	1
Clan_Alpine_fault_zone_M6.9_se	33	130000	0	0.2
Cortez_Mountain_fault_zone_M7.2_se	33	15000	0	0.2
Coyote_Spring_fault_M6.5_se	15	130000	0	0.2
Crescent_Dunes_fault_M7.0_se	50	130000	0	0.2
Desatoya_Mountains_fault_zone_M7.0_se	45	130000	0	0.2
Diamond_Mountains_fault_M7.3_se	80	130000	0	0.2
Diamond_Valley_fault_M6.7_se	27	1600000	0	0.2
Dixie_Valley_fault_zone_M7.0_se	57	60	0.2	1
Dry_Lake_fault_M7.0_se	58	130000	0	0.2
Dry_Valley-Smoke_Creek_Ranch_fault_zone_M7.0_se *5	50	1600000	0	0.2
Duck_Flat_fault_M6.5_se	16	1600000	0	0.2
Dunn_Glenn_fault_M6.5_se	18	130000	0	0.2

Scenario Name**	Length (km)	tMRE more recent than:	Slip Rate Lower Limit (mm/yr)(*1)	Slip Rate Upper Limit (mm/yr)
Eastern_Bilk_Creek_Mountains_fault_zone_M6.8_se	41	15000	0	0.2
Eastern_Edwards_Creek_Valley_fault_zone_M6.9_se	35	130000	0	0.2
Eastern_Granite_Range_fault_M6.8_se	32	1600000	0	0.2
Eastern_Independence_Valley_fault_zone_M7.0_se	42	130000	0	0.2
Eastern_Monitor_Range_fault_zone_M7.4_se	106	130000	0	0.2
Eastern_Osgood_Mountains_fault_zone_M6.8_se	37	1600000	0	0.2
Eastern_Osgood_Mountains_piedmont_fault_M6.8_se	29	130000	0	0.2
Eastern_Pine_Forest_Range_fault_zone_M6.2_se	28	130000	0	0.2
Eastern_Pyramid_Lake_fault_M7.0_se	42	130000	0	0.2
Eastern_Tuscarora_Mountains_fault_zone_M7.1_se	52	1600000	0	0.2
Edna_Mountain_fault_M6.9_se	33	130000	0	0.2
Eglinton_fault_M6.3_se	11	130000	0	0.2
Emigrant_Peak_fault_zone_M6.8_se	36	15000	0.2	1
Eugene_Mountains_fault_M6.2_se	10	15000	0	0.2
Fairview_fault_zone_M7.2_se	31	60	0	0.2
Fox_Range_fault_zone_M6.9_se	31	15000	0	0.2
Freds_Mountain_fault_M6.8_se	28	130000	0	0.2
Frenchman_Mountain_fault_M6.6_se	18	130000	0	0.2
Golden_Gate_fault_M6.9_se	30	15000	0	0.2
Granite_Springs_Valley_fault_zone_M7.0_se	50	15000	0.2	1
Grass_Valley_fault_zone_M7.1_se	53	15000	0	0.2
Hiko_fault_zone_M6.5_se	15	130000	0	0.2
Hoppin_Peaks_fault_zone_M7.4_se	99	750000	0	0.2
Hot_Springs_fault_zone_M6.7_se	25	60	0	0.2
Independence_Valley_fault_zone_M7.2_se	66	130000	0	0.2
Indian_Hills_fault_M6.1_se	15	15000	0	0.2
Ione_Valley_fault_M7.3_se	76	130000	0	0.2
Jackson_Mountains_fault_zone_M7.2_se	67	1600000	0	0.2
Jakes_Valley_fault_zone_M6.9_se	34	130000	0	0.2
Jersey_Valley_fault_zone_M6.9_se	33	130000	0	0.2
Kawich-Hot_Creek_Ranges_fault_zone_M7.5_se	110	130000	0.2	1
Kings_Canyon_fault_zone_M6.5_se	16	15000	0.2	1
Little_Fish_Lake_Valley_fault_M7.0_se	42	1600000	0	0.2
Little_Valley_fault_M6.5_se	17	15000	0.2	1
Lone_Mountain_fault_zone_M7.0_se	10	130000	0	0.2
Marys_Mountain_fault_M6.6_se	19	1600000	0	0.2

Scenario Name**	Length (km)	tMRE more recent than:	Slip Rate Lower Limit (mm/yr)(*1)	Slip Rate Upper Limit (mm/yr)
McGee_Mountain_fault_zone_M7.0_se	34	1600000	0	0.2
Middlegate_fault_zone_M6.9_se	37	130000	0	0.2
Montana_MountainsDesert_Valley_fault_zone_M7.4_se	65	15000	0	0.2
Mount_Irish_Range_fault_M6.3_se	11	1600000	0	0.2
Mount_Rose_fault_zone_M6.9_se	38	15000	1	5
NV3_Petersen_Mountain_fault_2_M6.5_se	25	130000	0	0.2
Nightingale_Mountains_fault_M6.9_se	35	1600000	0	0.2
Northern_Butte_Valley_fault_M6.5_se	17	130000	0	0.2
Northern_Huntington_Valley_fault_zone_M6.9_se	38	130000	0	0.2
Northern_Roberts_Mountains_fault_M6.7_se	22	750000	0	0.2
Northern_Simpson_Park_Mountains_fault_zone_M6.4_se	13	15000	0	0.2
NV4_Western_Smoke_Creek_Desert_fault_2_M6.6_se *3	20	15000	0.2	1
Paradise_Range_fault_zone_M7.0_se	38	130000	0	0.2
Peavine_Peak_fault_zone_M6.4_se	15	15000	0	0.2
Penoyer_fault_M7.1_se	49	130000	0	0.2
Petersen_Mountain_fault_M6.7_se	25	130000	0	0.2
Pleasant_Valley_fault_zone_M7.6_se	88	99	0	0.2
Railroad_Valley_fault_zone_M1.6_se	94	130000	0	0.2
Ruby_Mountains_fault_zone_M6.9_se	76	15000	0	0.2
Ruby_Mountains_fault_zone_M7.1_se *4	76	15000	0	0.2
Ruby_Valley_fault_zone_M7.3_se	78	130000	0	0.2
San_Emidio_fault_zone_M6.9_se	32	130000	0.2	1
Sand_Springs_Range_fault_M7.0_se	40	15000	0	0.2
Schell_Creek_Range_fault_system_M7.4_se	99	130000	0	0.2
Selenite_Range_fault_zone_M6.5_se	18	15000	0	0.2
Seven_Troughs_Range_fault_zone_M6.9_se	37	1600000	0	0.2
Sheep_Basin_fault_M6.7_se	38	1600000	0	0.2
Sheep_Creek_Range_southeastern_fault_M6.9_se	34	130000	0	0.2
Shoshone_Range_fault_zone_M7.5_se	118	15000	0	0.2
Simpson_Park_Mountains_fault_zone_M7.2_se	67	15000	0.2	1
Singatse_Range_fault_zone_M6.8_se	40	130000	0	0.2
Smith_Valley_fault_M7.4_se	96	15000	0.2	1
Southwest_Reese_River_Valley_fault_M7.3_se	73	130000	0	0.2
Spanish_Springs_Valley_fault_M6.6_se	13	1600000	0	0.2
Spruce_Mountain_Ridge_fault_zone_M6.8_se	31	130000	0	0.2
The_Lava_Beds_fault_M6.7_se	25	130000	0	0.2

Scenario Name**	Length (km)	tMRE more recent than:	Slip Rate Lower Limit (mm/yr)(*1)	Slip Rate Upper Limit (mm/yr)
Toiyabe_Range_fault_zone_M2.0_se	116	130000	0.2	1
Wassuk_Range_fault_zone_M7.5_se	116	15000	0.2	1
West_Gate_fault_M6.7_se	23	60	0	0.2
West_Spring_Mountains_fault_M7.1_se	48	15000	0	0.2
Western_Diamond_Mountains_fault_zone_M7.2_se	63	1600000	0	0.2
Western_Granite_Range_fault_M6.8_se	26	1600000	0.2	1
Western_Humboldt_Range_fault_zone_M7.3_se	105	15000	0	0.2
Western_Toiyabe_Range_fault_zone_M2.0_se *6	61	130000	0.2	1
White_River_Valley_fault_zone_M7.4_se	100	130000	0	0.2

Notes:

*1: 0 mm/yr is to give a number, but not to imply "inactive"

*2: Values from Carson_Range-Kings_Canyon_faults_M7.2_se

*3: length approximate, from magnitude; other parameters from Bonham Ranch Fault zone

*4 length approximate, from magnitude; other parameters from Ruby Mntn Fault zone

*5 length approximate, from magnitude; other parameters from the Dry Creek fault zone, Qfaults on-line map

*6: main section of fault zone used

Notes on column 3, geologic age bounding the most recent fault activity bounds of 15,000, 130,000, 750,000, and 1.6myr are geologic bounds (activity more recent than...) ages

Columns 4 and 5, Slip rates

Slip rate bounds are assigned based on freshness of the offset features, the ages of the deposits, and other geologic criteria

Minimum rates of 0.2 mm/yr normally means "slow slip of an unknown, but non-zero rate".

Most in the $0 < \text{rate} < 0.2 \text{ mm/yr}$ category will be much smaller than 0.2 mm/yr.

Faults with minimum rates of 0.2 mm/yr and greater are more likely to have been studied and the rate range is thus more likely to be accurate.

Table 2.2 Names, locations, physical descriptions, and damage state levels for four example bridges.

Bridge ID	Location (Long., Lat.)	Description	Damage Level - Sa(1 sec) in g		
			Moderate (Yellow)	Extensive (Orange)	Complete (Red)
G_863E -SPRR	-117.9056, 40.8902	3-span; 4; 02; 60 deg skew; 102.7 m Structure Length; 39.6 m Max Span Length; NBI Class 402; HAZUS Class HWB15; Built 1970	0.32	0.41	0.51
I1291 - US 395	-119.9964, 39.6680	2-span; 4; 02; 0 deg skew; 92 m Structure Length; 46 m Max Span Length; NBI Class 402; HAZUS Class HWB15; Built 1975	0.32	0.41	0.51
32_H_76 7W	-119.900, 39.5139	3-span; 2; 05; 11 deg skew; 36.6 m Structure Length; 21.9 m Max Span Length; NBI Class 205; HAZUS Class HWB10; Built 1966	0.18	0.27	0.36
H1412 - PECOS DR	-115.0982, 36.1667	1-span; 5; 05; 20 deg skew; 49.7 m Structure Length; 49.1 m Max Span Length; NBI Class 505; HAZUS Class HWB3; Built 1982	1.12	1.34	1.90



Figure 2.1 Southern Pacific water tank in Lovelock, Nevada, damaged by ground motions of the 1915 Pleasant Valley M7.3 earthquake. Lovelock is approximately 60 km from the nearest part of the surface rupture. (photo source: <http://www.nbmng.unr.edu/Geohazards/Earthquakes/1915centennial.html>, accessed 10/21/2015; used with permission)

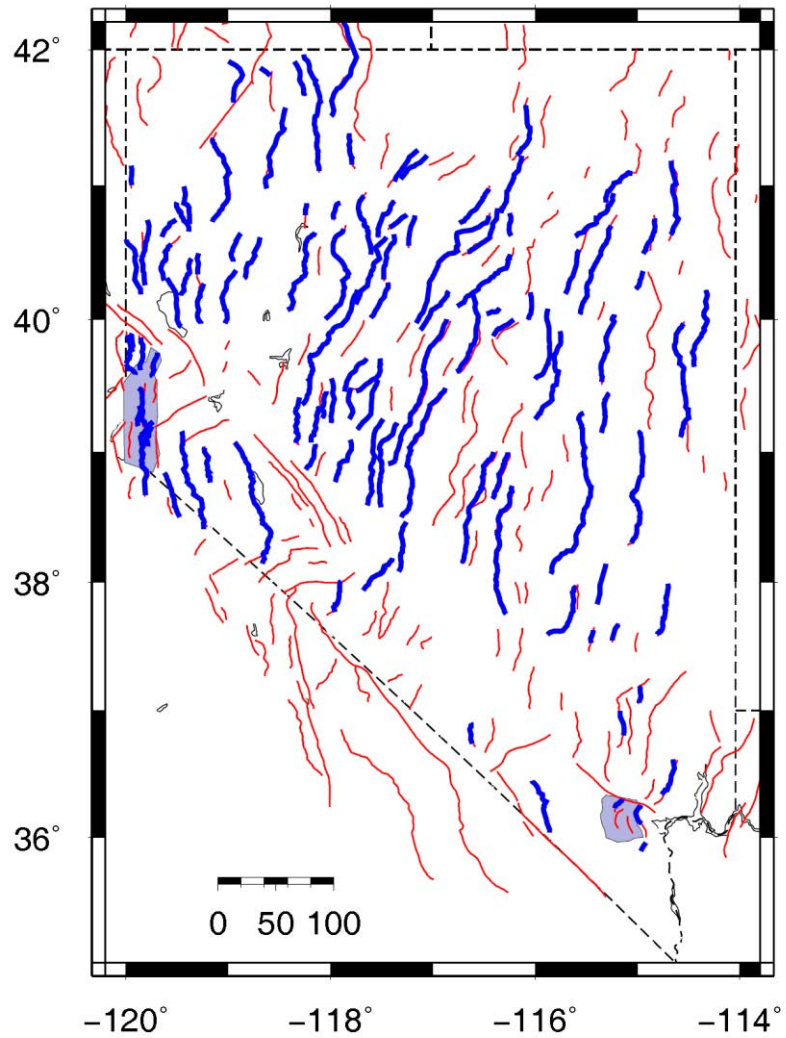


Figure 2.2 Map of ShakeMap fault scenarios used for bridge evaluation. Surface traces of fault rupture shown as heavy blue lines. Finer red lines are other known faults, generally having lower slip rates. Shaded areas of western and southern Nevada are the Reno-Carson City and the greater Las Vegas urban areas, respectively.

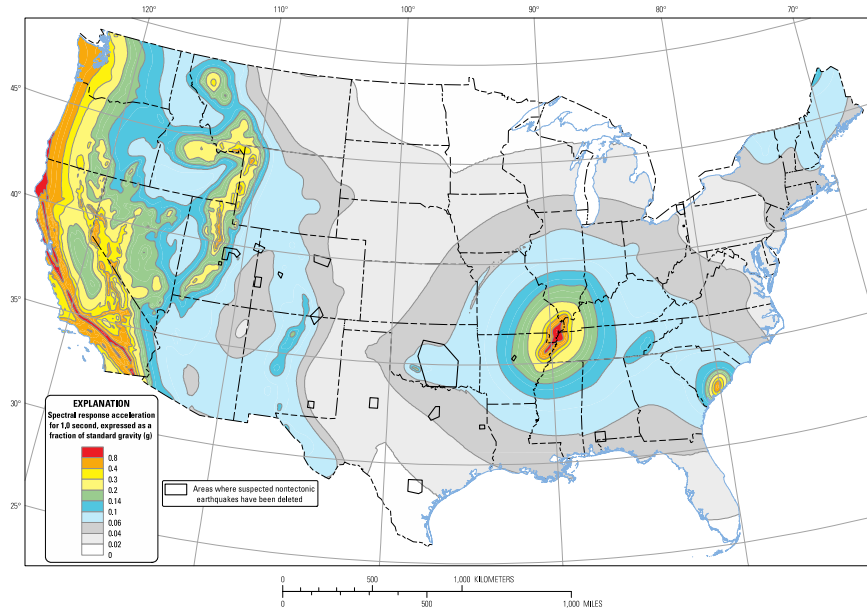


Figure 2.3 USGS National Seismic Hazard Map for spectral acceleration 1 Hz and return probability of 2% in 50 years (2475 year return time). Ground motions at 1000-year return will be lower (Peterson et al., 2014).

Description	Status Checks	Monitoring	Tags	Usage Instructions
Instance ID	running			
Instance state	running			
Instance type	t1.micro			
Private DNS	ip-172-31-52-3.ec2.internal			
Private IPs	172.31.52.3			
Secondary private IPs				
VPC ID	vpc-0983d36c			
Subnet ID	subnet-befd5795			
Network interfaces	eth0			
Source/dest. check	True			
EBS-optimized	False			
Root device type	ebs			
Root device	/dev/sda1			
Block devices	/dev/sda			
Public DNS	ec2-52-4-53-109.compute-1.amazonaws.com			
Public IP	52.4.53.109			
Elastic IP	-			
Availability zone	us-east-1d			
Security groups	FourthSCGroup. view rules			
Scheduled events	No scheduled events			
AMI ID	ShakeCast v3 - 9 (ami-58acd730)			
Platform	-			
IAM role	-			
Key pair name	rufus4th			
Owner	110820839138			
Launch time	March 31, 2015 at 3:46:39 PM UTC-7 (3697 hours)			
Termination protection	False			
Lifecycle	normal			
Monitoring	basic			
Alarm status	None			
Kernel ID	aki-b8aa75df			

Figure 2.4 Virtual machine instances are administered via a web interface at Amazon Web Services (AWS).

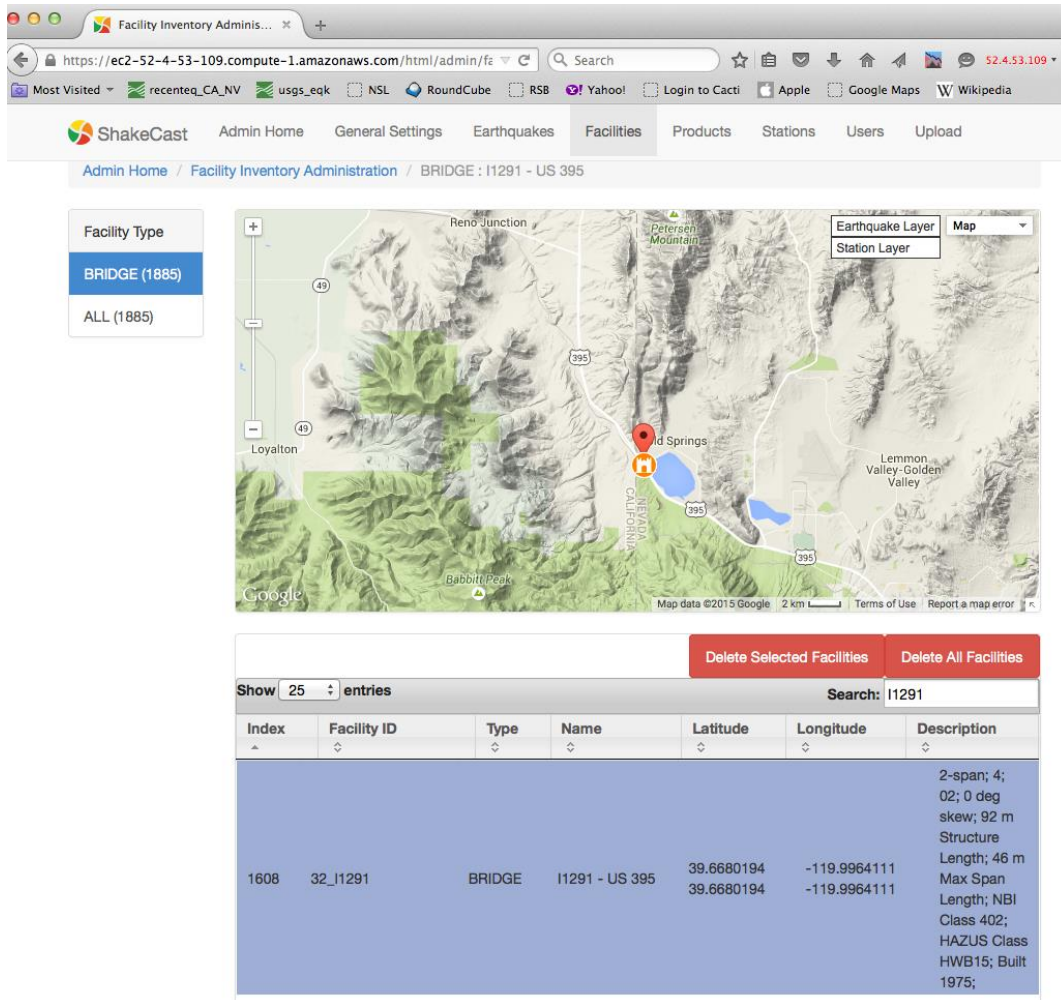


Figure 2.5 Bridges from the Nevada inventory located using a Search capability on the Facilities tab of ShakeCast 3.

BRIDGE I1291 - US 395 / ID 32_11291

Notification Fragility Fragility Probability

ID	Damage Level	Low Limit	High Limit	Metric
47875	RED	51	999999	PSA10
47874	ORANGE	41	51	PSA10
47873	YELLOW	32	41	PSA10
47872	GREEN	10	32	PSA10
47871	GREY	0.01	10	PSA10

Figure 2.6 Screen capture from the ShakeCast 3 Facilities tab for bridge 32_11291 on Highway 395 north of Reno near the California state line.

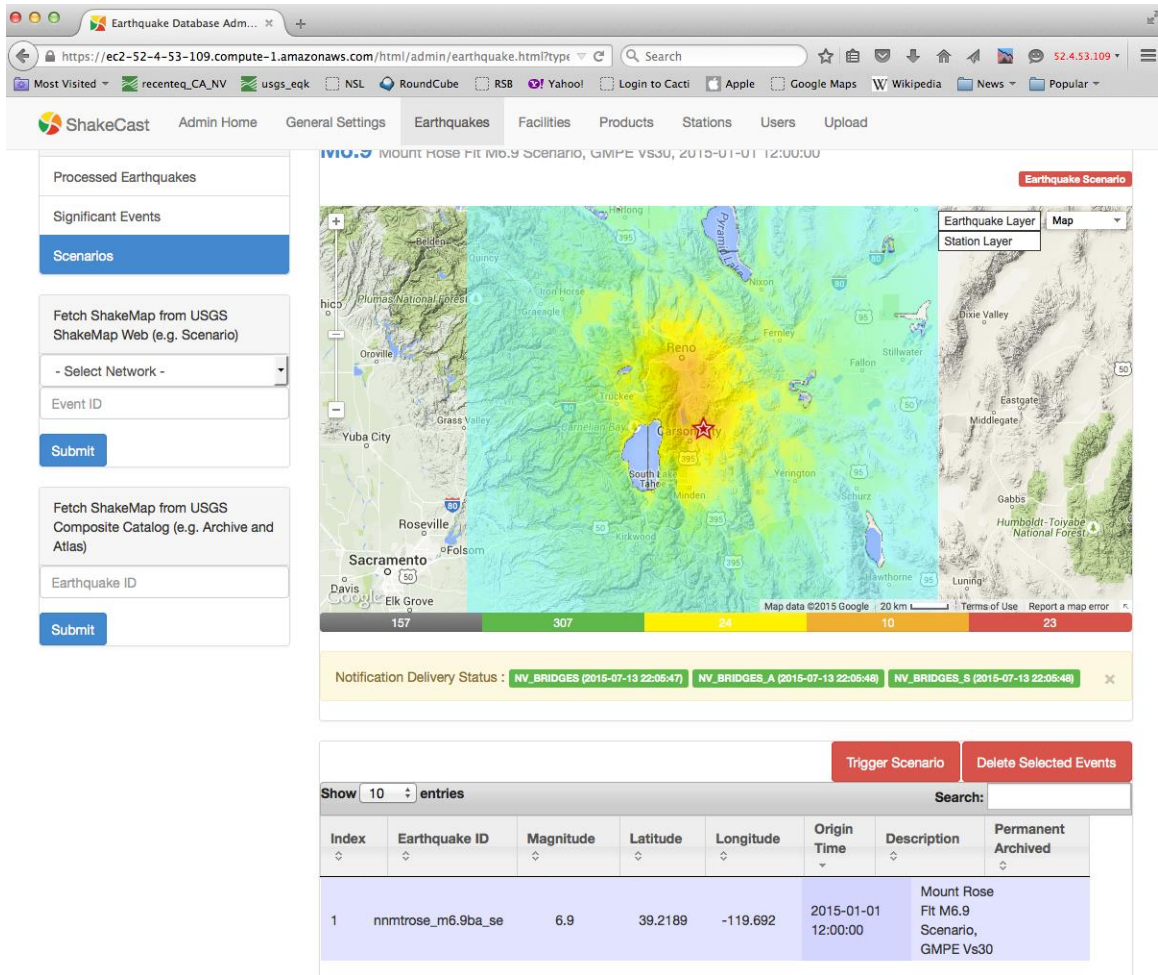


Figure 2.7 Summary level page in the ShakeCast 3 web interface for bridge assessment.

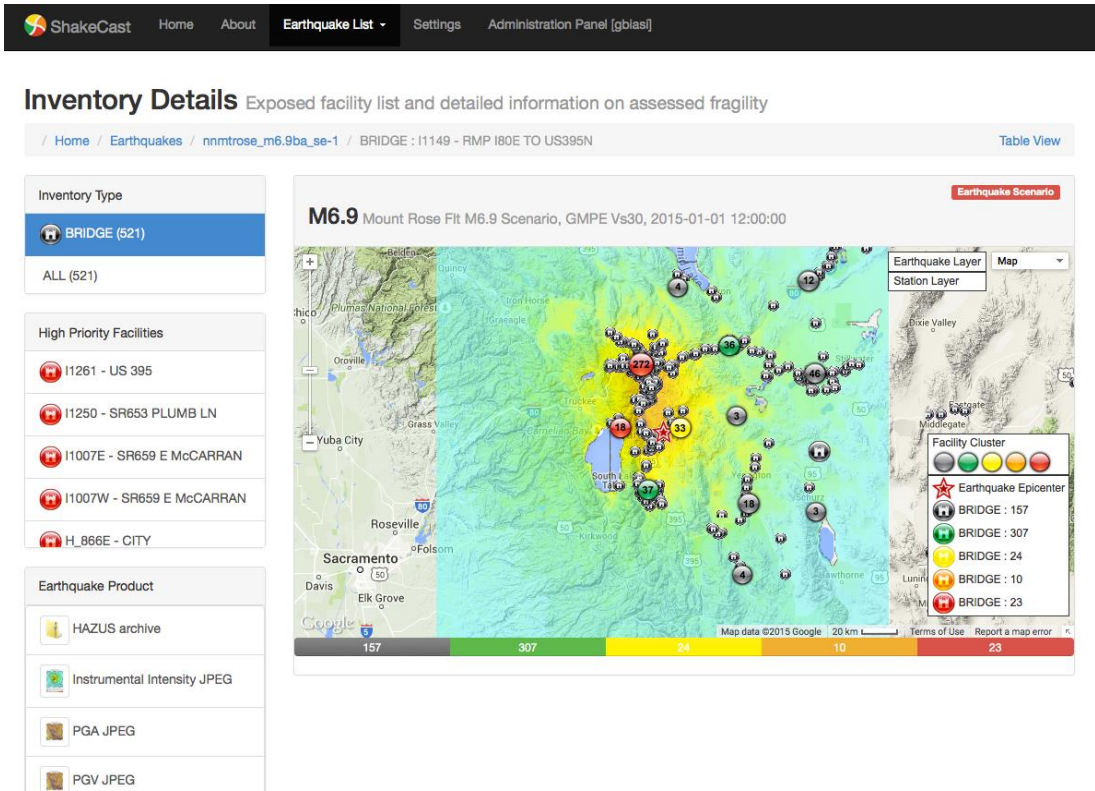


Figure 2.8 ShakeCast view showing bridges and damage states from the Mount Rose M6.9 scenario earthquake.

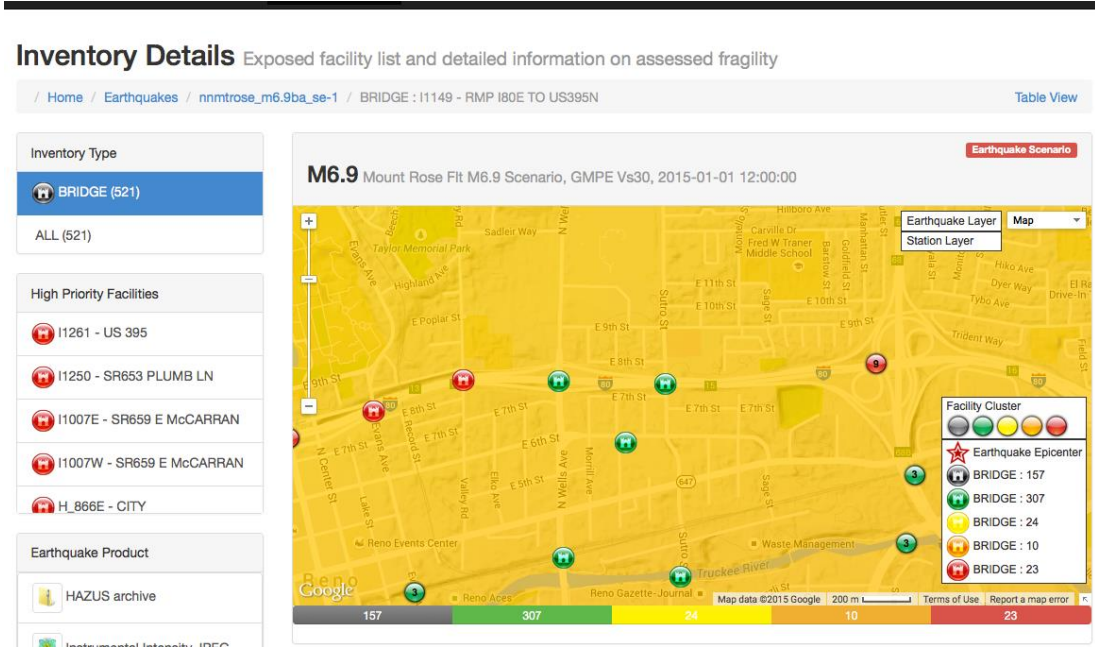


Figure 2.9 Detailed map view showing many individual bridges along and just south of I-80 in Reno.

ShakeCast Event: Magnitude 6.9

ShakeMap (Unnamed Event) Version 1
 Event Location: Mount Rose Flt M6.9 Scenario, GMPE Vs30
 Event Time: 2015-01-01 12:00:00
 Generated at 2015-07-13 20:29:35
 Reported by: Server ID = 1000, DNS = i386_Base_Image

Damage Summary

Number of Facilities Reported: 364
 Max Value: MMI: [NULL]; Acceleration: (not measured)
 Number of Reports of Likely Damage: 23
 Number of Reports of Possible Damage: 24



Facility Damage Estimates from ShakeMap

Facility	Inspection Priority	Metric	Value
I1261 - US 395	High	PSA10	58.25
I1250 - SR653 PLUMB LN	High	PSA10	46.13
I1007E - SR659 E McCARRAN	High	PSA10	41.48
I1007W - SR659 E McCARRAN	High	PSA10	41.48
H_866E - CITY STREETS(NUGGET)	High	PSA10	39.99

Figure 2.10 Facility Inspection Report generated by ShakeCast using as input a scenario M6.9 earthquake on the Mount Rose fault.

H_993 - I 80	High	PSA10	35.22
H_995 - I 80	High	PSA10	35.22
H_997 - I 80	High	PSA10	35.22
B1424 - BOYNTON SLOUGH	Moderate High	PSA10	58.64
B1425 - DRY CREEK	Moderate High	PSA10	53.24
B1300 - TRUCKEE RIVER	Moderate High	PSA10	51.35
B1534 - TRUCKEE RVR	Moderate High	PSA10	49.93
H1834 - HILTON INN ACCESS RD	Moderate High	PSA10	49.22
B1829 - DRY CRK	Moderate High	PSA10	49.08
B1801 - EVANS CREEK	Moderate High	PSA10	48.21
B1814 - EVANS CRK	Moderate High	PSA10	48.21
B1833 - DRY CREEK	Moderate High	PSA10	44.42
I1089 - SR663 ODDIE BL	Moderate High	PSA10	32.6
I1950 - SR430 S VIRGINIA ST	Moderate	PSA10	53.11
I2293N - US 50	Moderate	PSA10	52.07
I2293S - US 50	Moderate	PSA10	52.07

Figure 2.11 Excerpt from the M6.9 earthquake on the Mount Rose fault report of additional facilities likely or possibly having damage.

ShakeCast Overview Recent earthquake activities and ShakeCast summary

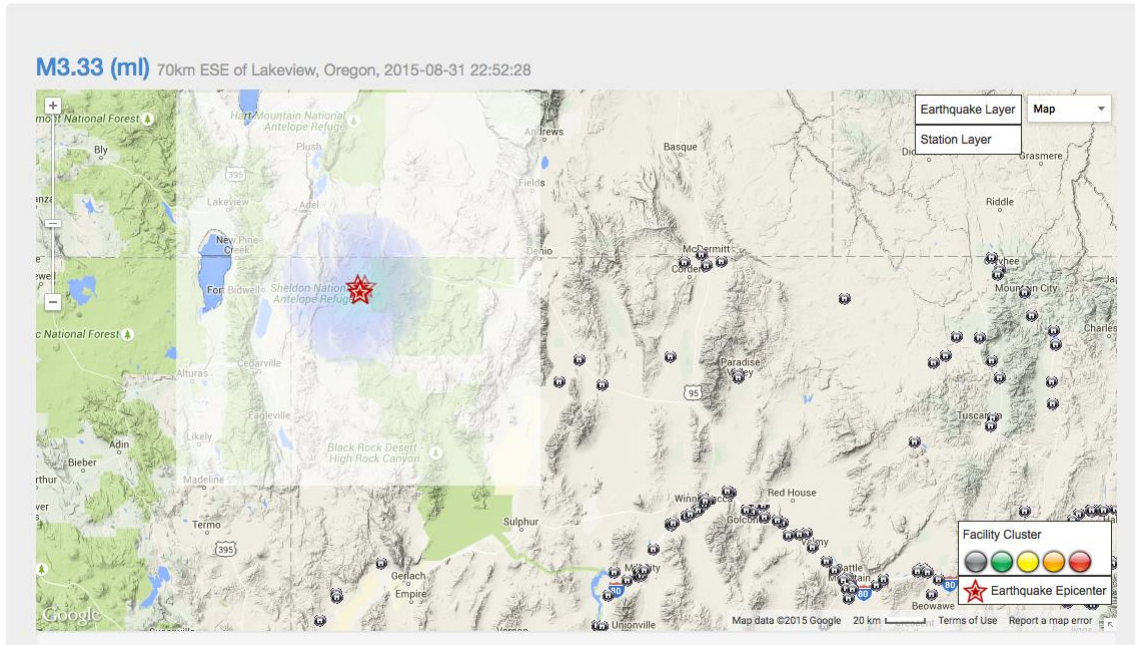


Figure 2.12 ShakeMap of a small real earthquake in northwest Nevada. Bridges are all grey because none reach the lowest green level at 0.1 g SA(1).

Chapter 3: Bridge Fragilities

3.1 Seismic Risk Assessment

The vulnerability of a bridge to earthquake event is expressed through a fragility function. These functions are used to describe the tendency of a bridge type to be damaged or fail due to specific earthquake responses. Since bridges are critical links in transportation networks, especially during and after an earthquake, many research projects have been conducted in order to describe their fragility functions. In **Figure 3.1**, Basoz and Kiremidjian, (1996) show the events that take place before and after an earthquake, which are divided into pre-disaster activities, and emergency response and post-disaster recovery activities. The figure shows that risk assessment is the first event in the pre-disaster activities. The pre-disaster phase in general includes all the work to identify the vulnerability of the existing bridges and plan their preparedness to the event in order to assure their survival during the disaster with limited damage. The pre-disaster planning will enhance the post-disaster response. Due to the high number of structures involved, the post-disaster response requires information that enables the engineer to make decisions concerning the priorities of inspection; this is where ShakeMap and ShakeCast can be used. Training inspectors in advance to assess the level of damage and understand standardized repair procedure would improve post-disaster response. Appendix D summarizes bridge damage assessment and repair procedures.

Figure 3.2 shows the basic steps in a seismic risk assessment which are:

- Hazard analysis or description of the ground shaking.
- Inventory Classification according to their vulnerability to damage.
- Fragility and sensitivity of the structures to damage from the shaking intensity.
- Loss estimation of direct and indirect losses.

3.2 Fragility Functions

A common nontechnical definition of fragility is “the quality of being easily broken or damaged.” The concept of a fragility function in earthquake engineering dates at least to Kennedy et al. (1980), who defined a fragility function as a probabilistic relationship between frequency of failure of a component of a nuclear power plant and peak ground acceleration in an earthquake. More broadly, one can define a fragility function as a mathematical function that expresses the probability that some undesirable event occurs (typically that an asset—a facility or a component reaches or exceeds some clearly defined limit state) as a function of some measure of environmental excitation (typically a measure of acceleration, deformation, or force in an earthquake, hurricane, or other extreme loading condition; Keith, 2015).

In structural engineering term, fragility functions express the probability of a structure exceeding a specific damage state for a given ground motion parameter. They represent the cumulative distribution function of the capacity of an asset to resist an undesirable limit state. Capacity is measured in terms of the degree of environment excitation at which the asset exceeds the undesirable limit state. For example, a fragility function could express the uncertain level of shaking that a building can tolerate before it collapses. The chance that it collapses at a given level

of shaking is the same as the probability that its strength is less than that level of shaking. This could be expressed in mathematical form as shown in Equation 3.1 (Keith, 2015):

$$P(DS/IM) = y \quad (3.1)$$

Where; DS is the damage level of the bridge or the bridge component and IM is the measure of the ground motion intensity [PGA, S_a (1 sec.), ...]. A graphical representation of this function is shown in **Figure 3.3**, which, typically take the form of a log-normal distribution where the vertical axis represents the probability of reaching a damage state and the horizontal axis represents ground motion intensity measure. Fragility functions or curves are classified into three main groups, which are:

- Fragility functions based on expert opinions.
- Empirical fragility functions.
- Analytical fragility functions.

3.2.1 Fragility Functions Based on Expert Opinion

The ATC-13 Report, Earthquake Damage Evaluation Data for California (ATC, 1985) was the first step in performing seismic risk assessment of infrastructure for California. This assessment was based on the opinion of 42 experts, they developed damage probability matrices for bridge infrastructure which were formed based on Modified Mercalli Intensity (MMI). A high level of uncertainty is present in this study as it is dependent on experience and on the number of experts participated in it.

3.2.2 Empirical Fragility Functions

Empirical fragility curves are generated from actual damage data observed in earthquakes. Many researchers developed empirical fragility curves after the 1989 Loma Prieta and 1994 Northridge earthquakes (Basoz and Kiremidjian, 1997, Der Kiureghian, 2002, Shinozuka et al. 2003, and Elnashai et al. 2004). The damage matrix for all the highway concrete bridges in Los Angeles area after the 1994 Northridge earthquake, from the work of Basoz and Kiremidjian (1997), is reported in **Table 3.1**. **Figure 3.4** shows an example of empirical fragility curves (Basoz and Kiremidjian, 1997). Yamazaki et al. (1999) and Shinozuka et al. (2000) developed empirical fragility curves for the 1995 Kobe earthquake. The number of bridges related to each level of damage at different PGA values for highway bridges after Kobe earthquake is shown in **Table 3.2** (Yamazaki et al. 1999).

3.2.3 Analytical Fragility Functions

Development of fragility curves using analytical methods has been highlighted due to the lack of sufficient earthquake damage data, and because of the improvements in modeling efficiency. The researchers used different methods to generate analytical fragility curves; some of these methods are introduced in the following sections.

3.2.3.1 Elastic Response Spectrum Analysis

One of the simplest methods to generate seismic fragility curves is by looking at the elastic response of a bridge. Yu et al. (1991) developed fragility curves for highway bridges in Kentucky; they used single degree of freedom models for the bridge piers and got their response using an elastic response spectrum. Hwang et al. (2000) improved this method by including uncertainties in the demands and the capacities.

3.2.3.2 Demand-Capacity Spectrum Method

The demand-capacity spectrum method is also called nonlinear static analysis. It is a simplified method to consider the nonlinear response of the bridge without performing a full nonlinear time history analysis. Dutta (1999), Basoz and Mander (1999) and Jeong and Elnashai (2007) used this method to develop fragility curves for highway bridges in the United States. The fragility curves that were proposed by Mander and Basoz (1999) were used in HAZUS-MH and then implemented in the ShakeCast. This approach is shown in **Figure 3.5** where the capacity is determined by performing nonlinear static pushover analysis of the structure, while the demand is determined using a scaled down response spectrum for a ground motion. The intersection of the two curves, the pushover and the response spectrum, is the expected level of performance. The pushover is converted from force-displacement to acceleration-displacement by dividing the force by the mass when plotted with the demand curve.

3.2.3.3 Nonlinear Time History Analysis (NLTHA)

Many researchers (Kim and Shinozuka, 2004; Mackie and Stojadinovic, 2004; Nielson, 2005; Ramanathan et al., 2010) have developed fragility curves using nonlinear time history analysis approach. This method is more reliable, although it is computationally expensive. In this approach, a group of ground motions representing the seismicity of a specific region is assembled. 3D analytical bridge models are created after the structural properties are probabilistically sampled. A nonlinear time history analysis for each ground motion-bridge sample is performed and the peak responses are recorded to build Probabilistic Seismic Demand Models (PSDM's). The PSDM's and the capacity models are then used to develop the fragility curves (see **Figure 3.6**).

3.2.3.4 Incremental Dynamic Analysis

Incremental dynamic analysis is a scaling type technique of nonlinear dynamic analysis. A series of nonlinear time history analysis for ground motions that are scaled incrementally is used until collapse. This method was established by the FEMA guidelines in 2000 to determine the global capacity. **Figure 3.7** shows the incremental dynamic analysis procedure to develop PSDM's. A drawback of this technique is that the ground motions might be unrealistic because of the scaling which might not be representative of the seismic hazard at bridge location.

3.3 ShakeCast Fragility Functions

The ShakeCast uses the HAZUS-MH fragility functions, which are based upon work originally done by Basoz and Mander in 1999. As previously mentioned, fragility curves typically

take the form of a log-normal distribution and are plotted with the ground motion intensity parameter on the horizontal axis and the probability of reaching a damage state on the vertical axis. The HAZUS fragility curves use the 1 sec peak spectral acceleration as the ground motion intensity parameter. Multiple curves are used to define the different damage states of a bridge as shown in the example in **Figure 3.8**. The definition of different damage states is shown in **Table 3.3**. In ShakeCast, the HAZUS fragility curves are simplified in order to assign a specific damage state to each bridge based on the ground motion intensity parameter. ShakeCast stores only the parameter corresponding to the 50% probability of exceeding a limit state as shown in **Figure 3.8**.

3.3.1 Bridge Classification Based on National Bridge Inventory (NBI) and HAZUS

The National Bridge Inventory (NBI, 2010) is a database for bridges in the United States. **Tables 3.4** and **3.5** summarize the key NBI characteristics used. HAZUS provides further classification scheme for highway bridges based on seismic design, number of spans and span continuity coupled with the material and type of construction from the NBI. A total of 28 classes (HWB1-HWB28) are defined as shown in **Table 3.6**.

3.3.2 Bridge fragilities in HAZUS

HAZUS fragility functions are described in more detail in Basoz and Mander (1999). **Table 3.7** shows the median (the 50% probability of exceeding a damage state) of these damage functions which are stored in ShakeCast.

3.3.3 Main steps for damage algorithm for bridges

This section presents the main steps for damage algorithms for different bridge types.

Step 1:

- Bridge location (longitude and latitude).
- Bridge class (HWB1 through HWB28)
- Number of spans (N)
- Skew angle (α)
- Bridge length (L)
- Maximum span length (L_{\max})

Step 2:

- Evaluate the demands at the bridge site (PGA and spectral accelerations) either from the ShakeMap (real ground motion) or using attenuation relationships (Scenarios).

Step 3:

- Calculate the following modification factors:
 - $K_{\text{skew}} = \sqrt{\sin(90 - \alpha)}$ (3.2)
where K_{skew} is a factor taking into account the effect of the skew angle.
 - $K_{3D} = 1 + A / (N - B)$ where A and B are as indicated in Table 3.6

Step 4:

- Modify the medians for the fragility functions in **Table 3.8** as follows (Capacity):
New median = Old median (K_{skew} , K_{3D})

Step 5:

- Compare the demand (Spectral acceleration at 1 sec.) with the capacity (New median) to determine the damage state for the bridge.

3.4 ShakeCast for Nevada Bridges

3.4.1. Limitations in the HAZUS fragility curves

There are limitations to the HAZUS fragility curves, which are:

- Simplified two-dimensional analyses is used (Demand-Capacity Spectrum Method).
- Limited uncertainty.
- The fragility curves were developed assuming that the vulnerability of the bridge is represented only by the vulnerability of the columns. **Table 3.9** shows the drift limits that were used for the different damage states.

Continuous bridges in most of the recent fragility studies are found to be more vulnerable than that predicted by the HAZUS. Ramanathan (2012) developed fragility curves for different classes of bridges in California (see **Tables 3.10** and **Table 3.11**) where:

- MSCC-BG-S: Multispan Continuous Concrete Box Girder - Single Column Bent.
- MSCC-BG-M: Multispan Continuous Concrete Box Girder - Multi Column Bent.
- BSST-0: Slight Damage State.
- BSST-1: Moderate Damage State.
- BSST-2: Extensive Damage State.
- BSST-3: Complete Damage State.
- E1: Pre 1971 Design Era.
- E2: 1971-1990 Design Era.
- E3: Post 1990 Design Era.
- S0: Diaphragm Abutment.
- S1: Seat length (4-12 in.).
- S2: Seat length (12-18 in.).
- S3: Seat length (18-24 in.).
- S4: Seat length (>24 in.).
- λ : Median.
- ζ : Dispersion.
- ζ^* : Average Dispersion.

Nielson (2005) developed seismic fragility curves for nine bridge classes in the central and southeastern United States using nonlinear time history analyses (**Table 3.12**). AmiriHormozaki (2013) developed fragility curves for seismically and non-seismically designed horizontally curved steel bridges in the United States (**Figures 3.9** and **3.10**).

3.4.2 Nevada bridge inventory

Table 3.13 shows bridge classes that represent about 67% of the total number of bridges in Nevada. The remaining bridges are distributed over a wide variety of bridge types for which

fragility functions are limited. Based on bridge plans from the Nevada Department of Transportation (NDOT), the seismic design started in 1983 not 1990 as given in HAZUS.

3.4.3. Modifications in ShakeCast fragility functions

As previously mentioned, there are considerable differences between the HAZUS fragility curves and those in the recent studies especially for continuous bridges (e.g. Nielson 2005, Ramanathan 2012, and AmiriHormozaki 2013). Fragility curves implemented by HAZUS are considerably simplified compared to a complete engineering evaluation of a structure. For bridges, HAZUS fragilities are based on a simplified two-dimensional analyses (demand-capacity spectrum method). Uncertainties from the analyses are limited, and assume that the vulnerability of the bridge is represented by the vulnerability of the columns (Basoz and Mander, 1999). Limit states were based on column drift limits for various damage states (see **Table 3.9**), resulting in relative large apparent bridge capacities.

Several researchers have sought to develop new fragility curves for bridges that overcome HAZUS fragility curve limitations (e.g. Nielson, 2005; Ramanathan et al., 2010; Ramanathan, 2012; and AmiriHormozaki, 2013). A major difference in approach is how the column limit states are determined, replacing the fixed drift limits in HAZUS with a curvature ductility approach. Curvature ductility is recognized as a more reliable index since it is a function only of section properties (Hwang et al., 2000; Saxena, 2000; and Kim, 2002). Recent research is also using more reliable techniques such as Nonlinear Time History Analysis and Incremental Dynamic Analysis to develop curves. Newer studies (Elnashai et al., 2004; Nielson, 2005; Ramanathan et al., 2010; Ramanathan, 2012; and AmiriHormozaki, 2013) have also expanded the vulnerability estimates to include other critical components than just the columns. For example, these studies found that seals, abutment seats, and columns in continuous concrete box girder and continuous prestressed concrete box girder bridges are prone to damage under strong ground motions.

New research suggested significant differences for continuous bridges from HAZUS fragility curves. At the same time, no defining research recommendations have yet been published with which to revise HAZUS fragility functions. Therefore, a need existed for revised values that could be used for Nevada bridge evaluation and ShakeCast application.

Revised values were proposed in consultation with NDOT engineers using a combination of literature review (Hwang et al., 2000; Saxena, 2000; and Kim, 2002; Elnashai et al., 2004; Nielson, 2005; Ramanathan et al., 2010; Ramanathan, 2012; and AmiriHormozaki, 2013), Nevada bridge plans, and Nevada bridge design spectra. The resulting new “50% probability of exceedance limit states” implemented for Nevada bridges are shown in **Table 3.14**. The need for revision was based on two primary points. First, HAZUS (remarkably) uses the same SA(1) capacities for both seismically and non-seismically designed continuous box girder bridges. Nevada adopted seismic design standards in 1983. A single criteria would not provide the granularity needed to evaluate pre- and post-seismic design cases. Second, the SA(1) capacity values from HAZUS were too high to be considered credible for some main types of Nevada bridges. **Figures 3.11** show the 1000-year return period design response spectra (AASHTO) for a high seismic zone city, Reno (site class D), and a medium seismic zone city, Las Vegas (site class D). The comparison between HAZUS values, proposed values, and the design response spectra is also shown. The SA(1) for the extensive damage state is used in the comparison as it corresponds to the 1000-year return period damage description stated by the AASHTO. The 1000-year return period corresponds with the

AASHTO design return period of seven percent probability of exceedance in 75 years, with acceptable damage consisting of inelastic hinges in the columns. The HAZUS SA(1) for seismically and non-seismically designed continuous box girder bridges (1.10g) are higher by about 70% than the SA(1) design value for Reno (high seismic zone), and by about 300% of the SA(1) design value for Las Vegas (medium seismic zone). The HAZUS capacities conspicuously overstate design capacities for continuous type bridges, and correspond to return times on the order of 45,500 and 280,000 years for the Reno (high hazard) and Las Vegas Valley (low hazard) cases, respectively.

From this synthesis, SA(1) for seismically designed continuous box girder bridges are almost the same as the SA(1) design value for Reno (**Figure 3.11a**), and the proposed SA(1) for non-seismically designed box girder bridges is almost the same as the SA(1) design value for Las Vegas (**Figure 3.11b**). Capacities for the non-seismically designed bridges are around half of those of the seismically designed bridges, resulting in more credible screening and ShakeCast evaluation comparisons. Proposed complete damage state SA(1) for non-seismically and seismically designed bridges, 0.36g, and 0.87g, for Reno give more realistic return times of 700 and 6,250 years respectively. Return times for non-seismically and seismically designed bridges for Las Vegas are 5,000 and 48,000 years respectively. Lower capacity values have been proposed (e.g., Ramanathan, 2012) for non-seismically designed continuous concrete box girder bridges, but these have not been accepted for operational use (DesRoches et al., 2012), and were not adopted in this study.

We reiterate that the above revised continuous bridge capacities values are being used for evaluation purposes only, and not recommended for new design. Values are approximations based on available studies, consultation with Nevada design practice and consideration of AASHTO design response spectra. Better fragility estimates can be expected in the future, but for the meantime, the proposed values provide a more realistic screening criteria than the original HAZUS fragilities. **Table 3.14** presents the fragility function median values that are used for the bridge classes that constitute the majority of Nevada bridge types.

Table 3.1 Damage matrix for highway concrete bridges in Los Angeles area (Basoz and Kiremidjian, 1997)

Observed Damage	Peak Ground Acceleration (g)										Total
	0.15-0.2	0.2-0.3	0.3-0.4	0.4-0.5	0.5-0.6	0.6-0.7	0.7-0.8	0.8-0.9	0.9-1.0	>1.0	
None	318	502	234	50	34	29	24	29	16	16	1252
Minor	2	10	25	2	6	4	6	1	7	3	66
Moderate	1	15	13	11	10	9	5	4	9	4	81
Major	0	10	2	6	7	3	2	5	11	1	47
Collapse	0	0	1	0	0	0	0	2	2	1	6

Table 3.2 Damage matrix for concrete bridges after Kobe earthquake (Yamazaki et al. 1999)

Observed Damage	Peak Ground Acceleration (g)										Total
	0.15-0.2	0.2-0.3	0.3-0.4	0.4-0.5	0.5-0.6	0.6-0.7	0.7-0.8	0.8-0.9	0.9-1.0	>1.0	
None	80	34	23	28	12	3	3	1	0	0	184
Minor	0	0	2	1	0	4	0	1	0	0	8
Moderate	0	0	1	3	3	6	0	0	0	0	13
Major	0	0	0	1	0	5	1	0	0	0	7
Collapse	0	0	0	2	0	2	0	0	0	0	4

Table 3.3 Definition of bridge damage states (Turner et al. 2009)

HAZUS Damage State	Definitions of HAZUS Damage States (FEMA 2009)	ShakeCast Inspection Priority	Definition of ShakeCast Inspection Priority
Complete (ds5)	ds5 is defined by any column collapsing and connection losing all bearing support, which may lead to imminent deck collapse, tilting of substructure due to foundation failure.	High	High Priority for full engineering assessment
Extensive (ds4)	ds4 is defined by any column degrading without collapse – shear failure - (column structurally unsafe), significant residual movement at connections, or major settlement approach, vertical offset of the abutment, differential settlement at connections, shear key failure at abutments.	Medium-High	Medium-High Priority for full engineering assessment
Moderate (ds3)	ds3 is defined by any column experiencing moderate (shear cracks) cracking and spalling (column structurally still sound), moderate movement of the abutment (<2"), extensive cracking and spalling of shear keys, any connection having cracked shear keys or bent bolts, keeper bar failure without unseating, rocker bearing failure or moderate settlement of the approach.	Medium	Medium Priority for full engineering assessment
Slight/Minor (ds2)	ds2 is defined by minor cracking and spalling to the abutment, cracks in shear keys at abutments, minor spalling and cracks at hinges, minor spalling at the column (damage requires no more than cosmetic repair) or minor cracking to the deck	Low	Low Priority for full engineering assessment; quick visual inspection likely sufficient. (1.0 second peak spectral acceleration exceeds 0.10g.)
None (ds1)			

Table 3.4 Bridge material classes in NBI (NBI, 1995)

Code	Description
1	Concrete
2	Concrete continuous
3	Steel
4	Steel continuous
5	Prestressed concrete
6	Prestressed concrete continuous
7	Timber
8	Masonry
9	Aluminum, Wrought Iron or Cast Iron
0	Other

Table 3.5 Bridge types in NBI (NBI, 1995)

Code	Description
01	Slab
02	Stringer/Multi-beam or Girder
03	Girder and Floor beam System
04	Tee Beam
05	Box Beam or Girders- Multiple
06	Box Beam or Girders- Single or Spread
07	Frame
08	Orthotropic
09	Truss-Deck
10	Truss-Thru
11	Arch-Deck
12	Arch-Thru
13	Suspension
14	Stayed Girder
15	Movable-Lift
16	Movable-Bascule
17	Movable-Swing
18	Tunnel
19	Culvert
20	Mixed Types (applicable only to approach spans)
21	Segmental Box Girder
22	Channel Beam
00	Other

Table 3.6 HAZUS bridge classification scheme (HAZUS-MH)

Class	NBI Class	State	Year Built	No. of Spans	Length of max. Span (meter)	Length less than 20 m	K3D (see note below)	Design ¹	Description
HWB1	All	Non-CA	<1990	Multi-span	>150	N/A	EQ1	Conventional	Major bridge- Length > 150m
HWB1	All	CA	<1975	Multi-span	>150	N/A	EQ1	Conventional	Major bridge- Length > 150
HWB2	All	Non-CA	≥1990	Multi-span	>150	N/A	EQ1	Seismic	Major bridge- Length > 150m
HWB2	All	CA	≥1975	Multi-span	>150	N/A	EQ1	Seismic	Major bridge- Length > 150m
HWB3	All	Non-CA	<1990	1		N/A	EQ1	Conventional	Single Span
HWB3	All	CA	<1975	1		N/A	EQ1	Conventional	Single Span
HWB4	All	Non-CA	≥1990	1		N/A	EQ1	Seismic	Single Span
HWB4	All	CA	≥1975	1		N/A	EQ1	Seismic	Single Span
HWB5	101-106	Non-CA	<1990	Multi-span		N/A	EQ1	Conventional	Multi-Col. bent, Simple support- Concrete
HWB6	101-106	CA	<1975	Multi-span		N/A	EQ1	Conventional	Multi-Col. bent, Simple support- Concrete
HWB7	101-106	Non-CA	≥1990	Multi-span		N/A	EQ1	Seismic	Multi-Col. bent, Simple support- Concrete
HWB7	101-106	CA	≥1975	Multi-span		N/A	EQ1	Seismic	Multi-Col. bent, Simple support- Concrete
HWB8	205-206	CA	<1975	Multi-span		N/A	EQ2	Conventional	Single Col., Box Girder- Continuous Concrete
HWB9	205-206	CA	≥1975	Multi-span		N/A	EQ3	Seismic	Single Col., Box Girder- Continuous Concrete
HWB10	201-206	Non-CA	<1990	Multi-span		N/A	EQ2	Conventional	Continuous Concrete
HWB10	201-206	CA	<1975	Multi-span		N/A	EQ2	Conventional	Continuous Concrete
HWB11	201-206	Non-CA	≥1990	Multi-span		N/A	EQ3	Seismic	Continuous Concrete

Class	NBI Class	State	Year Built	No. of Spans	Length of max. Span (meter)	Length less than 20 m	K3D (see note below)	Design ¹	Description
HWB11	201-206	CA	≥1975	Multi-span		N/A	EQ3	Seismic	Continuous Concrete
HWB12	301-306	Non-CA	<1990	Multi-span		No	EQ4	Conventional	Multi-Col. bent, Simple support-Steel
HWB13	301-306	CA	<1975	Multi-span		No	EQ4	Conventional	Multi-Col. bent, Simple support-Steel
HWB14	301-306	Non-CA	≥1990	Multi-span		N/A	EQ1	Seismic	Multi-Col. bent, Simple support-Steel
HWB14	301-306	CA	≥1975	Multi-span		N/A	EQ1	Seismic	Multi-Col. bent, Simple support-Steel
HWB15	402-410	Non-CA	<1990	Multi-span		No	EQ5	Conventional	Continuous Steel
HWB15	402-410	CA	<1975	Multi-span		No	EQ5	Conventional	Continuous Steel
HWB16	402-410	Non-CA	≥1990	Multi-span		N/A	EQ3	Seismic	Continuous Steel
HWB16	402-410	CA	≥1975	Multi-span		N/A	EQ3	Seismic	Continuous Steel
HWB17	501-506	Non-CA	<1990	Multi-span		N/A	EQ1	Conventional	Multi-Col. bent, Simple support-Prestressed Concrete
HWB18	501-506	CA	<1975	Multi-span		N/A	EQ1	Conventional	Multi-Col. bent, Simple support-Prestressed Concrete
HWB19	501-506	Non-CA	≥1990	Multi-span		N/A	EQ1	Seismic	Multi-Col. bent, Simple support-Prestressed Concrete
HWB19	501-506	CA	≥1975	Multi-span		N/A	EQ1	Seismic	Multi-Col. bent, Simple support-Prestressed Concrete
HWB20	605-606	CA	<1975	Multi-span		N/A	EQ2	Conventional	Single Col., Box Girder-Prestressed Continuous Concrete
HWB21	605-606	CA	≥1975	Multi-span		N/A	EQ3	Seismic	Single Col., Box Girder-Prestressed Continuous Concrete

Class	NBI Class	State	Year Built	No. of Spans	Length of max. Span (meter)	Length less than 20 m	K3D (see note below)	Design ¹	Description
HWB22	601-607	Non-CA	<1990	Multi-span		N/A	EQ2	Conventional	Continuous Concrete
HWB22	601-607	CA	<1975	Multi-span		N/A	EQ2	Conventional	Continuous Concrete
HWB23	601-607	Non-CA	≥1990	Multi-span		N/A	EQ3	Seismic	Continuous Concrete
HWB23	601-607	CA	≥1975	Multi-span		N/A	EQ3	Seismic	Continuous Concrete
HWB24	301-306	Non-CA	<1990	Multi-span		Yes	EQ6	Conventional	Multi-Col. bent, Simple support-Steel
HWB25	301-306	CA	<1975	Multi-span		Yes	EQ6	Conventional	Multi-Col. bent, Simple support-Steel
HWB26	402-410	Non-CA	<1990	Multi-span		Yes	EQ7	Conventional	Continuous Steel
HWB27	402-410	CA	<1975	Multi-span		Yes	EQ7	Conventional	Continuous Steel
HWB28									All other bridges that are not classified

-Note: EQ1 through EQ7 in Table 3.6 are the K_{3D} equations which modifies the pier's 2-dimensional capacity to take into account the 3-dimensional arch action in the deck. These equations take the same form; $K_{3D} = 1 + A / (N-B)$, where N is the number of spans and A and B are given in Table 3.6.

- 1 Conventional means seismic Reinforcement details are not followed by the time of design.

Table 3.7 Median of the HAZUS fragility functions (HAZUS-MH)

Class	SA (1 sec) for fragility functions (g)			
	Slight	Moderate	Extensive	Complete
HWB1	0.40	0.50	0.70	0.90
HWB2	0.60	0.90	1.10	1.70
HWB3	0.80	1.00	1.20	1.70
HWB4	0.80	1.00	1.20	1.70
HWB5	0.25	0.35	0.45	0.70
HWB6	0.30	0.50	0.60	0.90
HWB7	0.50	0.80	1.10	1.70
HWB8	0.35	0.45	0.55	0.80
HWB9	0.60	0.90	1.30	1.90
HWB10	0.60	0.90	1.10	1.50
HWB11	0.90	0.90	1.10	1.50
HWB12	0.25	0.35	0.45	0.70
HWB13	0.30	0.50	0.60	0.90
HWB14	0.50	0.80	1.10	1.70
HWB15	0.75	0.75	0.75	1.10
HWB16	0.90	0.90	1.10	1.50
HWB17	0.25	0.35	0.45	0.70
HWB18	0.30	0.50	0.60	0.90
HWB19	0.50	0.80	1.10	1.70
HWB20	0.35	0.45	0.55	0.80
HWB21	0.60	0.90	1.30	1.60
HWB22	0.60	0.90	1.10	1.50
HWB23	0.90	0.60	1.10	1.50
HWB24	0.25	0.35	0.45	0.70
HWB25	0.30	0.50	0.60	0.90
HWB26	0.75	0.75	0.75	1.10
HWB27	0.75	0.75	0.75	1.10
HWB28	0.80	1.00	1.20	1.70

-Note: For the slight damage state, a value of 0.1g is stored for all bridge classes.

Table 3.8 K_{3D} equations (HAZUS-MH)

Equation	A	B	K_{3D}
EQ1	0.25	1	$1 + 0.25 / (N-1)$
EQ2	0.33	0	$1 + 0.33 / N$
EQ3	0.33	1	$1 + 0.33 / (N-1)$
EQ4	0.09	1	$1 + 0.09 / (N-1)$
EQ5	0.05	0	$1 + 0.05 / N$
EQ6	0.20	1	$1 + 0.20 / (N-1)$
EQ7	0.10	0	$1 + 0.10 / (N-1)$

Table 3.9 Drift limits used by the HAZUS fragility curves (Mander and Basoz, 1999)

Damage State	Drift limits	
	Non-seismic	Seismic
Slight	0.005	0.010
Moderate	0.010	0.025
Extensive	0.020	0.05
Complete	0.05	0.075

Table 3.10 MSCC-BG bridge fragilities (Ramanathan, 2012)

Seismic performance sub-bin	BSST-0		BSST-1		BSST-2		BSST-3		ζ^*
	λ	ζ	λ	ζ	λ	ζ	λ	ζ	
<u>Pre 1971 design era</u>									
MSCC-BG-S-E1-S0	0.13	0.53	0.17	0.60	0.19	0.61	0.22	0.59	0.58
MSCC-BG-M-E1-S0	0.08	0.51	0.10	0.51	0.11	0.52	0.12	0.52	0.51
MSCC-BG-S-E1-S1	0.02	0.77	0.08	0.62	0.14	0.53	0.17	0.54	0.61
MSCC-BG-S-E1-S2	0.02	0.82	0.09	0.67	0.15	0.54	0.17	0.54	0.64
MSCC-BG-S-E1-S3	0.02	0.79	0.09	0.67	0.14	0.55	0.17	0.54	0.64
MSCC-BG-S-E1-S4	0.02	0.80	0.09	0.66	0.15	0.55	0.17	0.54	0.64
MSCC-BG-M-E1-S1	0.01	0.73	0.06	0.61	0.08	0.59	0.09	0.60	0.63
MSCC-BG-M-E1-S2	0.01	0.80	0.06	0.66	0.08	0.62	0.09	0.62	0.68
MSCC-BG-M-E1-S3	0.01	0.80	0.06	0.64	0.08	0.60	0.09	0.61	0.66
MSCC-BG-M-E1-S4	0.01	0.77	0.06	0.67	0.08	0.61	0.09	0.60	0.66
<u>1971-1990 design era</u>									
MSCC-BG-S-E2-S0	0.15	0.56	0.38	0.61	0.70	0.70	1.00	0.70	0.64
MSCC-BG-M-E2-S0	0.12	0.55	0.24	0.56	0.38	0.57	0.50	0.57	0.56
MSCC-BG-S-E2-S2	0.08	0.61	0.31	0.53	0.47	0.51	0.62	0.52	0.54
MSCC-BG-S-E2-S3	0.08	0.61	0.31	0.53	0.47	0.51	0.62	0.51	0.54
MSCC-BG-S-E2-S4	0.09	0.61	0.31	0.54	0.48	0.51	0.62	0.51	0.54
MSCC-BG-M-E2-S2	0.07	0.52	0.18	0.58	0.27	0.62	0.36	0.63	0.59
MSCC-BG-M-E2-S3	0.07	0.52	0.18	0.59	0.28	0.64	0.36	0.64	0.59
MSCC-BG-M-E2-S4	0.07	0.55	0.18	0.58	0.27	0.64	0.35	0.64	0.60
<u>Post 1990 design era</u>									
MSCC-BG-S-E3-S0	0.16	0.42	0.52	0.39	0.95	0.40	1.26	0.40	0.40
MSCC-BG-M-E3-S0	0.11	0.54	0.32	0.53	0.61	0.56	0.84	0.57	0.55
MSCC-BG-S-E3-S3	0.09	0.55	0.57	0.53	1.44	0.48	2.06	0.49	0.51
MSCC-BG-S-E3-S4	0.09	0.56	0.57	0.53	1.44	0.48	2.06	0.49	0.51
MSCC-BG-M-E3-S3	0.06	0.57	0.26	0.55	0.59	0.59	0.87	0.60	0.58
MSCC-BG-M-E3-S4	0.06	0.58	0.26	0.55	0.61	0.60	0.88	0.61	0.59

Table 3.11 Most vulnerable component for MSCC-BG bridge class with seat abutments
(Ramanathan, 2012)

Seismic performance sub-bin	Damage States			
	BSST-0	BSST-1	BSST-2	BSST-3
MSCC-BG-S-E1-S1	Abut seat	Abut seat	Abut seat	Abut seat
MSCC-BG-S-E1-S2	Joint seal	Abut seat	Columns	Columns
MSCC-BG-S-E1-S3	Joint seal	Abut seat	Columns	Columns
MSCC-BG-S-E1-S4	Joint seal	Abut seat	Columns	Columns
MSCC-BG-M-E1-S1	Joint seal	Abut seat	Abut seat	Abut seat
MSCC-BG-M-E1-S2	Joint seal	Abut seat	Columns	Columns
MSCC-BG-M-E1-S3	Joint seal	Abut seat	Columns	Columns
MSCC-BG-M-E1-S4	Joint seal	Abut seat	Columns	Columns
MSCC-BG-S-E2-S2	Joint seal	Columns	Columns	Columns
MSCC-BG-S-E2-S3	Joint seal	Columns	Columns	Columns
MSCC-BG-S-E2-S4	Joint seal	Columns	Columns	Columns
MSCC-BG-M-E2-S2	Joint seal	Columns	Columns	Columns
MSCC-BG-M-E2-S3	Joint seal	Columns	Columns	Columns
MSCC-BG-M-E2-S4	Joint seal	Columns	Columns	Columns
MSCC-BG-S-E3-S3	Joint seal	Abut seat	Columns	Columns
MSCC-BG-S-E3-S4	Joint seal	Abut seat	Columns	Columns
MSCC-BG-M-E3-S3	Joint seal	Columns	Columns	Columns
MSCC-BG-M-E3-S4	Joint seal	Columns	Columns	Columns

Table 3.12 Comparison between Nielson (2005) fragility curves and HAZUS (Nielson, 2005)

		Median PGA values (g)			
Bridge	Source	Slight	Moderate	Extensive	Complete
MSC Concrete	Proposed	0.16	0.53	0.75	1.01
	HAZUS	0.60	0.88	1.17	1.53
MSC Slab	Proposed	0.17	0.49	0.86	2.39
	HAZUS	0.60	0.88	1.17	1.53
MSC Steel	Proposed	0.19	0.32	0.41	0.51
	HAZUS	0.76	0.77	0.77	1.06
MSSS Concrete	Proposed	0.20	0.63	0.91	1.28
	HAZUS	0.26	0.39	0.50	0.73
MSSS Concrete-Box	Proposed	0.22	0.69	1.31	3.39
	HAZUS	0.26	0.39	0.50	0.73
MSSS Slab	Proposed	0.17	0.51	0.91	1.87
	HAZUS	0.26	0.39	0.50	0.73
MSSS Steel	Proposed	0.24	0.45	0.58	0.85
	HAZUS	0.26	0.39	0.48	0.72
SS Concrete	Proposed	0.35	1.33	1.83	2.50
	HAZUS	0.80	0.90	1.10	1.60
SS Steel	Proposed	0.64	1.19	1.59	2.59
	HAZUS	0.80	0.90	1.10	1.60

Where:

- MSC Concrete: Multi-Span Continuous Concrete Girder.
- MSC Slab: Multi-Span Continuous Slab.
- MSC Steel: Multi-Span Continuous Steel Girder.
- MSSS Concrete: Multi-Span Simply Supported Concrete Girder.
- MSSS Concrete-Box: Multi-Span Simply Supported Concrete Box Girder.
- MSSS Slab: Multi-Span Simply Supported Slab.
- MSSS Steel: Multi-Span Simply Supported Steel Girder.
- SS Concrete: Single-Span Concrete Girder.
- SS Steel: Single-Span Steel Girder.

Table 3.13 Predominant bridge classes in Nevada

HAZUS Class	NBI Class	Description	Year Built	Design	Percentage
HWB5	101	Simple/Slab type/Concrete	<1983	Conventional	1.5%
HWB7	101	Simple/Slab type/Concrete	≥1983	Seismic	1.8%
HWB10	201	Continuous/Slab type/Concrete	<1983	Conventional	9.4%
HWB11	201	Continuous/Slab type/Concrete	≥1983	Seismic	1.5%
HWB10	205	Continuous Concrete Box Girder Bridge/Multiple	<1983	Conventional	6.4%
HWB11	205	Continuous Concrete Box Girder Bridge/Multiple	≥1983	Seismic	0.9%
HWB12	302	Simply Supported Steel Bridge	<1983	Conventional	4%
HWB14	302	Simply Supported Steel Bridge	≥1983	Seismic	3.7%
HWB15	402	Continuous Steel Bridge	<1983	Conventional	3.7%
HWB16	402	Continuous Steel Bridge	≥1983	Seismic	4%
HWB17	505	Simply Supported Prestressed Concrete Box Girder Bridge/Multiple	<1983	Conventional	4.4%
HWB19	505	Simply Supported Prestressed Concrete Box Girder Bridge/Multiple	≥1983	Seismic	7%
HWB17	506	Simply Supported Prestressed Concrete Box Girder Bridge/Single	<1983	Conventional	0.4%
HWB19	506	Simply Supported Prestressed Concrete Box Girder Bridge/Single	≥1983	Seismic	2.25%
HWB22	605	Continuous Prestressed Concrete Box Girder Bridge/Multiple	<1983	Conventional	0.9%
HWB23	605	Continuous Prestressed Concrete Box Girder Bridge/Multiple	≥1983	Seismic	9.1%
HWB22	606	Continuous Prestressed Concrete Box Girder Bridge/Single	<1983	Conventional	0
HWB23	606	Continuous Prestressed Concrete Box Girder Bridge/Single	≥1983	Seismic	5.5%

Table 3.14 Medians for the proposed fragility functions (S_a at 1 sec.) (g)

HAZUS Class	NBI Class	Year Built	Source	Damage States		
				Moderate	Extensive	Complete
HWB10	205	<1983	Proposed	0.18	0.27	0.36
			HAZUS	0.90	1.10	1.50
HWB11	205	\geq 1983	Proposed	0.26	0.60	0.87
			HAZUS	0.90	1.10	1.50
HWB15	402	<1983	Proposed	0.32	0.41	0.51
			HAZUS	0.75	0.75	1.10
HWB22	605	<1983	Proposed	0.18	0.27	0.36
			HAZUS	0.90	1.10	1.50
HWB23	605	\geq 1983	Proposed	0.26	0.60	0.87
			HAZUS	0.90	1.10	1.50

-Note: Fragility functions for bridge classes that are not listed in Table 3.14 are not changed (same as HAZUS)

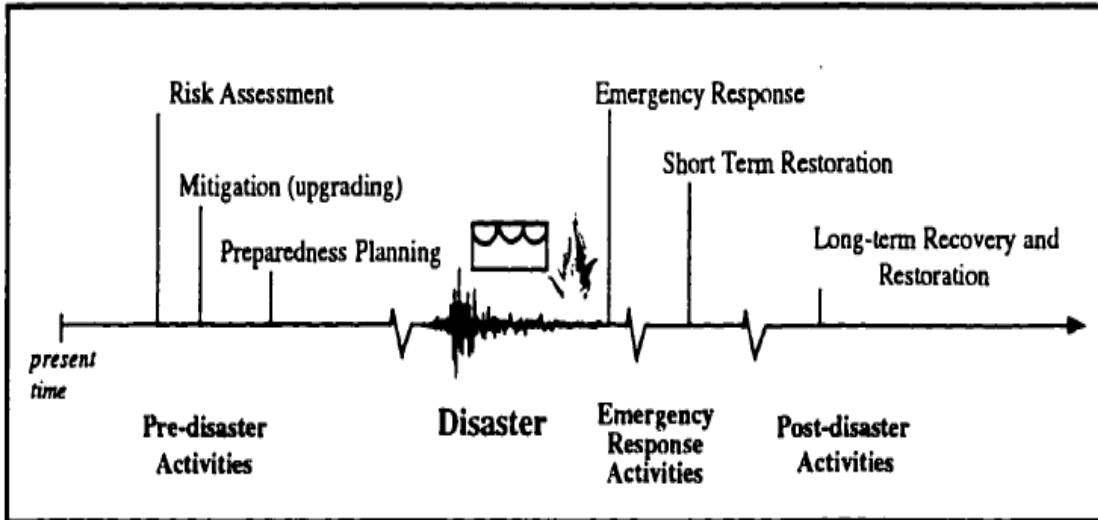


Figure 3.1 Before and after earthquake events (Basoz and Kiremidjian 1997)

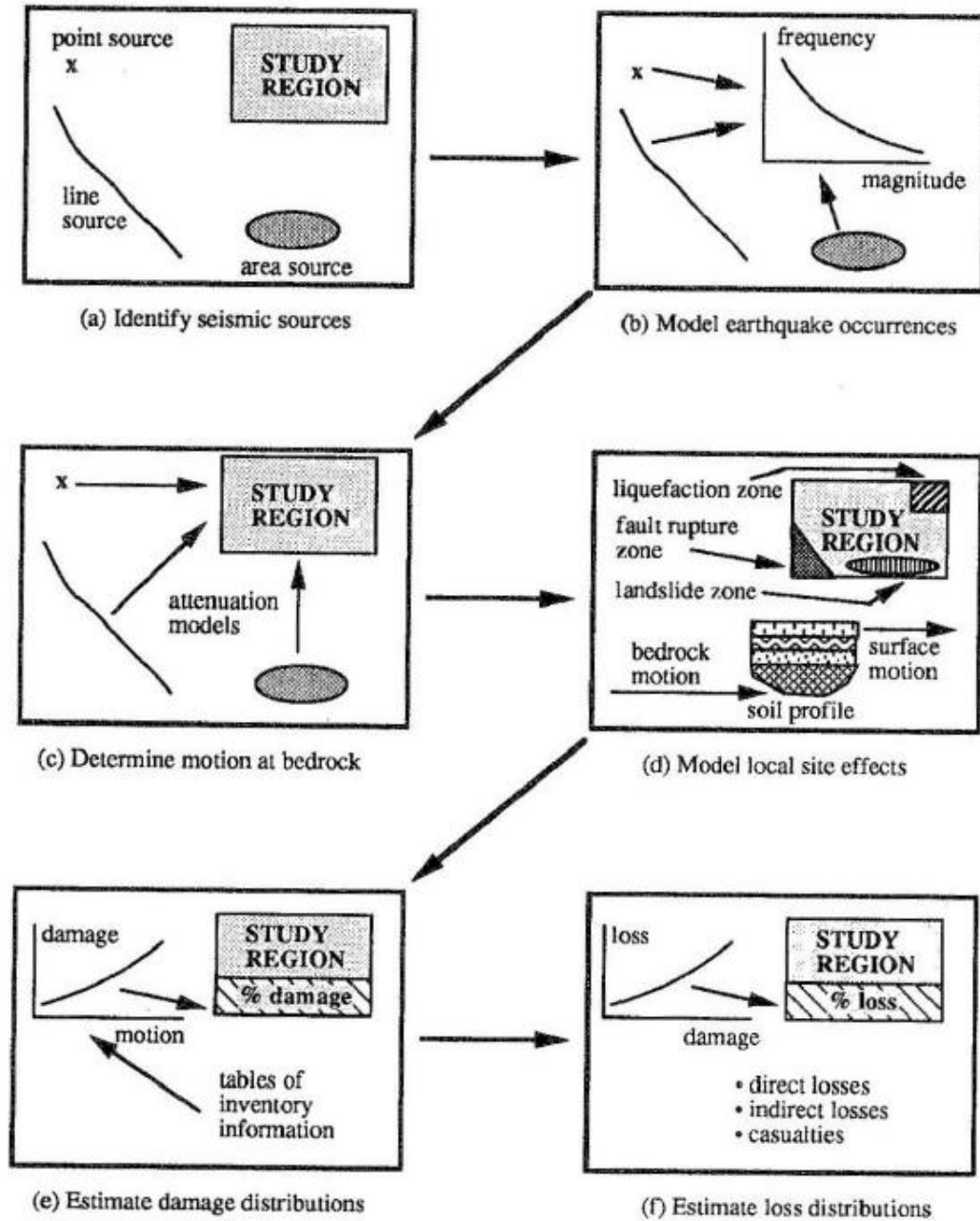


Figure 3.2 Basic steps in seismic risk assessment (King and Kiremidjian 1994)

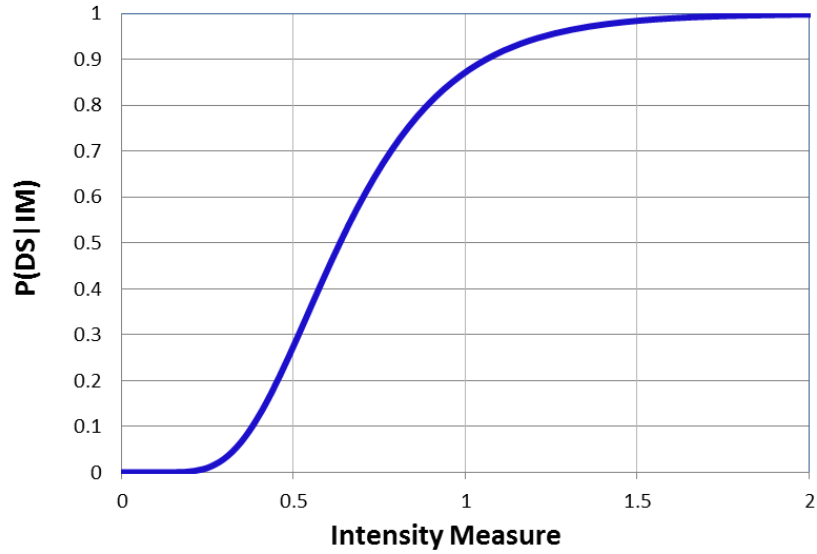


Figure 3.3 Fragility curve trend

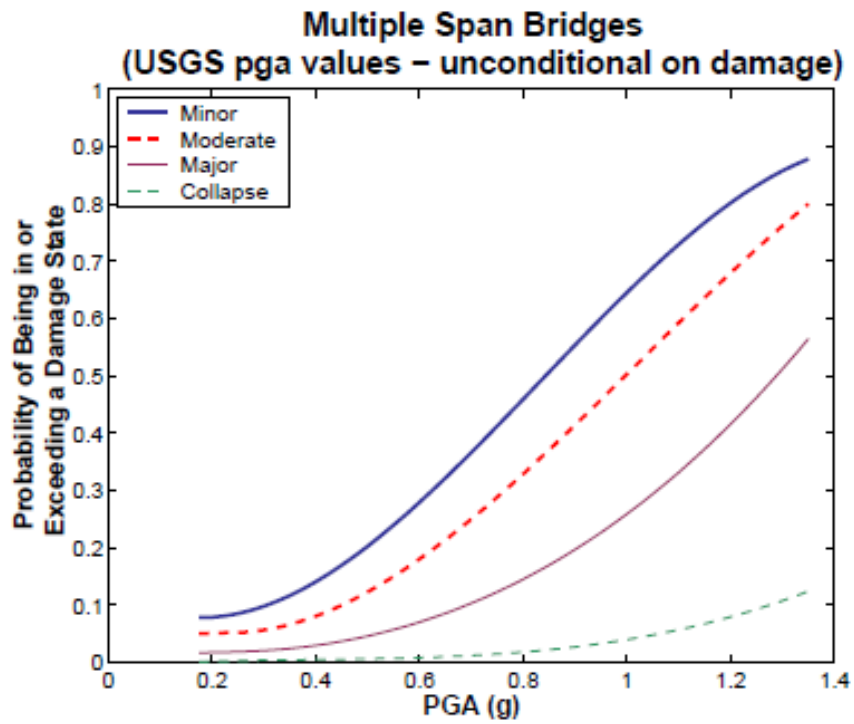


Figure 3.4 Empirical fragility curves for multi-span bridges (Basoz and Kiremidjian, 1997)

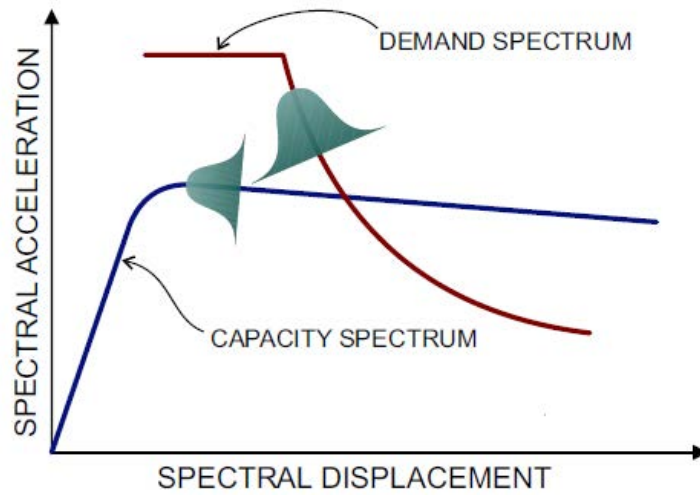


Figure 3.5 Demand and capacity response spectra (Mander and Basoz, 1999)

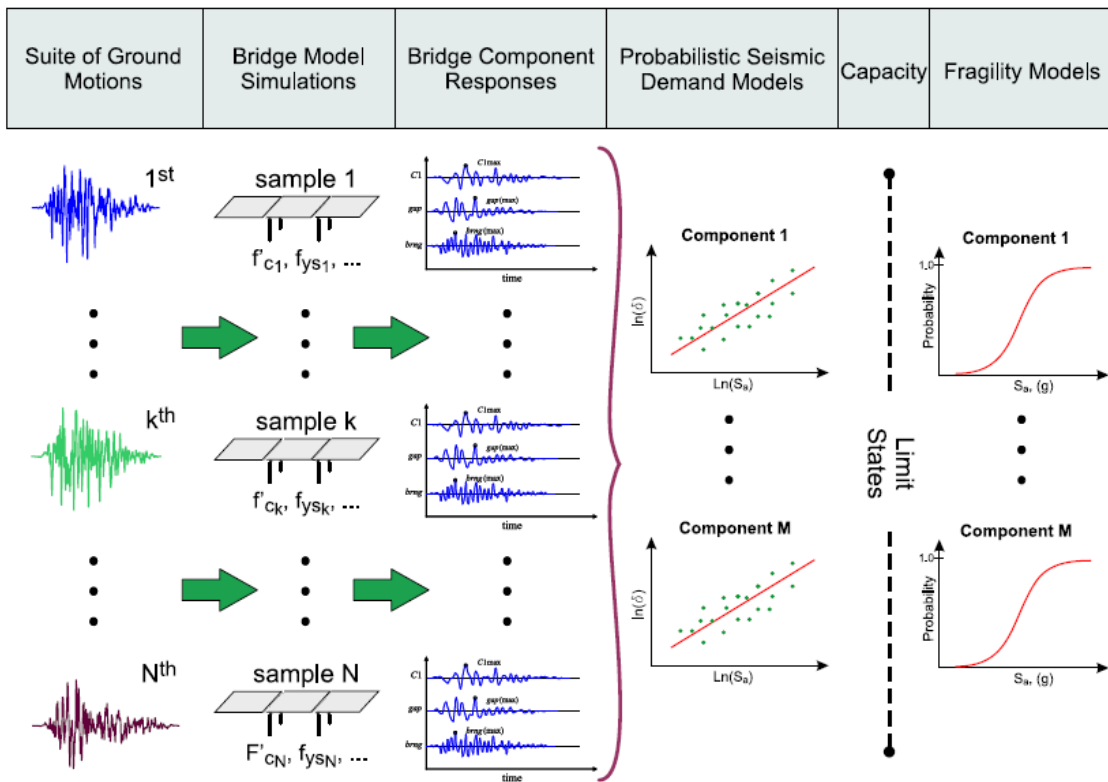


Figure 3.6 Generating of fragility curves using nonlinear time history analysis (Nielson, 2005)

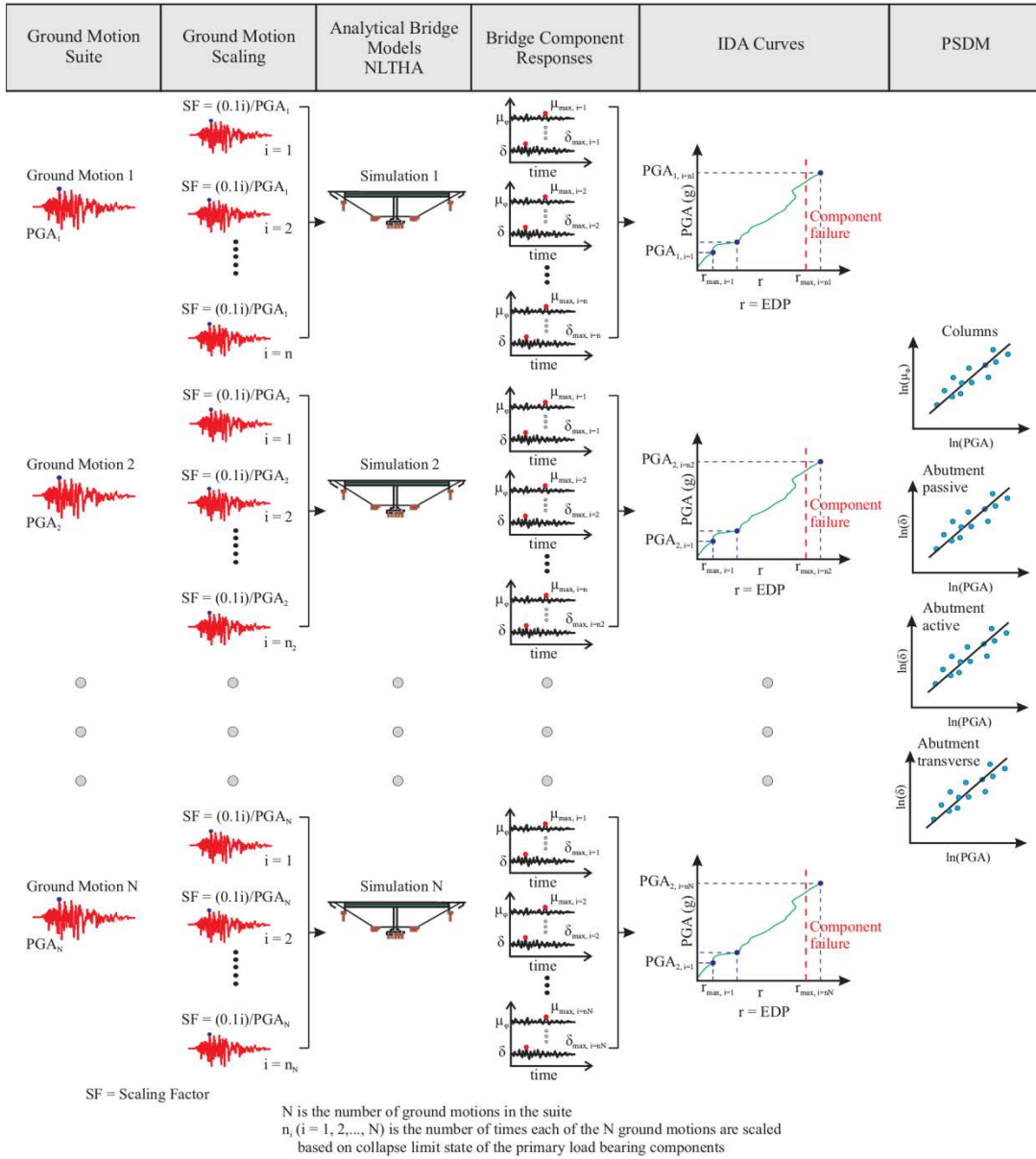


Figure 3.7 Incremental dynamic analysis procedure to develop PSDM's (Ramanathan, 2012)

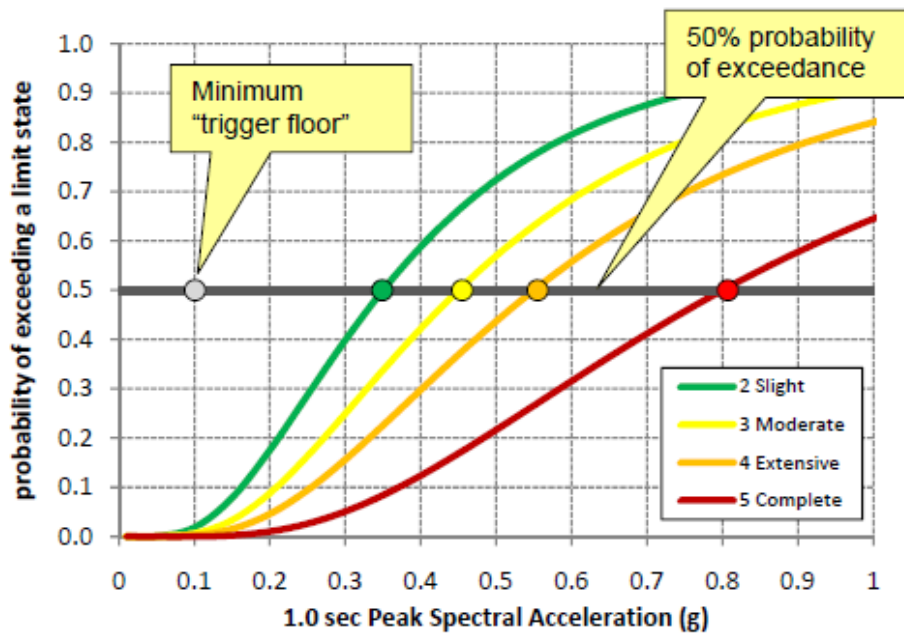


Figure 3.8 ShakeCast stores only the 50% probability of exceedance value (Turner et al. 2009)

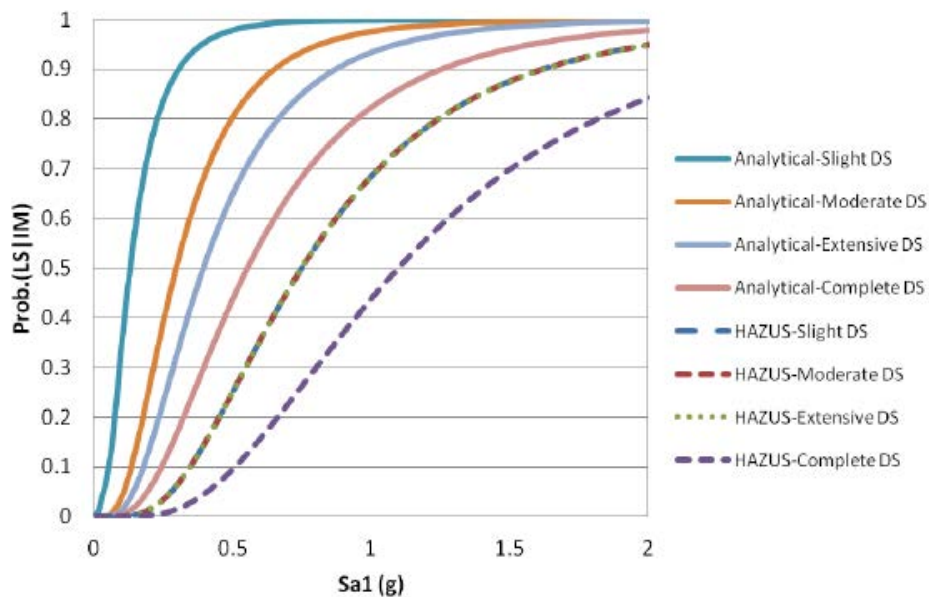


Figure 3.9 Comparison of analytical and HAZUS fragility curves for non-seismically designed bridges. LS: limit state, IM: intensity measure, and DS: damage state (AmiriHormozaki, 2013)

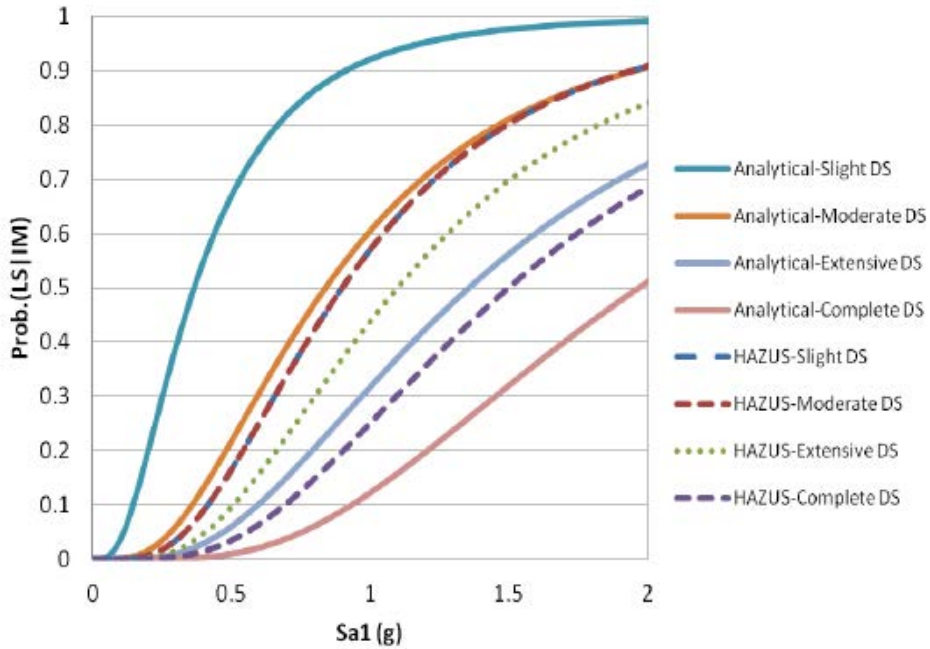


Figure 3.10 Comparison of analytical and HAZUS fragility curves for seismically designed bridges (AmiriHormozaki, 2013)

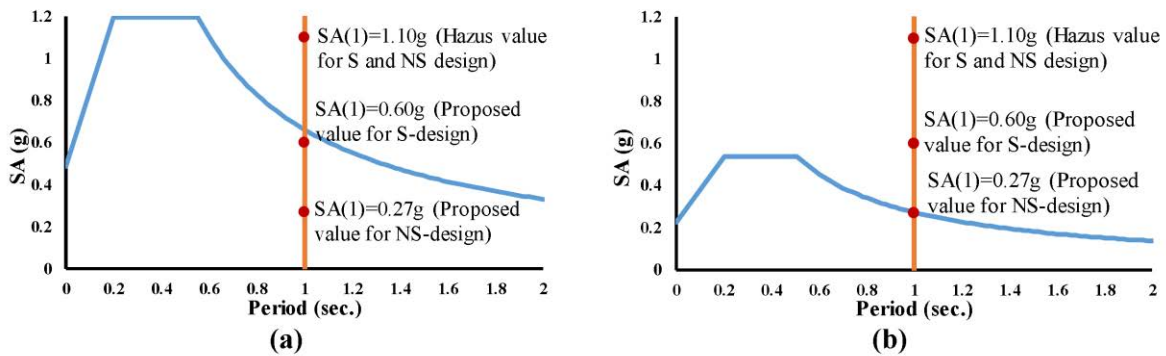


Figure 3.11 High (a) and medium (b) seismic design spectra for 1000-year return periods (AASHTO-site class D). Spectra represent the Reno and Las Vegas areas, respectively. HAZUS SA(1) values are seen to be much higher in both cases than actual Nevada bridge design. Proposed alternative values for seismically (S) and non-seismic (NS) are also shown.

Chapter 4: ShakeCast Results

4.1. ShakeCast Predictions for Nevada Bridges from Scenario Earthquakes

ShakeMap 3.5 was used to generate 112 earthquake scenarios, **Table 2.1**. Two ground motion prediction relations, Boore and Atkinson (2008, “BA08”) and Chiou and Youngs (2008, “CY08”), were used for each scenario. All were processed with ShakeCast 2. Some scenarios, especially in urbanized western Nevada, impact large numbers of bridges, while other scenarios especially in rural Nevada impact few bridges.

With the large number of scenarios, it became impractical to study scenarios individually using the ShakeCast web interface. Instead, ShakeCast predictions were compiled using crafted direct queries of the ShakeCast database, which uses the open-source standard software MySQL (<https://www.mysql.com>). Queries can readily be constructed that span multiple scenarios for a given facility, multiple facilities for one or more scenarios, or other combinations that involve one or multiple database fields. To find out which scenario events are most likely to cause damage, a query was developed that for each bridge finds all scenarios involved at the Possible (Yellow) or Likely (Orange or Red) damage states. For some bridges only one scenario is identified. For other bridges there may be several capable faults in the area, and any of several scenarios could produce damage.

An example query result for HWB10 with Continuous Concrete construction is provided in **Table 4.1**. Only the top few bridges of this type are shown; complete results are provided in Appendix A. The table shows scenario demands in PGA, PGV, and SA(1). SA(1) as used throughout ShakeCast for bridge damage expectation levels. Demand values include the effects of the site condition adjustments, as described in Section 4.3.2. The table also shows the bridge construction year, reported retrofit status, bridge location, and estimated site class. The Damage State column includes the name and ShakeCast color designation. The root of scenario names (briefly) refers to the fault hosting the earthquake. To this is added a short token, either BA or CY, to identify the scenario as being run with, respectively, the BA08 or CY08 GMPE (see Section 2.2.2.2 for more detail). Where the two differ, the BA08 GMPE tends to predict slightly higher ground motions. It can occur that only one of the two GMPEs predict a damage state above the Green level. It is important to keep in mind that the indicated damage states are conditioned on the scenario earthquake actually occurring. These scenarios do not comprise any even generalized prediction. It is shown in the next section how return frequency can be inferred for scenario ground motions at a point.

4.2 Developing Site Class Estimates for Bridges in ShakeCast Scenarios

Table 4.1 also includes an estimated Vs30 site class, mostly C or D, for Nevada bridges which were developed from available measurements and geologic and site physiographic mapping information. The year built, reported retrofit status and estimated site class are also shown. Damage State includes the name and ShakeCast color designation. Few bridge sites in Nevada have measured Vs30 values, and none were available for this project. Two methods were used to

develop an approximate site class for adjustment of bridge demands. The first method applies only in the greater Las Vegas Valley area. Clark County commissioned an extensive parcel mapping project that used the Refraction Micro-tremor surface wave method to develop measured site condition values in the valley. It can be accessed at <http://gisgate.co.clark.nv.us/openweb/>. For bridges on this parcel map and near it on geologically similar conditions (House et al., 2010), the bridge site condition was adopted from their estimate. Site conditions for other bridges were inferred using geologic and geomorphic evaluations of scenes in Google Earth at the individual bridges. For example, older alluvial surfaces can be recognized by patterns of incision and color. Such surfaces also have a significant local topographic gradient that favors deposition of sand to cobble-sized material. Sites like this were given site class C designations. Dry low gradient environments likely to be dominated by fine materials were given site class D. A few bridges occur in active channels dominated by saturated fines. These were given site class E. These site class designations were used to adjust National Seismic Hazard Map SA(1) hazards, as described in the next section.

4.3 Ground Motion Predictions for Bridge Sites

4.3.1 U.S. Geological Survey (USGS) National Seismic Hazard Map (NSHM) Hazard Curves

To evaluate predicted ground motions and rates at bridge sites evaluated by ShakeCast, tools to extract the spectral acceleration at one Hz (SA(1)) from the 2014 USGS National Seismic Hazard Map (NSHM) (**Figure 2.2**) were developed. The National Seismic Hazard Maps are probabilistic seismic hazard maps constructed from all known active fault sources in the U.S. Ground motion estimates at Nevada bridges will be dominated by Nevada faults, but also include fault sources in California and other states as they contribute to hazard. The rates and amplitudes at which each fault source contributes include the rates of earthquakes on the faults, the range of estimated magnitudes, and their potential rupture locations on the faults. Thus earthquake recurrence rate and how earthquakes occur, as a single large event or multiple small events, are all included. Given this source description, ground motions are estimated using several ground motion prediction equations. Maps also include the seismic contributions of background earthquakes. Background events cannot be definitely associated with known faults but are recognized from regional seismic monitoring. Other details regarding the inputs to the NSHMs and the process of their development are available at <http://earthquake.usgs.gov/hazards/products/>. National Seismic Hazard Maps are available for several ground motion parameters, including spectral acceleration at several periods, peak ground acceleration, and peak ground velocity. Historically, after a review process, the USGS NSHM is incorporated into relevant building codes governing construction in the U.S.

NSHM hazard curves are useful for bridge evaluation because they are an objective externally developed measure of the actual rate of ground motion demand. In contrast, ShakeCast estimates are conditioned on the occurrence of specific scenario earthquakes without reference to their likelihood. Thus the NSHM hazard curves provide a way to unite the two estimates.

Based on the ShakeCast results, capacities of the bridges evaluated for damage are used to get their corresponding earthquake return periods from the NSHM hazard curves (**Figure 4.1**).

Demand at a fixed return period (e.g., 1000 yrs.) can be used as a relative measure of the frequency that damaging earthquake ground motions can be expected. This frequency can be used as one measure in setting priorities for seismic upgrades or bridge improvements. For this project we used SA(1) because it is the most relevant NSHM ground motion measure for bridge evaluation and because it is available on a latitude and longitude grid of 0.05 by 0.05 degrees. These translate to grid point separations of approximately 5.5 km north-south by 4.2 km east-west in Nevada. The NSHM for SA(1) in the Conterminous U.S. is shown in **Figure 2.2**

Except by rare coincidence, bridges are unlikely to fall on a grid point from the USGS hazard map. In addition, near active faults the spatial rate of change of hazard can be significant (e.g., **Figure 2.2**, near bands along western faults). To improve the use of the grid estimates, we developed an interpolation of the grid SA(1) data to the actual locations of bridges of the Nevada inventory. The implementation finds the four nearest points to the bridge (**Figure 4.2**), then averages using summed inverse distance weighting approach. Specifically, each of the four nearest grid SA(1) values is given a weight $w_i = (1/d_i)/\Sigma(1/d_i)$, where the sum is over the 4 points. If $d_i < 0.001$ km it is set to 0.001 to prevent singularities. This weighting method emphasizes the nearest grid point if one is nearby, while smoothing among them when the bridge is between grid points. In **Figure 4.4** and subsequent similar figures, SA(1) values at the four grid points are shown as small dots, while the solid line shows the weighted result. For bridge sites where the hazard changes over short spatial distances (e.g., western Nevada) the dots will be spread out. Where the hazard is spatially more constant (e.g. eastern Nevada) grid point values will be similar and the range among them will be small.

4.3.2 Adjusting NSHM Hazard Curves for Bridge Site Conditions

The NSHM hazard curves assume a site condition of 760 m/s, corresponding to the NEHRP B-C soil class boundary. This relatively high value has been assumed by the USGS with the expectation that users would adjust from there according to the project site conditions. Site conditions from parcel-mapping in Clark County and geologic estimates elsewhere to adjust the NSHM hazard curves were used. Site condition amplifications from AASHTO (**Table 4.2**) were adopted. These values were used to adjust NSHM SA(1sec) hazard curves for site-specific soil class estimates (AASHTO 2014). The corrections are amplitude dependent, and applied as such to the NSHM hazard curves. Because the AASHTO site amplification table has no “B-C Boundary” site class, all sites were de-amplified to site class B, then increased according to the bridge site conditions. The AASHTO standard prescribes linear extrapolation between SA values; this was done both to de-amplify to site class B and to amplify to the site value. **Figure 4.3** shows the net corrections for site conditions C, D, and E. The inflection in site condition E is due to differing correction rates of the deamplification to site class B and amplification to the indicated conditions. These amplification factors were applied to NSHM hazard curves to estimate actual demands at Nevada bridge sites.

Examples for two bridges identified in this project as potentially subject to damage are shown in **Figures 4.4** and **4.5**. Both were identified as potentially at risk from scenario earthquakes using the ShakeCast system. In **Figure 4.4**, bridge 32_G_863W is a freeway overpass southwest of Winnemucca. The gray line is the hazard curve at the bridge site as extrapolated using four nearest grid points of the USGS NSHM for SA(1). Small dots show the individual grid values. Green, yellow, orange, and red vertical bars are respective ShakeCast damage levels. Black vertical bars are demands of scenario earthquakes; stars on the ends are added for visibility.

Intersections of the vertical bars with the red line give the predicted annual frequencies for the respective ground motions. For this bridge, all of the three scenarios are less frequent than once in the reference return period of 1000 years. The red curve is the NSHM hazard curve shifted up with the frequency-dependent AASHTO amplitude correction to the individual site condition of the bridge. The circle highlights the point of curve intersection at 1000-year return time. Entries in the title are the bridge type, name, location, site class (“sc”), SA(1) at 1000 year return time, in g’s, and whether or not the bridge has been retrofitted. The 1000 year return SA(1) of 0.136 g compares with 0.182 at 2% probability in 50 years ($4e-4$ annual frequency) from the NSHM map. The red line shifts this curve as a function of frequency according to the AASHTO site correction. The expected NSHM demand at 2% probability in 50 years ($4e-4$ annual frequency) is 0.182 g. This is the value one would get from **Figure 2.2** for the bridge site. ShakeCast identified three scenarios with likely or probable damage, with the largest demand being 0.58 g; this level is capable of damage (vertical bars with stars, **Figure 4.4**). The difference between the two is that ShakeCast considers the earthquake occurrence as given, and describes ground motions as though that the earthquake has occurred. The NSHM hazard curve includes the relative rates of sources. In this case earthquakes as large as the scenario are more rare than $4e-4$ /year. At a 1000 year return time ($1e-3$ /yrs.), SA(1) is expected to reach only 0.136 g.

As a second example, in **Figure 4.5** is the hazard curve for bridge 32_I1291, the freeway overpass to Bordertown, near where US Highway 395 crosses into northern California (**Figure 2.7**). Figure and title field explanations are the same as in the previous figure. Bridge metadata and damage levels are also found in **Figures 2.7 and 2.8**. The NSHM hazard curve is shown in light gray; the hazard map (**Figure 2.2**) value ($4e-4$ annual frequency) for this site is 0.457 g, compared to a 1000-year return of 0.366 g after site condition adjustment. Compared to the previous figure the fault sources affecting this bridge are closer and slip at a higher rate. Western Nevada is seismically more active than near Winnemucca, and this is reflected in the higher expected demand at 2% in 50 years of 0.457 g. The Winnemucca Bridge is expected to see these accelerations, but at return frequencies of $\sim 4.5e-5$, or about 22,000 years (**Figure 4.4**). With site conditions, 32_I1291 is expected to experience 0.366 g at the 1000-year return period. Neither bridge is likely in an absolute sense to be damaged by an earthquake, since $1e-3$ or $4e-4$ are both a relatively low probability event, but between the bridges, the second is more likely to experience strong ground shaking than is the first.

Table 4.3 presents the return periods corresponding to different damage states for some bridges. They are sorted from lower to higher return periods for the extensive damage state (orange). A threshold of 1000-year return period is used to separate bridges with higher priority to be retrofitted. The complete bridge list is presented in Appendix C.

Hazard curves for bridges identified under this project as potentially at risk from scenario earthquakes are provided in appendices to this report. Bridges with damage expected on return times of less than 1000 years (colored lines intersect the hazard curve above $1e-3$ annual frequency) are at greatest probabilistic risk based on National Seismic Hazard Map estimates. In some cases the site correction may be important in evaluating priorities. Before work is done on such bridges we encourage that the Vs30 and total site condition be measured to confirm estimates provided here.

The main objective of **Tables 4.1 and 4.3**, which are expanded in Appendices A and C, is to present bridges with the highest priority to be retrofitted. Many of the bridges in **Tables 4.1, A.1, A.2, A.3, A.4, and A.5** are expected to experience ground motions with SA(1 sec.), at the

bridge site, exceeding 0.3g. These values of the expected spectral accelerations could be highly damaging, especially that most of these bridges were built before 1983 (non-seismically designed).

By taking the first four bridges from **Table 4.3**, as an example (I-1172, I-1250, H-1003, and I-1010), it is found that, based on the USGS hazard curves, the return periods for earthquakes causing extensive damage are less than 300 years and those causing complete damage are around 500 years. These return periods are less than what is specified by the AASHTO. AASHTO specifies a design return period corresponding to a seven percent probability of exceedance in 75 years (1000 year return period). Table A.1 shows that these bridges are surrounded by a number of faults, such as Mountain Rose, Freds Mountain and Spanish Springs. The predicted scenarios from these faults are producing ground motions that can exceed a SA(1sec.) of 0.4g.

Based on the scenarios and the predicted response of the bridges, it is recommended that NDOT personnel should consider this information while planning bridge retrofiting.

Appendix D presents a damage assessment and repair manual for various bridge components such as columns, shear keys and abutments. This manual can be used as a post-earthquake response to damage in bridges.

Table 4.1 Top 12 bridges of type HWB10-205, with scenario names (attenuation model indicated by “BA” or “CY”), and scenario demands in PGA, PGV, and SA(1).

Bridge ID	PGA (%)	PGV	Sa (1 sec) (%)	Year Built	Retrofitted?	Scenario	Damage State	Site Class
32_B1544N	28.98	26.68	31.45	1968	no	Frenchman_Mntn_M6.6BA_se	Orange	C
32_B1544N	25.18	28.02	24.93	1968	no	Frenchman_Mntn_M6.6CY_se	Yellow	
32_B1544S	28.98	26.68	31.45	1968	no	Frenchman_Mntn_M6.6BA_se	Orange	C
32_B1544S	25.18	28.02	24.93	1968	no	Frenchman_Mntn_M6.6CY_se	Yellow	
32_B_839S	40.67	46.83	55.22	1961	no	California_Wash_M6.9BA_se	Red	C
32_B_839S	41.97	62.98	56.1	1961	no	California_Wash_M6.9CY_se	Red	
32_B_954N	35.34	31.84	40.12	1970	no	Eglington_M6.3BA_se	Red	D
32_B_954N	28.21	37.17	32.77	1970	no	Eglington_M6.3CY_se	Orange	
32_B_954N	39.04	40.19	52.31	1970	no	Frenchman_Mntn_M6.6BA_se	Red	
32_B_954N	27.56	37.52	33.93	1970	no	Frenchman_Mntn_M6.6CY_se	Orange	
32_B_954S	35.34	31.84	40.12	1970	no	Eglington_M6.3BA_se	Red	D
32_B_954S	28.21	37.17	32.77	1970	no	Eglington_M6.3CY_se	Orange	
32_B_954S	39.04	40.19	52.31	1970	no	Frenchman_Mntn_M6.6BA_se	Red	
32_B_954S	27.56	37.52	33.93	1970	no	Frenchman_Mntn_M6.6CY_se	Orange	
32_G1153	26.11	30.83	32.82	1967	no	Grass_Valley_M7.1BA_se	Orange	C
32_G1153	33.02	48.34	44.05	1967	no	Grass_Valley_M7.1CY_se	Red	
32_G_925E	20.08	20.63	20.97	1974	no	Independence_V_M7.2BA_se	Yellow	D
32_G_925E	21.82	28.87	26.89	1974	no	Independence_V_M7.2CY_se	Yellow	
32_G_925W	20.44	21.33	21.81	1974	no	Independence_V_M7.2BA_se	Yellow	D
32_G_925W	22.11	29.86	27.85	1974	no	Independence_V_M7.2CY_se	Orange	
32_G_941	31.84	25.1	28.98	1968	no	Eglington_M6.3BA_se	Orange	C
32_G_941	24.91	26.79	23.25	1968	no	Eglington_M6.3CY_se	Yellow	
32_G_941	37.03	32.48	38.78	1968	no	Frenchman_Mntn_M6.6BA_se	Red	
32_G_941	23.99	26.68	23.81	1968	no	Frenchman_Mntn_M6.6CY_se	Yellow	
32_G_947	31.84	25.1	28.98	1968	no	Eglington_M6.3BA_se	Orange	C
32_G_947	24.91	26.79	23.25	1968	no	Eglington_M6.3CY_se	Yellow	
32_G_947	37.03	32.48	38.78	1968	no	Frenchman_Mntn_M6.6BA_se	Red	
32_G_947	23.99	26.68	23.81	1968	no	Frenchman_Mntn_M6.6CY_se	Yellow	
32_G_953	34.56	29.24	35.62	1971	no	Eglington_M6.3BA_se	Red	D
32_G_953	27.12	32.89	28.77	1971	no	Eglington_M6.3CY_se	Orange	
32_G_953	38.23	36.93	46.44	1971	no	Frenchman_Mntn_M6.6BA_se	Red	
32_G_953	27.12	34.23	30.71	1971	no	Frenchman_Mntn_M6.6CY_se	Orange	
32_G_961N	27.34	24.79	29.81	1963	yes	Eglington_M6.3BA_se	Yellow	C
32_G_961N	27.12	33.15	29.02	1963	yes	Eglington_M6.3CY_se	Yellow	
32_G_961N	35.16	35.83	45.12	1963	yes	Frenchman_Mntn_M6.6BA_se	Yellow	
32_G_961N	30.8	40.82	36.48	1963	yes	Frenchman_Mntn_M6.6CY_se	Yellow	

Table 4.2 Amplitude-dependent site corrections for SA(1 sec).

Site Class	Spectral Acceleration Coefficient at Period 1 sec (S_1)				
	$S_1 < 0.1g$	$S_1 = 0.2g$	$S_1 = 0.3g$	$S_1 = 0.4g$	$S_1 > 0.5g$
A	0.8	0.8	0.8	0.8	0.8
B	1.0	1.0	1.0	1.0	1.0
C	1.7	1.6	1.5	1.4	1.3
D	2.4	2.0	1.8	1.6	1.5
E	3.5	3.2	2.8	2.4	2.4

Table 4.3 Return periods corresponding to different damage states for 28 example bridges

Bridge ID	SA(1 sec) %	Annual Frequency	Return Period (Years)	SA(1 sec) %	Annual Frequency	Return Period (Years)	SA(1 sec) %	Annual Frequency	Return Period (Years)
32_I1172	18	7.48E-03	133.7	27	3.67E-03	272.4	35	2.08E-03	481.6
32_I1250	18	7.46E-03	134.0	27	3.66E-03	273.5	35	2.06E-03	484.9
32_H1003	18	7.34E-03	136.2	27	3.53E-03	283.2	35	1.94E-03	515.0
32_I1010	18	7.34E-03	136.3	27	3.53E-03	283.4	35	1.94E-03	515.4
32_H_866W	18	7.30E-03	137.0	27	3.50E-03	285.4	35	1.92E-03	519.8
32_H_866E	18	7.30E-03	137.0	27	3.50E-03	285.4	35	1.92E-03	519.9
32_I1007E	18	7.08E-03	141.3	27	3.37E-03	297.0	35	1.83E-03	546.4
32_I1007W	18	7.08E-03	141.3	27	3.37E-03	297.1	35	1.83E-03	546.7
32_H_767W	18	4.61E-03	217.0	27	2.27E-03	440.2	35	1.44E-03	694.0
32_H_990	18	4.40E-03	227.0	27	2.19E-03	456.1	35	1.39E-03	717.1
32_H_991	18	4.40E-03	227.4	27	2.19E-03	457.2	35	1.39E-03	719.2
32_H_993	18	4.37E-03	228.6	27	2.17E-03	461.1	35	1.38E-03	727.1
32_H_995	18	4.36E-03	229.4	27	2.16E-03	463.5	35	1.37E-03	732.1
32_I1149	18	4.22E-03	236.9	27	2.08E-03	480.7	35	1.31E-03	760.8
32_I1002	18	4.21E-03	237.4	27	2.08E-03	481.1	35	1.31E-03	760.5
32_I1086	18	4.21E-03	237.3	27	2.07E-03	482.3	35	1.31E-03	764.5
32_I1001	18	4.21E-03	237.3	27	2.07E-03	482.4	35	1.31E-03	764.7
32_I1087	18	4.21E-03	237.3	27	2.07E-03	482.4	35	1.31E-03	764.6
32_I1000	18	4.21E-03	237.3	27	2.07E-03	482.4	35	1.31E-03	764.8
32_I1088	18	4.21E-03	237.3	27	2.07E-03	482.4	35	1.31E-03	764.6
32_I1173	18	4.21E-03	237.7	27	2.07E-03	484.1	35	1.30E-03	768.4
32_H_997	18	4.24E-03	235.8	27	2.06E-03	484.7	35	1.29E-03	775.6
32_I1171	18	4.21E-03	237.4	27	2.05E-03	488.8	35	1.28E-03	782.9
32_I1089	18	4.20E-03	238.4	27	2.03E-03	493.1	35	1.26E-03	792.7
32_I_770	18	4.39E-03	227.6	27	1.96E-03	511.0	35	1.16E-03	862.1
32_I1093S	18	4.07E-03	245.7	27	1.91E-03	523.4	35	1.17E-03	855.9
32_I1093N	18	4.07E-03	245.8	27	1.91E-03	523.6	35	1.17E-03	856.3
<i>32_I1005W</i>	<i>29</i>	<i>3.04E-03</i>	<i>328.8</i>	<i>59</i>	<i>5.36E-04</i>	<i>1867.1</i>	<i>87</i>	<i>1.93E-04</i>	<i>5174.2</i>

-Note: Bridges that are written in Italic are retrofitted bridges.

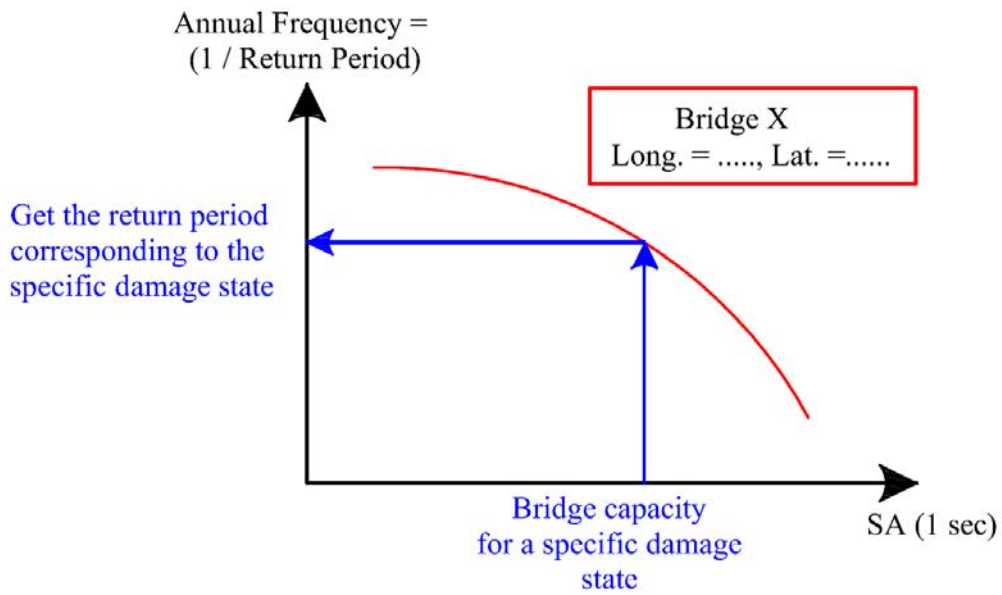


Figure 4.1 Schematic diagram showing how to get the return period corresponding to a specific damage state for a specific bridge

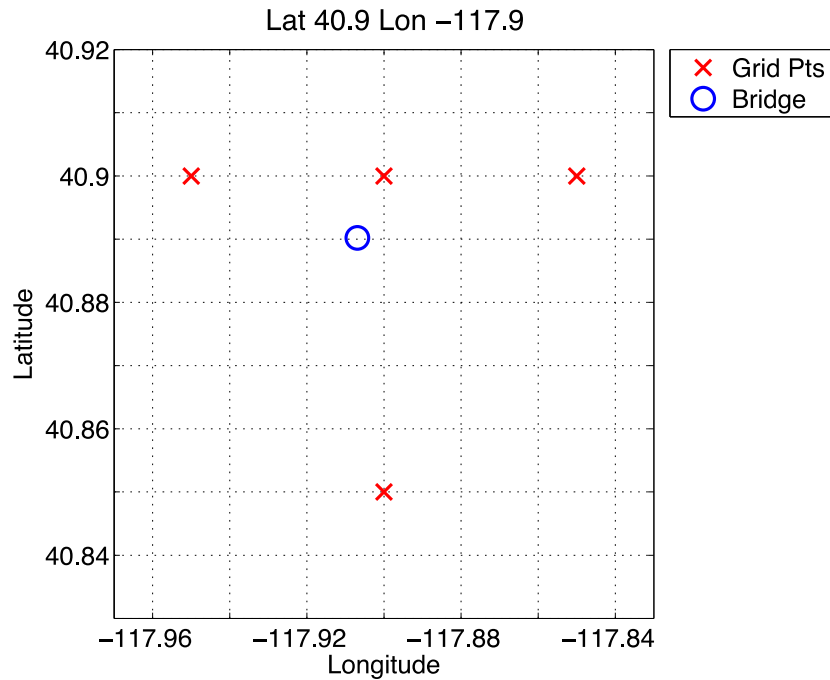


Figure 4.2 Illustration of an NSHM grid point configuration (red “X”) for extrapolating gridded SA(1) to bridge 32_G_863W (blue circle). In this case the four nearest points do not form a rectangle around the bridge. For scale, 0.01 degrees latitude is 900 meters.

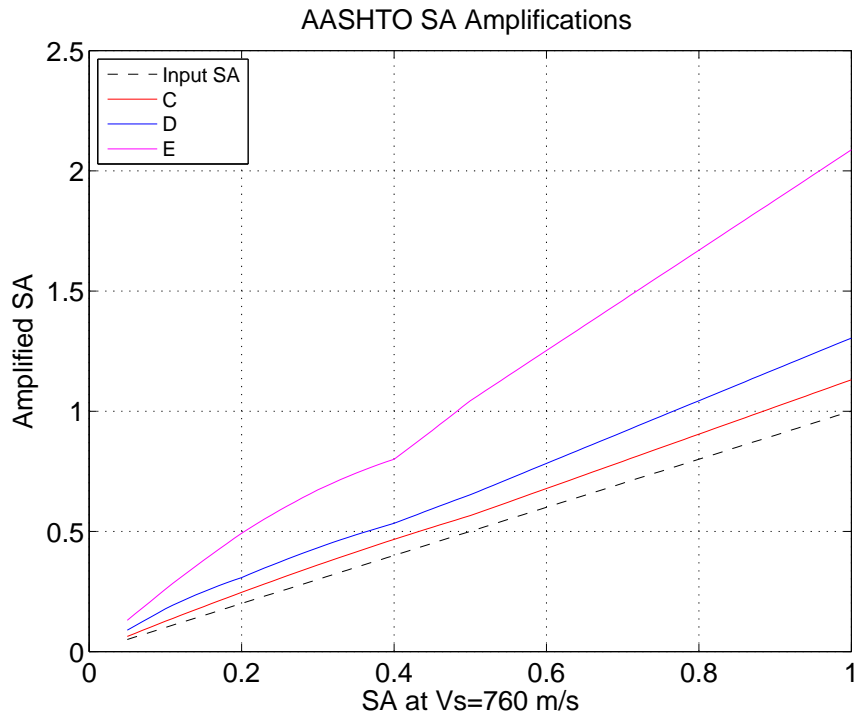


Figure 4.3 Net site amplifications for non-linear corrections and three NEHRP site classes

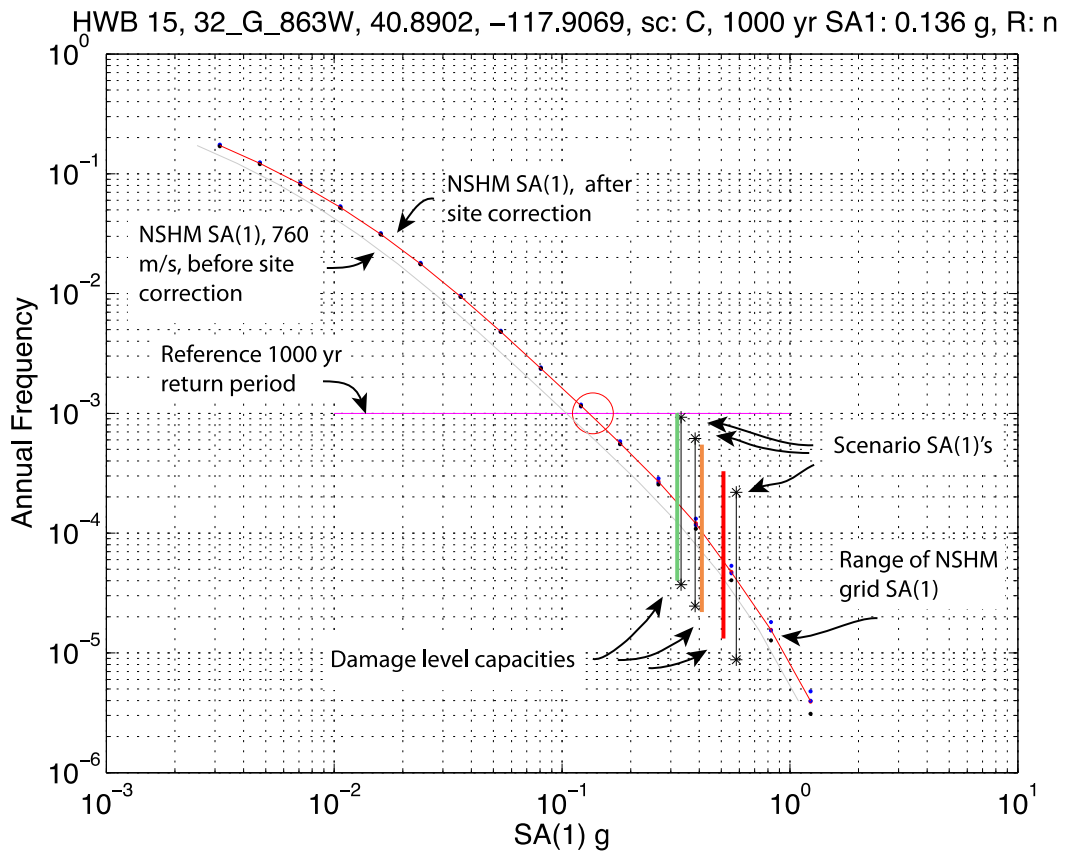


Figure 4.4 Bridge 32_G_863W, near Winnemucca in north-central Nevada. HAZUS category HWB-15, continuous steel girder construction, built before 1983. Data identifying the individual bridge type, bridge identifier, and bridge location are given in the title of each figure. Latitude and longitude are in decimal degrees. An estimated site class is given after the “sc” label, generally either “C” or “D”. Spectral acceleration at a reference return period of 1000 years follows, in units of “g”. The intersection of the reference return period with the hazard curve is circled. The “R: “ refers to bridge seismic retrofit status, followed by “y” or “n” for Yes or No. Small dots near the hazard curve represent discrete values at the four grid points of the NSHM nearest to the bridge. See **Figure 4.2** for the grid map. The spread among these dots is a measure of how spatially variable the hazard estimate is at the bridge site. Vertical green, yellow, orange, and red bars on the hazard curve indicate estimated bridge capacities for the respective damage state bounds in ShakeCast. Black vertical bars show demands from scenarios affecting the bridge where the demand exceeds the “green” damage state bound.

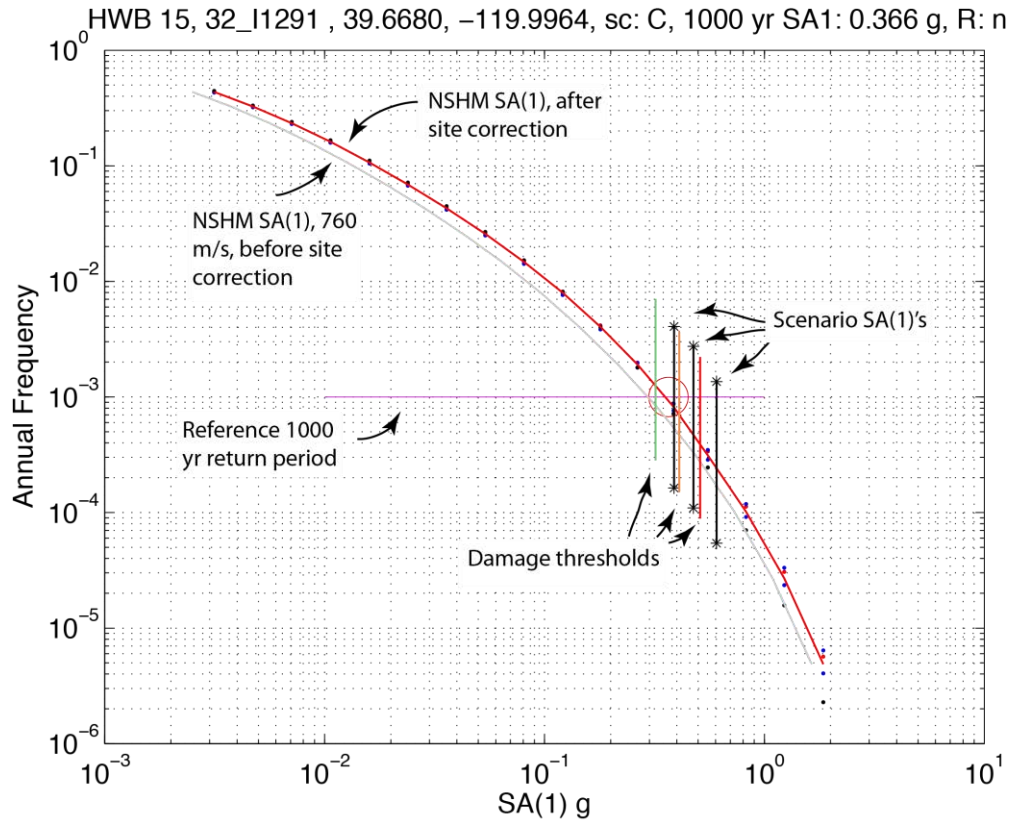


Figure 4.5 Bridge 32_I1291, HAZUS category HWB-15, continuous steel girder construction built before 1983. This bridge in western Nevada near Reno is predicted to experience SA(1) values over 2.5 times larger than the previous example bridge. The detailed figure description is given in **Figure 4.4**.

Chapter 5: Recommendations and Future work

5.1 Recommendations

Demand for Nevada bridges has been estimated by using large scenario earthquakes on mapped Nevada faults. Hazard curves from the USGS National Seismic Hazard Map give a standardized basis for evaluating the relative return times for damaging levels of ground motion at bridge sites. It is recommended that this information be included as objective inputs for setting priorities for bridge retrofit and replacement.

Demands estimated in this project depend on site conditions coming from a variety of sources. Available measured categories have come from the relatively coarse Clark County Parcel Map. Elsewhere soil class estimates are rough categorizations using local geologic and geomorphic assessments. Realistically, site conditions at individual bridge sites could be better or some worse than have been assessed. It is recommended that shallow shear-wave velocity profiles be obtained for bridges considered candidates for retrofit and or replacement. Site condition data would allow NDOT to adjust hazard curves provided in this report and refine relative probabilities among bridges of ground motion exceeding capacity.

ShakeCast has been implemented as a method for extrapolating scenario earthquake ground motions to Nevada bridge sites. It is currently running and evaluating ShakeMaps developed in and near the Nevada region. Alerts are being sent out and earthquake Inspection priority reports are automatically developed. In the event of a damaging earthquake, ShakeCast will provide NDOT with prompt evaluation of potential issues in the bridge inventory. ShakeCast requires a certain level of monthly maintenance expense. In addition, arrangements will be needed to maintain it in a longer-term computing environment. It is recommended that NDOT consider some level of maintenance and upkeep of the ShakeCast system to maintain the ShakeCast capability. This maintenance might be most efficiently achieved by some combination of UNR support and by NDOT participating in a FHWA Transportation Pooled Fund project with other DOTs. Continuing UNR involvement would ensure that local needs and bridge updates to the NBI could be incorporated as they become available. Depending on scope, UNR might be enlisted to integrate emerging research on other bridge types as was shown in this project to be important for some common designs.

FHWA Transportation Pooled Fund (TFP) project would provide for the long-term health of the ShakeCast software system itself. Funding through a TFP would be an appropriate mechanism for multi-state shared engagement with ShakeCast. Support would help ensure the long-term stability of ShakeCast core development and integration among the 36 states that currently have an earthquake hazard.

5.2 Future Research

Our research suggests opportunities to improve understanding of demand and potential earthquake consequences for bridges in Nevada.

True scenario evaluation. ShakeCast results are intrinsically scenario based, but the scenario earthquakes used in this project were not developed to study any individual hazard carefully. Realistic scenarios developed by UNR in collaboration with NDOT could be useful for planning and preparedness evaluation. Scenario earthquakes could also be used to compliment NDOT design evaluations of new or prospective projects. Scenario earthquakes could also be postulated on smaller faults, or in areas of particular interest or importance. It would be useful to ask, using scenario earthquakes, whether there are places in which a background earthquake in the $6 < M < 6.5$ magnitude range could be consequential. Earthquakes in this magnitude range are part of the “background” source used in the USGS National Seismic Hazard Map and not associated with known faults. Scenario evaluation could be approached in phases (e.g., **Figure 3.1**), including immediate evaluation in minutes to perhaps hours, engineering response in hours to days, and repair/reconstruction response that could involve traffic disruption for days to months. Serious disruption of city traffic could have economic consequences.

Attenuation in regressions compared to NV conditions. The Boore and Atkinson (2008) and Chiou and Youngs (2008) regressions are well vetted against global data, but it have not been checked whether either or both produce unbiased predictions using data for Nevada conditions. Regional attenuation studies suggest that California and Nevada have similar attenuation. California data with (the small) available contributions from Nevada could be used to check whether Nevada is well served by either or both of these GMPEs.

Soil conditions. Given the potential importance of site class for earthquake demand, it is very important to take steps to improve confidence in implied site response. Site-specific geophysics at selected bridges would provide a basis for evaluating the uncertainty and consequences of the soil condition estimates we have provided here.

References

- AASHTO (2014). AASHTO LRFD Bridge Design Specifications. *American Association of State Highway and Transportation Officials, Washington, D.C.*
- Abrahamson, N., G. Atkinson, D. Boore, Y. Bozorgnia, K. Campbell, B. Chiou, I. M. Idriss, W. Silva, and R. Youngs (2008). Comparisons of the NGA ground-motion relations, *Earthquake Spectra*, 24 45-66.
- AmiriHormozaki, E. (2013). Analytical Fragility Curves for Horizontally Curved Steel Girder Highway Bridges, *Ph.D. Dissertation, University of Nevada, Reno.*
- ATC (1985). Earthquake Damage Evaluation Data for California, *Report No. ATC-13, Applied Technology Council.*
- Basoz, N. and Kiremidjian, Anne, S. (1996). Risk Assessment of Highway Transportation Systems, *Report No. NCEER-118, John A. Blume Earthquake Engineering Center.*
- Basoz, N. and Kiremidjian, Anne, S. (1997). Evaluation of Bridge Damage Data from the Loma Prieta and Northridge, CA Earthquakes. *Report No. MCEER-98-0004, MCEER.*
- Biasi, G., Mohammed, M. S., and Sanders, D. H., (in press). Earthquake Damage Estimations: ShakeCast Case Study on Nevada Bridges. *Earthquake Spectra.*
- Boore, D. M. and G. M. Atkinson (2008). Ground motion prediction equations for the average horizontal component of PGA, PGV, and 5%-damped PSA at spectral periods between 0.01 and 10.0 s., *Earthquake Spectra*, 24(S1), 99-138.
- Boore, D. M., W. B. Joyner, and T. E. Fumal (1997). Equations for estimating horizontal response spectra and peak acceleration from western North American earthquakes: A summary of recent work, *Seismological Research Letters*, 68, 128-153.
- Chiou, B. S. -J. and R. R. Youngs (2008). Chiou and Youngs PEER-NGA empirical ground motion model for the average horizontal component of peak acceleration and pseudo-spectral acceleration for spectral periods of 0.01 to 10 seconds. *Earthquake Spectra*, 24(S1), 173-216.
- DePolo, C. M. (2012). Damaging earthquakes in Nevada: 1840s to 2010, *Nevada Bureau of Mines and Geology Special Publication 37, (map and text).*
- DePolo, C. M. (2008). *Quaternary faults in Nevada, Nevada Bureau of Mines and Geology Map 167.*
- DePolo, C. M., J. G. Anderson, D. M. DePolo, and J. G. Price (1997). Earthquake occurrence in the Reno-Carson City Urban Corridor, *Seismological Research Letters*, 68, 401-412.

- DePolo, D. M. and C. M. DePolo, (2012). Earthquakes in Nevada, 1840's to 2010, *Nevada Bureau of Mines and Geology Map 179*.
- Der Kiureghian, A. (2002). Bayesian Methods for Seismic Fragility Assessment of Lifeline Components, *Acceptable Risk Processes: Lifelines and Natural Hazards, Monograph No. 21, A. D. Kiureghian, ed., Technical Council on Lifeline Earthquake Engineering, ASCE, Reston VA USA*.
- DesRoches, R., J. Padgett, K. Ramanathan, and J. Dukes (2012). Final Report: Feasibility Studies for Improving Caltrans' Bridge Fragility Relationships, California Department of Transportation Report Number CA12-1775, 540 pp.
- Dutta, A. (1999). On Energy Based Seismic Analysis and Design of Highway Bridges, *PhD thesis, State University of New York at Buffalo*.
- Elnashai, A., Borzi, B., and Vlachos, S. (2004). Deformation-Based Vulnerability Functions for RC Bridges, *Structural Engineering and Mechanics, 17(2), 215–244*.
- FEMA-350 (2000). Recommended seismic design criteria for new steel moment-frame buildings, *Report No. FEMA-350, SAC Joint Venture, Federal Emergency Management Agency, Washington, DC*.
- FEMA-351 (2000). Recommended seismic evaluation and upgrade criteria for existing welded steel moment-frame buildings, *Report No. FEMA-351, SAC Joint Venture, Federal Emergency Management Agency, Washington, DC*.
- Hanks, T. C. and H. Kanamori (1979). A moment magnitude scale, *Journal of Geophysical Research, 84, 2348-2350*.
- HAZUS (1997). Technical Manual, *Federal Emergency Management Agency, Washington DC*.
- HAZUS-MH (2011). Multi-Hazard Loss Estimation Methodology: Earthquake Model HAZUS-MH MR5 Technical Manual, *Federal Emergency Management Agency, Washington DC*.
- House, P. K., H. Green, A. Grimmer, and the Nevada Digital Dirt Mapping Team (2010). Preliminary surficial geologic map of Clark County, Nevada, *Nevada Bureau of Mines and Geology Open File Report 2010-07, Plate 1*.
- Hwang, H., Jernigan, J. B., and Lin, Y.-W. (2000). Evaluation of Seismic Damage to Memphis Bridges and Highway Systems, *Journal of Bridge Engineering, 5(4), p 322–330*.
- Hwang, H., Liu, J. B., and Chiu, Y.-H. (2000). Seismic Fragility Analysis of Highway Bridges, *Report No. MAEC RR-4, Center for Earthquake Research Informaion*.

- Jeong, S. H., Elnashai, A. S. (2007). Probabilistic Fragility Analysis Parameterized by Fundamental Response Quantities, *Engineering Structures*, 29, pp: 1238-1251.
- Kim, S.H. (2002). Fragility analysis of bridges under ground motion with spatial variation, Ph.D. Dissertation. Department of Civil Engineering, University of California, Irvin.
- Kim, S.-H. and Shinozuka, M. (2004). Development of Fragility Curves of Bridges Retrofitted by Column Jacketing, *Probabilistic Engineering Mechanics*, 19, 105–112.
- King SA and Kiremidjian, A (1994). Regional seismic hazard and risk analysis through geographic information systems, *Report No. 111, The John A. Blume Earthquake Engineering Centre*.
- Lay, T. and T. C. Wallace (1995). *Modern Global Seismology*, Academic Press, San Diego, California, 521 p.
- Mackie, K. and Stojadinovic, B. (2004). Fragility Curves for Reinforced Concrete Highway Overpass Bridges, 13th World Conference on Earthquake Engineering, Vancouver, B.C. Canada.
- Mander, J. B. and Basoz, N. (1999). Seismic Fragility Curve Theory for Highway Bridges, *5th US Conference on Lifeline Earthquake Engineering, Seattle, WA, USA. ASCE*.
- Nielson, B. G. (2005). Analytical Fragility Curves for Highway Bridges in Moderate Seismic Zones, *Ph.D. Dissertation, Georgia Institute of Technology, Atlanta, GA*.
- Pancha, A., J. G. Anderson, and C. Kreemer (2006). Comparison of seismic and geodetic scalar moment rates across the Basin and Range Province, *Bulletin of the Seismological Society of America*, 96, 11-32.
- Petersen, M. D., Moschetti, M. P., Powers, P. M., Mueller, C. S., Haller, K. M., Frankel, A. D., Zeng, Y., Rezaeian, S., Harmsen, S. C., Boyd, O. S., Field, E. H., Chen, R., Rukstales, K. S., Luco, N., Wheeler, R. L., Williams, R. A., Olsen, A. H. and K. S. Rukstales (2014). Seismic-hazard maps for the conterminous United States, 2014: U.S. Geological Seismic Investigations Map 3325. <http://pubs.usgs.gov/sim/3325/>.
- Porter, Keith, (2015). A Beginner's Guide to Fragility, Vulnerability, and Risk, *University of Colorado Boulder and SPA Risk LLC, Denver CO USA*
- Ramanathan, K. N. (2012). Next Generation Seismic Fragility Curves For California Bridges Incorporating The Evolution in Seismic Design Philosophy, *Ph.D. Dissertation, Georgia Institute of Technology, Atlanta, GA*.
- Ramanathan, K., DesRoches, R., Padgett, J. E. (2010). Analytical Fragility Curves for Multispan Continuous Steel Girder Bridges in Moderate Seismic Zones,

Transportation Research Record: Journal of the Transportation Research Board, 2202, pp: 173-182.

- Saxena, V. (2000). Spatial variation of earthquake ground motion and development of bridge fragility curves, Ph.D. Dissertation. Department of Civil Engineering and Operations Research, Princeton University, Ann Arbor.
- Scott, J. B., M. Clark, T. Rennie, A. Pancha, H. Park, and J. N. Louie (2004). A Shallow Shear-Wave Velocity Transect across the Reno, Nevada, Area Basin, *Bulletin of the Seismological Society of America*, 94, 2222-2228.
- Seekins, L. C., and J. Boatwright (2010). Rupture Directivity of Moderate Earthquakes in Northern California, *Bulletin of the Seismological Society of America*, 100, 1107-1119.
- Shinozuka, M., Feng, M. Q., Kim, H., Uzawa, T., and Ueda, T. (2003). Statistical Analysis of Fragility Curves, *Report No. MCEER-03-0002*, MCEER.
- Shinozuka, M., Feng, Maria, Q., Lee, J., and Naganuma, T. (2000). Statistical Analysis of Fragility Curves, *Journal of Engineering Mechanics*, 126(12), 1224–1231.
- Turner, L. L., D. Wald, and K-W. Lin (2009). ShakeCast – Developing a tool for rapid post-earthquake response, *CALTRANS Final Report No. CA09-0734, June 2009*, 325 p.
- Wald, D. J., and T. I. Allen (2007). Topographic slope as a proxy for seismic site conditions and amplification, *Bulletin of the Seismological Society of America*, 97, 1379-1395.
- Wald, D., Worden, B. C., Quitoriano, V., and Pankow, K. (2005). ShakeMap Manual: Technical Manual, User's Guide, and Software Guide: US Geological Survey.
- Yamazaki, F., Hamada, T., Motoyama, H., and Yamauchi, H. (1999). Earthquake Damage Assessment of Expressway Bridges in Japan, *Technical Council on Lifeline Earthquake Engineering Monograph*, (16), p 361–370.
- Yu, O., Allen, D. L., and Drnevich, V. P. (1991). Seismic Vulnerability Assessment of Bridges on Earthquake Priority Routes in Western Kentucky, *3rd US Conference on Lifeline Earthquake Engineering, Los Angeles, CA, USA. ASCE*.

APPENDIX A: Demand vs. Capacity

This Appendix presents vulnerable bridges, with scenario demands in PGA, PGV, and SA(1). The year built, reported retrofit status and estimated site class are also shown. Damage State includes the name and ShakeCast color designation. Scenarios with a common root name but differing at the end with labels BA or CY refer to a single fault source but run with the BA08 and CY08 GMPE's, respectively.

Table A.1 Bridges of type HWB10-205 (Demand vs Capacity)

Bridge ID	PGA	PGV	SA (1 sec)	Year Built	Retrofitted?	Scenario	Damage State	Site Class
32_B1544N	28.98	26.68	31.45	1968	no	Frenchman_Mntn_M6.6BA_se	Orange	C
32_B1544N	25.18	28.02	24.93	1968	no	Frenchman_Mntn_M6.6CY_se	Yellow	
32_B1544S	28.98	26.68	31.45	1968	no	Frenchman_Mntn_M6.6BA_se	Orange	C
32_B1544S	25.18	28.02	24.93	1968	no	Frenchman_Mntn_M6.6CY_se	Yellow	
32_B_839S	40.67	46.83	55.22	1961	no	California_Wash_M6.9BA_se	Red	C
32_B_839S	41.97	62.98	56.1	1961	no	California_Wash_M6.9CY_se	Red	
32_B_954N	35.34	31.84	40.12	1970	no	Eglington_M6.3BA_se	Red	D
32_B_954N	28.21	37.17	32.77	1970	no	Eglington_M6.3CY_se	Orange	
32_B_954N	39.04	40.19	52.31	1970	no	Frenchman_Mntn_M6.6BA_se	Red	
32_B_954N	27.56	37.52	33.93	1970	no	Frenchman_Mntn_M6.6CY_se	Orange	
32_B_954S	35.34	31.84	40.12	1970	no	Eglington_M6.3BA_se	Red	D
32_B_954S	28.21	37.17	32.77	1970	no	Eglington_M6.3CY_se	Orange	
32_B_954S	39.04	40.19	52.31	1970	no	Frenchman_Mntn_M6.6BA_se	Red	
32_B_954S	27.56	37.52	33.93	1970	no	Frenchman_Mntn_M6.6CY_se	Orange	
32_G1153	26.11	30.83	32.82	1967	no	Grass_Valley_M7.1BA_se	Orange	C
32_G1153	33.02	48.34	44.05	1967	no	Grass_Valley_M7.1CY_se	Red	
32_G_925E	20.08	20.63	20.97	1974	no	Independence_V_M7.2BA_se	Yellow	D
32_G_925E	21.82	28.87	26.89	1974	no	Independence_V_M7.2CY_se	Yellow	
32_G_925W	20.44	21.33	21.81	1974	no	Independence_V_M7.2BA_se	Yellow	D
32_G_925W	22.11	29.86	27.85	1974	no	Independence_V_M7.2CY_se	Orange	
32_G_941	31.84	25.1	28.98	1968	no	Eglington_M6.3BA_se	Orange	C
32_G_941	24.91	26.79	23.25	1968	no	Eglington_M6.3CY_se	Yellow	
32_G_941	37.03	32.48	38.78	1968	no	Frenchman_Mntn_M6.6BA_se	Red	
32_G_941	23.99	26.68	23.81	1968	no	Frenchman_Mntn_M6.6CY_se	Yellow	
32_G_947	31.84	25.1	28.98	1968	no	Eglington_M6.3BA_se	Orange	C
32_G_947	24.91	26.79	23.25	1968	no	Eglington_M6.3CY_se	Yellow	
32_G_947	37.03	32.48	38.78	1968	no	Frenchman_Mntn_M6.6BA_se	Red	
32_G_947	23.99	26.68	23.81	1968	no	Frenchman_Mntn_M6.6CY_se	Yellow	
32_G_953	34.56	29.24	35.62	1971	no	Eglington_M6.3BA_se	Red	D
32_G_953	27.12	32.89	28.77	1971	no	Eglington_M6.3CY_se	Orange	
32_G_953	38.23	36.93	46.44	1971	no	Frenchman_Mntn_M6.6BA_se	Red	
32_G_953	27.12	34.23	30.71	1971	no	Frenchman_Mntn_M6.6CY_se	Orange	
32_G_961N	27.34	24.79	29.81	1963	yes	Eglington_M6.3BA_se	Yellow	

Bridge ID	PGA	PGV	SA (1 sec)	Year Built	Retrofitted?	Scenario	Damage State	Site Class
32_G_961N	27.12	33.15	29.02	1963	yes	Eglington_M6.3CY_se	Yellow	C
32_G_961N	35.16	35.83	45.12	1963	yes	Frenchman_Mntn_M6.6BA_se	Yellow	
32_G_961N	30.8	40.82	36.48	1963	yes	Frenchman_Mntn_M6.6CY_se	Yellow	
32_G_961S	27.34	24.79	29.81	1963	yes	Eglington_M6.3BA_se	Yellow	C
32_G_961S	27.12	33.15	29.02	1963	yes	Eglington_M6.3CY_se	Yellow	
32_G_961S	35.16	35.83	45.12	1963	yes	Frenchman_Mntn_M6.6BA_se	Yellow	
32_G_961S	30.8	40.82	36.48	1963	yes	Frenchman_Mntn_M6.6CY_se	Yellow	
32_H1003	21.46	19.78	24.55	1969	no	Freds_Mountain_M6.8BA_se	Yellow	D
32_H1003	23.5	30.6	28.07	1969	no	Freds_Mountain_M6.8CY_se	Orange	
32_H1003	28.78	33.24	39.07	1969	no	Mount_Rose_M6.9BA_se	Red	
32_H1003	29.46	40.99	37.36	1969	no	Mount_Rose_M6.9CY_se	Red	
32_H1003	17.24	20.36	18.41	1969	no	Peavine_Peak_M6.4CY_se	Yellow	
32_H1003	17.79	14.42	18.33	1969	no	Petersen_Mountain_M6.7BA_se	Yellow	
32_H1003	25.17	24.58	30.93	1969	no	Spanish_Springs_V_M6.6BA_se	Orange	
32_H1003	34.51	48.41	43.15	1969	no	Spanish_Springs_V_M6.6CY_se	Red	
32_H1042	25.08	22.5	27.01	1964	yes	Eglington_M6.3BA_se	Green	C
32_H1042	24.69	29.69	26.11	1964	yes	Eglington_M6.3CY_se	Green	
32_H1042	35.04	35.52	44.59	1964	yes	Frenchman_Mntn_M6.6BA_se	Yellow	
32_H1042	22.79	28.06	25.41	1964	yes	Frenchman_Mntn_M6.6CY_se	Green	
32_H_767W	24.8	23.22	24.75	1966	no	Mount_Rose_M6.9BA_se	Yellow	C
32_H_767W	35.23	40.76	35.87	1966	no	Mount_Rose_M6.9CY_se	Red	
32_H_767W	21.98	21.65	18.92	1966	no	Peavine_Peak_M6.4CY_se	Yellow	
32_H_788	20.01	16.48	20.02	2012	yes	Frenchman_Mntn_M6.6BA_se	Green	C
32_H_856	42.72	65.25	64.67	1976	no	W_Humboldt_Range_M7.3BA_se	Red	D
32_H_856	44.38	75.7	68.19	1976	no	W_Humboldt_Range_M7.3CY_se	Red	
32_H_866E	21.53	19.92	24.76	1966	no	Freds_Mountain_M6.8BA_se	Yellow	D
32_H_866E	22.75	29.57	27.17	1966	no	Freds_Mountain_M6.8CY_se	Orange	
32_H_866E	29.2	34.01	39.99	1966	no	Mount_Rose_M6.9BA_se	Red	
32_H_866E	28.07	38.64	35.32	1966	no	Mount_Rose_M6.9CY_se	Red	
32_H_866E	26.72	26.96	34.01	1966	no	Spanish_Springs_V_M6.6BA_se	Orange	
32_H_866E	37.01	53.31	47.36	1966	no	Spanish_Springs_V_M6.6CY_se	Red	
32_H_866W	21.53	19.92	24.76	1966	no	Freds_Mountain_M6.8BA_se	Yellow	D
32_H_866W	22.75	29.57	27.17	1966	no	Freds_Mountain_M6.8CY_se	Orange	
32_H_866W	29.2	34.01	39.99	1966	no	Mount_Rose_M6.9BA_se	Red	
32_H_866W	28.07	38.64	35.32	1966	no	Mount_Rose_M6.9CY_se	Red	
32_H_866W	26.72	26.96	34.01	1966	no	Spanish_Springs_V_M6.6BA_se	Orange	
32_H_866W	37.01	53.31	47.36	1966	no	Spanish_Springs_V_M6.6CY_se	Red	
32_H_918E	21.71	22.2	23.18	1976	no	Ruby_Mountains_M7.1BA_se	Yellow	C
32_H_918E	18.4	22.47	20.94	1976	no	Ruby_Mountains_M7.1CY_se	Yellow	
32_H_918W	19.16	18.57	19.72	1976	no	Ruby_Mountains_M7.1BA_se	Yellow	C
32_H_918W	15.67	19.53	18.41	1976	no	Ruby_Mountains_M7.1CY_se	Yellow	
32_H_933	25.08	22.5	27.01	1966	no	Eglington_M6.3BA_se	Orange	

Bridge ID	PGA	PGV	SA (1 sec)	Year Built	Retrofitted?	Scenario	Damage State	Site Class
32_H_933	24.69	29.69	26.11	1966	no	Eglington_M6.3CY_se	Yellow	C
32_H_933	32.49	33.16	41.32	1966	no	Frenchman_Mntn_M6.6BA_se	Red	
32_H_933	22.03	26.78	24.26	1966	no	Frenchman_Mntn_M6.6CY_se	Yellow	
32_H_935	29.3	26.22	31.49	1970	no	Eglington_M6.3BA_se	Orange	C
32_H_935	27.63	33.53	29.29	1970	no	Eglington_M6.3CY_se	Orange	
32_H_935	35.04	35.52	44.59	1970	no	Frenchman_Mntn_M6.6BA_se	Red	
32_H_935	22.79	28.06	25.41	1970	no	Frenchman_Mntn_M6.6CY_se	Yellow	
32_H_936	29.3	26.22	31.49	1968	yes	Eglington_M6.3BA_se	Yellow	C
32_H_936	27.63	33.53	29.29	1968	yes	Eglington_M6.3CY_se	Yellow	
32_H_936	37.18	36.28	45.43	1968	yes	Frenchman_Mntn_M6.6BA_se	Yellow	
32_H_936	23.03	28	25.3	1968	yes	Frenchman_Mntn_M6.6CY_se	Green	
32_H_946	31.84	25.1	28.98	1968	yes	Eglington_M6.3BA_se	Green	C
32_H_946	24.91	26.79	23.25	1968	yes	Eglington_M6.3CY_se	Green	
32_H_946	37.03	32.48	38.78	1968	yes	Frenchman_Mntn_M6.6BA_se	Yellow	
32_H_946	23.99	26.68	23.81	1968	yes	Frenchman_Mntn_M6.6CY_se	Green	
32_H_970	21.8	19.87	22.05	1963	no	California_Wash_M6.9BA_se	Yellow	C
32_H_970	19.91	21.99	20.08	1963	no	California_Wash_M6.9CY_se	Yellow	
32_H_970	20.71	16.89	20	1963	no	Frenchman_Mntn_M6.6BA_se	Yellow	
32_H_970	28.55	32.52	28.74	1963	no	Frenchman_Mntn_M6.6CY_se	Orange	
32_H_990	20.53	17.99	21.79	1970	no	Freds_Mountain_M6.8BA_se	Yellow	C
32_H_990	24.75	30.49	27.69	1970	no	Freds_Mountain_M6.8CY_se	Orange	
32_H_990	27.4	30.46	35.52	1970	no	Mount_Rose_M6.9BA_se	Red	
32_H_990	33.91	47.95	43.28	1970	no	Mount_Rose_M6.9CY_se	Red	
32_H_990	21.48	25.79	23.08	1970	no	Peavine_Peak_M6.4CY_se	Yellow	
32_H_990	20.61	17.65	21.86	1970	no	Spanish_Springs_V_M6.6BA_se	Yellow	
32_H_990	26.48	33.25	29.87	1970	no	Spanish_Springs_V_M6.6CY_se	Orange	
32_H_991	20.53	17.99	21.79	1969	no	Freds_Mountain_M6.8BA_se	Yellow	C
32_H_991	24.75	30.49	27.69	1969	no	Freds_Mountain_M6.8CY_se	Orange	
32_H_991	27.4	30.46	35.52	1969	no	Mount_Rose_M6.9BA_se	Red	
32_H_991	33.91	47.95	43.28	1969	no	Mount_Rose_M6.9CY_se	Red	
32_H_991	21.48	25.79	23.08	1969	no	Peavine_Peak_M6.4CY_se	Yellow	
32_H_991	20.61	17.65	21.86	1969	no	Spanish_Springs_V_M6.6BA_se	Yellow	
32_H_991	26.48	33.25	29.87	1969	no	Spanish_Springs_V_M6.6CY_se	Orange	
32_H_993	21.22	19.31	23.84	1970	no	Freds_Mountain_M6.8BA_se	Yellow	C
32_H_993	24.67	31.96	29.19	1970	no	Freds_Mountain_M6.8CY_se	Orange	
32_H_993	27.52	30.41	35.22	1970	no	Mount_Rose_M6.9BA_se	Red	
32_H_993	32.51	44.65	40.31	1970	no	Mount_Rose_M6.9CY_se	Red	
32_H_993	23.4	27.92	24.82	1970	no	Peavine_Peak_M6.4CY_se	Yellow	
32_H_993	22.2	20.08	25.12	1970	no	Spanish_Springs_V_M6.6BA_se	Yellow	
32_H_993	29.17	38.57	34.61	1970	no	Spanish_Springs_V_M6.6CY_se	Orange	
32_H_995	22.53	21.08	25.77	1969	no	Freds_Mountain_M6.8BA_se	Yellow	C
32_H_995	27.63	35.85	32.49	1969	no	Freds_Mountain_M6.8CY_se	Orange	

Bridge ID	PGA	PGV	SA (1 sec)	Year Built	Retrofitted?	Scenario	Damage State	Site Class
32_H_995	27.52	30.41	35.22	1969	no	Mount_Rose_M6.9BA_se	Red	
32_H_995	32.51	44.65	40.31	1969	no	Mount_Rose_M6.9CY_se	Red	
32_H_995	23.4	27.92	24.82	1969	no	Peavine_Peak_M6.4CY_se	Yellow	
32_H_995	22.2	20.08	25.12	1969	no	Spanish_Springs_V_M6.6BA_se	Yellow	
32_H_995	29.17	38.57	34.61	1969	no	Spanish_Springs_V_M6.6CY_se	Orange	
32_H_997	22.53	21.08	25.77	1970	no	Freds_Mountain_M6.8BA_se	Yellow	C
32_H_997	27.63	35.85	32.49	1970	no	Freds_Mountain_M6.8CY_se	Orange	
32_H_997	27.52	30.41	35.22	1970	no	Mount_Rose_M6.9BA_se	Red	
32_H_997	32.51	44.65	40.31	1970	no	Mount_Rose_M6.9CY_se	Red	
32_H_997	21.63	26.15	23.41	1970	no	Peavine_Peak_M6.4CY_se	Yellow	
32_H_997	22.2	20.08	25.12	1970	no	Spanish_Springs_V_M6.6BA_se	Yellow	
32_H_997	29.17	38.57	34.61	1970	no	Spanish_Springs_V_M6.6CY_se	Orange	
32_I1000	22.93	21.93	27.11	1969	no	Freds_Mountain_M6.8BA_se	Orange	C
32_I1000	26.94	35.76	32.56	1969	no	Freds_Mountain_M6.8CY_se	Orange	
32_I1000	28.33	32.37	37.98	1969	no	Mount_Rose_M6.9BA_se	Red	
32_I1000	30.97	43.45	39.48	1969	no	Mount_Rose_M6.9CY_se	Red	
32_I1000	19.99	24.23	21.8	1969	no	Peavine_Peak_M6.4CY_se	Yellow	
32_I1000	17.79	14.42	18.33	1969	no	Petersen_Mountain_M6.7BA_se	Yellow	
32_I1000	23.78	22.54	28.4	1969	no	Spanish_Springs_V_M6.6BA_se	Orange	
32_I1000	31.85	43.86	39.27	1969	no	Spanish_Springs_V_M6.6CY_se	Red	
32_I1001	22.93	21.93	27.11	1969	no	Freds_Mountain_M6.8BA_se	Orange	C
32_I1001	26.94	35.76	32.56	1969	no	Freds_Mountain_M6.8CY_se	Orange	
32_I1001	28.33	32.37	37.98	1969	no	Mount_Rose_M6.9BA_se	Red	
32_I1001	30.97	43.45	39.48	1969	no	Mount_Rose_M6.9CY_se	Red	
32_I1001	19.99	24.23	21.8	1969	no	Peavine_Peak_M6.4CY_se	Yellow	
32_I1001	17.79	14.42	18.33	1969	no	Petersen_Mountain_M6.7BA_se	Yellow	
32_I1001	23.78	22.54	28.4	1969	no	Spanish_Springs_V_M6.6BA_se	Orange	
32_I1001	31.85	43.86	39.27	1969	no	Spanish_Springs_V_M6.6CY_se	Red	
32_I1002	23.18	22.47	27.96	1969	no	Freds_Mountain_M6.8BA_se	Orange	C
32_I1002	26.04	34.9	31.89	1969	no	Freds_Mountain_M6.8CY_se	Orange	
32_I1002	28.78	33.24	39.07	1969	no	Mount_Rose_M6.9BA_se	Red	
32_I1002	29.46	40.99	37.36	1969	no	Mount_Rose_M6.9CY_se	Red	
32_I1002	19.99	24.23	21.8	1969	no	Peavine_Peak_M6.4CY_se	Yellow	
32_I1002	17.79	14.42	18.33	1969	no	Petersen_Mountain_M6.7BA_se	Yellow	
32_I1002	25.17	24.58	30.93	1969	no	Spanish_Springs_V_M6.6BA_se	Orange	
32_I1002	34.51	48.41	43.15	1969	no	Spanish_Springs_V_M6.6CY_se	Red	
32_I1005E	21.53	19.92	24.76	1968	yes	Freds_Mountain_M6.8BA_se	Green	C
32_I1005E	22.75	29.57	27.17	1968	yes	Freds_Mountain_M6.8CY_se	Green	
32_I1005E	29.2	34.01	39.99	1968	yes	Mount_Rose_M6.9BA_se	Yellow	
32_I1005E	28.07	38.64	35.32	1968	yes	Mount_Rose_M6.9CY_se	Yellow	
32_I1005E	17.24	20.36	18.41	1968	yes	Peavine_Peak_M6.4CY_se	Green	
32_I1005E	26.72	26.96	34.01	1968	yes	Spanish_Springs_V_M6.6BA_se	Yellow	
32_I1005E	37.01	53.31	47.36	1968	yes	Spanish_Springs_V_M6.6CY_se	Yellow	

Bridge ID	PGA	PGV	SA (1 sec)	Year Built	Retrofitted?	Scenario	Damage State	Site Class
32_I1005W	21.53	19.92	24.76	1968	yes	Freds_Mountain_M6.8BA_se	Green	D
32_I1005W	22.75	29.57	27.17	1968	yes	Freds_Mountain_M6.8CY_se	Green	
32_I1005W	29.2	34.01	39.99	1968	yes	Mount_Rose_M6.9BA_se	Yellow	
32_I1005W	28.07	38.64	35.32	1968	yes	Mount_Rose_M6.9CY_se	Yellow	
32_I1005W	17.24	20.36	18.41	1968	yes	Peavine_Peak_M6.4CY_se	Green	
32_I1005W	26.72	26.96	34.01	1968	yes	Spanish_Springs_V_M6.6BA_se	Yellow	
32_I1005W	37.01	53.31	47.36	1968	yes	Spanish_Springs_V_M6.6CY_se	Yellow	
32_I1007E	21.57	19.99	24.85	1964	no	Freds_Mountain_M6.8BA_se	Yellow	D
32_I1007E	21.94	28.34	26.09	1964	no	Freds_Mountain_M6.8CY_se	Yellow	
32_I1007E	29.75	35.14	41.48	1964	no	Mount_Rose_M6.9BA_se	Red	
32_I1007E	26.78	36.79	33.74	1964	no	Mount_Rose_M6.9CY_se	Orange	
32_I1007E	27.82	28.76	36.49	1964	no	Spanish_Springs_V_M6.6BA_se	Red	
32_I1007E	38.33	56.63	50.3	1964	no	Spanish_Springs_V_M6.6CY_se	Red	
32_I1007W	21.57	19.99	24.85	1964	no	Freds_Mountain_M6.8BA_se	Yellow	D
32_I1007W	21.94	28.34	26.09	1964	no	Freds_Mountain_M6.8CY_se	Yellow	
32_I1007W	29.75	35.14	41.48	1964	no	Mount_Rose_M6.9BA_se	Red	
32_I1007W	26.78	36.79	33.74	1964	no	Mount_Rose_M6.9CY_se	Orange	
32_I1007W	27.82	28.76	36.49	1964	no	Spanish_Springs_V_M6.6BA_se	Red	
32_I1007W	38.33	56.63	50.3	1964	no	Spanish_Springs_V_M6.6CY_se	Red	
32_I1010	21.46	19.78	24.55	1969	no	Freds_Mountain_M6.8BA_se	Yellow	D
32_I1010	23.5	30.6	28.07	1969	no	Freds_Mountain_M6.8CY_se	Orange	
32_I1010	28.78	33.24	39.07	1969	no	Mount_Rose_M6.9BA_se	Red	
32_I1010	29.46	40.99	37.36	1969	no	Mount_Rose_M6.9CY_se	Red	
32_I1010	18.43	21.96	19.81	1969	no	Peavine_Peak_M6.4CY_se	Yellow	
32_I1010	17.79	14.42	18.33	1969	no	Petersen_Mountain_M6.7BA_se	Yellow	
32_I1010	25.17	24.58	30.93	1969	no	Spanish_Springs_V_M6.6BA_se	Orange	
32_I1010	34.51	48.41	43.15	1969	no	Spanish_Springs_V_M6.6CY_se	Red	
32_I1075N	18.92	18.32	19.57	1963	no	W_Spring_Mntns_M7.1BA_se	Yellow	C
32_I1075N	19.37	25.24	23.62	1963	no	W_Spring_Mntns_M7.1CY_se	Yellow	
32_I1075S	18.92	18.32	19.57	1963	no	W_Spring_Mntns_M7.1BA_se	Yellow	C
32_I1075S	19.37	25.24	23.62	1963	no	W_Spring_Mntns_M7.1CY_se	Yellow	
32_I1086	22.93	21.93	27.11	1969	no	Freds_Mountain_M6.8BA_se	Orange	C
32_I1086	26.94	35.76	32.56	1969	no	Freds_Mountain_M6.8CY_se	Orange	
32_I1086	28.33	32.37	37.98	1969	no	Mount_Rose_M6.9BA_se	Red	
32_I1086	30.97	43.45	39.48	1969	no	Mount_Rose_M6.9CY_se	Red	
32_I1086	19.99	24.23	21.8	1969	no	Peavine_Peak_M6.4CY_se	Yellow	
32_I1086	17.79	14.42	18.33	1969	no	Petersen_Mountain_M6.7BA_se	Yellow	
32_I1086	23.78	22.54	28.4	1969	no	Spanish_Springs_V_M6.6BA_se	Orange	
32_I1086	31.85	43.86	39.27	1969	no	Spanish_Springs_V_M6.6CY_se	Red	
32_I1087	23.18	22.47	27.96	1969	no	Freds_Mountain_M6.8BA_se	Orange	C
32_I1087	26.04	34.9	31.89	1969	no	Freds_Mountain_M6.8CY_se	Orange	
32_I1087	28.33	32.37	37.98	1969	no	Mount_Rose_M6.9BA_se	Red	

Bridge ID	PGA	PGV	SA (1 sec)	Year Built	Retrofitted?	Scenario	Damage State	Site Class
32_I1087	30.97	43.45	39.48	1969	no	Mount_Rose_M6.9CY_se	Red	
32_I1087	19.99	24.23	21.8	1969	no	Peavine_Peak_M6.4CY_se	Yellow	
32_I1087	17.79	14.42	18.33	1969	no	Petersen_Mountain_M6.7BA_se	Yellow	
32_I1087	23.78	22.54	28.4	1969	no	Spanish_Springs_V_M6.6BA_se	Orange	
32_I1087	31.85	43.86	39.27	1969	no	Spanish_Springs_V_M6.6CY_se	Red	
32_I1088	23.18	22.47	27.96	1969	no	Freds_Mountain_M6.8BA_se	Orange	C
32_I1088	26.04	34.9	31.89	1969	no	Freds_Mountain_M6.8CY_se	Orange	
32_I1088	28.33	32.37	37.98	1969	no	Mount_Rose_M6.9BA_se	Red	
32_I1088	30.97	43.45	39.48	1969	no	Mount_Rose_M6.9CY_se	Red	
32_I1088	19.99	24.23	21.8	1969	no	Peavine_Peak_M6.4CY_se	Yellow	
32_I1088	17.79	14.42	18.33	1969	no	Petersen_Mountain_M6.7BA_se	Yellow	
32_I1088	23.78	22.54	28.4	1969	no	Spanish_Springs_V_M6.6BA_se	Orange	
32_I1088	31.85	43.86	39.27	1969	no	Spanish_Springs_V_M6.6CY_se	Red	
32_I1089	22.93	21.93	27.11	1967	no	Freds_Mountain_M6.8BA_se	Orange	C
32_I1089	26.94	35.76	32.56	1967	no	Freds_Mountain_M6.8CY_se	Orange	
32_I1089	25.64	27.68	32.6	1967	no	Mount_Rose_M6.9BA_se	Orange	
32_I1089	28.29	39.08	35.71	1967	no	Mount_Rose_M6.9CY_se	Red	
32_I1089	19.99	24.23	21.8	1967	no	Peavine_Peak_M6.4CY_se	Yellow	
32_I1089	17.79	14.42	18.33	1967	no	Petersen_Mountain_M6.7BA_se	Yellow	
32_I1089	24.29	22.28	27.11	1967	no	Spanish_Springs_V_M6.6BA_se	Orange	
32_I1089	34.74	44.62	39.36	1967	no	Spanish_Springs_V_M6.6CY_se	Red	
32_I1093N	30.65	31.1	36.28	1967	no	Freds_Mountain_M6.8BA_se	Red	C
32_I1093N	41.64	54.28	47.56	1967	no	Freds_Mountain_M6.8CY_se	Red	
32_I1093N	20.68	18.95	21.74	1967	no	Mount_Rose_M6.9BA_se	Yellow	
32_I1093N	23.86	29.41	26.86	1967	no	Mount_Rose_M6.9CY_se	Yellow	
32_I1093N	24.06	21.98	26.83	1967	no	Peavine_Peak_M6.4BA_se	Yellow	
32_I1093N	28.1	35.71	31.59	1967	no	Peavine_Peak_M6.4CY_se	Orange	
32_I1093N	20.47	16.9	20.37	1967	no	Petersen_Mountain_M6.7BA_se	Yellow	
32_I1093N	22.13	19.94	24.9	1967	no	Spanish_Springs_V_M6.6BA_se	Yellow	
32_I1093N	29.16	38.35	34.39	1967	no	Spanish_Springs_V_M6.6CY_se	Orange	
32_I1093S	30.65	31.1	36.28	1967	no	Freds_Mountain_M6.8BA_se	Red	C
32_I1093S	41.64	54.28	47.56	1967	no	Freds_Mountain_M6.8CY_se	Red	
32_I1093S	20.68	18.95	21.74	1967	no	Mount_Rose_M6.9BA_se	Yellow	
32_I1093S	23.86	29.41	26.86	1967	no	Mount_Rose_M6.9CY_se	Yellow	
32_I1093S	24.06	21.98	26.83	1967	no	Peavine_Peak_M6.4BA_se	Yellow	
32_I1093S	28.1	35.71	31.59	1967	no	Peavine_Peak_M6.4CY_se	Orange	
32_I1093S	20.47	16.9	20.37	1967	no	Petersen_Mountain_M6.7BA_se	Yellow	
32_I1093S	22.13	19.94	24.9	1967	no	Spanish_Springs_V_M6.6BA_se	Yellow	
32_I1093S	29.16	38.35	34.39	1967	no	Spanish_Springs_V_M6.6CY_se	Orange	
32_I1149	22.93	21.93	27.11	1969	no	Freds_Mountain_M6.8BA_se	Orange	C
32_I1149	26.94	35.76	32.56	1969	no	Freds_Mountain_M6.8CY_se	Orange	
32_I1149	28.33	32.37	37.98	1969	no	Mount_Rose_M6.9BA_se	Red	
32_I1149	30.97	43.45	39.48	1969	no	Mount_Rose_M6.9CY_se	Red	

Bridge ID	PGA	PGV	SA (1 sec)	Year Built	Retrofitted?	Scenario	Damage State	Site Class
32_I1149	19.99	24.23	21.8	1969	no	Peavine_Peak_M6.4CY_se	Yellow	
32_I1149	17.79	14.42	18.33	1969	no	Petersen_Mountain_M6.7BA_se	Yellow	
32_I1149	23.78	22.54	28.4	1969	no	Spanish_Springs_V_M6.6BA_se	Orange	
32_I1149	31.85	43.86	39.27	1969	no	Spanish_Springs_V_M6.6CY_se	Red	
32_I1159E	21.37	21.11	19.89	1973	no	Independence_V_M7.2BA_se	Yellow	C
32_I1159E	28.09	32.5	29.28	1973	no	Independence_V_M7.2CY_se	Orange	
32_I1159W	21.37	21.11	19.89	1973	no	Independence_V_M7.2BA_se	Yellow	C
32_I1159W	28.09	32.5	29.28	1973	no	Independence_V_M7.2CY_se	Orange	
32_I1171	22.93	21.93	27.11	1969	no	Freds_Mountain_M6.8BA_se	Orange	C
32_I1171	26.94	35.76	32.56	1969	no	Freds_Mountain_M6.8CY_se	Orange	
32_I1171	28.33	32.37	37.98	1969	no	Mount_Rose_M6.9BA_se	Red	
32_I1171	30.97	43.45	39.48	1969	no	Mount_Rose_M6.9CY_se	Red	
32_I1171	19.99	24.23	21.8	1969	no	Peavine_Peak_M6.4CY_se	Yellow	
32_I1171	17.79	14.42	18.33	1969	no	Petersen_Mountain_M6.7BA_se	Yellow	
32_I1171	23.78	22.54	28.4	1969	no	Spanish_Springs_V_M6.6BA_se	Orange	
32_I1171	31.85	43.86	39.27	1969	no	Spanish_Springs_V_M6.6CY_se	Red	
32_I1172	22.93	21.93	27.11	1969	no	Freds_Mountain_M6.8BA_se	Orange	D
32_I1172	26.94	35.76	32.56	1969	no	Freds_Mountain_M6.8CY_se	Orange	
32_I1172	28.33	32.37	37.98	1969	no	Mount_Rose_M6.9BA_se	Red	
32_I1172	30.97	43.45	39.48	1969	no	Mount_Rose_M6.9CY_se	Red	
32_I1172	19.99	24.23	21.8	1969	no	Peavine_Peak_M6.4CY_se	Yellow	
32_I1172	17.79	14.42	18.33	1969	no	Petersen_Mountain_M6.7BA_se	Yellow	
32_I1172	23.78	22.54	28.4	1969	no	Spanish_Springs_V_M6.6BA_se	Orange	
32_I1172	31.85	43.86	39.27	1969	no	Spanish_Springs_V_M6.6CY_se	Red	
32_I1173	23.18	22.47	27.96	1969	no	Freds_Mountain_M6.8BA_se	Orange	C
32_I1173	26.04	34.9	31.89	1969	no	Freds_Mountain_M6.8CY_se	Orange	
32_I1173	28.33	32.37	37.98	1969	no	Mount_Rose_M6.9BA_se	Red	
32_I1173	30.97	43.45	39.48	1969	no	Mount_Rose_M6.9CY_se	Red	
32_I1173	19.99	24.23	21.8	1969	no	Peavine_Peak_M6.4CY_se	Yellow	
32_I1173	17.79	14.42	18.33	1969	no	Petersen_Mountain_M6.7BA_se	Yellow	
32_I1173	23.78	22.54	28.4	1969	no	Spanish_Springs_V_M6.6BA_se	Orange	
32_I1173	31.85	43.86	39.27	1969	no	Spanish_Springs_V_M6.6CY_se	Red	
32_I1250	19.4	16.54	20.14	1980	no	Freds_Mountain_M6.8BA_se	Yellow	D
32_I1250	21.4	25.93	23.74	1980	no	Freds_Mountain_M6.8CY_se	Yellow	
32_I1250	32.54	39.32	46.13	1980	no	Mount_Rose_M6.9BA_se	Red	
32_I1250	33.86	48.55	43.89	1980	no	Mount_Rose_M6.9CY_se	Red	
32_I1250	17.94	20.1	18.04	1980	no	Peavine_Peak_M6.4CY_se	Yellow	
32_I1250	20.59	17.88	22.43	1980	no	Spanish_Springs_V_M6.6BA_se	Yellow	
32_I1250	25.62	33.13	29.93	1980	no	Spanish_Springs_V_M6.6CY_se	Orange	
32_I_754	19.24	16.71	18.94	1960	no	Edna_Mntn_M6.9BA_se	Yellow	C
32_I_754	22.79	26.85	24.48	1960	no	Edna_Mntn_M6.9CY_se	Yellow	
32_I_754	20.29	23.19	21.17	1960	no	E_Osgood_Mntns_M6.8CY_se	Yellow	

Bridge ID	PGA	PGV	SA (1 sec)	Year Built	Retrofitted?	Scenario	Damage State	Site Class
32_I_754	20.14	23.76	21.93	1960	no	Grass_Valley_M7.1CY_se	Yellow	
32_I_770	26.81	29.09	25.99	1964	no	Mount_Rose_M6.9CY_se	Yellow	C
32_I_796	22.85	20.28	24.65	1964	yes	Frenchman_Mntn_M6.6BA_se	Green	C
32_I_796	18.18	20.41	18.54	1964	yes	Frenchman_Mntn_M6.6CY_se	Green	
32_I_862	16.8	21.53	20.35	1970	no	Buena_Vista_V_M7.4CY_se	Yellow	C
32_I_862	26.31	25.56	31.7	1970	no	Dunn_Glenn_M6.5BA_se	Orange	
32_I_862	37.69	52.9	46.54	1970	no	Dunn_Glenn_M6.5CY_se	Red	
32_I_862	30.48	39.01	40.85	1970	no	Grass_Valley_M7.1BA_se	Red	
32_I_862	25.51	33.96	31.26	1970	no	Grass_Valley_M7.1CY_se	Orange	
32_I_889	19.7	21.93	20.11	1967	no	Beowawe_M7.0CY_se	Yellow	C
32_I_889	20.8	20.78	20.09	1967	no	Cortez_Mntn_M7.2BA_se	Yellow	
32_I_889	20.6	23.83	21.95	1967	no	Cortez_Mntn_M7.2CY_se	Yellow	
32_I_889	18.31	20.39	18.82	1967	no	E_Tuscarora_Mntns_M7.1CY_se	Yellow	
32_I_889	36.1	29.66	34.17	1967	no	Marys_Mountain_M6.6BA_se	Orange	
32_I_889	53.14	68	57.57	1967	no	Marys_Mountain_M6.6CY_se	Red	
32_I_889	18.61	21.66	20.14	1967	no	Shoshone_Rng_M7.5CY_se	Yellow	
32_I_892	22.92	23.83	24.46	1967	no	E_Tuscarora_Mntns_M7.1BA_se	Yellow	C
32_I_892	19.53	23.13	21.4	1967	no	E_Tuscarora_Mntns_M7.1CY_se	Yellow	
32_I_892	37.5	34.22	41.75	1967	no	Marys_Mountain_M6.6BA_se	Red	
32_I_892	24.82	28.95	25.9	1967	no	Marys_Mountain_M6.6CY_se	Yellow	
32_I_908	41.03	48.55	58.08	1965	no	Ruby_Mountains_M6.9BA_se	Red	C
32_I_908	34.03	49.46	44.77	1965	no	Ruby_Mountains_M6.9CY_se	Red	
32_I_908	25.01	28.39	29.97	1965	no	Ruby_Mountains_M7.1BA_se	Orange	
32_I_908	24.54	32.6	30.08	1965	no	Ruby_Mountains_M7.1CY_se	Orange	
32_I_915	40.65	46.74	55.06	1968	no	Ruby_Mountains_M6.9BA_se	Red	C
32_I_915	45.92	70.93	62.8	1968	no	Ruby_Mountains_M6.9CY_se	Red	
32_I_915	18.57	17.65	18.71	1968	no	Ruby_Mountains_M7.1BA_se	Yellow	
32_I_915	18.89	23.93	22.35	1968	no	Ruby_Mountains_M7.1CY_se	Yellow	
32_I_924E	22	23.48	23.46	1973	no	Independence_V_M7.2BA_se	Yellow	C
32_I_924E	27.03	35.79	32.81	1973	no	Independence_V_M7.2CY_se	Orange	
32_I_924W	22	23.48	23.46	1973	no	Independence_V_M7.2BA_se	Yellow	C
32_I_924W	27.03	35.79	32.81	1973	no	Independence_V_M7.2CY_se	Orange	
32_I_934	25.08	22.5	27.01	1970	no	Eglington_M6.3BA_se	Orange	C
32_I_934	24.69	29.69	26.11	1970	no	Eglington_M6.3CY_se	Yellow	
32_I_934	35.04	35.52	44.59	1970	no	Frenchman_Mntn_M6.6BA_se	Red	
32_I_934	22.79	28.06	25.41	1970	no	Frenchman_Mntn_M6.6CY_se	Yellow	
32_I_937	29.3	26.22	31.49	1968	no	Eglington_M6.3BA_se	Orange	C
32_I_937	27.63	33.53	29.29	1968	no	Eglington_M6.3CY_se	Orange	
32_I_937	37.03	32.48	38.78	1968	no	Frenchman_Mntn_M6.6BA_se	Red	
32_I_937	23.99	26.68	23.81	1968	no	Frenchman_Mntn_M6.6CY_se	Yellow	
32_I_938	29.3	26.22	31.49	1968	no	Eglington_M6.3BA_se	Orange	C
32_I_938	27.63	33.53	29.29	1968	no	Eglington_M6.3CY_se	Orange	

Bridge ID	PGA	PGV	SA (1 sec)	Year Built	Retrofitted?	Scenario	Damage State	Site Class
32_I_938	37.03	32.48	38.78	1968	no	Frenchman_Mntn_M6.6BA_se	Red	
32_I_938	23.99	26.68	23.81	1968	no	Frenchman_Mntn_M6.6CY_se	Yellow	
32_I_947L	31.84	25.1	28.98	1968	no	Eglington_M6.3BA_se	Orange	C
32_I_947L	24.91	26.79	23.25	1968	no	Eglington_M6.3CY_se	Yellow	
32_I_947L	37.03	32.48	38.78	1968	no	Frenchman_Mntn_M6.6BA_se	Red	
32_I_947L	23.99	26.68	23.81	1968	no	Frenchman_Mntn_M6.6CY_se	Yellow	
32_I_947M	31.84	25.1	28.98	1968	no	Eglington_M6.3BA_se	Orange	C
32_I_947M	24.91	26.79	23.25	1968	no	Eglington_M6.3CY_se	Yellow	
32_I_947M	37.03	32.48	38.78	1968	no	Frenchman_Mntn_M6.6BA_se	Red	
32_I_947M	23.99	26.68	23.81	1968	no	Frenchman_Mntn_M6.6CY_se	Yellow	
32_I_947R	31.84	25.1	28.98	1968	no	Eglington_M6.3BA_se	Orange	C
32_I_947R	24.91	26.79	23.25	1968	no	Eglington_M6.3CY_se	Yellow	
32_I_947R	37.03	32.48	38.78	1968	no	Frenchman_Mntn_M6.6BA_se	Red	
32_I_947R	23.99	26.68	23.81	1968	no	Frenchman_Mntn_M6.6CY_se	Yellow	
32_I_969N	21.71	20.24	22.98	1963	no	California_Wash_M6.9BA_se	Yellow	C
32_I_969N	19.29	22.38	20.59	1963	no	California_Wash_M6.9CY_se	Yellow	
32_I_969N	20.71	16.89	20	1963	no	Frenchman_Mntn_M6.6BA_se	Yellow	
32_I_969N	28.55	32.52	28.74	1963	no	Frenchman_Mntn_M6.6CY_se	Orange	
32_I_969S	21.71	20.24	22.98	1963	no	California_Wash_M6.9BA_se	Yellow	C
32_I_969S	19.29	22.38	20.59	1963	no	California_Wash_M6.9CY_se	Yellow	
32_I_969S	20.71	16.89	20	1963	no	Frenchman_Mntn_M6.6BA_se	Yellow	
32_I_969S	28.55	32.52	28.74	1963	no	Frenchman_Mntn_M6.6CY_se	Orange	
32_I_992	21.02	18.91	23.2	1968	yes	Freds_Mountain_M6.8BA_se	Green	C
32_I_992	24.03	30.44	27.79	1968	yes	Freds_Mountain_M6.8CY_se	Green	
32_I_992	27.52	30.41	35.22	1968	yes	Mount_Rose_M6.9BA_se	Yellow	
32_I_992	32.51	44.65	40.31	1968	yes	Mount_Rose_M6.9CY_se	Yellow	
32_I_992	19.79	23.05	20.65	1968	yes	Peavine_Peak_M6.4CY_se	Green	
32_I_992	17.83	14.4	18.2	1968	yes	Petersen_Mountain_M6.7BA_se	Green	
32_I_992	22.2	20.08	25.12	1968	yes	Spanish_Springs_V_M6.6BA_se	Green	
32_I_992	29.17	38.57	34.61	1968	yes	Spanish_Springs_V_M6.6CY_se	Yellow	
32_I_994	21.22	19.31	23.84	1969	yes	Freds_Mountain_M6.8BA_se	Green	C
32_I_994	24.67	31.96	29.19	1969	yes	Freds_Mountain_M6.8CY_se	Yellow	
32_I_994	27.52	30.41	35.22	1969	yes	Mount_Rose_M6.9BA_se	Yellow	
32_I_994	32.51	44.65	40.31	1969	yes	Mount_Rose_M6.9CY_se	Yellow	
32_I_994	23.4	27.92	24.82	1969	yes	Peavine_Peak_M6.4CY_se	Green	
32_I_994	22.2	20.08	25.12	1969	yes	Spanish_Springs_V_M6.6BA_se	Green	
32_I_994	29.17	38.57	34.61	1969	yes	Spanish_Springs_V_M6.6CY_se	Yellow	

Table A.2 Bridges of type HWB11-205 (Demand vs Capacity)

Bridge ID	PGA	PGV	SA (1 sec)	Year built	Retrofitted?	Scenario	Damage State	Site Class
32_H1815	27.13	26.23	32.05	1985	no	Frenchman_Mntn_M6.6BA_se	Yellow	C
32_H1816	27.13	26.23	32.05	1985	no	Frenchman_Mntn_M6.6BA_se	Yellow	C
32_H1817	27.13	26.23	32.05	1985	no	Frenchman_Mntn_M6.6BA_se	Yellow	C
32_I1126	34.73	29.81	36.6	1999	yes	Eglington_M6.3BA_se	Yellow	
32_I1126	30.2	38.2	33.32	1999	yes	Eglington_M6.3CY_se	Yellow	
32_I1126	38.23	36.93	46.44	1999	yes	Frenchman_Mntn_M6.6BA_se	Yellow	
32_I1126	26.52	33.32	29.92	1999	yes	Frenchman_Mntn_M6.6CY_se	Yellow	
32_I1452	37.49	34.13	41.57	1986	yes	Frenchman_Mntn_M6.6BA_se	Yellow	
32_I1452	30.28	36.74	32.55	1986	yes	Frenchman_Mntn_M6.6CY_se	Yellow	
32_I_947	33.85	27.03	31.93	1985	no	Eglington_M6.3BA_se	Yellow	C
32_I_947	37.28	33.36	40.27	1985	no	Frenchman_Mntn_M6.6BA_se	Yellow	C
32_I_947E	33.85	27.03	31.93	1985	no	Eglington_M6.3BA_se	Yellow	C
32_I_947E	37.5	34.16	41.62	1985	no	Frenchman_Mntn_M6.6BA_se	Yellow	C
32_I_947W	33.85	27.03	31.93	1985	no	Eglington_M6.3BA_se	Yellow	C
32_I_947W	37.5	34.16	41.62	1985	no	Frenchman_Mntn_M6.6BA_se	Yellow	C

Table A.3 Bridges of type HWB15-402 (Demand vs Capacity)

Bridge ID	PGA	PGV	SA (1 sec)	Year built	Retrofitted?	Scenario	Damage State	Site Class
32_B1327W	27.52	30.41	35.22	1974	no	Mount_Rose_M6.9BA_se	Yellow	
32_B1327W	32.51	44.65	40.31	1974	no	Mount_Rose_M6.9CY_se	Yellow	C
32_B1327W	29.17	38.57	34.61	1974	no	Spanish_Springs_V_M6.6CY_se	Yellow	
32_B1489	39.81	47.25	40.84	1976	no	Marys_Mountain_M6.6CY_se	Yellow	
32_B_303	27.52	30.41	35.22	1937	no	Mount_Rose_M6.9BA_se	Yellow	C
32_B_303	32.51	44.65	40.31	1937	no	Mount_Rose_M6.9CY_se	Yellow	C
32_B_433N	40.67	46.83	55.22	1945	no	California_Wash_M6.9BA_se	Red	C
32_B_433N	41.97	62.98	56.1	1945	no	California_Wash_M6.9CY_se	Red	C
32_G1233	28.33	32.37	37.98	1971	yes	Mount_Rose_M6.9BA_se	Green	
32_G1233	30.97	43.45	39.48	1971	yes	Mount_Rose_M6.9CY_se	Green	C
32_G1233	31.85	43.86	39.27	1971	yes	Spanish_Springs_V_M6.6CY_se	Green	
32_G1233L	28.33	32.37	37.98	1971	yes	Mount_Rose_M6.9BA_se	Green	
32_G1233L	30.97	43.45	39.48	1971	yes	Mount_Rose_M6.9CY_se	Green	C
32_G1233L	31.85	43.86	39.27	1971	yes	Spanish_Springs_V_M6.6CY_se	Green	
32_G1233R	28.33	32.37	37.98	1971	yes	Mount_Rose_M6.9BA_se	Green	
32_G1233R	30.97	43.45	39.48	1971	yes	Mount_Rose_M6.9CY_se	Green	C
32_G1233R	31.85	43.86	39.27	1971	yes	Spanish_Springs_V_M6.6CY_se	Green	
32_G1296	32.57	37.45	33.16	1977	no	Ruby_Mountains_M6.9CY_se	Yellow	C
32_G_387	32.59	31.27	38.37	1939	no	Dunn_Glenn_M6.5BA_se	Yellow	

Bridge ID	PGA	PGV	SA (1 sec)	Year built	Retrofitted?	Scenario	Damage State	Site Class
32_G_387	46.96	67.32	58.14	1939	no	Dunn_Glenn_M6.5CY_se	Red	C
32_G_387	28.52	33.2	33.27	1939	no	Grass_Valley_M7.1BA_se	Yellow	
32_G_863E	32.59	31.27	38.37	1970	no	Dunn_Glenn_M6.5BA_se	Yellow	C
32_G_863E	46.96	67.32	58.14	1970	no	Dunn_Glenn_M6.5CY_se	Red	
32_G_863E	28.52	33.2	33.27	1970	no	Grass_Valley_M7.1BA_se	Yellow	
32_G_863W	32.59	31.27	38.37	1970	no	Dunn_Glenn_M6.5BA_se	Yellow	C
32_G_863W	46.96	67.32	58.14	1970	no	Dunn_Glenn_M6.5CY_se	Red	
32_G_863W	28.52	33.2	33.27	1970	no	Grass_Valley_M7.1BA_se	Yellow	
32_G_872E	26.11	30.83	32.82	1979	no	Grass_Valley_M7.1BA_se	Yellow	C
32_G_872E	33.02	48.34	44.05	1979	no	Grass_Valley_M7.1CY_se	Orange	
32_G_872R	26.11	30.83	32.82	1979	no	Grass_Valley_M7.1BA_se	Yellow	C
32_G_872R	33.02	48.34	44.05	1979	no	Grass_Valley_M7.1CY_se	Orange	
32_G_872W	26.11	30.83	32.82	1979	no	Grass_Valley_M7.1BA_se	Yellow	C
32_G_872W	33.02	48.34	44.05	1979	no	Grass_Valley_M7.1CY_se	Orange	
32_G_913E	41.34	50.01	60.56	1965	no	Ruby_Mountains_M6.9BA_se	Red	D
32_G_913E	35.52	53.73	48.67	1965	no	Ruby_Mountains_M6.9CY_se	Orange	
32_G_913W	41.34	50.01	60.56	1965	no	Ruby_Mountains_M6.9BA_se	Red	D
32_G_913W	35.52	53.73	48.67	1965	no	Ruby_Mountains_M6.9CY_se	Orange	
32_G_919E	32.57	37.45	33.16	1977	no	Ruby_Mountains_M6.9CY_se	Yellow	C
32_G_919W	32.57	37.45	33.16	1977	no	Ruby_Mountains_M6.9CY_se	Yellow	C
32_H1234	28.33	32.37	37.98	1971	yes	Mount_Rose_M6.9BA_se	Green	
32_H1234	30.97	43.45	39.48	1971	yes	Mount_Rose_M6.9CY_se	Green	
32_H1234	31.85	43.86	39.27	1971	yes	Spanish_Springs_V_M6.6CY_se	Green	
32_H1443	32.56	29.97	37.17	1982	no	Eglington_M6.3BA_se	Yellow	D
32_H1443	38.44	37.74	47.88	1982	no	Frenchman_Mntn_M6.6BA_se	Orange	
32_H1443	31.89	42.65	38.05	1982	no	Frenchman_Mntn_M6.6CY_se	Yellow	
32_I1255	35.5	49.35	52.78	1970	no	Grass_Valley_M7.1BA_se	Red	D
32_I1255	31.45	46.14	42.23	1970	no	Grass_Valley_M7.1CY_se	Orange	
32_I1290	42.82	46.86	38.68	1975	no	Peavine_Peak_M6.4CY_se	Yellow	D
32_I1290	28.78	27.5	32.82	1975	no	Petersen_Mountain_M6.7BA_se	Yellow	
32_I1290	38.97	49.01	42.9	1975	no	Petersen_Mountain_M6.7CY_se	Orange	
32_I1291	46.16	56.32	47.57	1975	no	Peavine_Peak_M6.4CY_se	Orange	C
32_I1291	37.24	32.98	38.82	1975	no	Petersen_Mountain_M6.7BA_se	Yellow	
32_I1291	53.25	70.94	60.57	1975	no	Petersen_Mountain_M6.7CY_se	Red	
32_I_868	31.45	41.49	43.92	1976	yes	Grass_Valley_M7.1BA_se	Green	D
32_I_868	35.43	52.59	47.69	1976	yes	Grass_Valley_M7.1CY_se	Green	

Table A.4 Bridges of type HWB22-605 (Demand vs Capacity)

Bridge ID	PGA	PGV	SA (1 sec)	Year built	Retrofitted?	Scenario	Damage State	Site Class
32_B1526	20.31	20.45	21.88	1979	no	Ruby_Mountains_M7.1BA_se	Yellow	D
32_B1526	16.73	21.47	20.23	1979	no	Ruby_Mountains_M7.1CY_se	Yellow	
32_G1414	20.99	21.4	22.76	1980	no	Ruby_Mountains_M7.1BA_se	Yellow	D
32_G1414	17.54	22.26	20.89	1980	no	Ruby_Mountains_M7.1CY_se	Yellow	
32_H1205	20.12	19.47	20.14	1976	no	E_Tuscarora_Mntns_M7.1BA_se	Yellow	C
32_H1205	17.01	19.95	18.6	1976	no	E_Tuscarora_Mntns_M7.1CY_se	Yellow	
32_H1205	26.77	25.4	30.76	1976	no	Marys_Mountain_M6.6BA_se	Orange	
32_H1205	19.79	22.4	20.27	1976	no	Marys_Mountain_M6.6CY_se	Yellow	
32_H_869E	25.23	28.55	29.82	1977	no	Grass_Valley_M7.1BA_se	Orange	D
32_H_869E	31.72	43.64	39.63	1977	no	Grass_Valley_M7.1CY_se	Red	
32_H_869W	25.23	28.55	29.82	1977	no	Grass_Valley_M7.1BA_se	Orange	D
32_H_869W	31.72	43.64	39.63	1977	no	Grass_Valley_M7.1CY_se	Red	
32_I1261	26.15	30.71	29.95	1968	no	Carson-Kings_Cnyn_M7.2BA_se	Orange	D
32_I1261	36.7	50.3	45.12	1968	no	Carson-Kings_Cnyn_M7.2CY_se	Red	
32_I1261	19.08	15.15	18.17	1968	no	Carson_City_M6.5BA_se	Yellow	
32_I1261	25.35	29.42	26.12	1968	no	Carson_City_M6.5CY_se	Yellow	
32_I1261	20.3	24.25	22.4	1968	no	Carson_Rng_M7.1CY_se	Yellow	
32_I1261	23.51	21.91	27.33	1968	no	Kings_Canyon_M6.5BA_se	Orange	
32_I1261	32.32	44.32	39.4	1968	no	Kings_Canyon_M6.5CY_se	Red	
32_I1261	36.36	31.9	38.63	1968	no	Little_Valley_M6.5BA_se	Red	
32_I1261	33.49	41.38	36.24	1968	no	Little_Valley_M6.5CY_se	Red	
32_I1261	41.06	48.69	58.25	1968	no	Mount_Rose_M6.9BA_se	Red	
32_I1261	46.57	75.24	66.82	1968	no	Mount_Rose_M6.9CY_se	Red	
32_I1977	24.62	22.81	27.81	1944	no	Frenchman_Mntn_M6.6BA_se	Orange	C
32_I1977	19.87	22.83	20.69	1944	no	Frenchman_Mntn_M6.6CY_se	Yellow	
32_I_871E	26.11	30.83	32.82	1977	no	Grass_Valley_M7.1BA_se	Orange	C
32_I_871E	33.02	48.34	44.05	1977	no	Grass_Valley_M7.1CY_se	Red	
32_I_871W	26.11	30.83	32.82	1977	no	Grass_Valley_M7.1BA_se	Orange	C
32_I_871W	33.02	48.34	44.05	1977	no	Grass_Valley_M7.1CY_se	Red	
32_I_873	26.11	30.83	32.82	1979	no	Grass_Valley_M7.1BA_se	Orange	C
32_I_873	33.02	48.34	44.05	1979	no	Grass_Valley_M7.1CY_se	Red	
32_I_878	18.68	17.41	19.59	1976	no	Beowawe_M7.0BA_se	Yellow	D
32_I_878	16.13	20.3	19.05	1976	no	Sheep_Crk_Rng_SE_M6.9CY_se	Yellow	
32_I_878	30.23	45.2	40.69	1976	no	Shoshone_Rng_M7.5BA_se	Red	
32_I_878	27.39	40.26	37.34	1976	no	Shoshone_Rng_M7.5CY_se	Red	
32_I_879	20.02	19.29	21.67	1976	no	Beowawe_M7.0BA_se	Yellow	D
32_I_879	16.12	20.39	19.19	1976	no	Beowawe_M7.0CY_se	Yellow	
32_I_879	15.98	20.04	18.8	1976	no	Sheep_Crk_Rng_SE_M6.9CY_se	Yellow	
32_I_879	32.03	49.93	44.78	1976	no	Shoshone_Rng_M7.5BA_se	Red	
32_I_879	28.79	42.7	39.48	1976	no	Shoshone_Rng_M7.5CY_se	Red	

Bridge ID	PGA	PGV	SA (1 sec)	Year built	Retrofitted?	Scenario	Damage State	Site Class
32_I_882	21.67	21.94	24.7	1976	no	Beowawe_M7.0BA_se	Yellow	D
32_I_882	17.6	22.69	21.29	1976	no	Beowawe_M7.0CY_se	Yellow	
32_I_882	17.64	15.37	18.17	1976	no	Sheep_Crk_Rng_SE_M6.9BA_se	Yellow	
32_I_882	16.99	21.57	20.2	1976	no	Sheep_Crk_Rng_SE_M6.9CY_se	Yellow	
32_I_882	37.37	62.96	56.34	1976	no	Shoshone_Rng_M7.5BA_se	Red	
32_I_882	32.24	49.28	45.28	1976	no	Shoshone_Rng_M7.5CY_se	Red	
32_I_896	21.31	21.48	22.38	1976	no	E_Tuscarora_Mntns_M7.1BA_se	Yellow	D
32_I_896	18.05	21.81	20.32	1976	no	E_Tuscarora_Mntns_M7.1CY_se	Yellow	
32_I_896	30.36	30.12	36.92	1976	no	Marys_Mountain_M6.6BA_se	Red	
32_I_896	21.53	25.27	22.84	1976	no	Marys_Mountain_M6.6CY_se	Yellow	

Table A.5 Bridges of type HWB23-605 (Demand vs Capacity)

Bridge ID	PGA	PGV	SA (1 sec)	Year built	Retrofitted?	Scenario	Damage State	Site Class
32_B1014	32.56	51.59	46.45	2000	no	Shoshone_Rng_M7.5BA_se	Yellow	D
32_B1014	28.89	43.32	40.1	2000	no	Shoshone_Rng_M7.5CY_se	Yellow	
32_B1533	24.67	31.96	29.19	1998	no	Freds_Mountain_M6.8CY_se	Yellow	C
32_B1533	27.52	30.41	35.22	1998	no	Mount_Rose_M6.9BA_se	Yellow	
32_B1533	32.51	44.65	40.31	1998	no	Mount_Rose_M6.9CY_se	Yellow	
32_B1533	26.51	33.5	30.11	1998	no	Spanish_Springs_V_M6.6CY_se	Yellow	
32_B_455	33.56	41.6	36.95	1992	no	E_Osgood_Mntns_M6.8CY_se	Yellow	D
32_G1748N	30.65	31.1	36.28	1988	no	Freds_Mountain_M6.8BA_se	Yellow	C
32_G1748N	41.64	54.28	47.56	1988	no	Freds_Mountain_M6.8CY_se	Yellow	
32_G1748N	30.33	34.6	30.07	1988	no	Peavine_Peak_M6.4CY_se	Yellow	
32_G1748N	27.8	32.93	29.29	1988	no	Spanish_Springs_V_M6.6CY_se	Yellow	
32_G1748S	30.65	31.1	36.28	1988	no	Freds_Mountain_M6.8BA_se	Yellow	C
32_G1748S	41.64	54.28	47.56	1988	no	Freds_Mountain_M6.8CY_se	Yellow	
32_G1748S	30.33	34.6	30.07	1988	no	Peavine_Peak_M6.4CY_se	Yellow	
32_G2012	26.31	25.23	30.89	1996	no	Frenchman_Mntn_M6.6BA_se	Yellow	C
32_G2014	26.31	25.23	30.89	1998	no	Frenchman_Mntn_M6.6BA_se	Yellow	C
32_G2014R	26.31	25.23	30.89	1999	no	Frenchman_Mntn_M6.6BA_se	Yellow	C
32_G_805R	26.31	25.23	30.89	1999	no	Frenchman_Mntn_M6.6BA_se	Yellow	C
32_G_941L	37.03	32.48	38.78	2000	no	Frenchman_Mntn_M6.6BA_se	Yellow	C
32_G_961R	27.34	24.79	29.81	2001	no	Eglington_M6.3BA_se	Yellow	C
32_G_961R	27.12	33.15	29.02	2001	no	Eglington_M6.3CY_se	Yellow	
32_G_961R	35.16	35.83	45.12	2001	no	Frenchman_Mntn_M6.6BA_se	Yellow	
32_G_961R	30.8	40.82	36.48	2001	no	Frenchman_Mntn_M6.6CY_se	Yellow	
32_H1212	30.95	36.34	31.37	1991	no	Eglington_M6.3CY_se	Yellow	C

Bridge ID	PGA	PGV	SA (1 sec)	Year built	Retrofitted?	Scenario	Damage State	Site Class
32_H1214	36.38	46.46	39.96	1990	no	Eglington_M6.3CY_se	Yellow	C
32_H1446	30.61	27.72	33.7	1986	no	Eglington_M6.3BA_se	Yellow	D
32_H1446	37.88	35.57	44.05	1986	no	Frenchman_Mntn_M6.6BA_se	Yellow	
32_H1446	30.45	38.26	34.01	1986	no	Frenchman_Mntn_M6.6CY_se	Yellow	
32_H1458	37.49	34.13	41.57	1987	no	Frenchman_Mntn_M6.6BA_se	Yellow	C
32_H1458	30.28	36.74	32.55	1987	no	Frenchman_Mntn_M6.6CY_se	Yellow	
32_H1460	29.83	36.43	32.34	1988	no	Frenchman_Mntn_M6.6CY_se	Yellow	C
32_H1804	29.74	29.31	35.81	1987	no	Frenchman_Mntn_M6.6BA_se	Yellow	C
32_H1804	30.4	38.08	33.85	1987	no	Frenchman_Mntn_M6.6CY_se	Yellow	
32_H2013	30.15	30.31	37.41	1996	no	Frenchman_Mntn_M6.6BA_se	Yellow	C
32_H2013W	30.15	30.31	37.41	1996	no	Frenchman_Mntn_M6.6BA_se	Yellow	C
32_H2290	41.66	57.48	58.14	2009	no	Carson-Kings_Cnyn_M7.2BA_se	Yellow	D
32_H2290	43.93	69.37	62.05	2009	no	Carson-Kings_Cnyn_M7.2CY_se	Orange	
32_H2290	37.27	35.16	44.28	2009	no	Carson_City_M6.5BA_se	Yellow	
32_H2290	47.25	70.76	61.36	2009	no	Carson_City_M6.5CY_se	Orange	
32_H2290	27.48	32.77	34.07	2009	no	Carson_Rng_M7.1BA_se	Yellow	
32_H2290	28	37.19	33.98	2009	no	Carson_Rng_M7.1CY_se	Yellow	
32_H2290	36.89	33.77	41.85	2009	no	Kings_Canyon_M6.5BA_se	Yellow	
32_H2290	36.82	49	42.93	2009	no	Kings_Canyon_M6.5CY_se	Yellow	
32_H2290	26.99	26.3	32.52	2009	no	Little_Valley_M6.5BA_se	Yellow	
32_H2290	29.45	33.29	38.24	2009	no	Mount_Rose_M6.9BA_se	Yellow	
32_H2290	34.48	47.24	42.43	2009	no	Mount_Rose_M6.9CY_se	Yellow	
32_H2331	27.05	24.99	30.34	2004	no	Eglington_M6.3BA_se	Yellow	
32_H2331	40.45	56.58	48.73	2004	no	Eglington_M6.3CY_se	Yellow	
32_H2348	35.11	33.93	41.7	1997	no	Frenchman_Mntn_M6.6BA_se	Yellow	C
32_H2349	35.11	33.93	41.7	1997	no	Frenchman_Mntn_M6.6BA_se	Yellow	C
32_H2350	35.11	33.93	41.7	1997	no	Frenchman_Mntn_M6.6BA_se	Yellow	C
32_H2486	35.58	48.35	41.98	2002	no	Eglington_M6.3CY_se	Yellow	C
32_H2710	29.3	26.22	31.49	2007	no	Eglington_M6.3BA_se	Yellow	C
32_H2710	27.63	33.53	29.29	2007	no	Eglington_M6.3CY_se	Yellow	
32_H2710	37.18	36.28	45.43	2007	no	Frenchman_Mntn_M6.6BA_se	Yellow	
32_H2711	29.3	26.22	31.49	2007	no	Eglington_M6.3BA_se	Yellow	C
32_H2711	27.63	33.53	29.29	2007	no	Eglington_M6.3CY_se	Yellow	
32_H2711	37.18	36.28	45.43	2007	no	Frenchman_Mntn_M6.6BA_se	Yellow	
32_H_936R	29.3	26.22	31.49	1999	no	Eglington_M6.3BA_se	Yellow	C
32_H_936R	27.63	33.53	29.29	1999	no	Eglington_M6.3CY_se	Yellow	
32_H_936R	37.18	36.28	45.43	1999	no	Frenchman_Mntn_M6.6BA_se	Yellow	
32_I1091N	29.67	37.1	33.3	2006	no	Freds_Mountain_M6.8CY_se	Yellow	

Bridge ID	PGA	PGV	SA (1 sec)	Year built	Retrofitted?	Scenario	Damage State	Site Class
32_I1091N	34.74	44.62	39.36	2006	no	Spanish_Springs_V_M6.6CY_se	Yellow	C
32_I1091S	29.67	37.1	33.3	2006	no	Freds_Mountain_M6.8CY_se	Yellow	C
32_I1091S	34.74	44.62	39.36	2006	no	Spanish_Springs_V_M6.6CY_se	Yellow	C
32_I1219	26.97	24.7	29.86	1990	no	Eglington_M6.3BA_se	Yellow	C
32_I1219	40.58	56.13	48.27	1990	no	Eglington_M6.3CY_se	Yellow	C
32_I1456	29.74	29.31	35.81	1987	no	Frenchman_Mntn_M6.6BA_se	Yellow	C
32_I1456	30.4	38.08	33.85	1987	no	Frenchman_Mntn_M6.6CY_se	Yellow	C
32_I1949	38.02	35.72	37.71	1995	no	Mount_Rose_M6.9BA_se	Yellow	C
32_I1949	33.2	37.59	33.15	1995	no	Mount_Rose_M6.9CY_se	Yellow	C
32_I1950	40.39	45.59	53.11	1995	no	Mount_Rose_M6.9BA_se	Yellow	C
32_I1950	32.79	44.61	40.21	1995	no	Mount_Rose_M6.9CY_se	Yellow	C
32_I1952	39.77	42.83	48.65	1995	no	Mount_Rose_M6.9BA_se	Yellow	C
32_I1952	35.69	47.12	42.03	1995	no	Mount_Rose_M6.9CY_se	Yellow	C
32_I2139	29.3	26.22	31.49	1999	no	Eglington_M6.3BA_se	Yellow	C
32_I2139	27.63	33.53	29.29	1999	no	Eglington_M6.3CY_se	Yellow	C
32_I2139	37.18	36.28	45.43	1999	no	Frenchman_Mntn_M6.6BA_se	Yellow	C
32_I2139R	34.08	28.26	33.99	1999	no	Eglington_M6.3BA_se	Yellow	C
32_I2139R	30.52	37.04	32.13	1999	no	Eglington_M6.3CY_se	Yellow	C
32_I2139R	37.18	36.28	45.43	1999	no	Frenchman_Mntn_M6.6BA_se	Yellow	C
32_I2140	29.3	26.22	31.49	1999	no	Eglington_M6.3BA_se	Yellow	C
32_I2140	27.63	33.53	29.29	1999	no	Eglington_M6.3CY_se	Yellow	C
32_I2140	37.18	36.28	45.43	1999	no	Frenchman_Mntn_M6.6BA_se	Yellow	C
32_I2141R	29.3	26.22	31.49	2000	no	Eglington_M6.3BA_se	Yellow	C
32_I2141R	27.63	33.53	29.29	2000	no	Eglington_M6.3CY_se	Yellow	C
32_I2141R	37.18	36.28	45.43	2000	no	Frenchman_Mntn_M6.6BA_se	Yellow	C
32_I2288	41.11	54.64	54.18	2009	no	Carson-Kings_Cnyn_M7.2BA_se	Yellow	C
32_I2288	41.56	61.52	54.97	2009	no	Carson-Kings_Cnyn_M7.2CY_se	Yellow	C
32_I2288	36.79	33.43	41.26	2009	no	Carson_City_M6.5BA_se	Yellow	C
32_I2288	45.14	63.37	54.82	2009	no	Carson_City_M6.5CY_se	Yellow	C
32_I2288	30.59	38.47	39.75	2009	no	Carson_Rng_M7.1BA_se	Yellow	C
32_I2288	31.48	42.64	38.67	2009	no	Carson_Rng_M7.1CY_se	Yellow	C
32_I2288	36.89	33.77	41.85	2009	no	Kings_Canyon_M6.5BA_se	Yellow	C
32_I2288	36.82	49	42.93	2009	no	Kings_Canyon_M6.5CY_se	Yellow	C
32_I2293N	41.48	56.51	56.78	2005	no	Carson-Kings_Cnyn_M7.2BA_se	Yellow	D
32_I2293N	46.31	73.31	65.23	2005	no	Carson-Kings_Cnyn_M7.2CY_se	Orange	D
32_I2293N	37.11	34.57	43.24	2005	no	Carson_City_M6.5BA_se	Yellow	D
32_I2293N	51.28	77.8	66.98	2005	no	Carson_City_M6.5CY_se	Orange	D
32_I2293N	27.48	32.77	34.07	2005	no	Carson_Rng_M7.1BA_se	Yellow	D
32_I2293N	28	37.19	33.98	2005	no	Carson_Rng_M7.1CY_se	Yellow	D
32_I2293N	37.58	36.35	46.39	2005	no	Kings_Canyon_M6.5BA_se	Yellow	D
32_I2293N	39.52	57.54	50.62	2005	no	Kings_Canyon_M6.5CY_se	Yellow	D

Bridge ID	PGA	PGV	SA (1 sec)	Year built	Retrofitted?	Scenario	Damage State	Site Class
32_I2293N	32.67	31.95	39.57	2005	no	Little_Valley_M6.5BA_se	Yellow	
32_I2293N	35.65	43.99	52.07	2005	no	Mount_Rose_M6.9BA_se	Yellow	
32_I2293N	36.72	54.7	49.31	2005	no	Mount_Rose_M6.9CY_se	Yellow	
32_I2293S	41.48	56.51	56.78	2005	no	Carson-Kings_Cnyn_M7.2BA_se	Yellow	D
32_I2293S	46.31	73.31	65.23	2005	no	Carson-Kings_Cnyn_M7.2CY_se	Orange	
32_I2293S	37.11	34.57	43.24	2005	no	Carson_City_M6.5BA_se	Yellow	
32_I2293S	51.28	77.8	66.98	2005	no	Carson_City_M6.5CY_se	Orange	
32_I2293S	25.92	30.52	32.57	2005	no	Carson_Rng_M7.1BA_se	Yellow	
32_I2293S	26.38	36.71	33.88	2005	no	Carson_Rng_M7.1CY_se	Yellow	
32_I2293S	37.58	36.35	46.39	2005	no	Kings_Canyon_M6.5BA_se	Yellow	
32_I2293S	39.52	57.54	50.62	2005	no	Kings_Canyon_M6.5CY_se	Yellow	
32_I2293S	32.67	31.95	39.57	2005	no	Little_Valley_M6.5BA_se	Yellow	
32_I2293S	35.65	43.99	52.07	2005	no	Mount_Rose_M6.9BA_se	Yellow	
32_I2293S	36.72	54.7	49.31	2005	no	Mount_Rose_M6.9CY_se	Yellow	
32_I2296N	41.43	56.28	56.45	2001	no	Carson-Kings_Cnyn_M7.2BA_se	Yellow	C
32_I2296N	49.23	79.38	70.29	2001	no	Carson-Kings_Cnyn_M7.2CY_se	Orange	
32_I2296N	32.03	28	32.82	2001	no	Carson_City_M6.5BA_se	Yellow	
32_I2296N	47.6	61.52	52.48	2001	no	Carson_City_M6.5CY_se	Yellow	
32_I2296N	25.2	28.65	30.1	2001	no	Carson_Rng_M7.1BA_se	Yellow	
32_I2296N	27.41	36.93	33.85	2001	no	Carson_Rng_M7.1CY_se	Yellow	
32_I2296N	36.38	31.96	38.75	2001	no	Kings_Canyon_M6.5BA_se	Yellow	
32_I2296N	48.05	66.08	56.69	2001	no	Kings_Canyon_M6.5CY_se	Yellow	
32_I2296N	36.38	31.97	38.75	2001	no	Little_Valley_M6.5BA_se	Yellow	
32_I2296N	35.9	42.66	49.6	2001	no	Mount_Rose_M6.9BA_se	Yellow	
32_I2296N	39.95	58.34	52.06	2001	no	Mount_Rose_M6.9CY_se	Yellow	
32_I2296S	41.43	56.28	56.45	2001	no	Carson-Kings_Cnyn_M7.2BA_se	Yellow	C
32_I2296S	49.23	79.38	70.29	2001	no	Carson-Kings_Cnyn_M7.2CY_se	Orange	
32_I2296S	32.03	28	32.82	2001	no	Carson_City_M6.5BA_se	Yellow	
32_I2296S	47.6	61.52	52.48	2001	no	Carson_City_M6.5CY_se	Yellow	
32_I2296S	25.2	28.65	30.1	2001	no	Carson_Rng_M7.1BA_se	Yellow	
32_I2296S	27.41	36.93	33.85	2001	no	Carson_Rng_M7.1CY_se	Yellow	
32_I2296S	36.38	31.96	38.75	2001	no	Kings_Canyon_M6.5BA_se	Yellow	
32_I2296S	48.05	66.08	56.69	2001	no	Kings_Canyon_M6.5CY_se	Yellow	
32_I2296S	36.38	31.97	38.75	2001	no	Little_Valley_M6.5BA_se	Yellow	
32_I2296S	35.9	42.66	49.6	2001	no	Mount_Rose_M6.9BA_se	Yellow	
32_I2296S	39.95	58.34	52.06	2001	no	Mount_Rose_M6.9CY_se	Yellow	
32_I2339	31.27	38.83	33.7	2000	no	Eglington_M6.3CY_se	Yellow	C
32_I2499	27.34	24.79	29.81	2002	no	Eglington_M6.3BA_se	Yellow	C
32_I2499	27.12	33.15	29.02	2002	no	Eglington_M6.3CY_se	Yellow	
32_I2499	28.65	28.91	35.93	2002	no	Frenchman_Mntn_M6.6BA_se	Yellow	
32_I2499	28.32	36.38	32.61	2002	no	Frenchman_Mntn_M6.6CY_se	Yellow	
32_I_806N	26.31	25.23	30.89	1994	no	Frenchman_Mntn_M6.6BA_se	Yellow	C

Bridge ID	PGA	PGV	SA (1 sec)	Year built	Retrofitted?	Scenario	Damage State	Site Class
32_I_806S	26.31	25.23	30.89	1994	no	Frenchman_Mntn_M6.6BA_se	Yellow	C
32_I_944N	28.95	35.6	31.05	2007	yes	Eglington_M6.3CY_se	Yellow	C
32_I_944N	31.43	31.95	39.65	2007	yes	Frenchman_Mntn_M6.6BA_se	Yellow	C
32_I_944S	28.95	35.6	31.05	2007	yes	Eglington_M6.3CY_se	Yellow	C
32_I_944S	31.43	31.95	39.65	2007	yes	Frenchman_Mntn_M6.6BA_se	Yellow	C
32_I_950	33.9	27.17	32.16	2009	yes	Eglington_M6.3BA_se	Yellow	D
32_I_950	29.02	33.64	29.13	2009	yes	Eglington_M6.3CY_se	Yellow	
32_I_950	37.32	33.49	40.49	2009	yes	Frenchman_Mntn_M6.6BA_se	Yellow	

APPENDIX B: Hazard Curves and ShakeCast Predicted Demand For Selected Bridge Types

ShakeCast was used to estimate seismic demand at all Nevada bridges. Five HAZUS bridge types were identified as having potentially lower capacities than originally estimated. In this Appendix scenario-predicted demands for these bridges are shown in a standardized format that provides estimated return times for scenario demands. The relative return frequencies of damaging demands comprise one basis for assigning priority for bridge retrofit or replacement.

The basic plots in this appendix are 1 Hz spectral acceleration hazard curves (red line) at individual bridge sites estimated from tables provided with the 2014 USGS National Seismic Hazard Map (NSHM). Original NSHM values (gray line) have been adjusted for non-linear site response using AASHTO parameters (see main text for an explanation). The NSHM hazard is calculated for the B-C site class boundary, which is stiffer than most Nevada bridge sites, so the actual hazard at bridge sites is generally higher than the unadjusted NSHM values.

Data identifying the individual bridge type, bridge identifier, and bridge location are given in the title of each figure. Latitude and longitude are in decimal degrees. An estimated site class is given after the “sc” label, generally either “C” or “D”. Spectral acceleration at a reference return period of 1000 years follows, in units of “g”. The intersection of the reference return period with the hazard curve is circled in the figure. The “R: “ refers to bridge seismic retrofit status, followed by “y” or “n” for Yes or No. Small dots near the hazard curve represent discrete values at the four grid points of the NSHM nearest to the bridge. The spread among these dots is a measure of how spatially variable the hazard estimate is at the bridge site. Vertical green, yellow, orange, and red bars on the hazard curve indicate estimated bridge capacities for the respective damage state bounds in ShakeCast. Black vertical bars show demands from scenarios affecting the bridge where the demand exceeds the “green” damage state bound. See Appendix A for the individual scenario names. Black stars at the ends of the bars are for display only. The predicted return period of a given scenario can be inferred from its intersection with the hazard curve. The relative return period of smaller earthquakes will be more frequent, but the relative rate cannot otherwise be inferred from these data. Smaller magnitude earthquakes may nevertheless produce damaging demands. Project-specific scenarios are recommended if such earthquakes could affect seismic design.

The reference return period line in each figure can be used to evaluate relative probabilities of ground motions expected to exceed capacity. The intersection of green bar with the hazard curve indicates the ShakeCast Green->Yellow damage state transition level. For HWB 10, 32_B_839S (Figure B-1.1) potentially damaging demand is expected less often than the reference with a return period of 1640 years. As a counter-example, damaging ground motions are expected more frequently than the reference period at HWB 10, 32_H_767W (Figure B-1.14) with a return period of 217 years. From a predicted exposure viewpoint, 32_H_767W is over seven times as likely to experience damaging ground motions as the first example. Thus as bridges are evaluated for retrofitting or replacement, from a hazard standpoint, 32_H_767W would have a higher priority. Other criteria affecting upgrade priorities such as upgrade costs, traffic levels, and

availability of alternate routes, are outside the scope of this report. Bridges expected to experience potentially damaging demand at return periods shorter than 1000 years are tabulated in Appendix C, "Return Periods Corresponding to Different Damage States".

B.1 HWB10 -205 Bridges

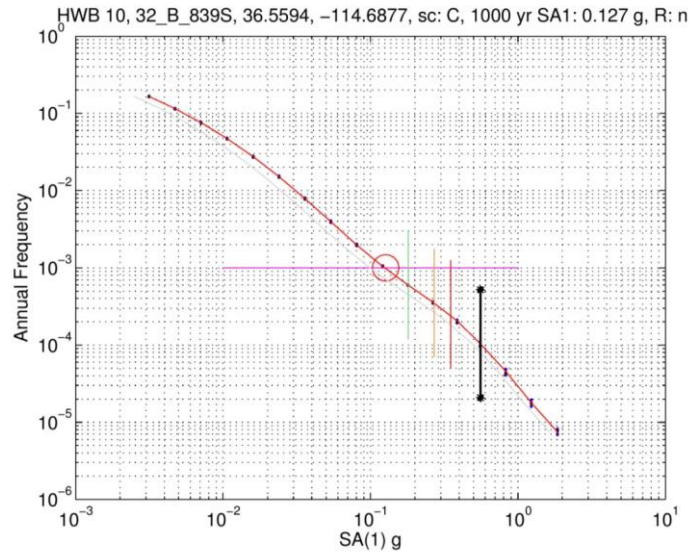


Figure B-1.1 HWB 10, 32_B_839S SA(1 Hz) hazard curve and capacity estimates, southeast Nevada and not near any high activity faults. Return frequency of ground motions able to damage this bridge are expected less frequently than the 1000 year reference return period. The scenario affecting this bridge (black vertical bar) is expected even less often, but should it occur, it is predicted to develop demand significantly in excess of bridge capacity.

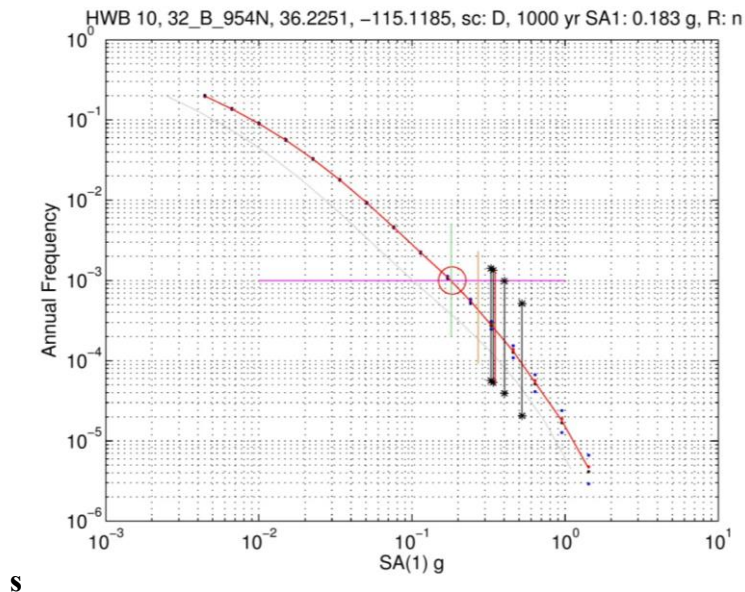


Figure B-1.2 HWB 10, 32_B_954N SA(1 Hz) hazard curve and capacity estimates. At the 1000 year reference return, the site class adjustment from B-C to D (gray line to red line) increases expected demand by a factor of 1.8.

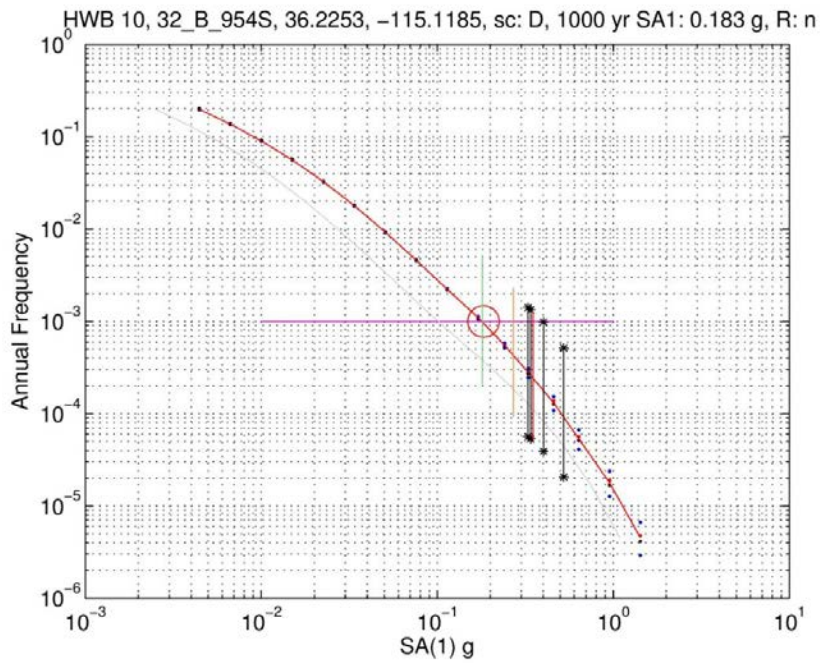


Figure B-1.3 HWB 10, 32_B_954S SA(1 Hz) hazard curve and capacity estimates. Ground motions capable of producing damage are expected at about the reference return period of 1000 years.

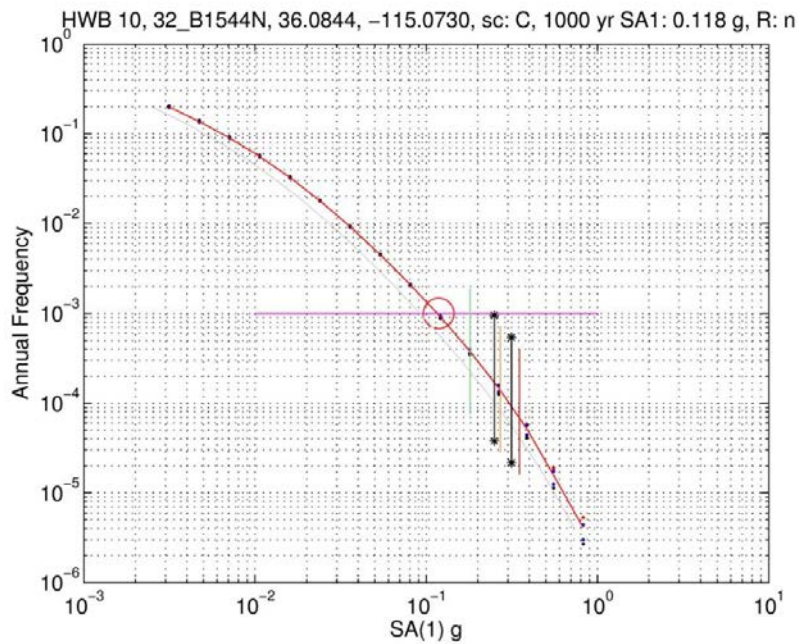


Figure B-1.4 HWB 10, 32_B1544N SA(1 Hz) hazard curve and capacity estimates.

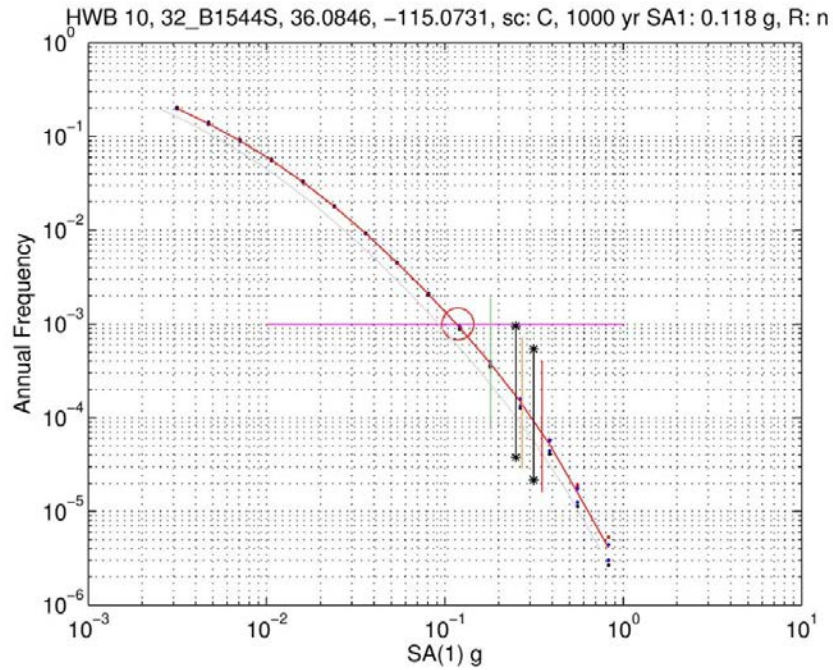


Figure B-1.5 HWB 10, 32_B1544S SA(1 Hz) hazard curve and capacity estimates.

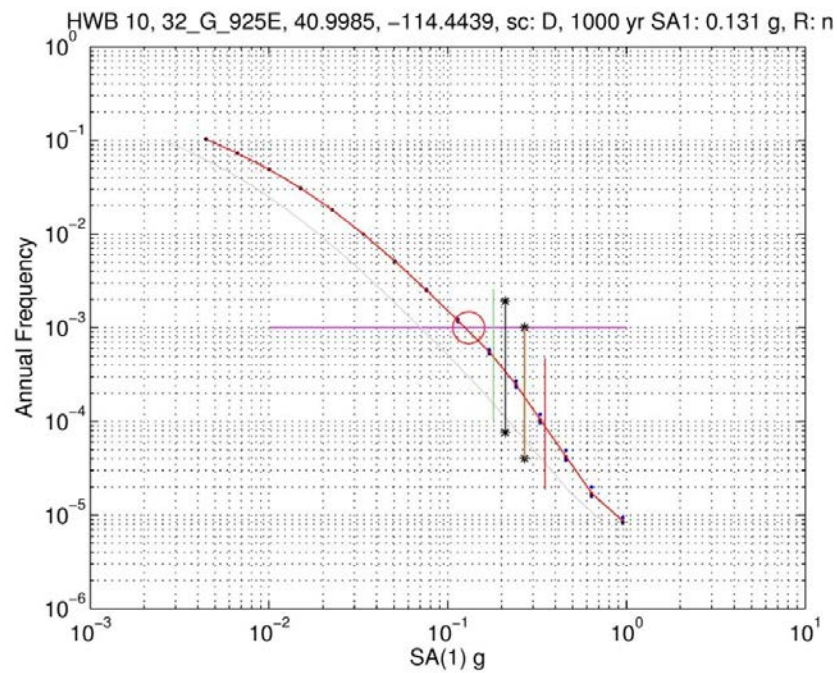


Figure B-1.6 HWB 10, 32_G_925E SA(1 Hz) hazard curve and capacity estimates.

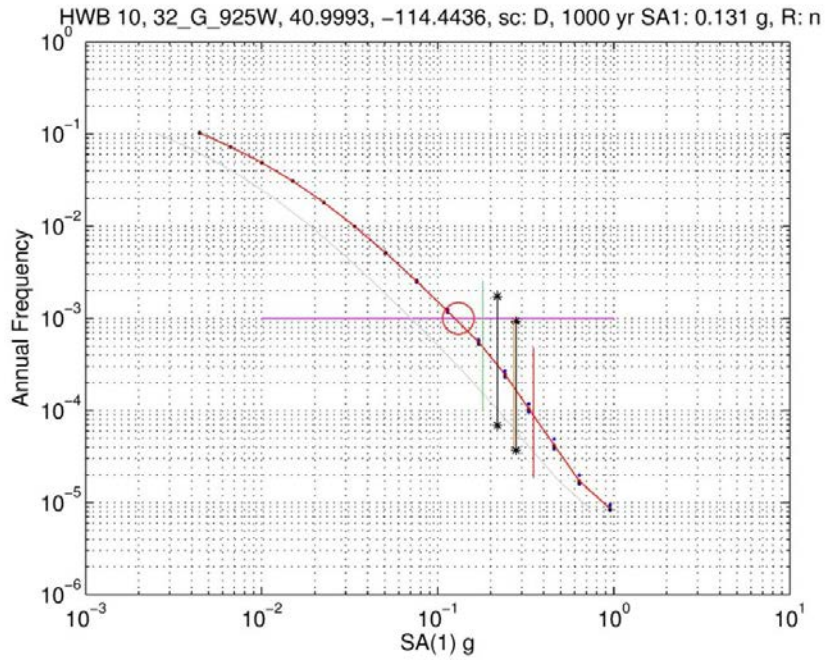


Figure B-1.7 HWB 10, 32_G_925W SA(1 Hz) hazard curve and capacity estimates.

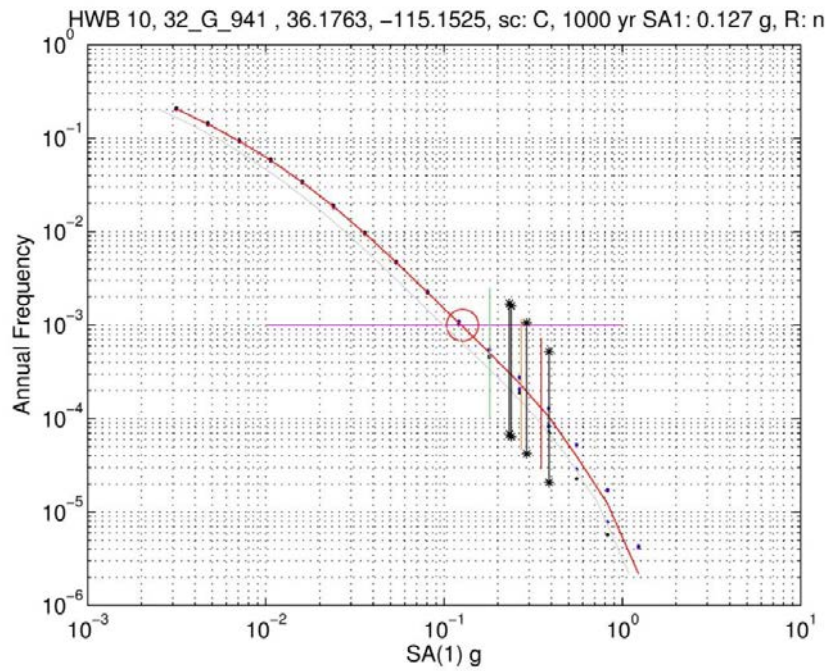


Figure B-1.8 HWB 10, 32_G_941 SA(1 Hz) hazard curve and capacity estimates.

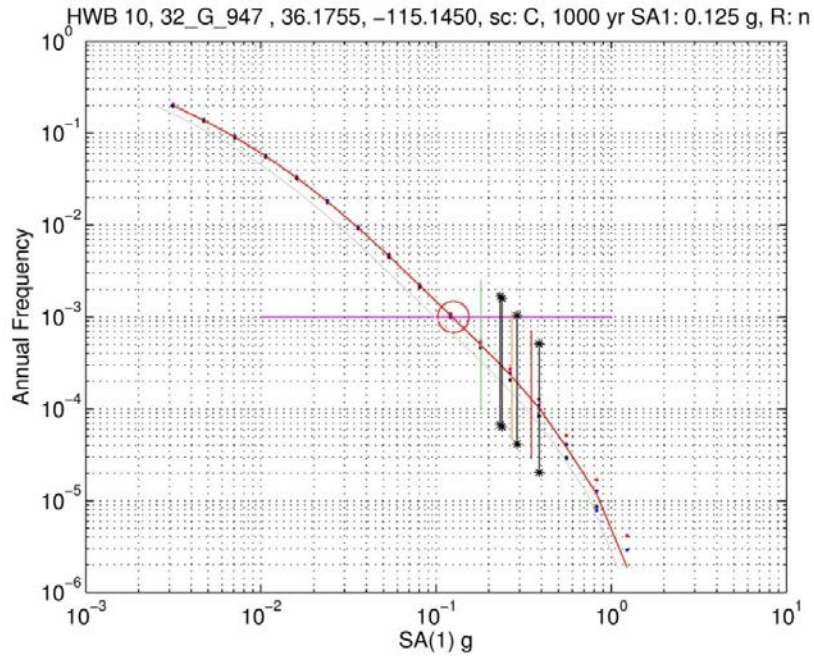


Figure B-1.9 HWB 10, 32_G_947 SA(1 Hz) hazard curve and capacity estimates.

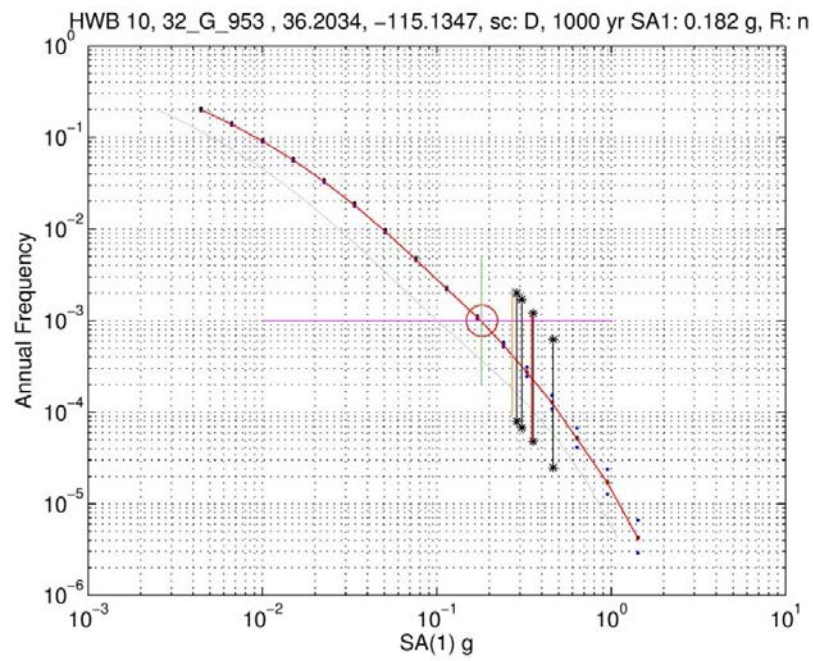


Figure B-1.10 HWB 10, 32_G_953 SA(1 Hz) hazard curve and capacity estimates.

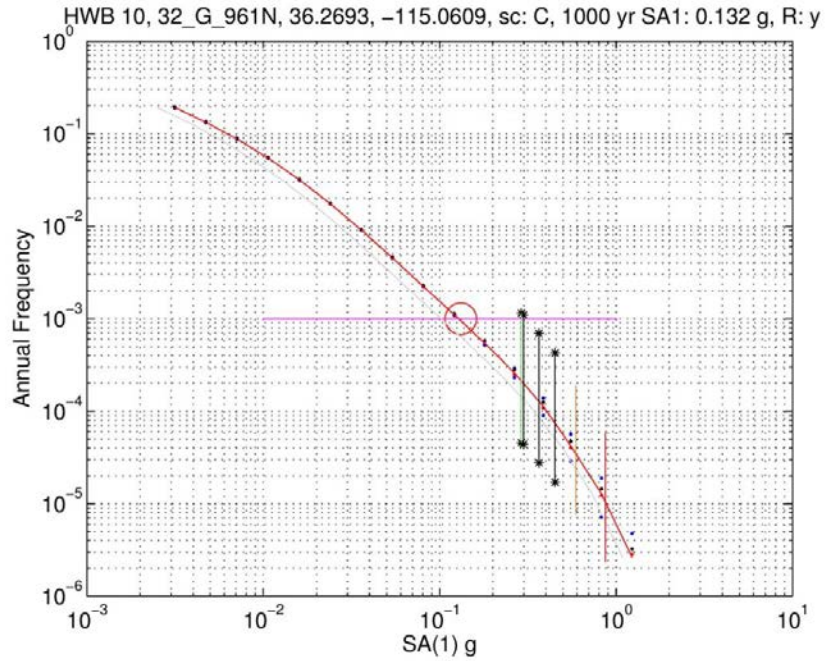


Figure B-1.11 HWB 10, 32_G_961N SA(1 Hz) hazard curve and capacity estimates.

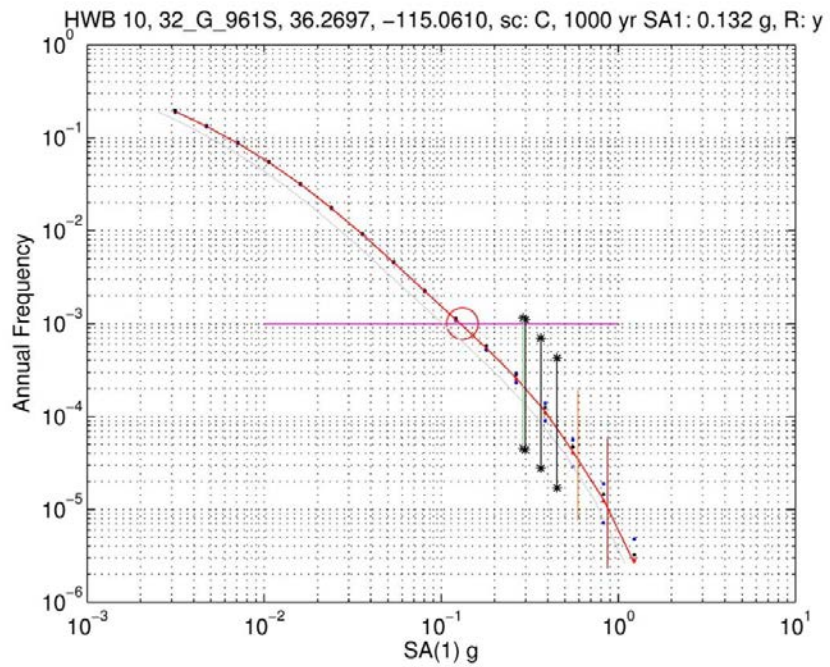


Figure B-1.12 HWB 10, 32_G_961S SA(1 Hz) hazard curve and capacity estimates.

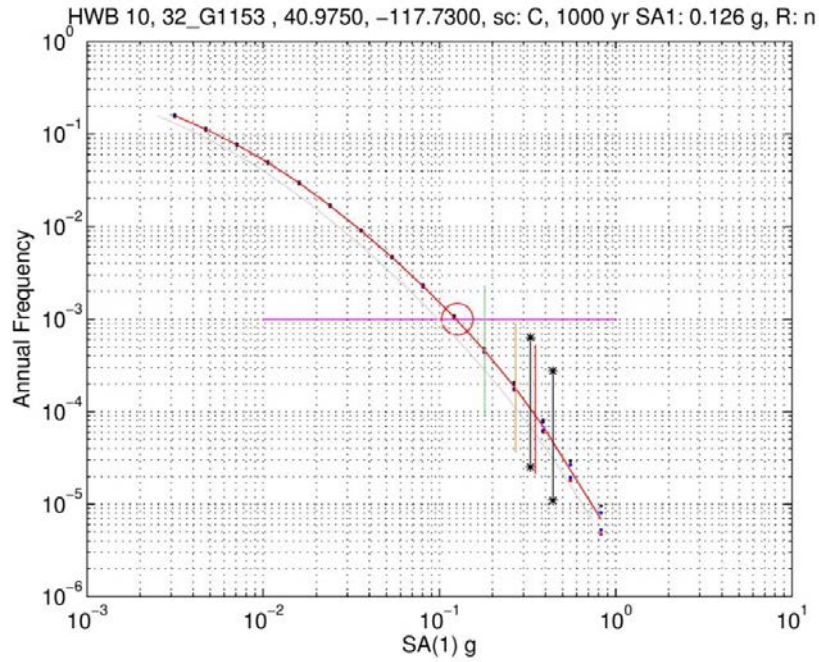


Figure B-1.13 HWB 10, 32_G1153 SA(1 Hz) hazard curve and capacity estimates.

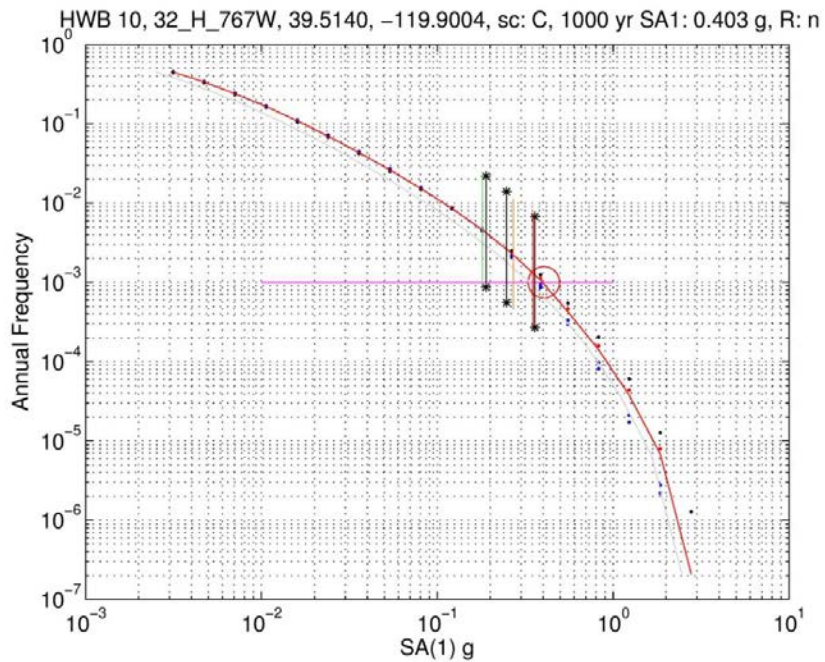


Figure B-1.14 HWB 10, 32_H_767W SA(1 Hz) hazard curve and capacity estimates. Damaging demand (intersection point of green line with hazard curve) is expected more frequently than the reference return period. Hazard is higher because bridge is near to higher slip-rate faults of northwest Nevada.

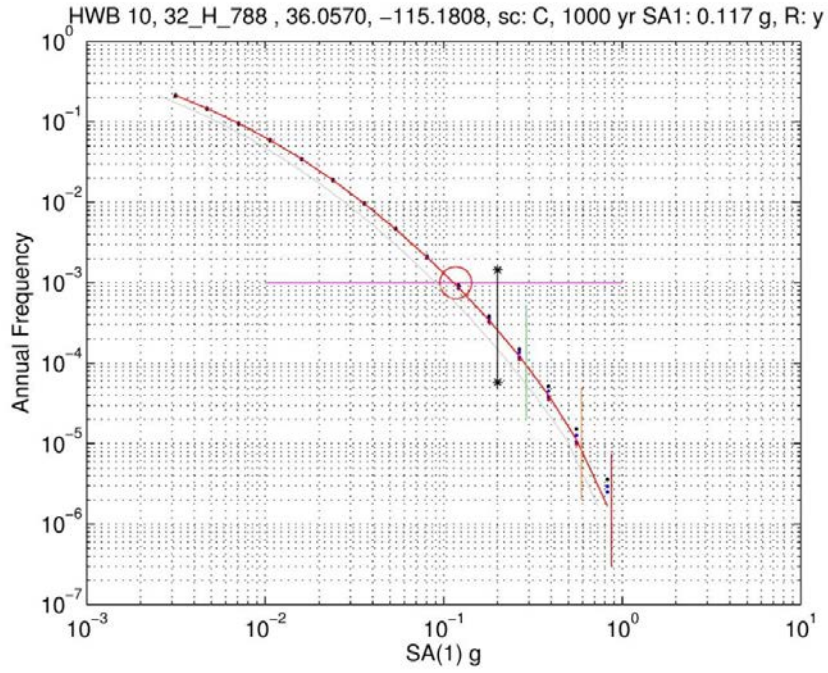


Figure B-1.15 HWB 10, 32_H_788 SA(1 Hz) hazard curve and capacity estimates.

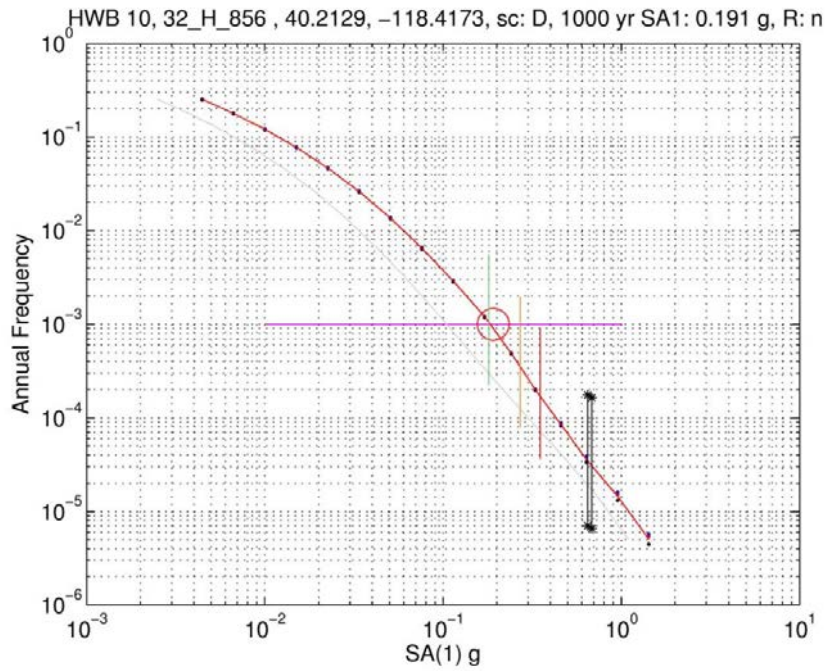


Figure B-1.16 HWB 10, 32_H_856 SA(1 Hz) hazard curve and capacity estimates.

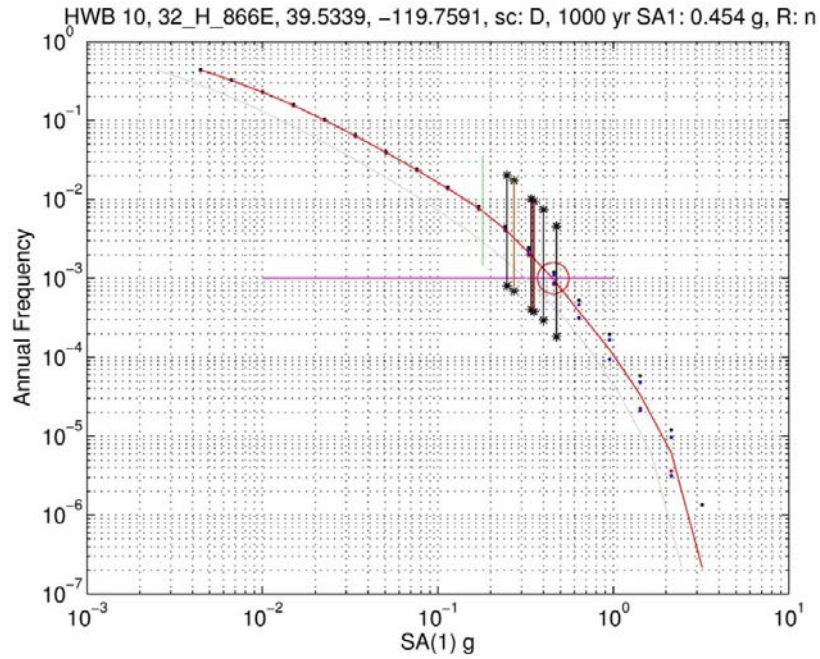


Figure B-1.17 HWB 10, 32_H_866E SA(1 Hz) hazard curve and capacity estimates.

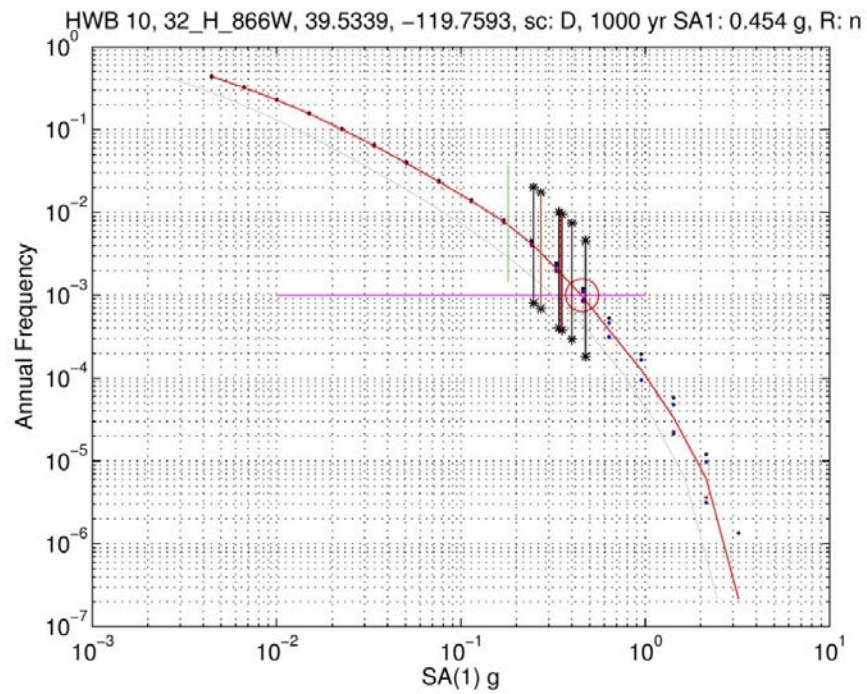


Figure B-1.18 HWB 10, 32_H_866W SA(1 Hz) hazard curve and capacity estimates.

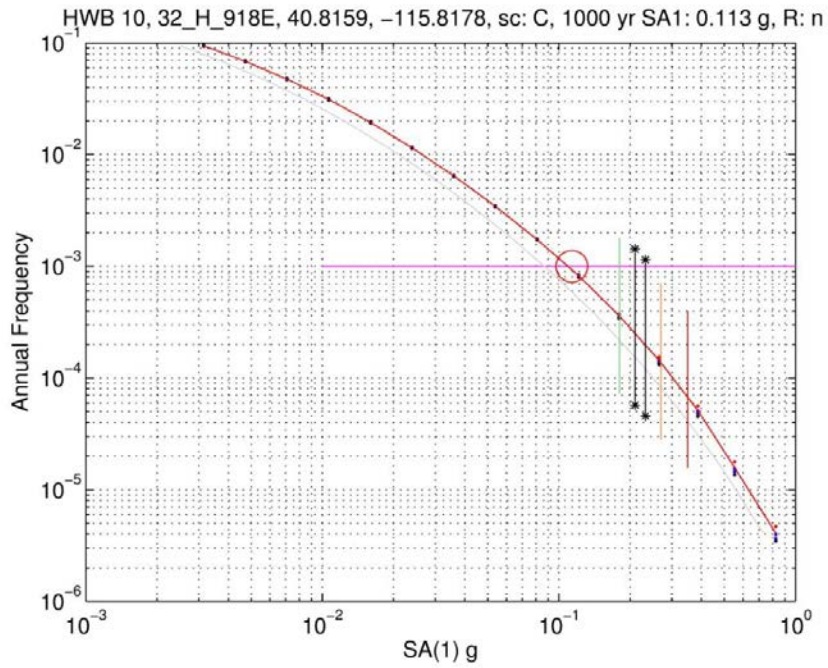


Figure B-1.19 HWB 10, 32_H_918W SA(1 Hz) hazard curve and capacity estimates.

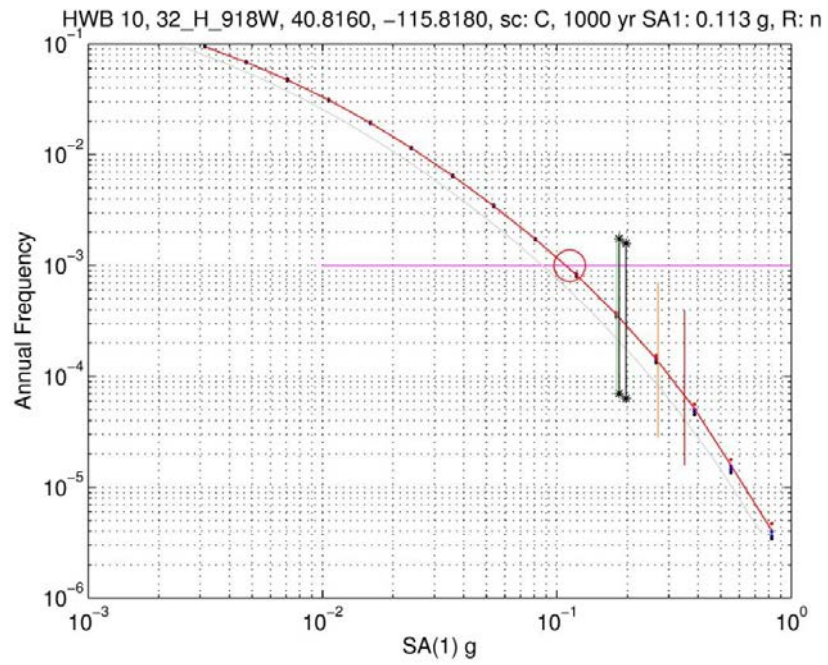


Figure B-1.20 HWB 10, 32_H_918W SA(1 Hz) hazard curve and capacity estimates.

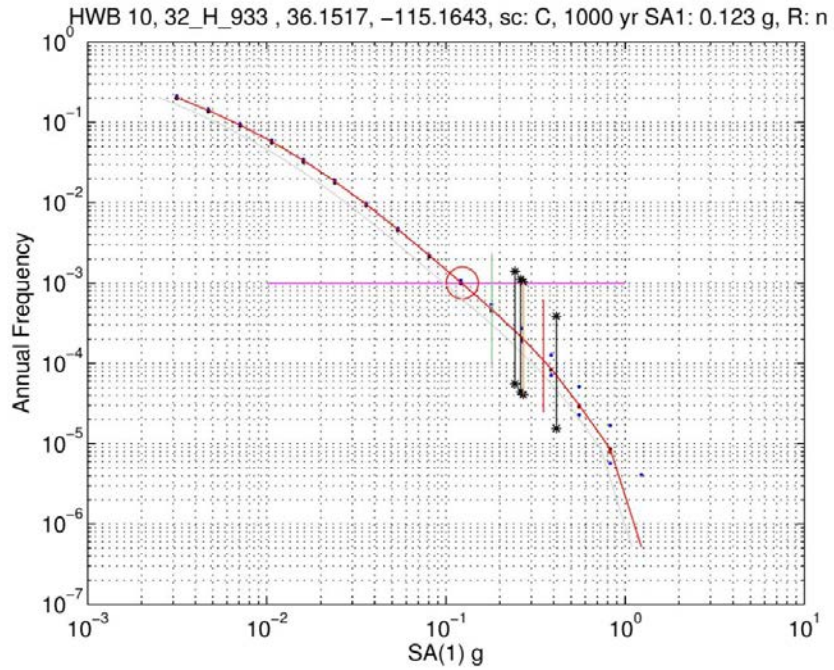


Figure B-1.21 HWB 10, 32_H_933 SA(1 Hz) hazard curve and capacity estimates.

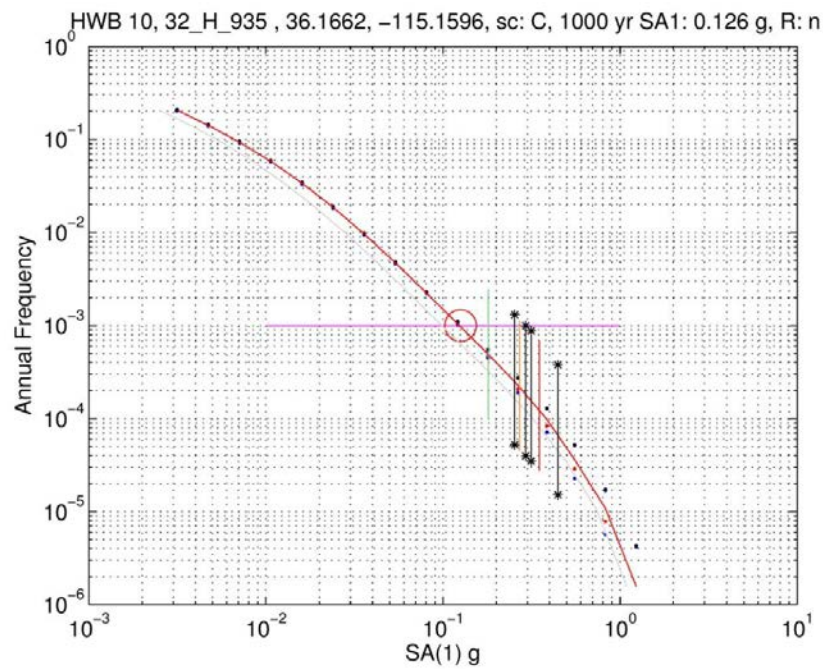


Figure B-1.22 HWB 10, 32_H_935 SA(1 Hz) hazard curve and capacity estimates.

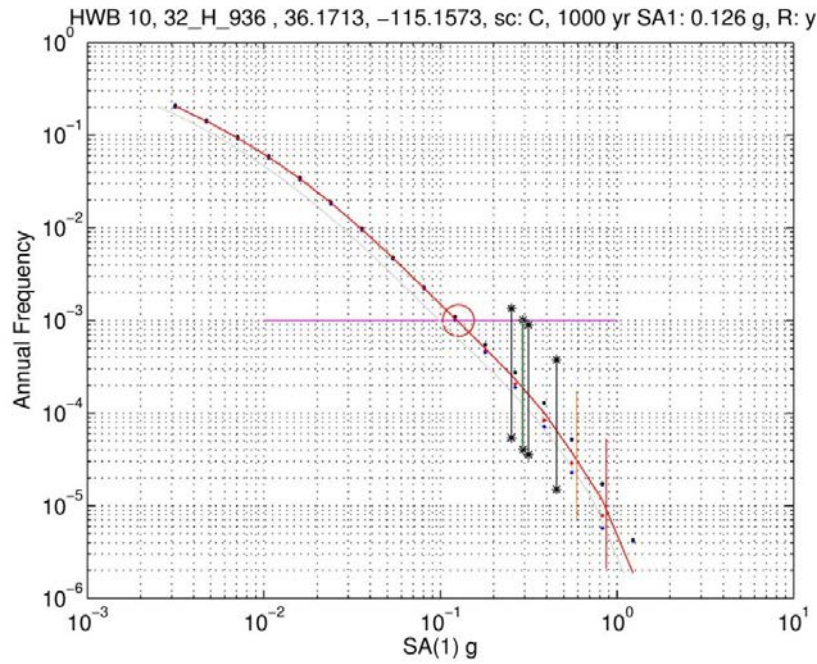


Figure B-1.23 HWB 10, 32_H_936 SA(1 Hz) hazard curve and capacity estimates.

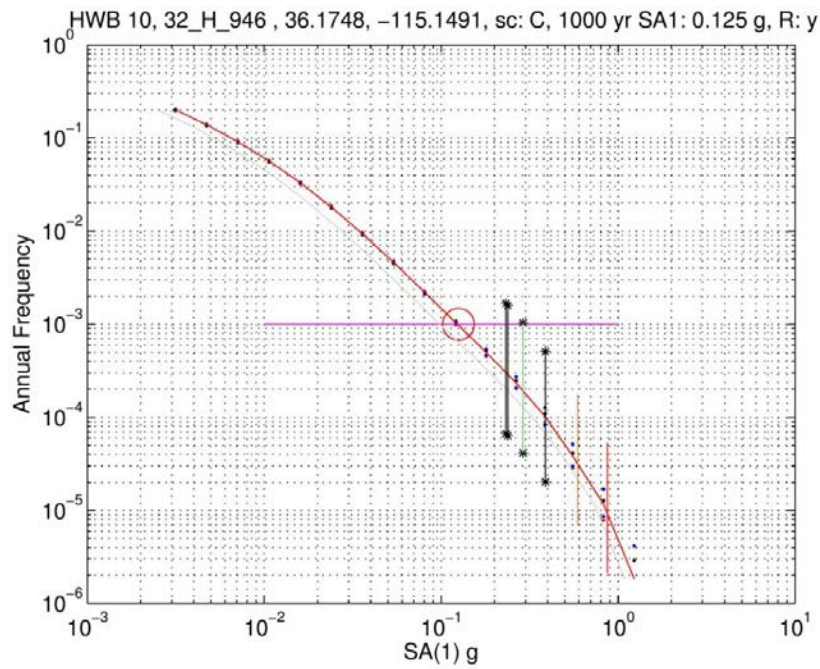


Figure B-1.24 HWB 10, 32_H_946 SA(1 Hz) hazard curve and capacity estimates.

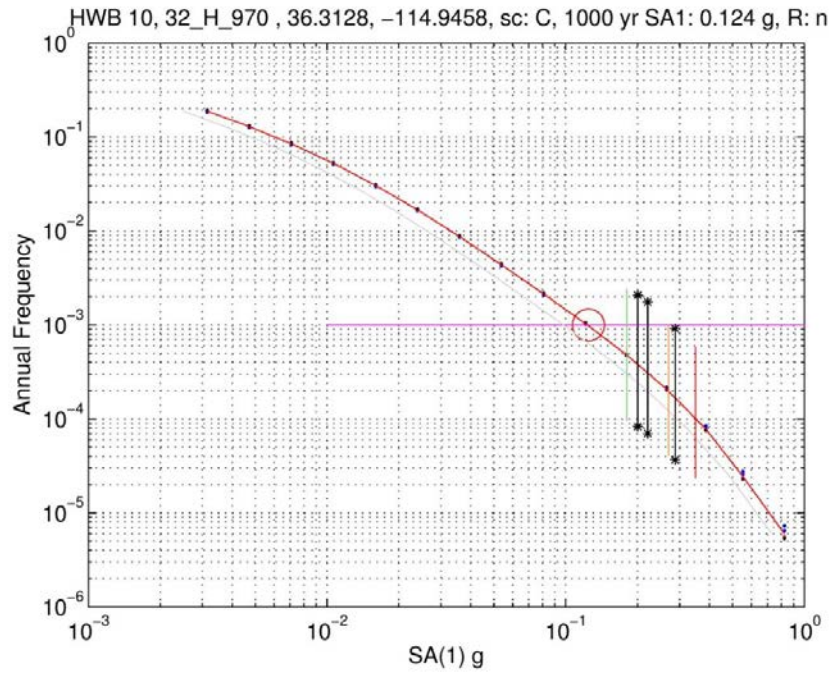


Figure B-1.25 HWB 10, 32_H_970 SA(1 Hz) hazard curve and capacity estimates.

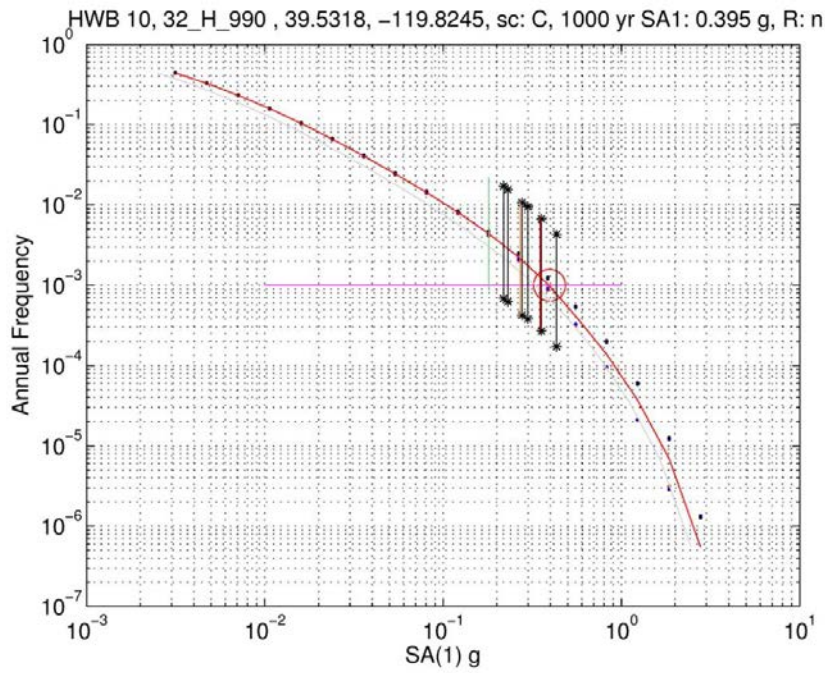


Figure B-1.26 HWB 10, 32_H_990 SA(1 Hz) hazard curve and capacity estimates.

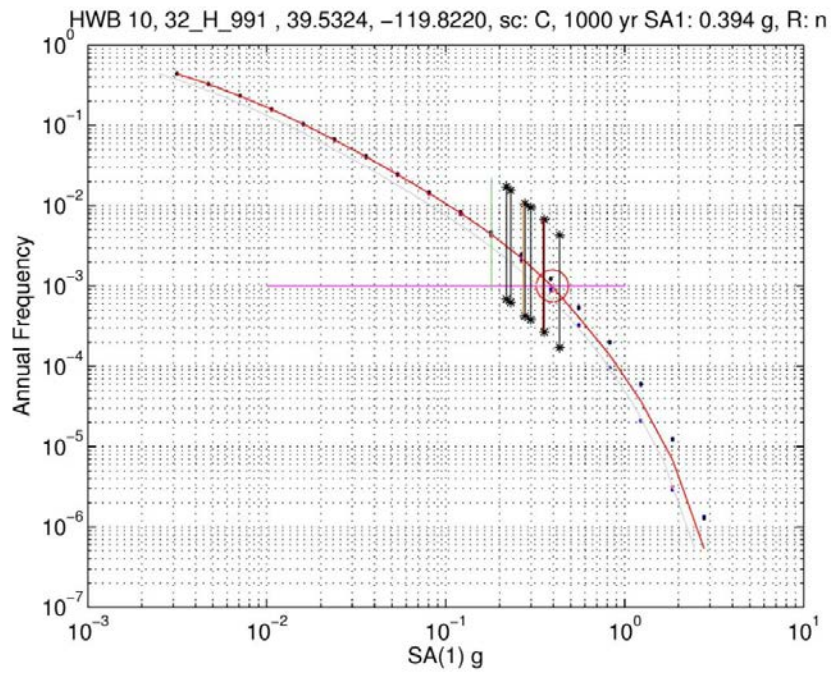


Figure B-1.27 HWB 10, 32_H_991 SA(1 Hz) hazard curve and capacity estimates.

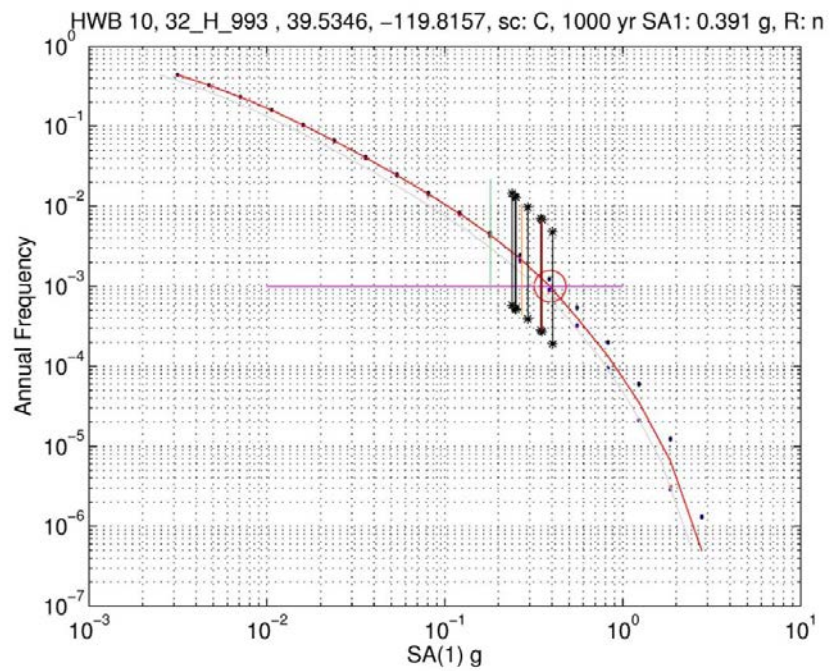


Figure B-1.28 HWB 10, 32_H_993 SA(1 Hz) hazard curve and capacity estimates.

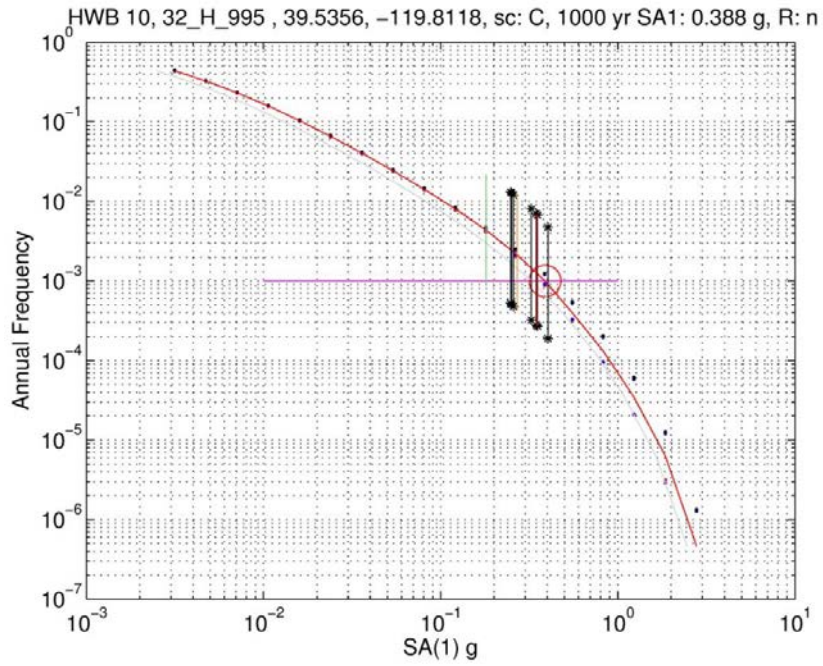


Figure B-1.29 HWB 10, 32_H_995 SA(1 Hz) hazard curve and capacity estimates.

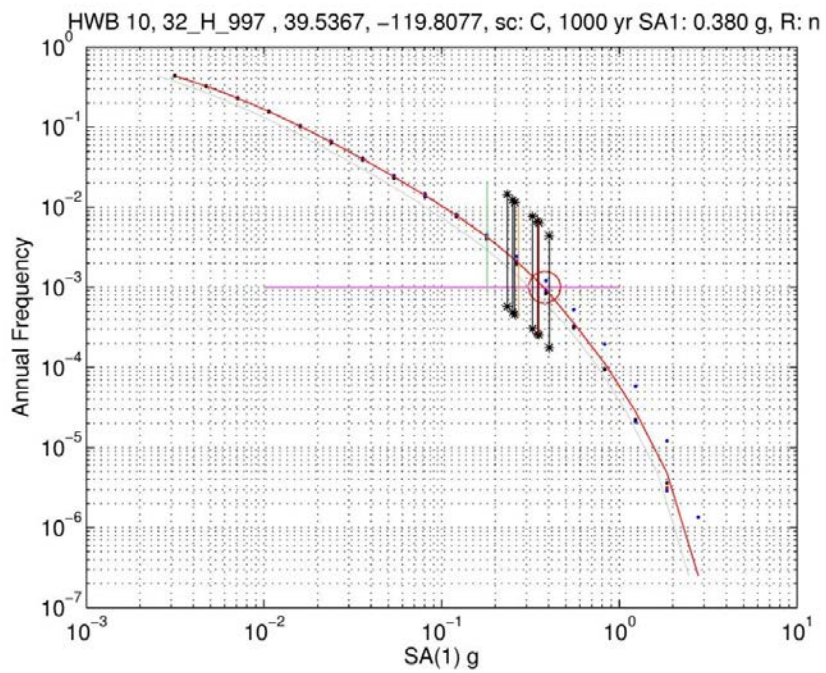


Figure B-1.30 HWB 10, 32_H_997 SA(1 Hz) hazard curve and capacity estimates.

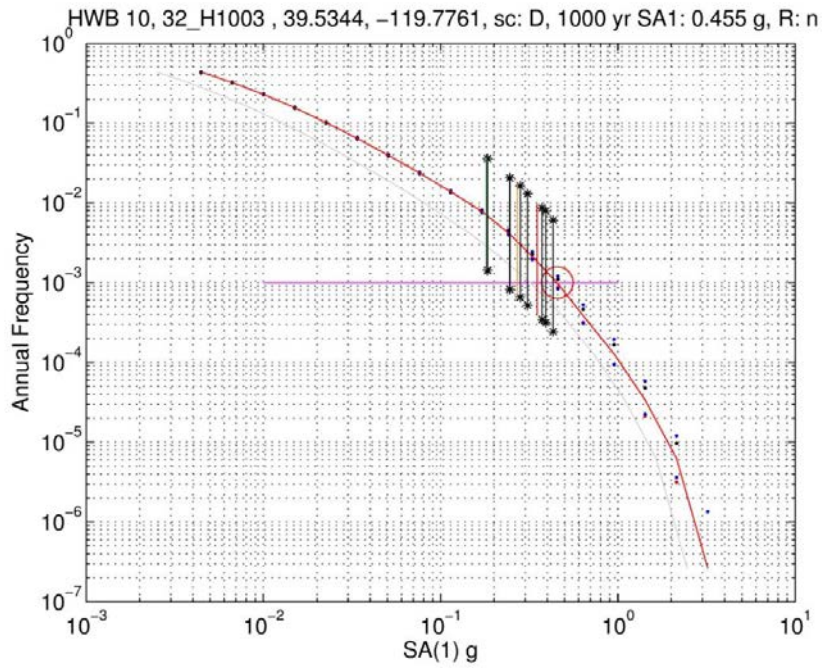


Figure B-1.31 HWB 10, 32_H1003 SA(1 Hz) hazard curve and capacity estimates.

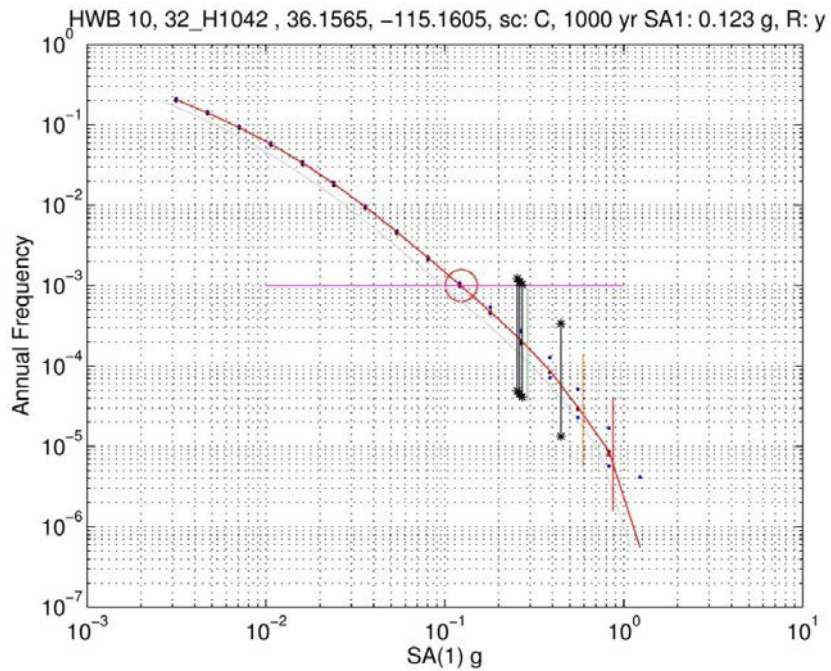


Figure B-1.32 HWB 10, 32_H1042 SA(1 Hz) hazard curve and capacity estimates.

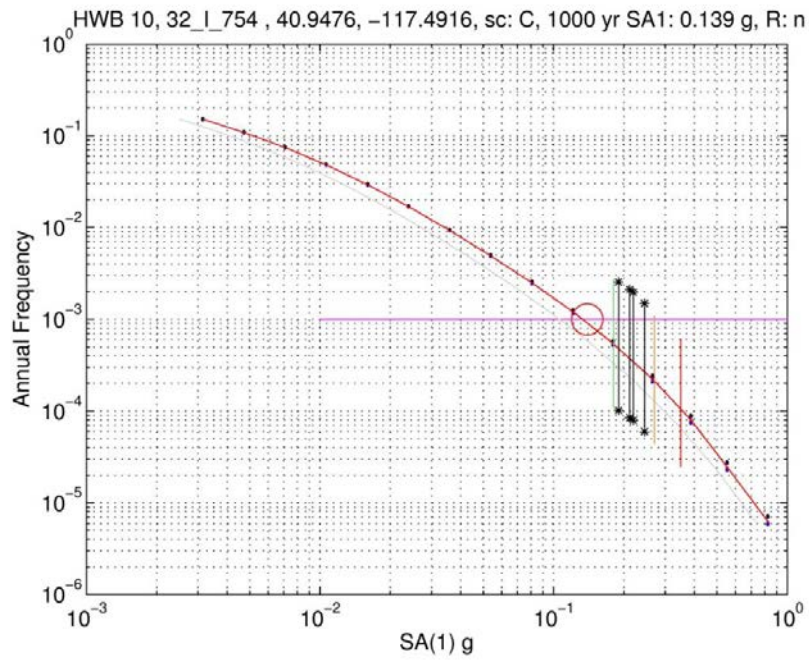


Figure B-1.33 HWB 10, 32_I_754 SA(1 Hz) hazard curve and capacity estimates.

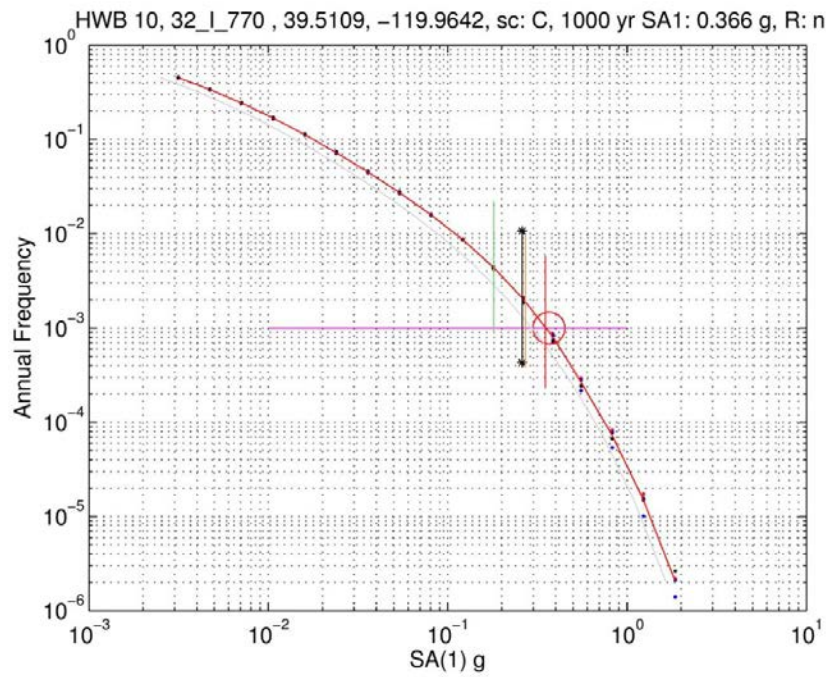


Figure B-1.34 HWB 10, 32_I_770 SA(1 Hz) hazard curve and capacity estimates.

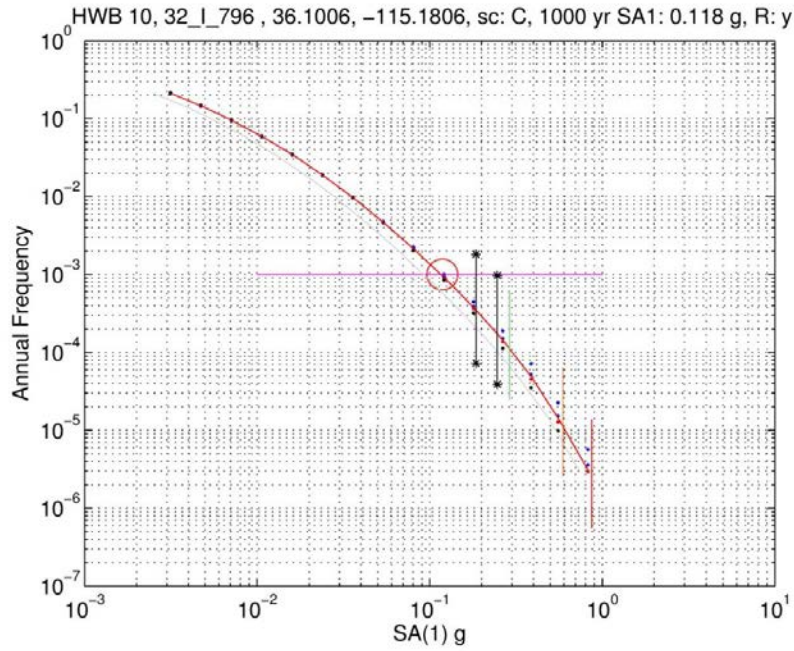


Figure B-1.35 HWB 10, 32_I_796 SA(1 Hz) hazard curve and capacity estimates.

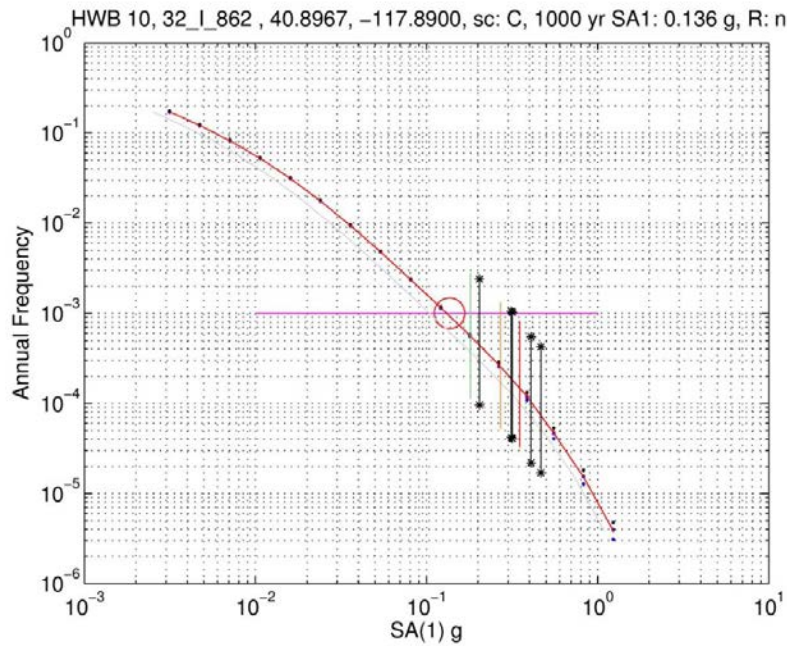


Figure B-1.36 HWB 10, 32_I_862 SA(1 Hz) hazard curve and capacity estimates.

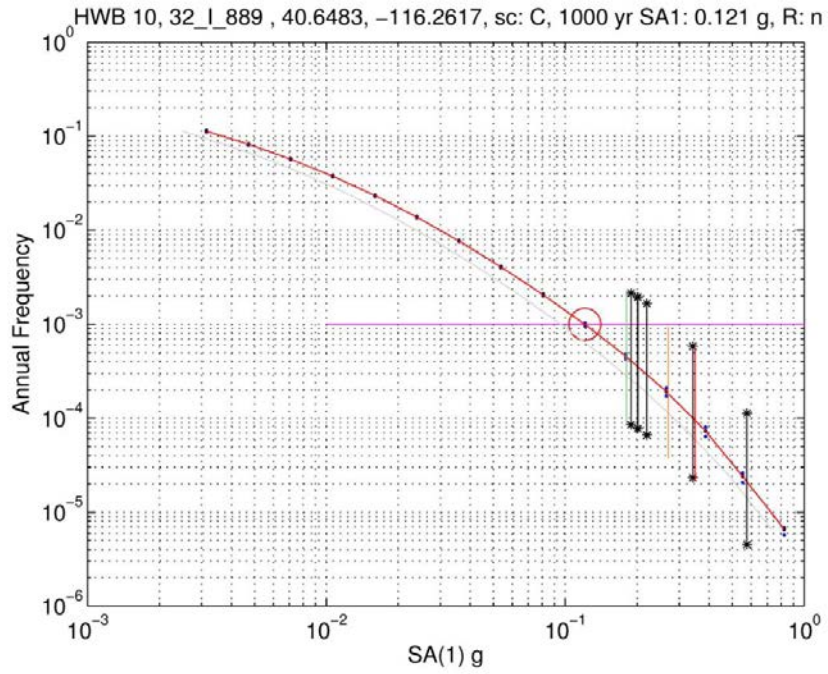


Figure B-1.37 HWB 10, 32_I_889 SA(1 Hz) hazard curve and capacity estimates.

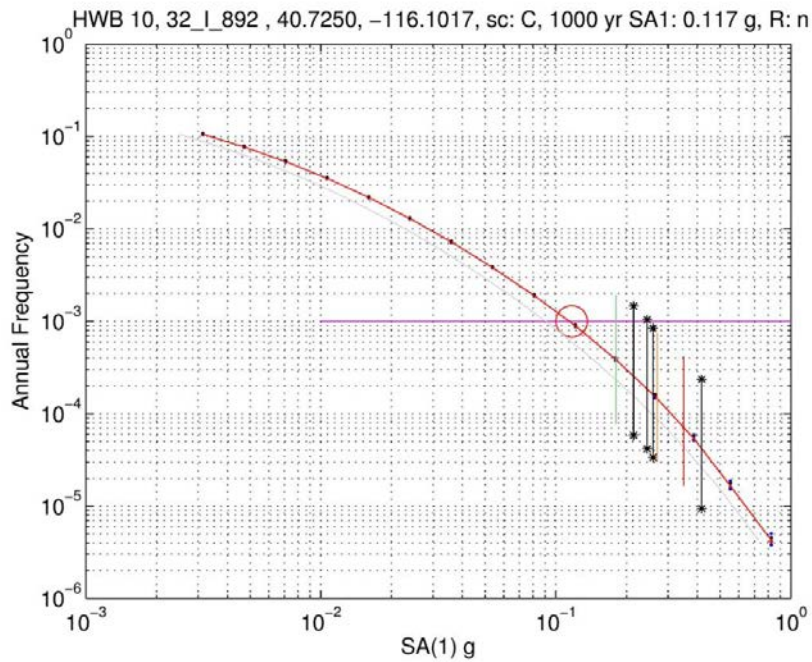


Figure B-1.38 HWB 10, 32_I_892 SA(1 Hz) hazard curve and capacity estimates.

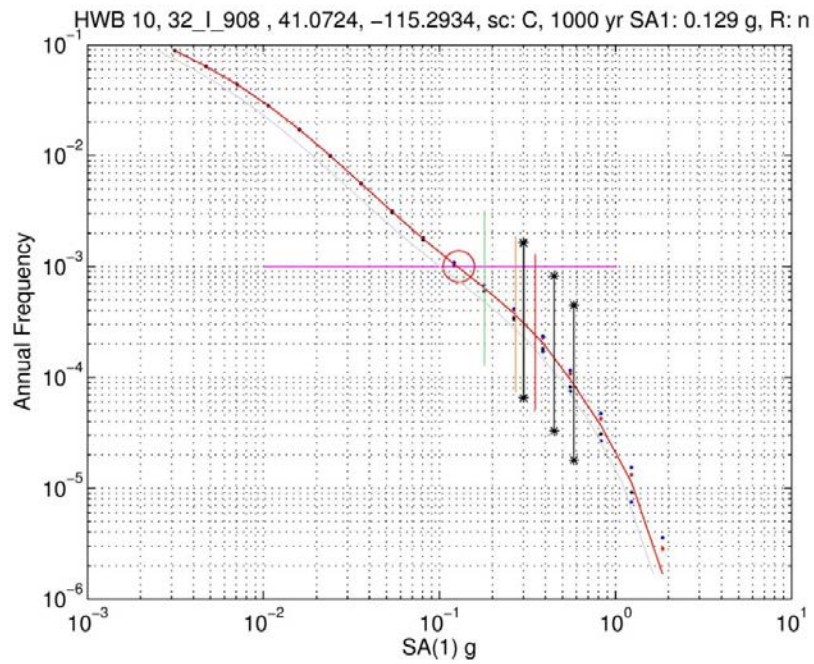


Figure B-1.39 HWB 10, 32_I_908 SA(1 Hz) hazard curve and capacity estimates.

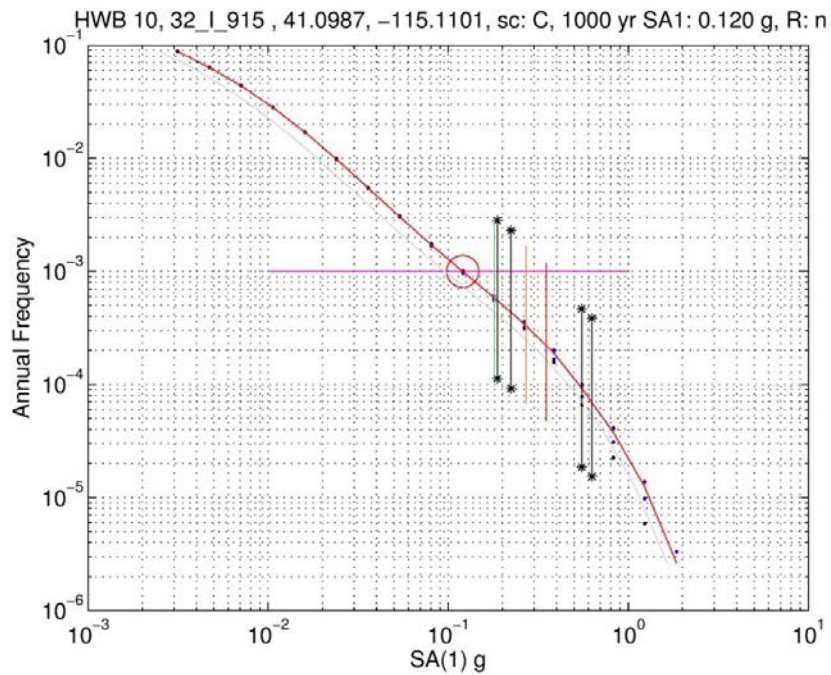


Figure B-1.40 HWB 10, 32_I_915 SA(1 Hz) hazard curve and capacity estimates.

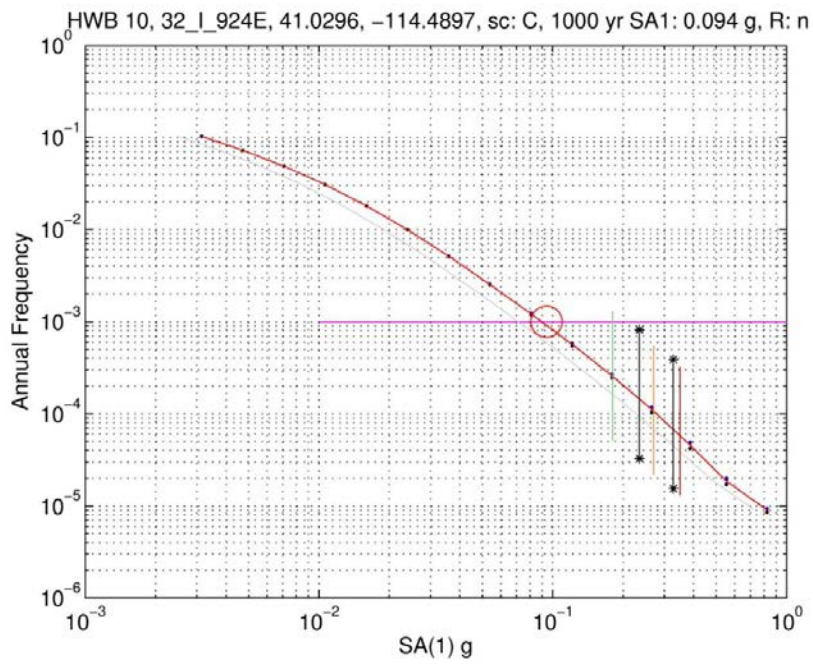


Figure B-1.41 HWB 10, 32_I_924E SA(1 Hz) hazard curve and capacity estimates.

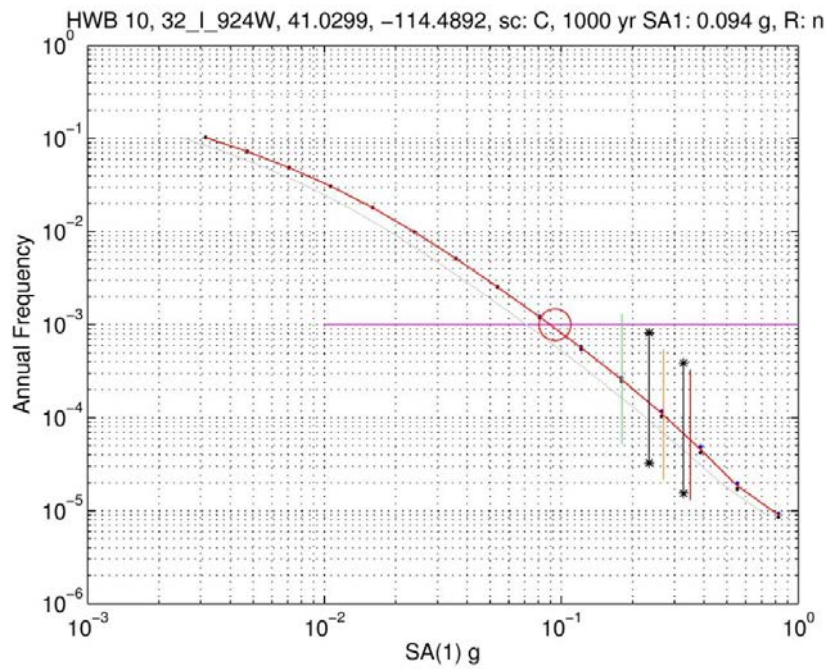


Figure B-1.42 HWB 10, 32_I_924W SA(1 Hz) hazard curve and capacity estimates.

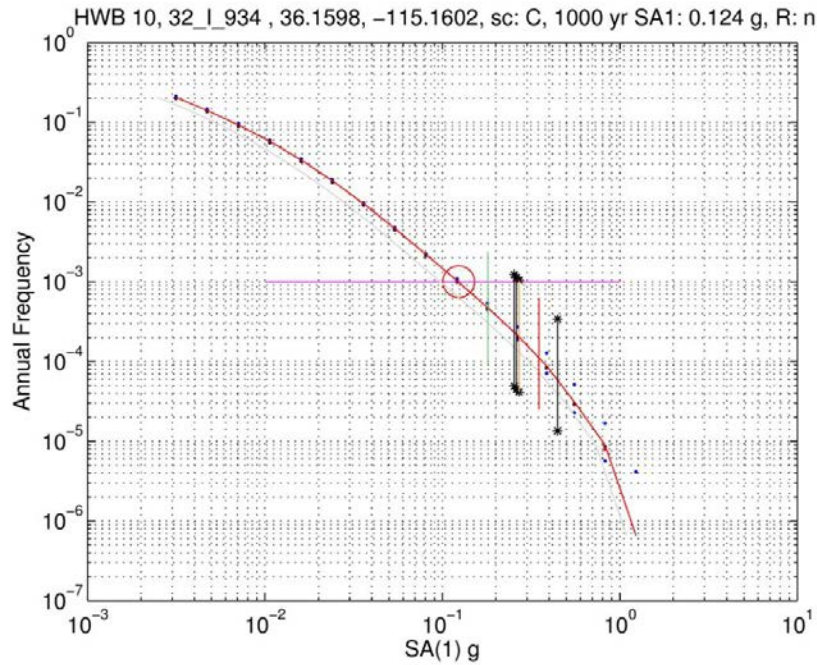


Figure B-1.43 HWB 10, 32_I_934 SA(1 Hz) hazard curve and capacity estimates.

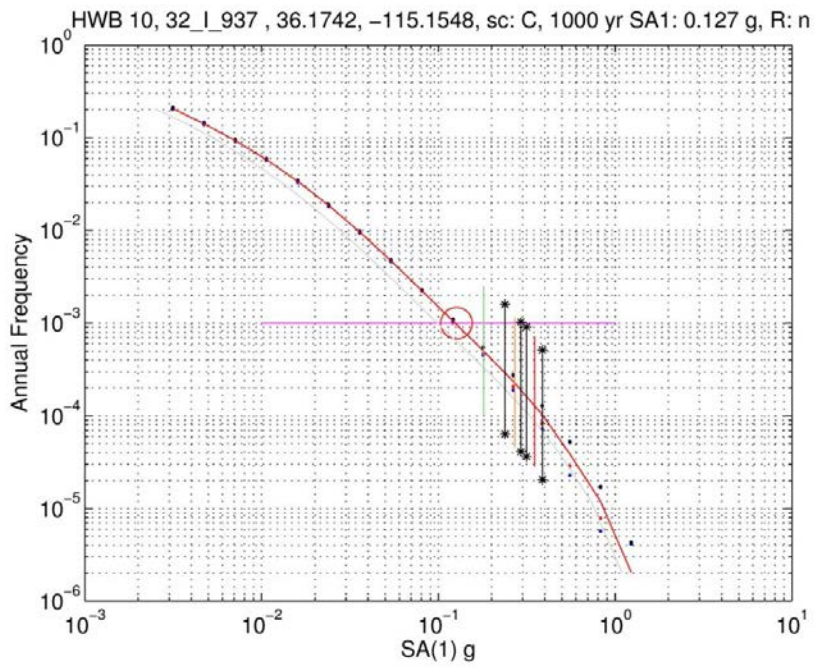


Figure B-1.44 HWB 10, 32_I_937 SA(1 Hz) hazard curve and capacity estimates.

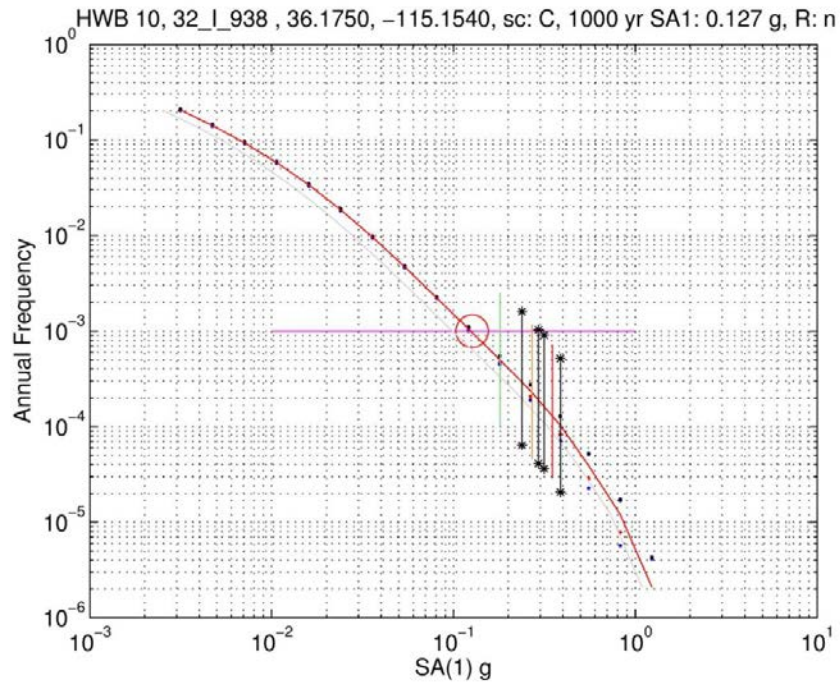


Figure B-1.45 HWB 10, 32_I_938 SA(1 Hz) hazard curve and capacity estimates.

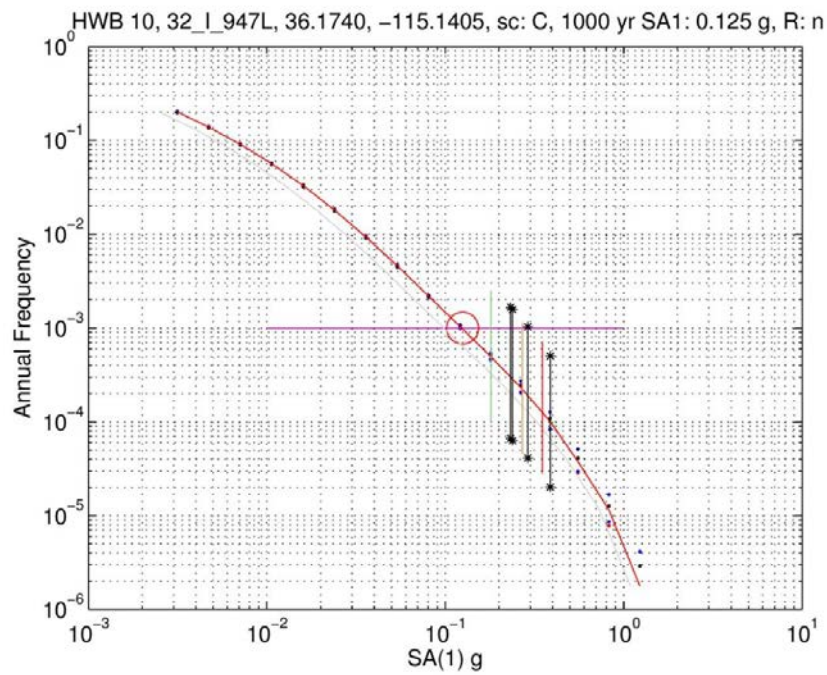


Figure B-1.46 HWB 10, 32_I_947L SA(1 Hz) hazard curve and capacity estimates.

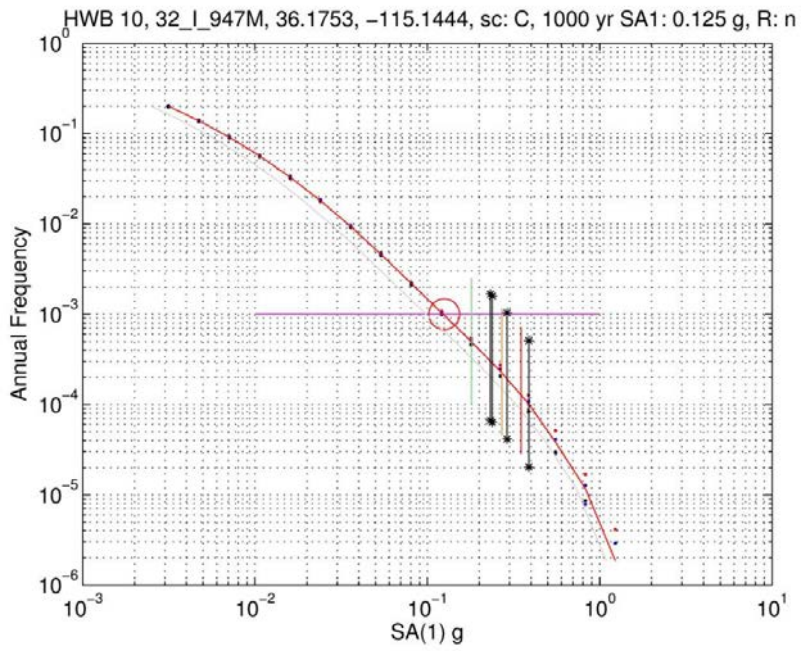


Figure B-1.47 HWB 10, 32_I_947M SA(1 Hz) hazard curve and capacity estimates.

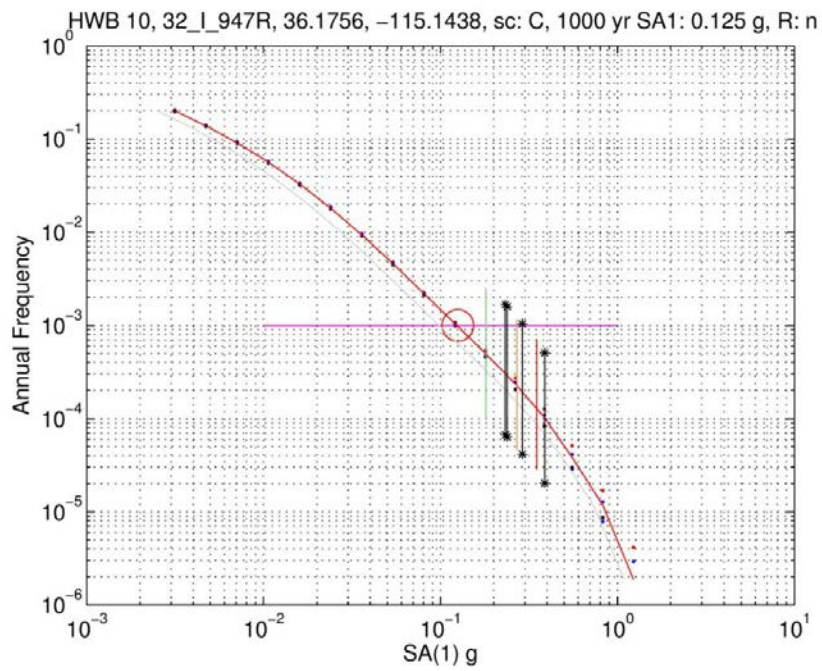


Figure B-1.48 HWB 10, 32_I_947R SA(1 Hz) hazard curve and capacity estimates.

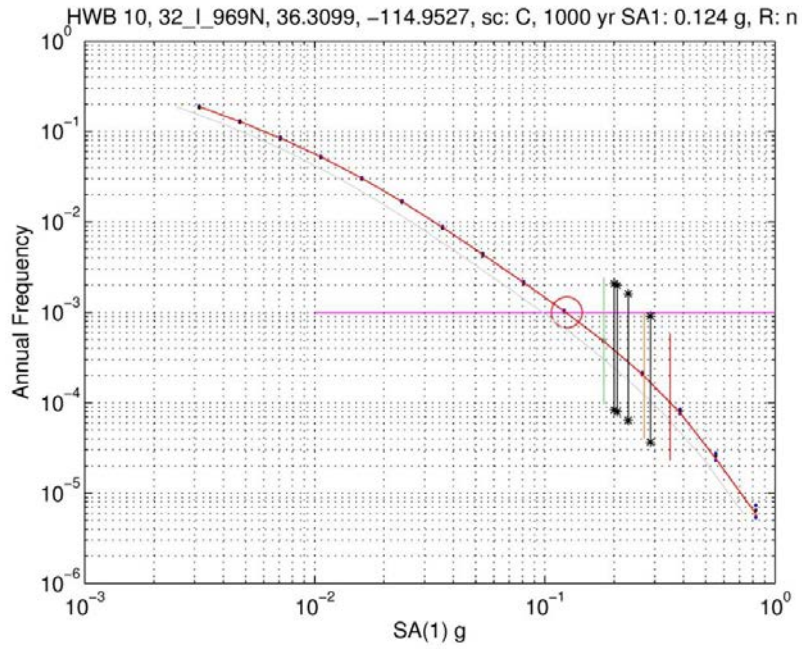


Figure B-1.49 HWB 10, 32_I_969N SA(1 Hz) hazard curve and capacity estimates.

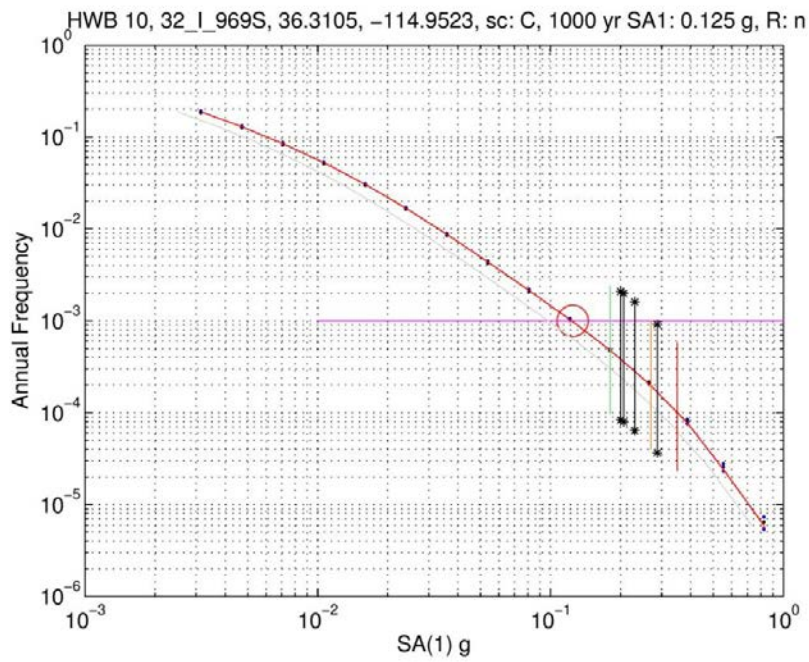


Figure B-1.50 HWB 10, 32_I_969S SA(1 Hz) hazard curve and capacity estimates.

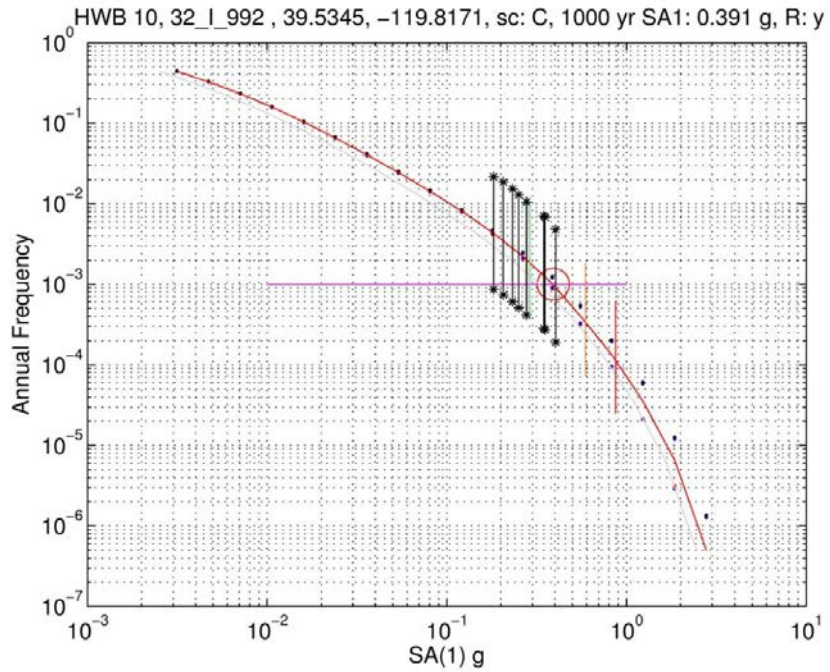


Figure B-1.51 HWB 10, 32_I_992 SA(1 Hz) hazard curve and capacity estimates.

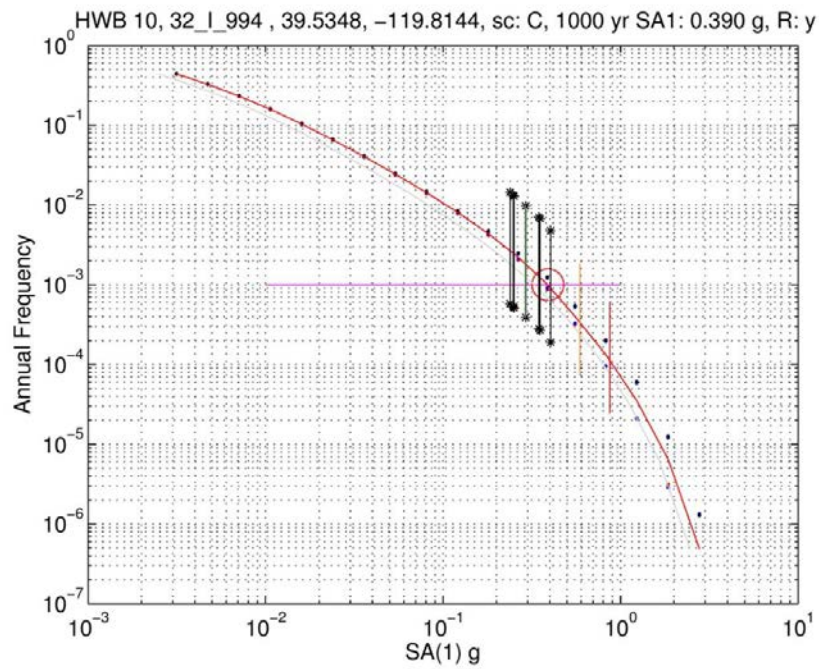


Figure B-1.52 HWB 10, 32_I_994 SA(1 Hz) hazard curve and capacity estimates.

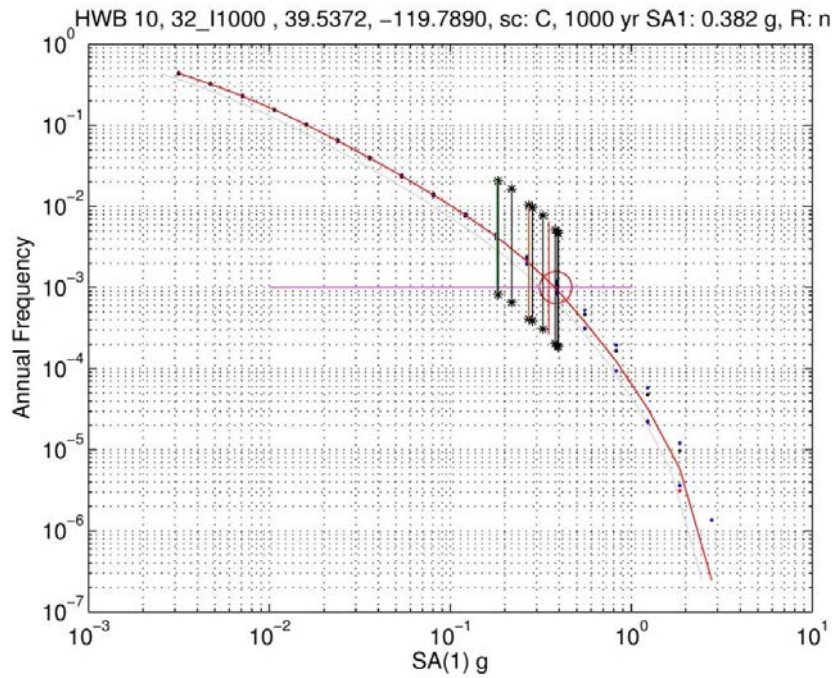


Figure B-1.53 HWB 10, 32_I1000 SA(1 Hz) hazard curve and capacity estimates.

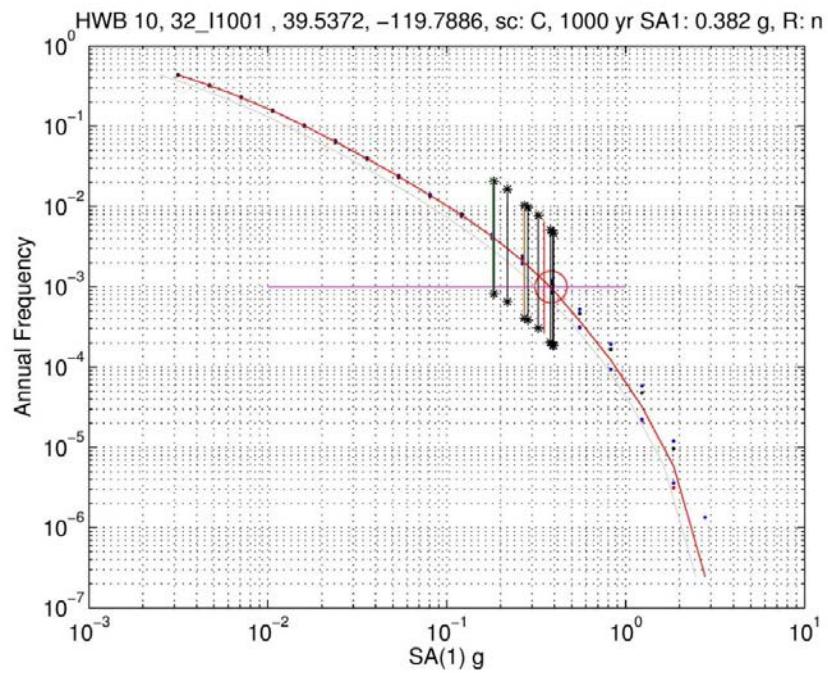


Figure B-1.54 HWB 10, 32_I1001 SA(1 Hz) hazard curve and capacity estimates.

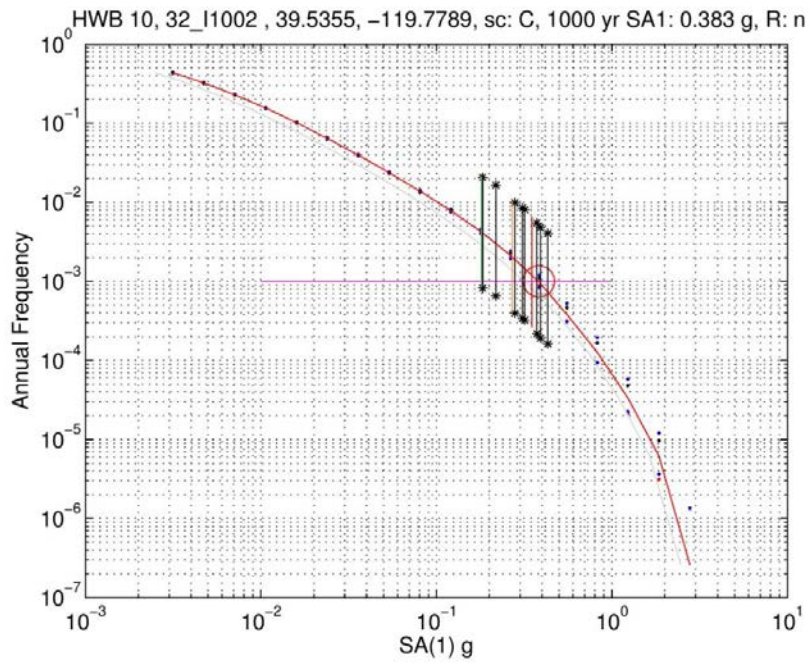


Figure B-1.55 HWB 10, 32_I1002 SA(1 Hz) hazard curve and capacity estimates.

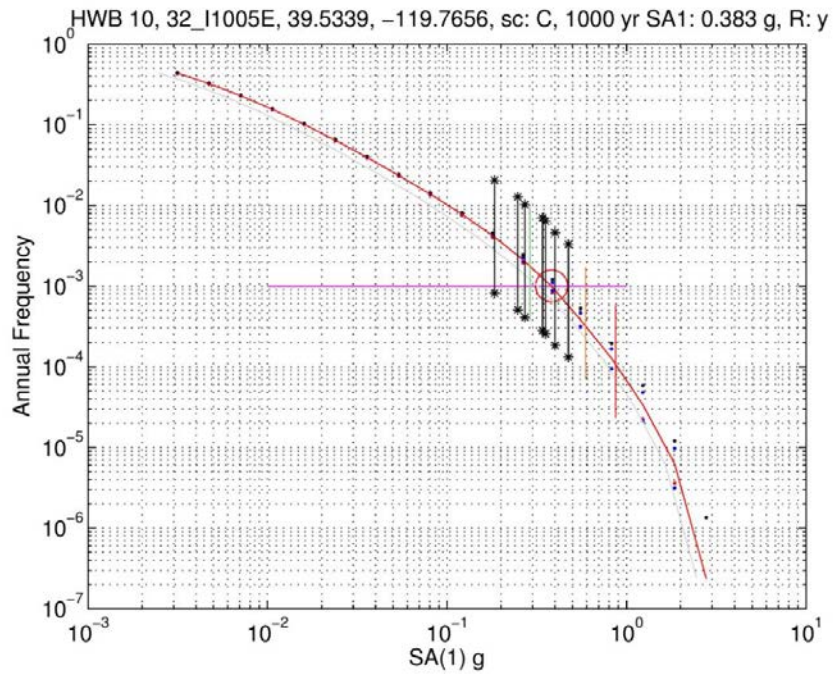


Figure B-1.56 HWB 10, 32_I1005E SA(1 Hz) hazard curve and capacity estimates.

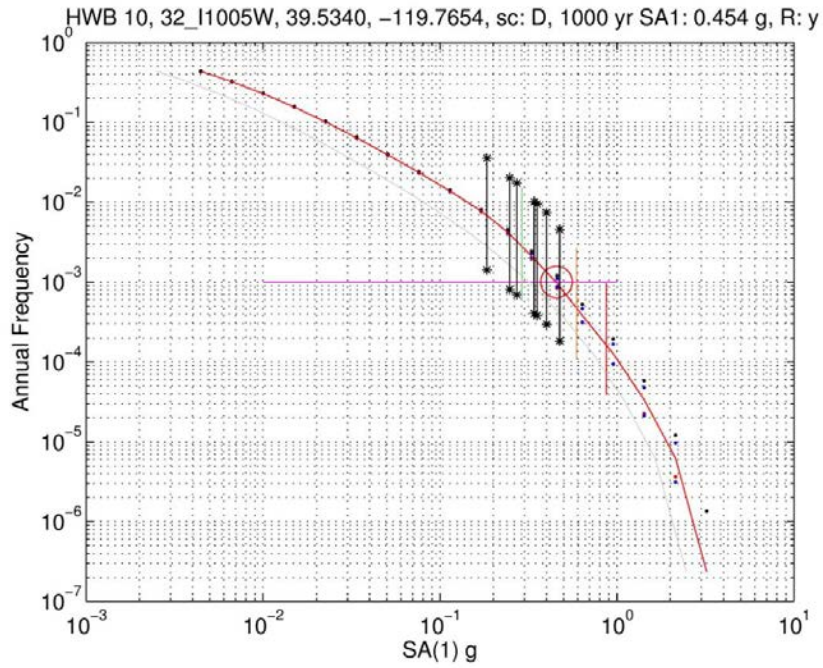


Figure B-1.57 HWB 10, 32_I1005W SA(1 Hz) hazard curve and capacity estimates.

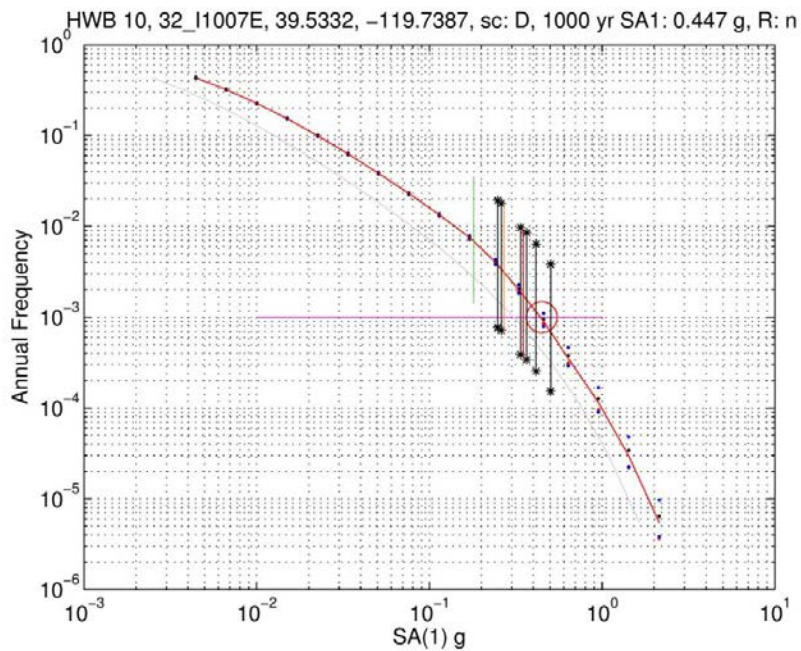


Figure B-1.58 HWB 10, 32_I1007E SA(1 Hz) hazard curve and capacity estimates.

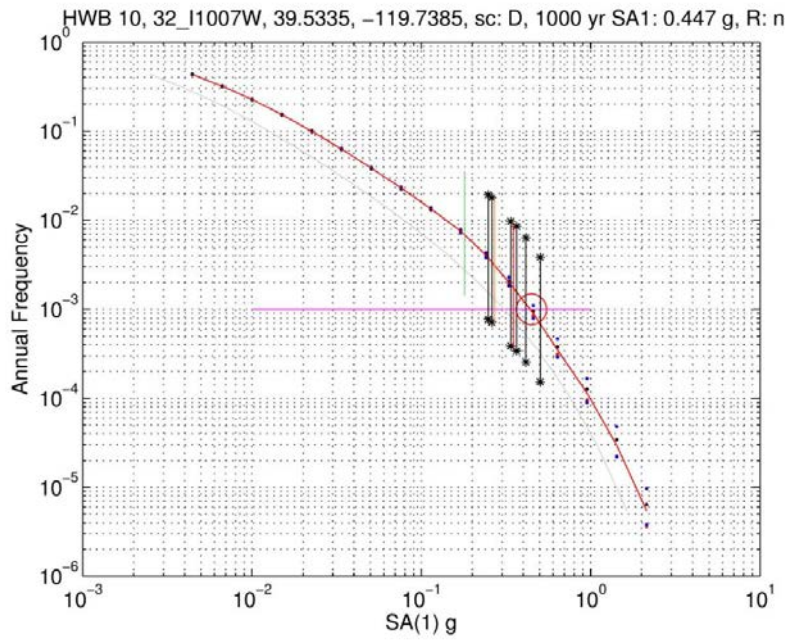


Figure B-1.59 HWB 10, 32_I1007W SA(1 Hz) hazard curve and capacity estimates.

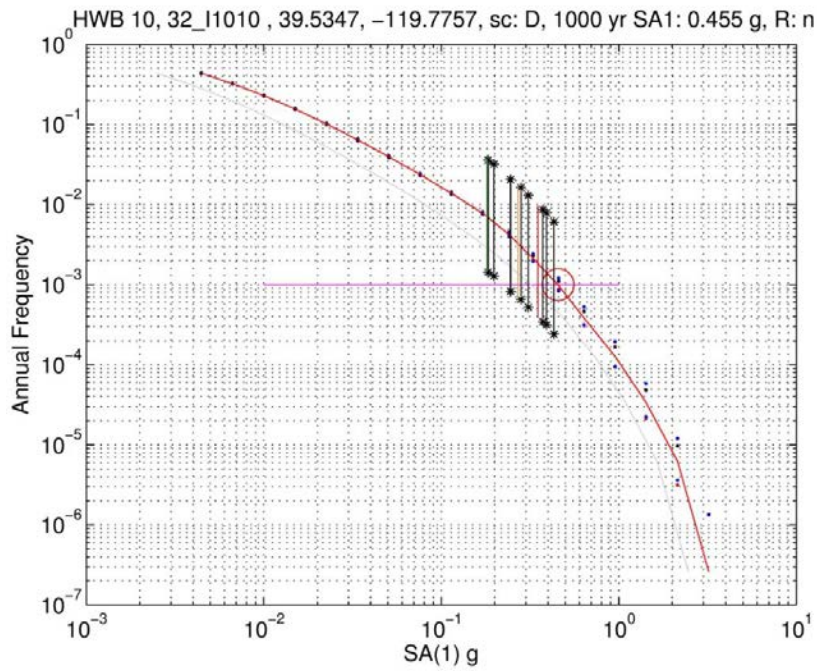


Figure B-1.60 HWB 10, 32_I1010 SA(1 Hz) hazard curve and capacity estimates.

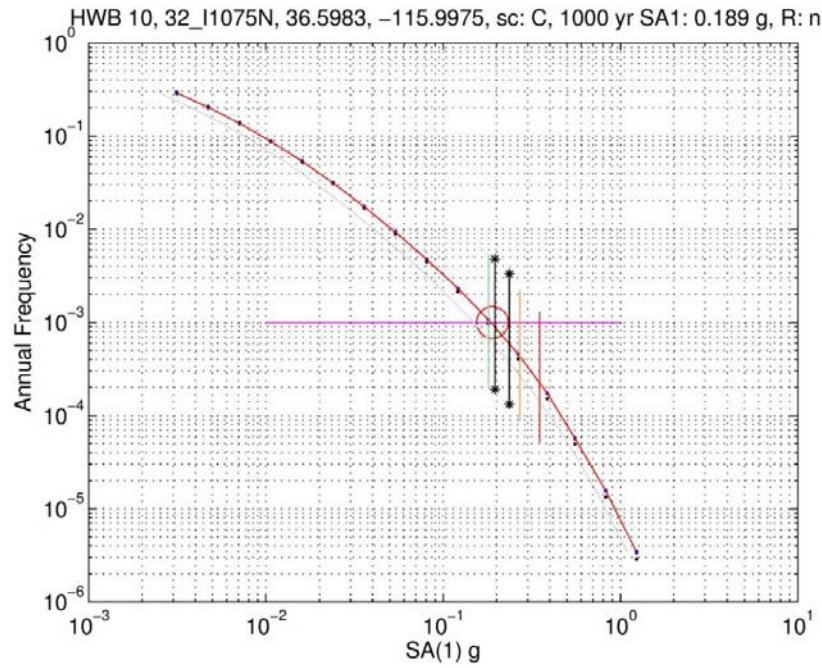


Figure B-1.61 HWB 10, 32_I1075N SA(1 Hz) hazard curve and capacity estimates.

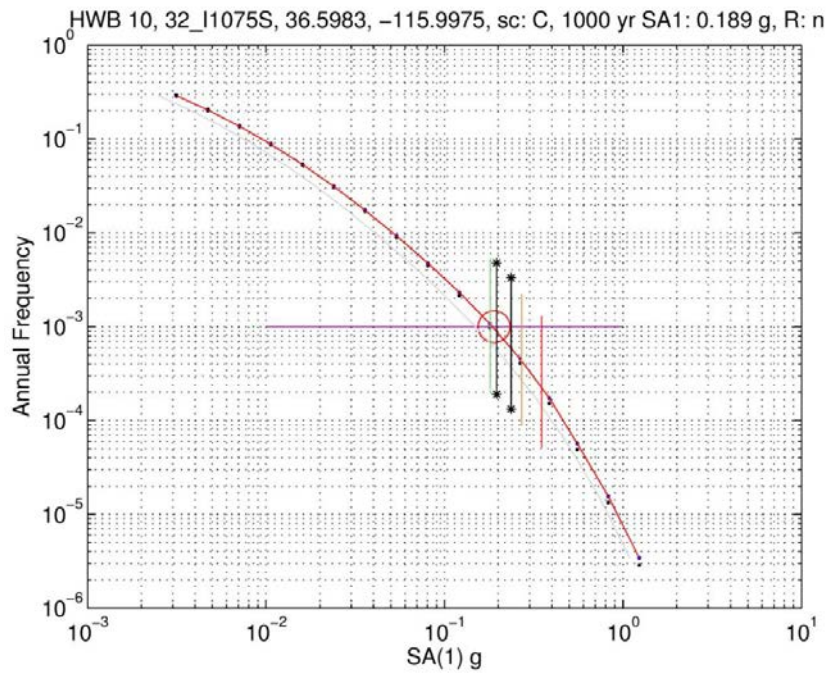


Figure B-1.62 HWB 10, 32_I1075S SA(1 Hz) hazard curve and capacity estimates.

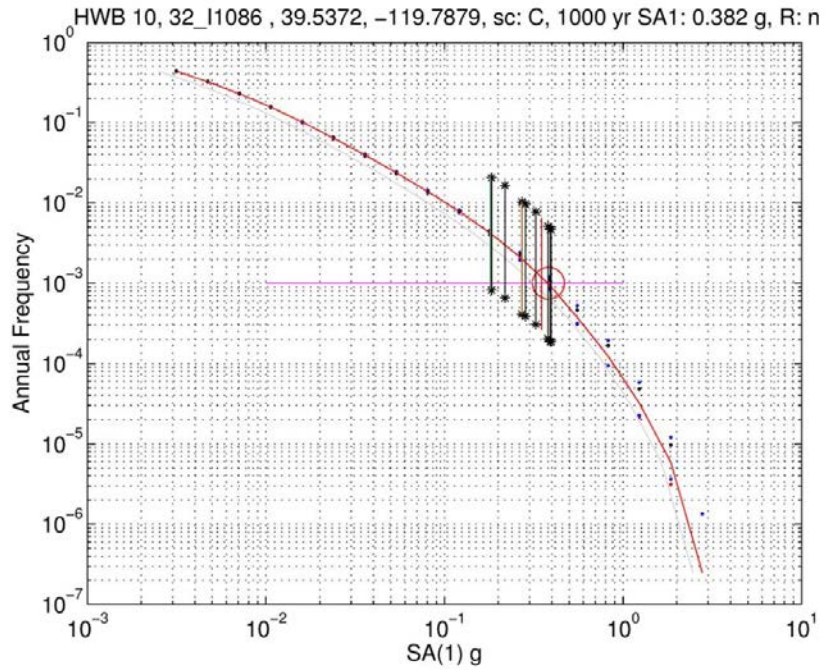


Figure B-1.63 HWB 10, 32_I1086 SA(1 Hz) hazard curve and capacity estimates.

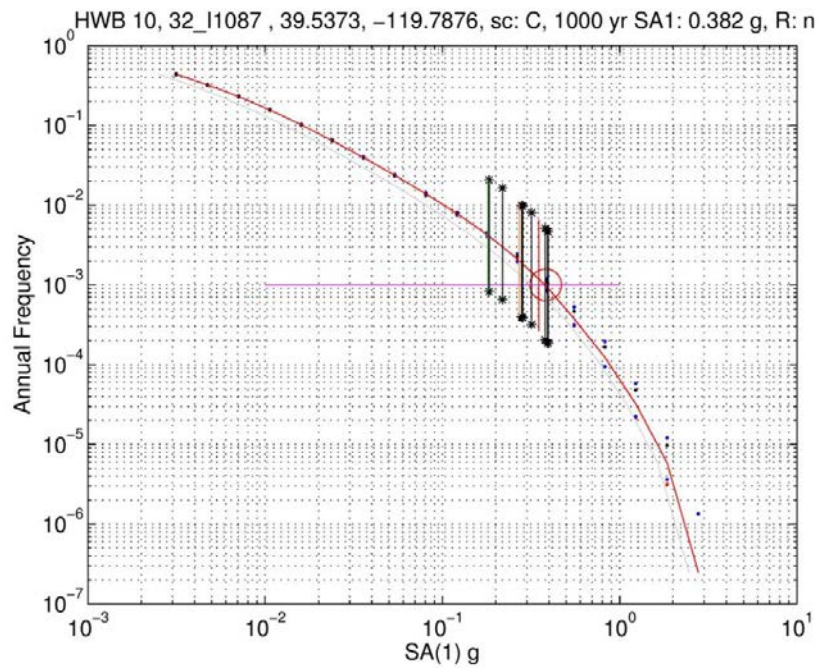


Figure B-1.64 HWB 10, 32_I1087 SA(1 Hz) hazard curve and capacity estimates.

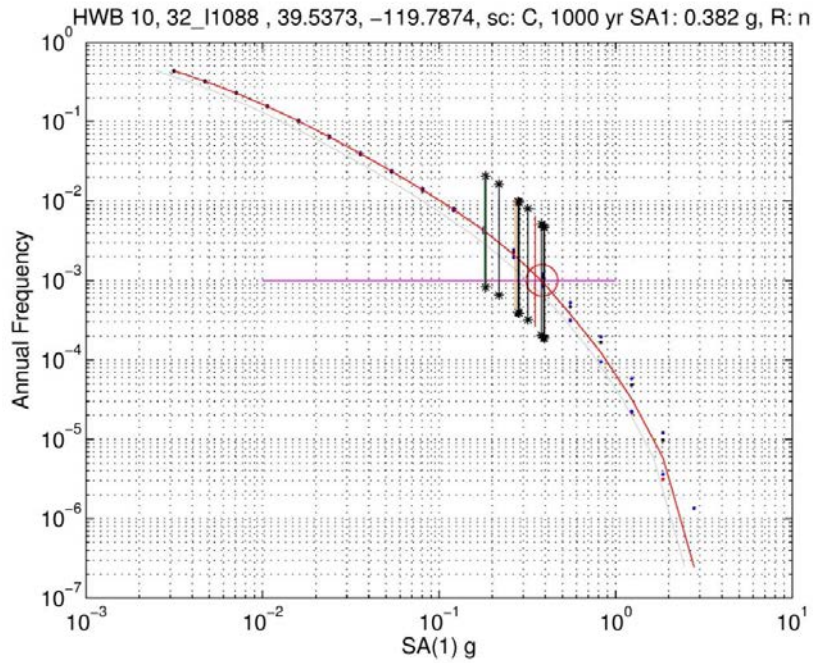


Figure B-1.65 HWB 10, 32_I1088 SA(1 Hz) hazard curve and capacity estimates.

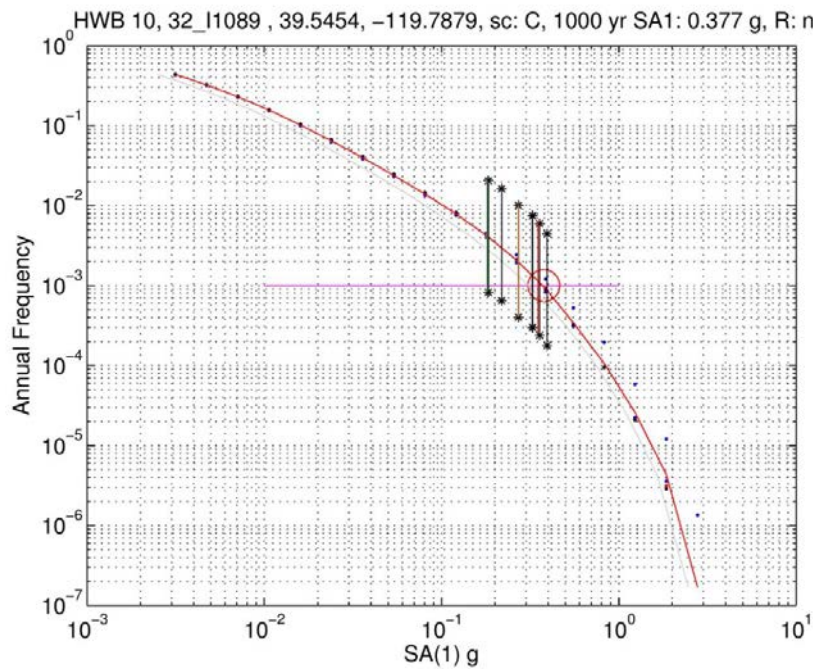


Figure B-1.66 HWB 10, 32_I1089 SA(1 Hz) hazard curve and capacity estimates.

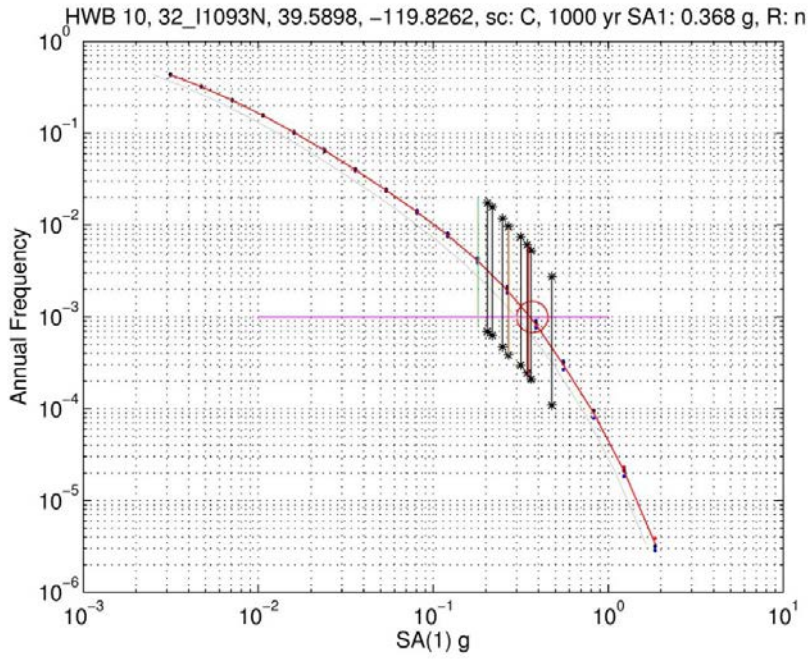


Figure B-1.67 HWB 10, 32_I1093N SA(1 Hz) hazard curve and capacity estimates.

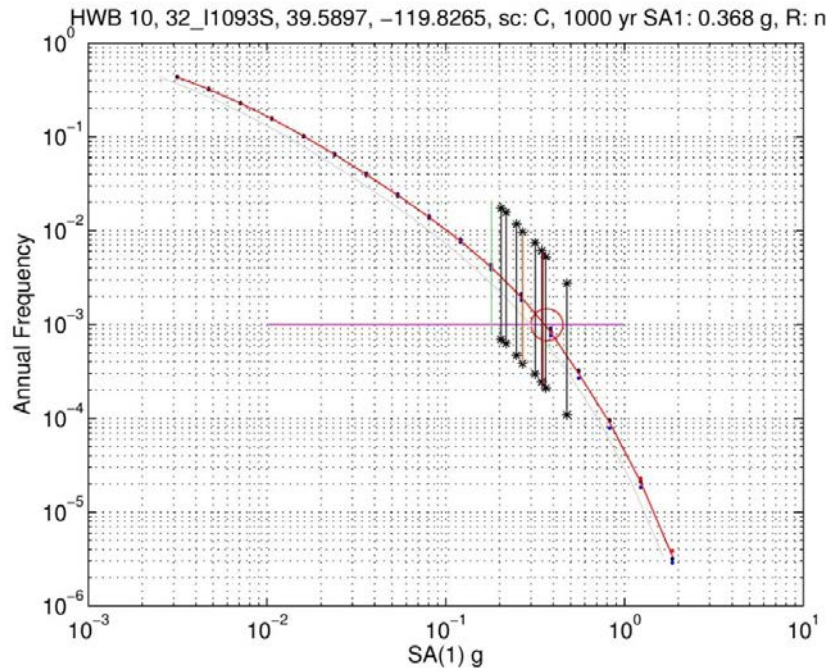


Figure B-1.68 HWB 10, 32_I1093S SA(1 Hz) hazard curve and capacity estimates.

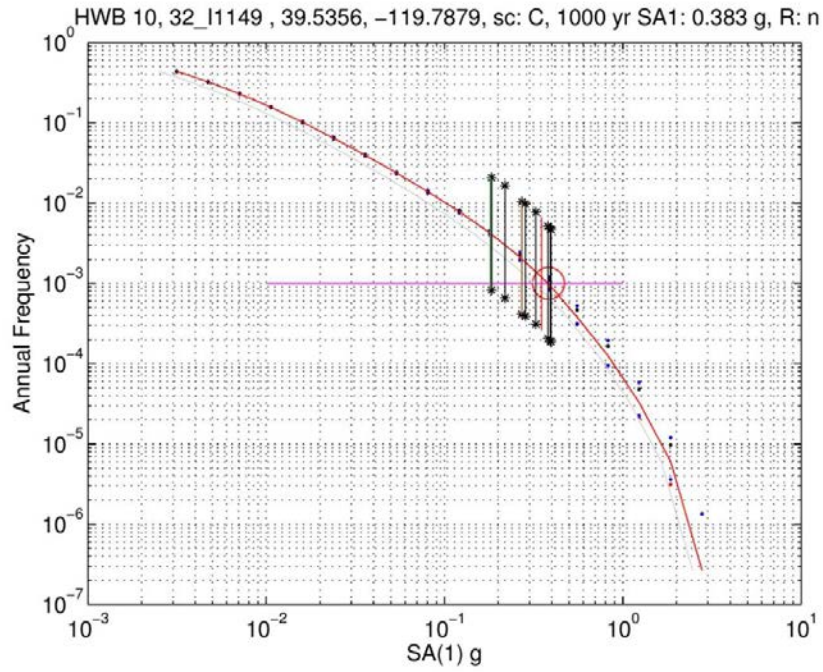


Figure B-1.69 HWB 10, 32_I1149 SA(1 Hz) hazard curve and capacity estimates.

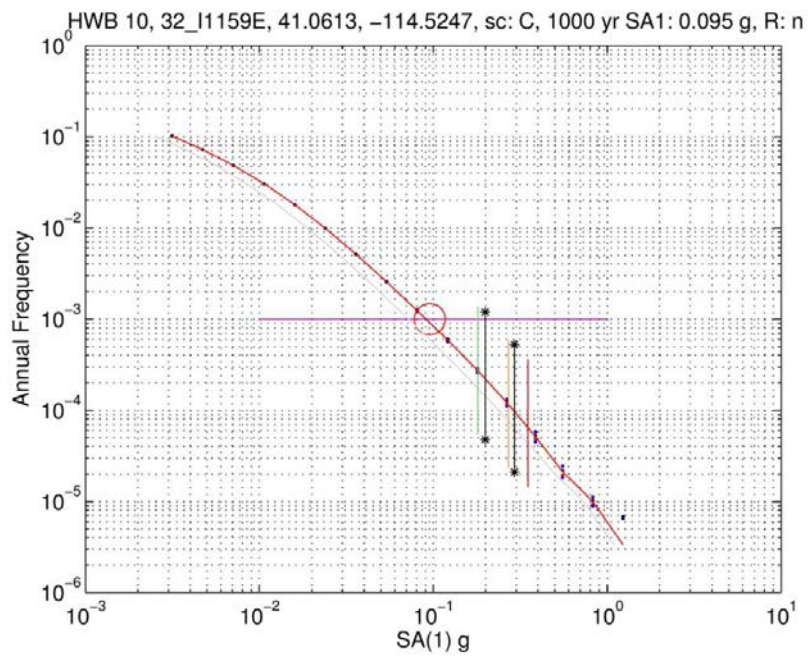


Figure B-1.70 HWB 10, 32_I1159E SA(1 Hz) hazard curve and capacity estimates.

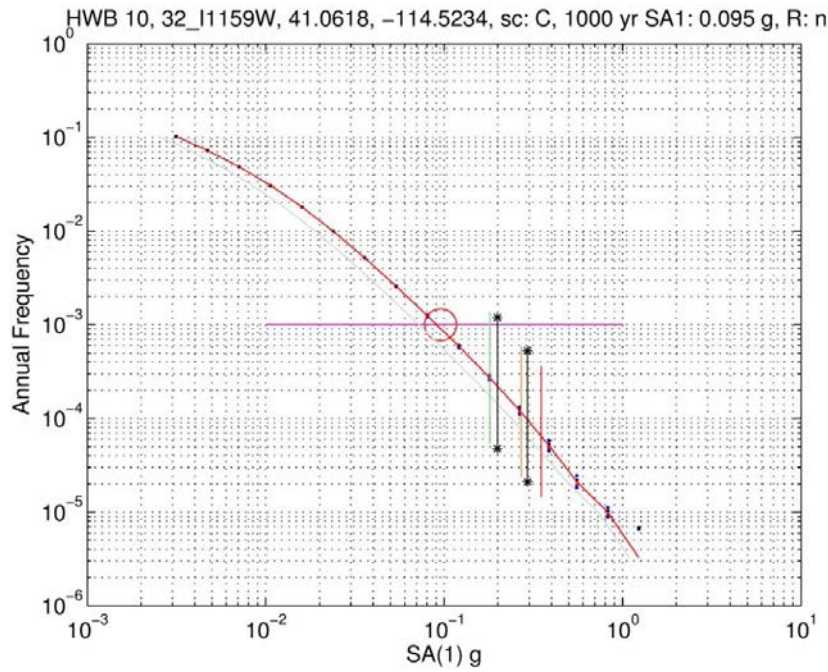


Figure B-1.71 HWB 10, 32_I1159W SA(1 Hz) hazard curve and capacity estimates.

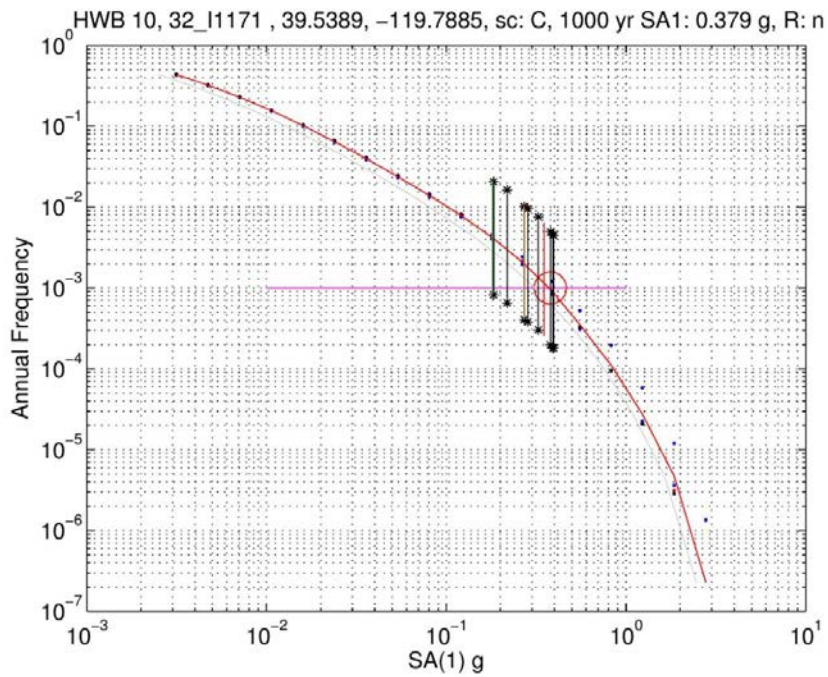


Figure B-1.72 HWB 10, 32_I1171 SA(1 Hz) hazard curve and capacity estimates.

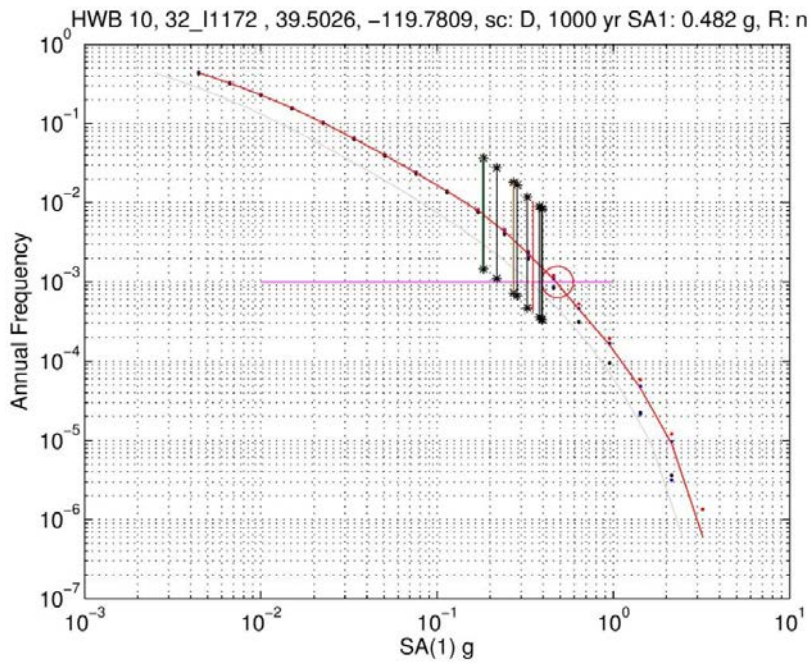


Figure B-1.73 HWB 10, 32_I1172 SA(1 Hz) hazard curve and capacity estimates.

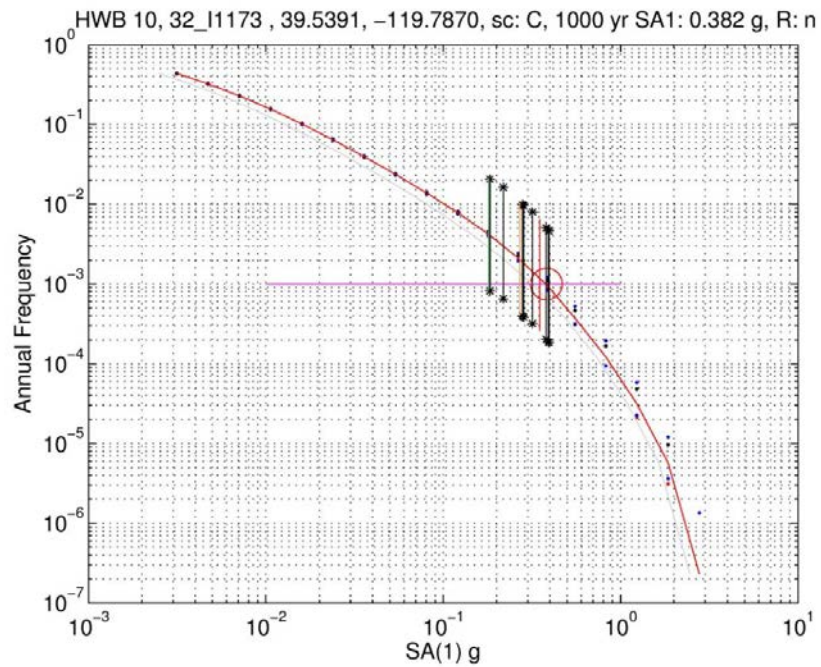


Figure B-1.74 HWB 10, 32_I1173 SA(1 Hz) hazard curve and capacity estimates.

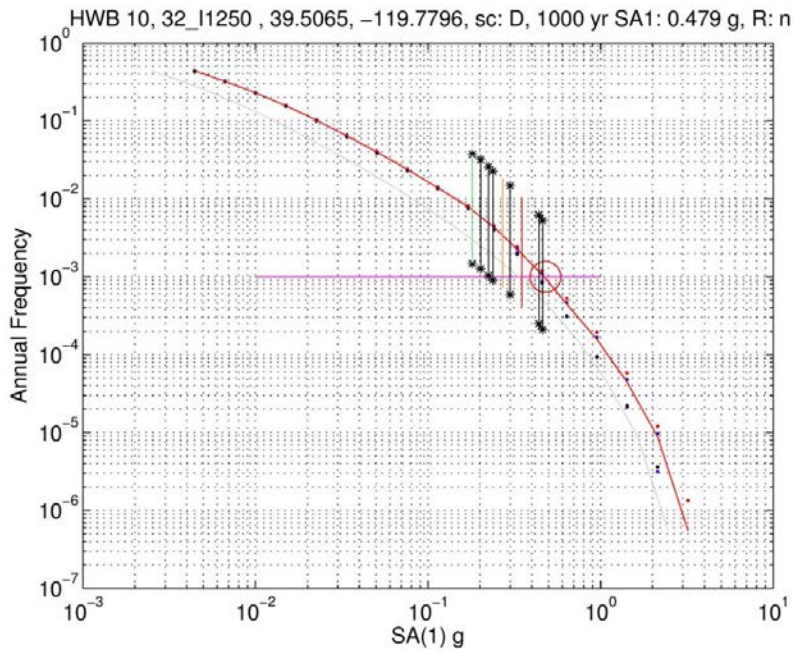


Figure B-1.75 HWB 10, 32_I1250 SA(1 Hz) hazard curve and capacity estimates.

B.2 HWB11 -205 Bridges

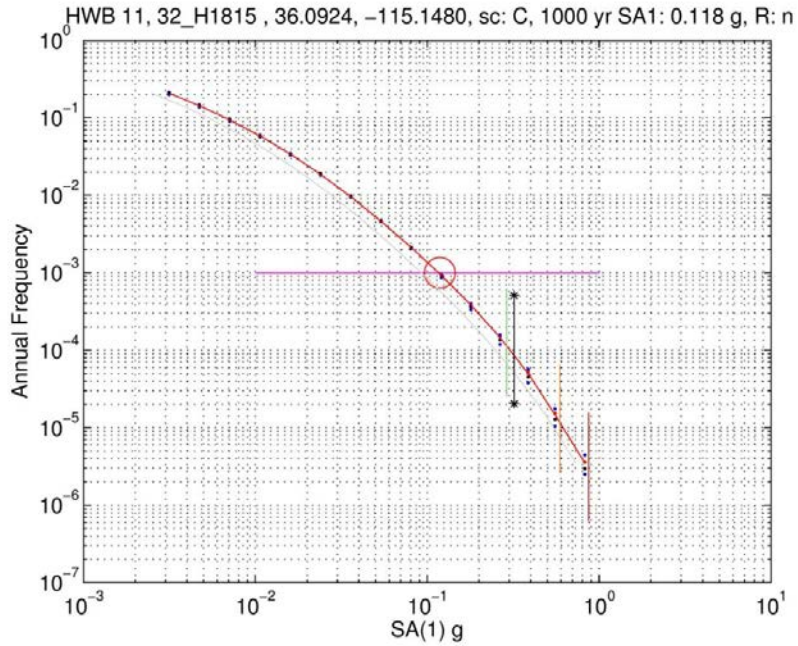


Figure B-2.1 HWB 11, 32_H1815 SA(1 Hz) hazard curve and capacity estimates.

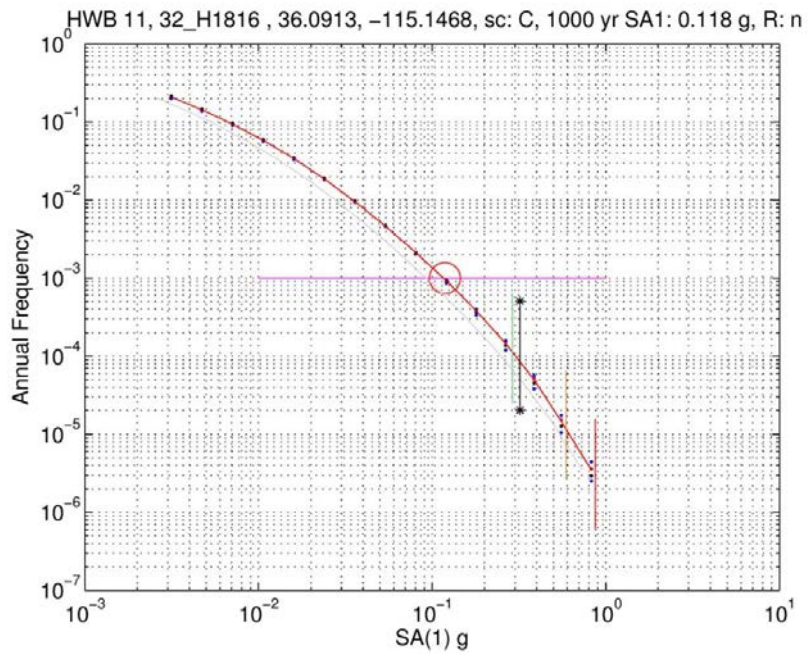


Figure B-2.2 HWB 11, 32_H1816 SA(1 Hz) hazard curve and capacity estimates.

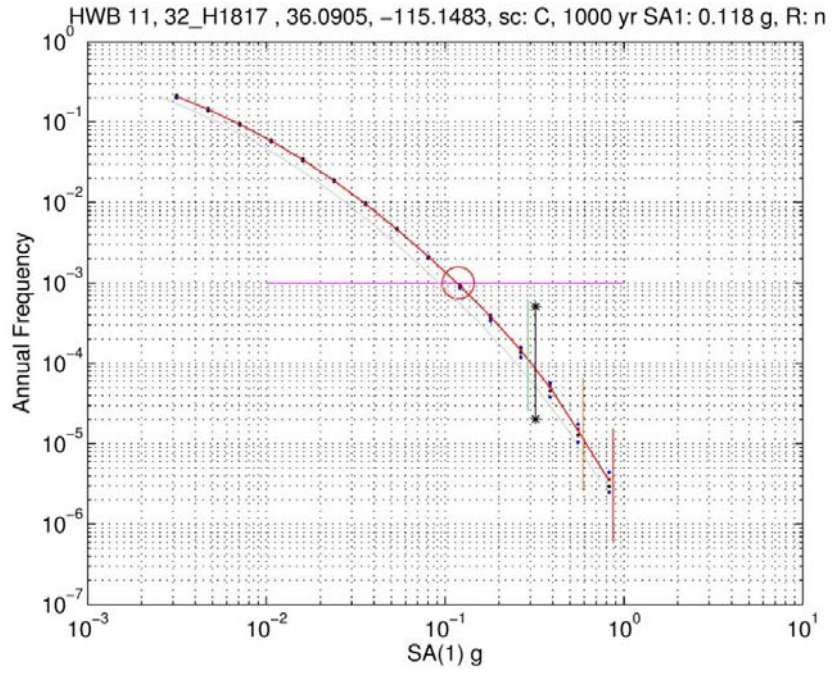


Figure B-2.3 HWB 11, 32_H1817 SA(1 Hz) hazard curve and capacity estimates.

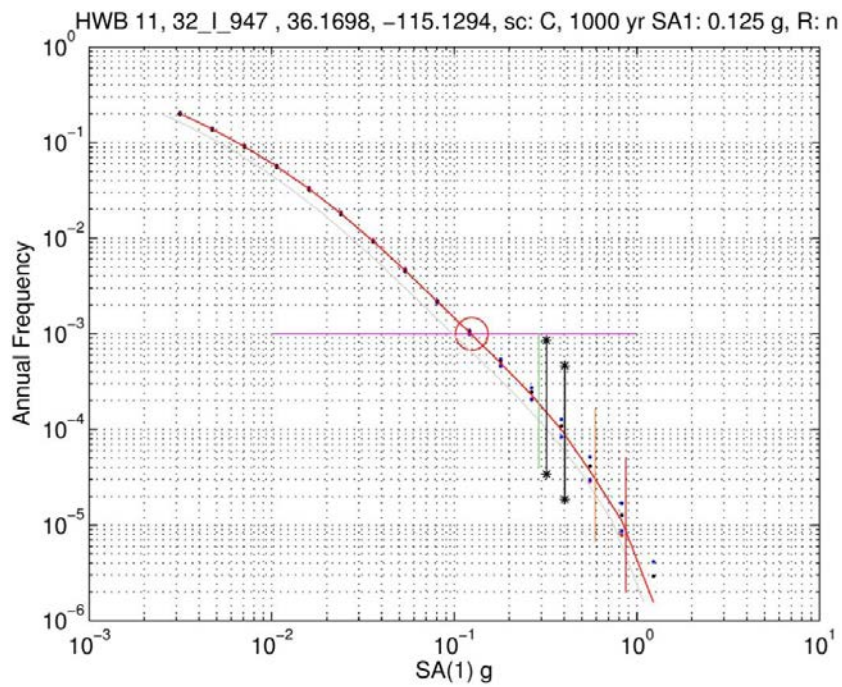


Figure B-2.4 HWB 11, 32_I_947 SA(1 Hz) hazard curve and capacity estimates.

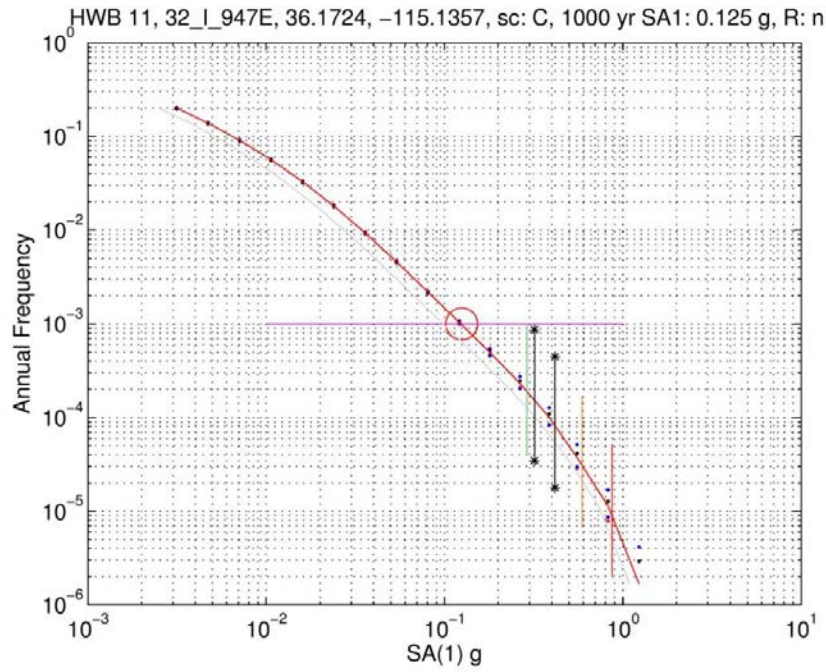


Figure B-2.5 HWB 11, 32_I_947E SA(1 Hz) hazard curve and capacity estimates.

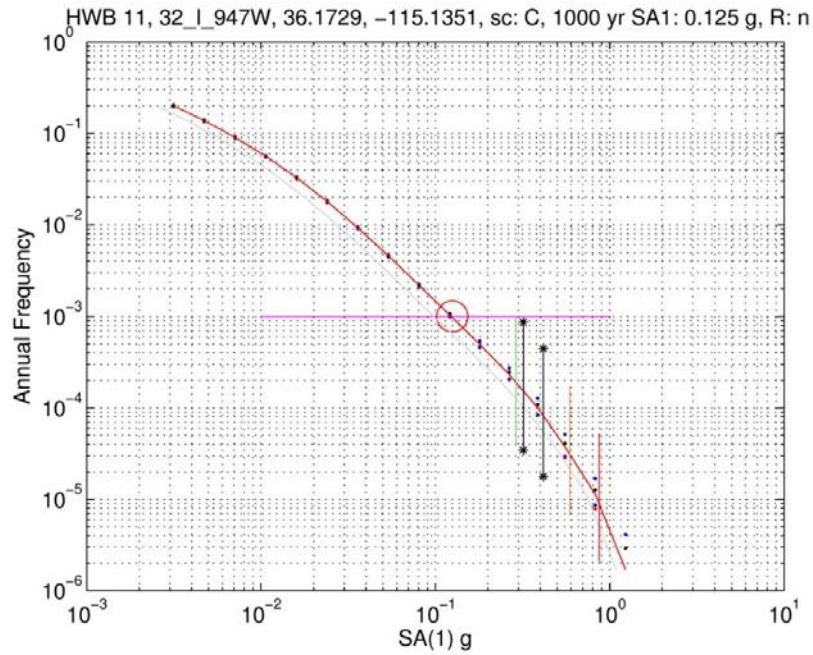


Figure B-2.6 HWB 11, 32_I_947W SA(1 Hz) hazard curve and capacity estimates

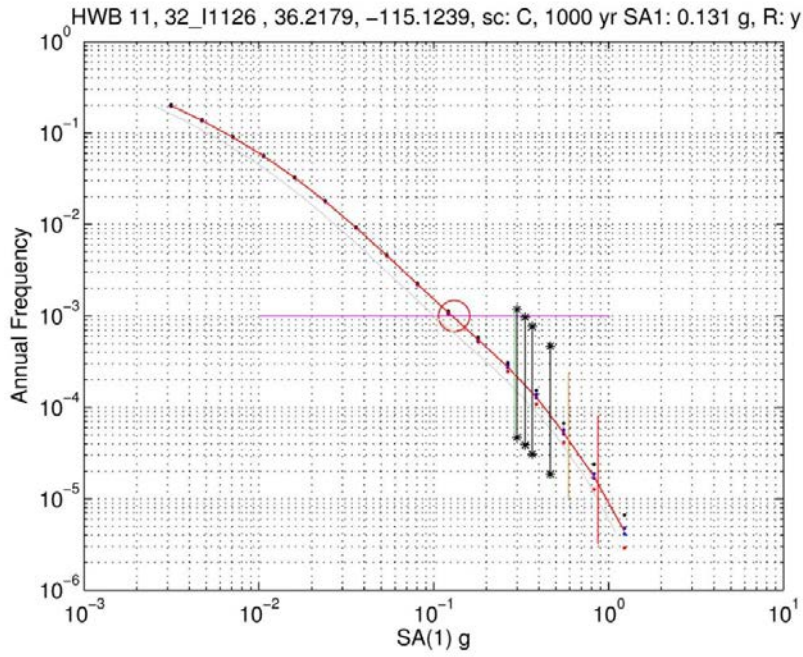


Figure B-2.7 HWB 11, 32_I1126 SA(1 Hz) hazard curve and capacity estimates.

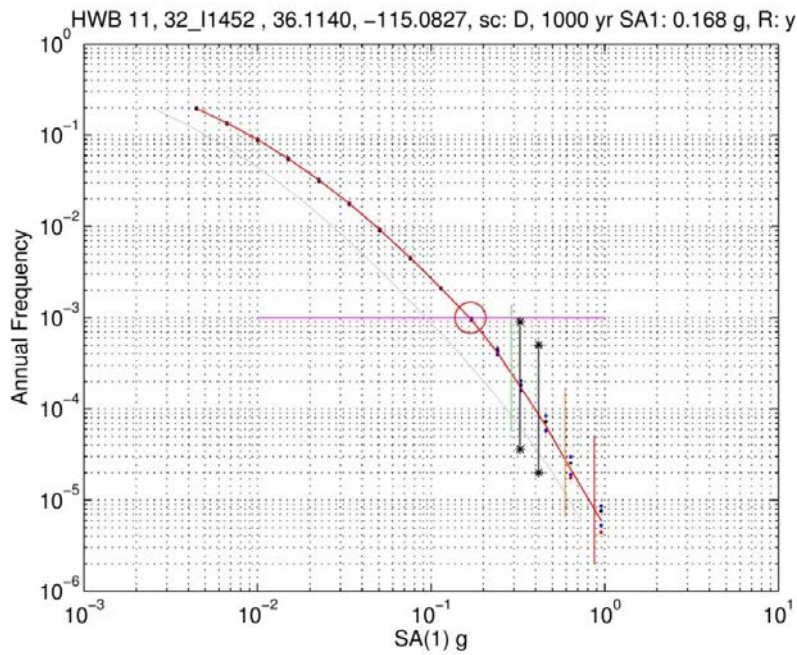


Figure B-2.8 HWB 11, 32_I1452 SA(1 Hz) hazard curve and capacity estimates.

B.3 HWB15 -402 Bridges

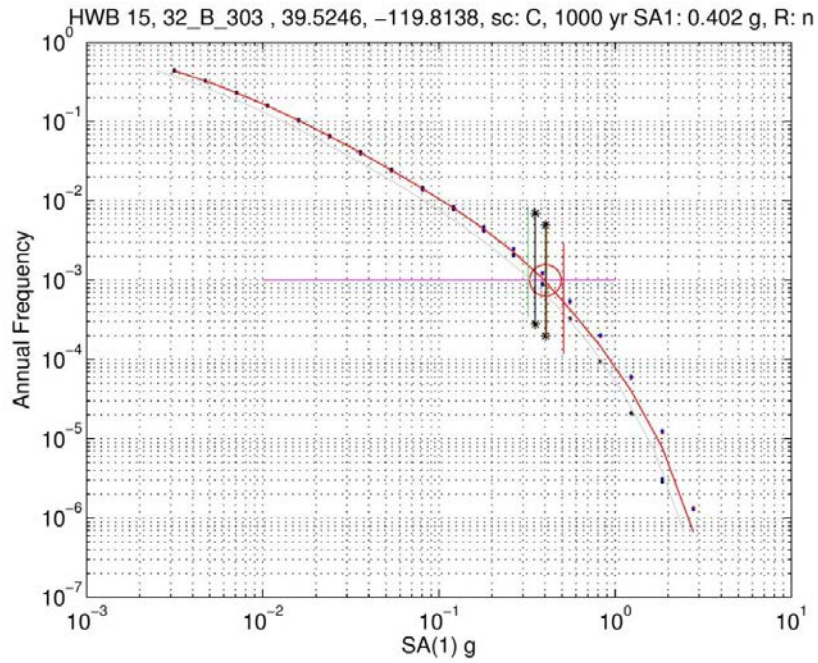


Figure B-3.1 HWB 15, 32_B_303 SA(1 Hz) hazard curve and capacity estimates.

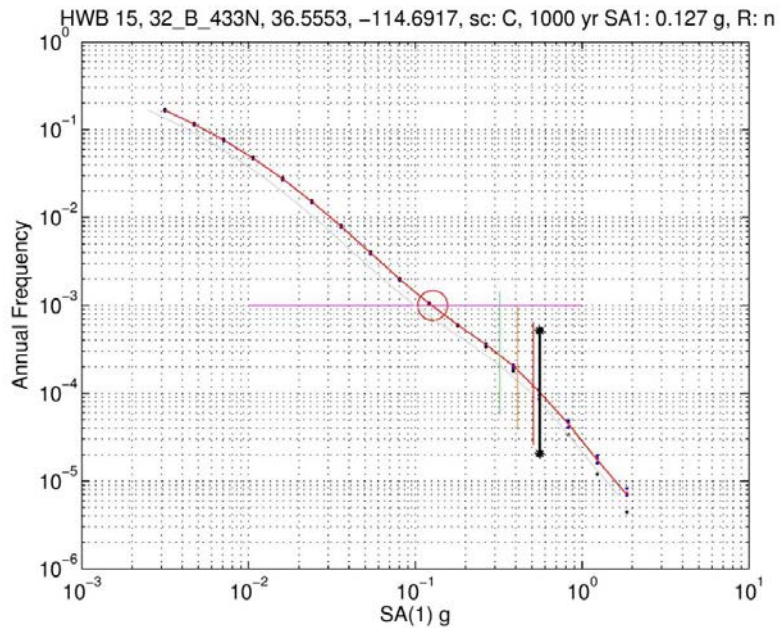


Figure B-3.2 HWB 15, 32_B_433N SA(1 Hz) hazard curve and capacity estimates.

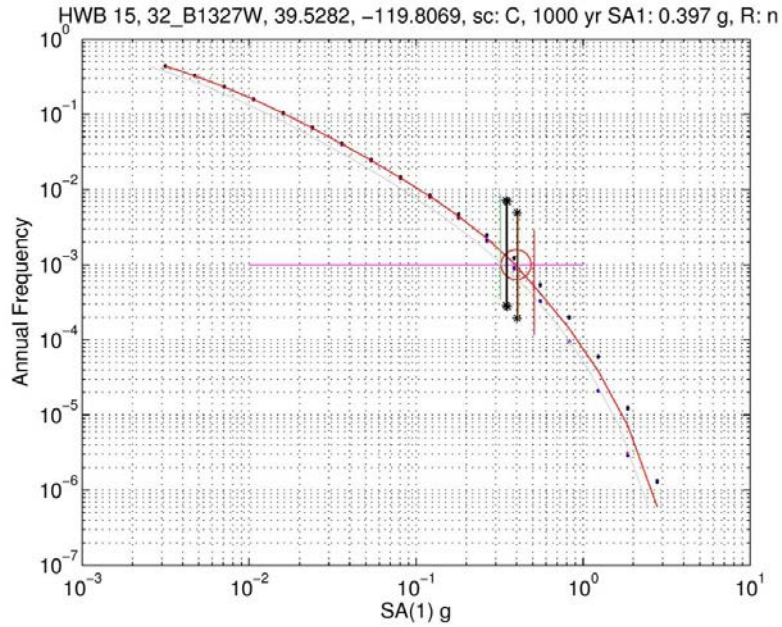


Figure B-3.3 HWB 15, 32_B1327W SA(1 Hz) hazard curve and capacity estimates.

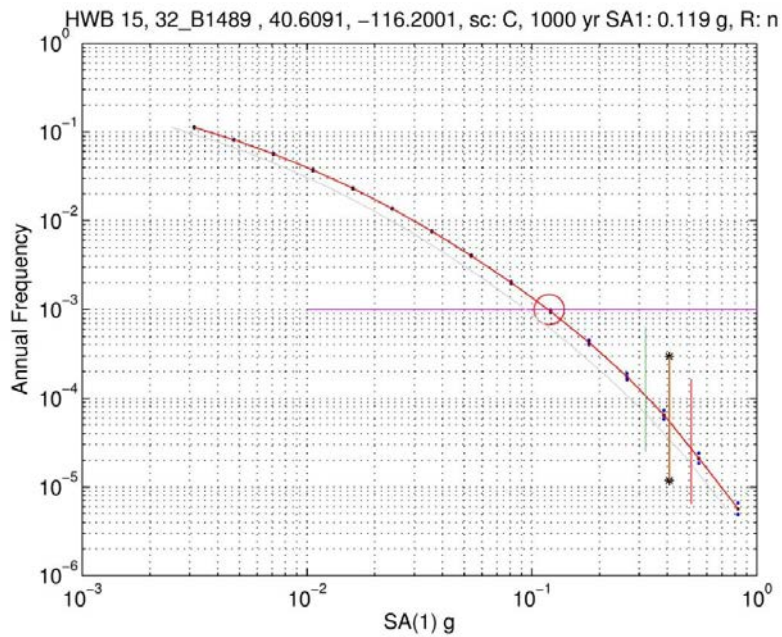


Figure B-3.4 HWB 15, 32_B1489 SA(1 Hz) hazard curve and capacity estimates.

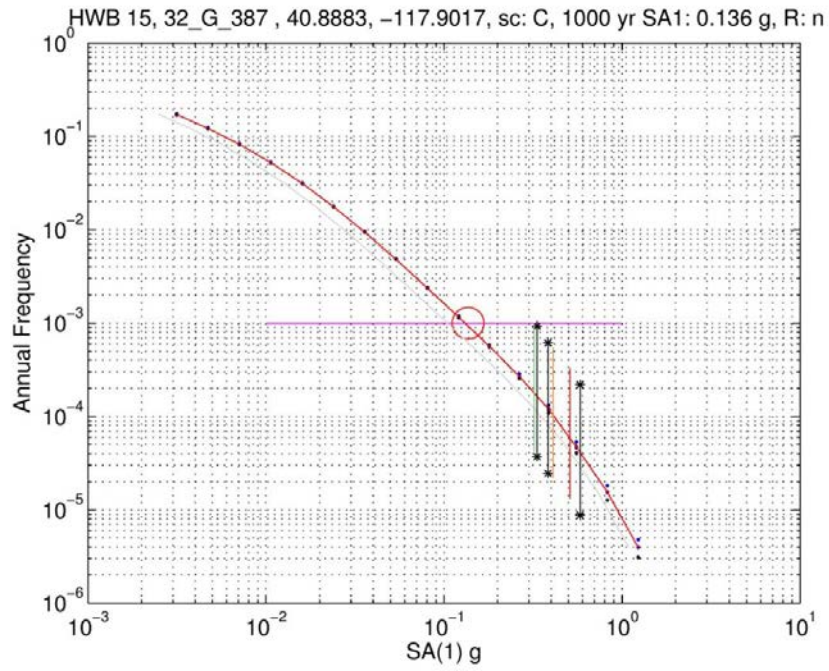


Figure B-3.5 HWB 15, 32_G_387 SA(1 Hz) hazard curve and capacity estimates.

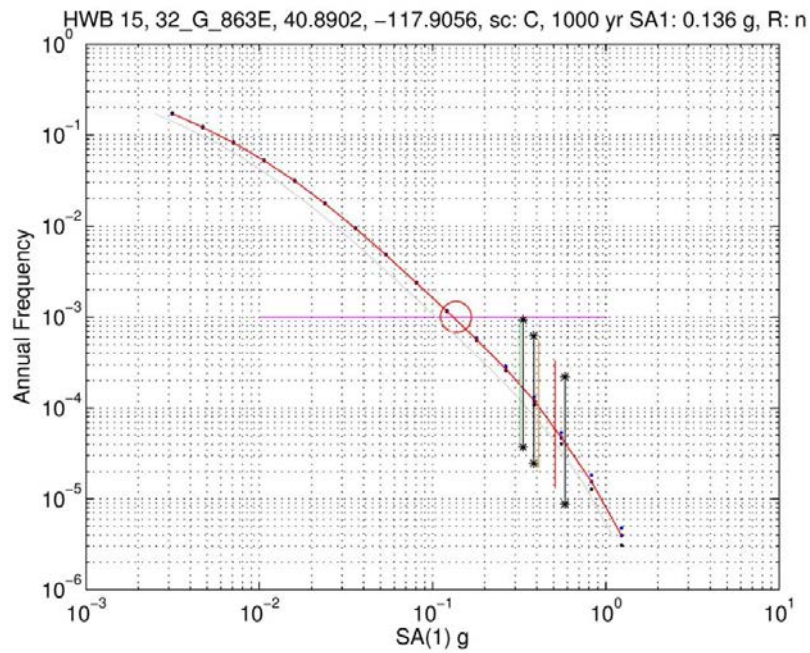


Figure B-3.6 HWB 15, 32_G_863E SA(1 Hz) hazard curve and capacity estimates.

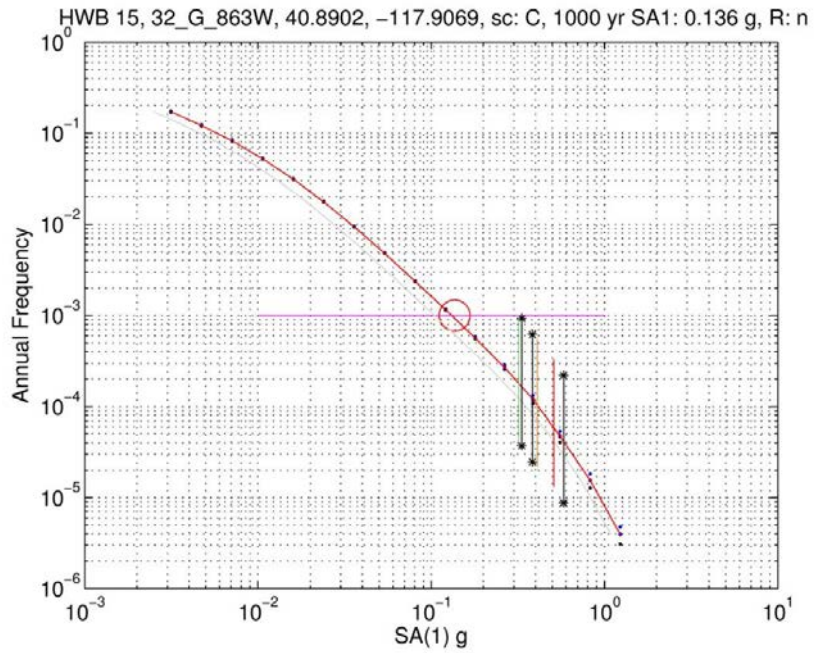


Figure B-3.7 HWB 15, 32_G_863W SA(1 Hz) hazard curve and capacity estimates.

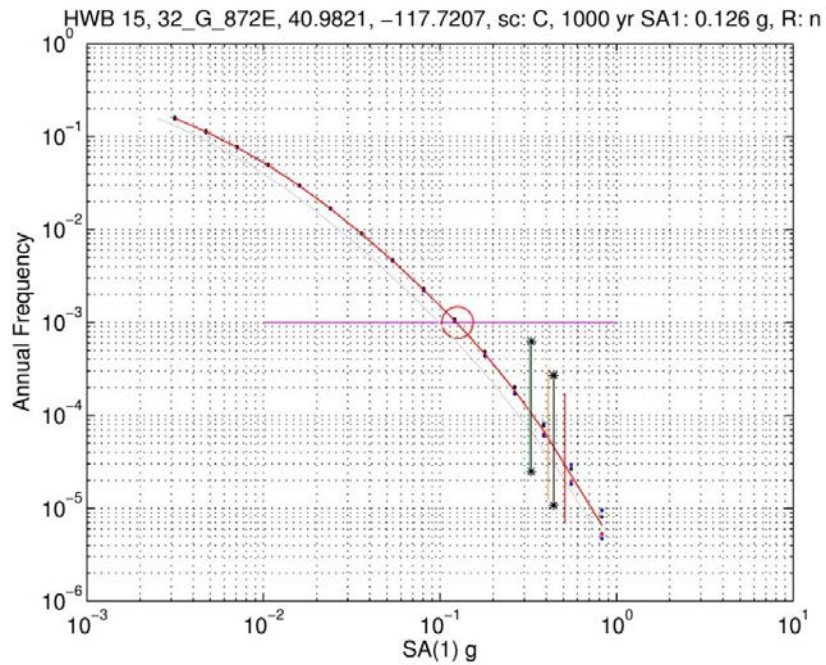


Figure B-3.8 HWB 15, 32_G_872E SA(1 Hz) hazard curve and capacity estimates.

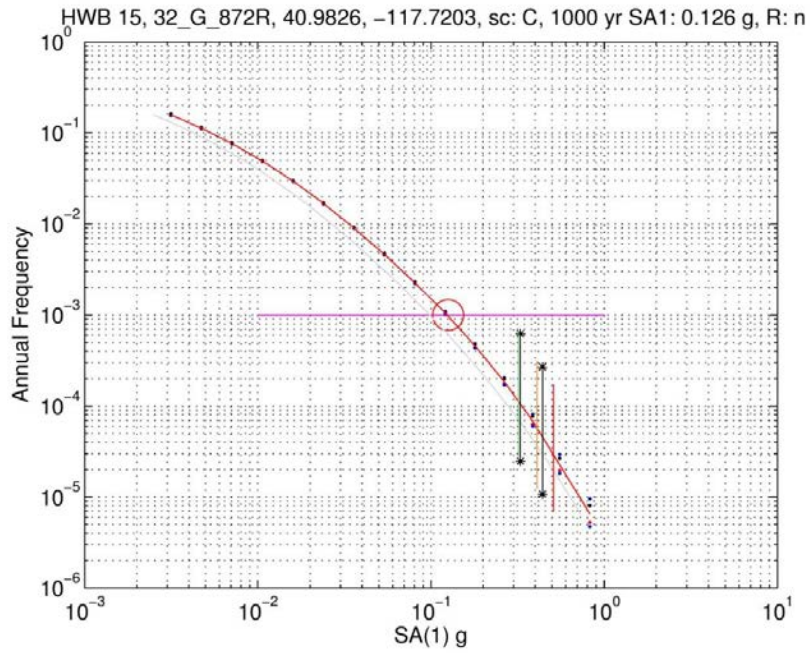


Figure B-3.9 HWB 15, 32_G_872R SA(1 Hz) hazard curve and capacity estimates.

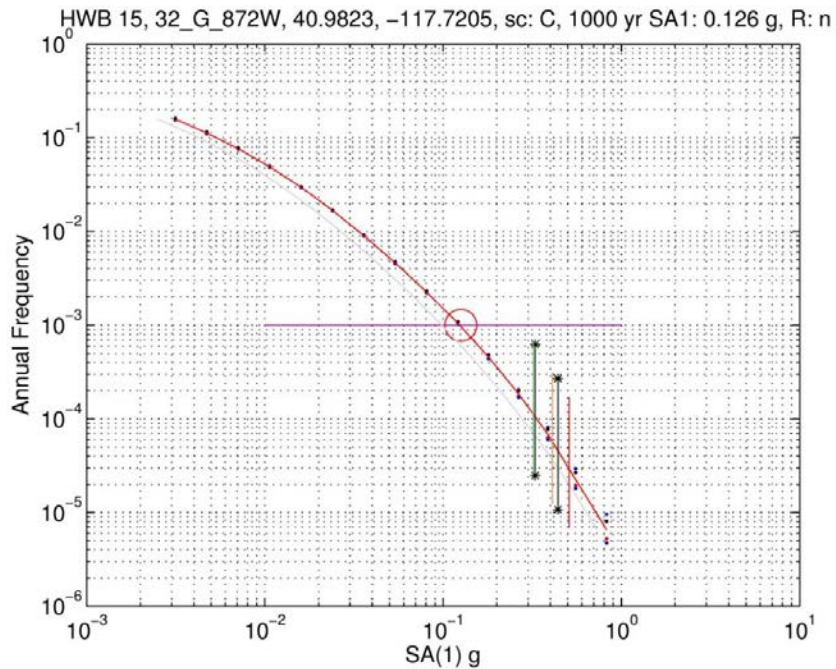


Figure B-3.10 HWB 15, 32_G_872W SA(1 Hz) hazard curve and capacity estimates.

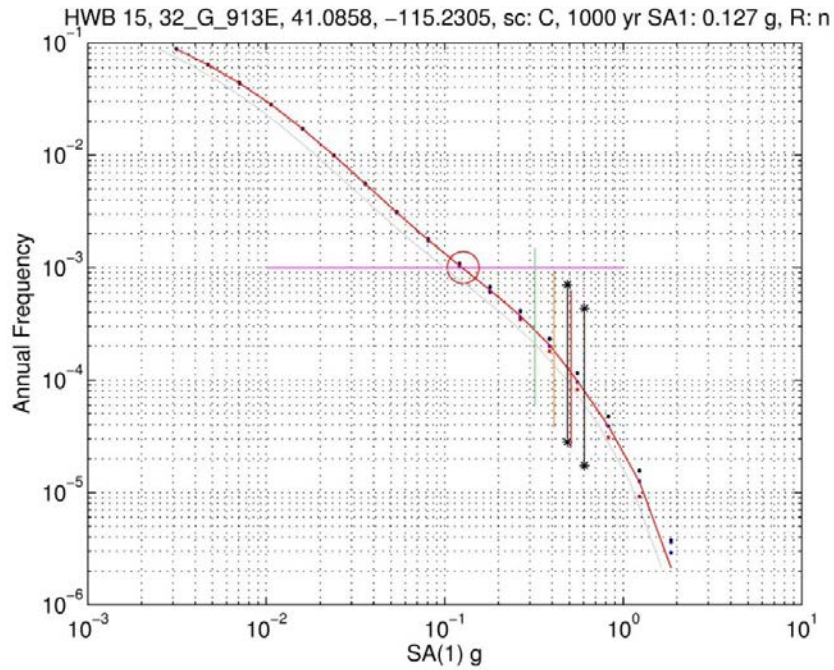


Figure B-3.11 HWB 15, 32_G_913E SA(1 Hz) hazard curve and capacity estimates.

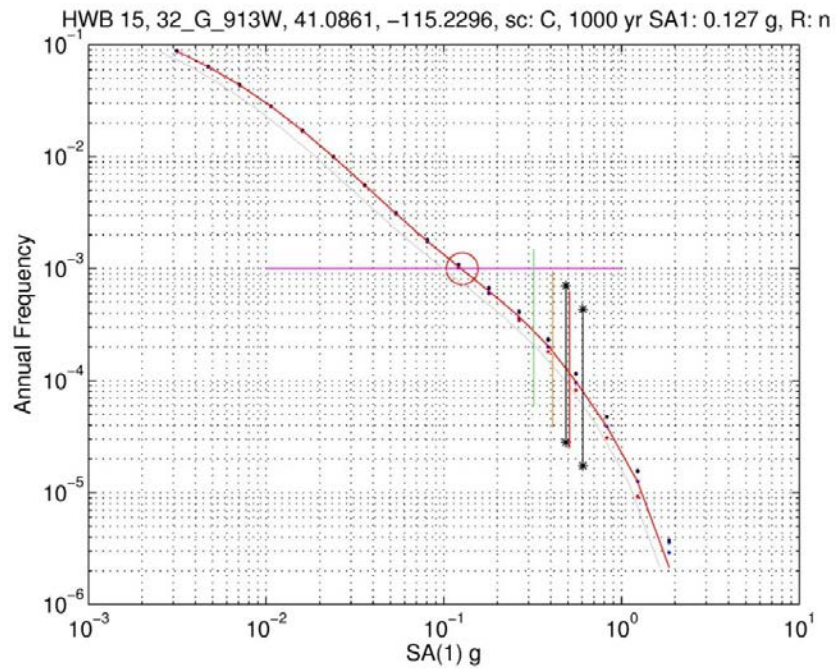


Figure B-3.12 HWB 15, 32_G_913W SA(1 Hz) hazard curve and capacity estimates.

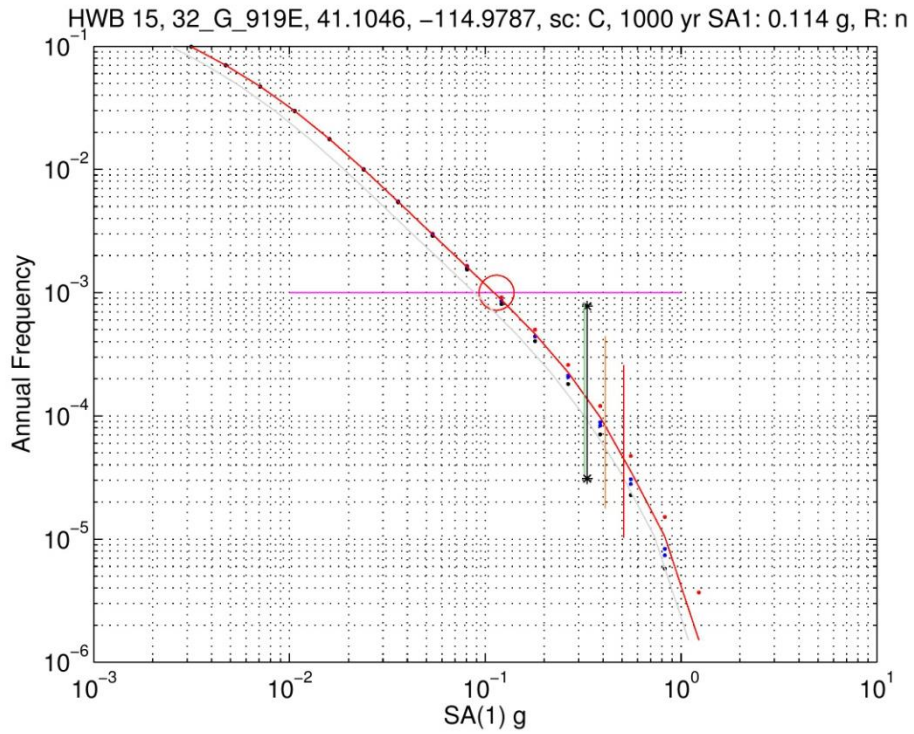


Figure B-3.13 HWB 15, 32_G_919E SA(1 Hz) hazard curve and capacity estimates.

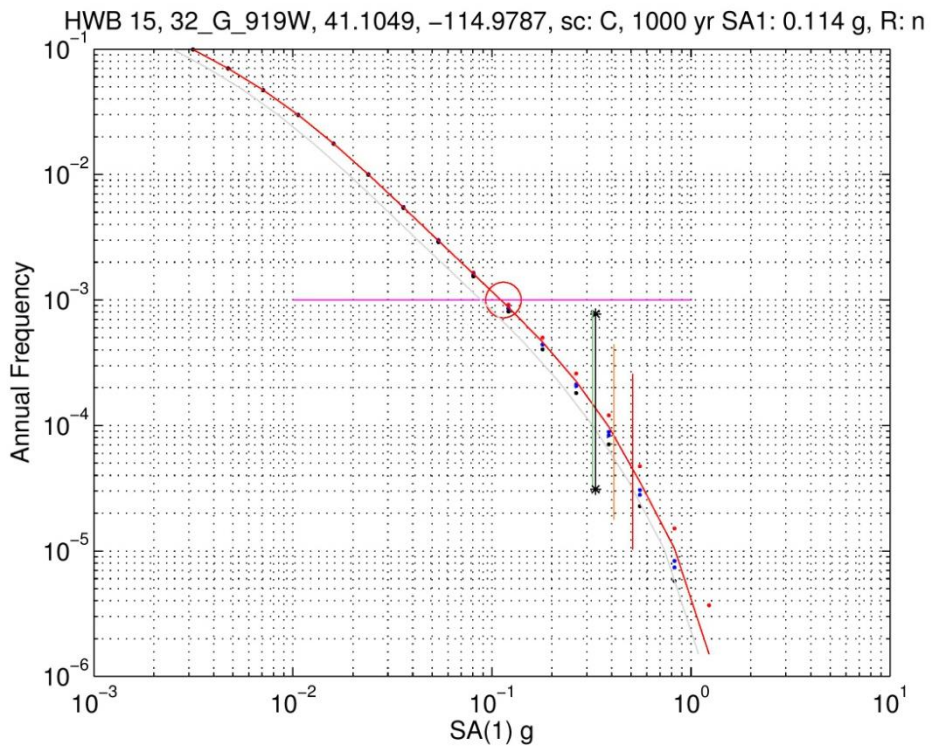


Figure B-3.14 HWB 15, 32_G_919W SA(1 Hz) hazard curve and capacity estimates.

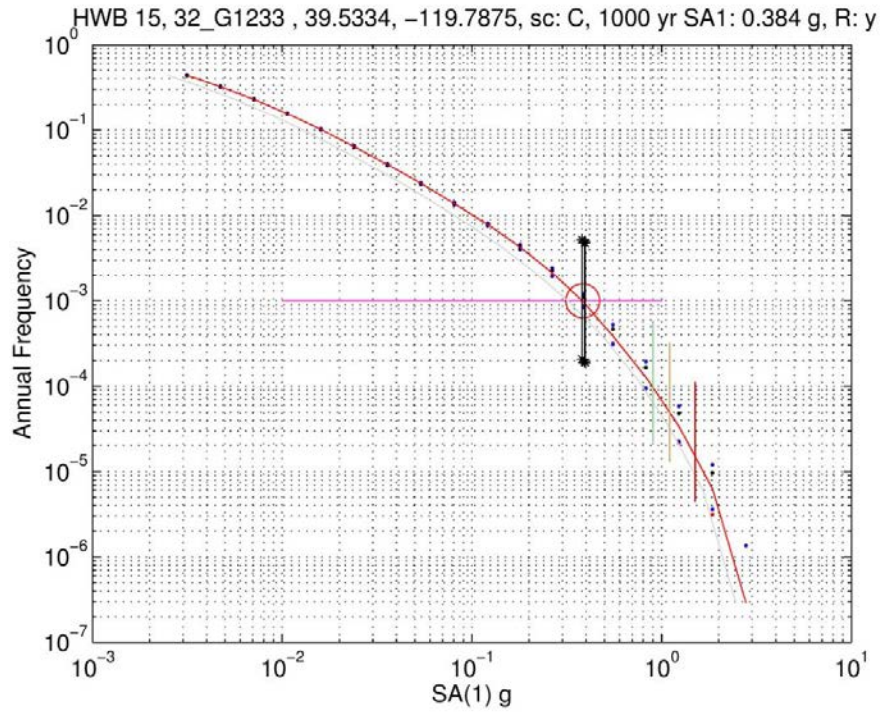


Figure B-3.15 HWB 15, 32_G1233 SA(1 Hz) hazard curve and capacity estimates.

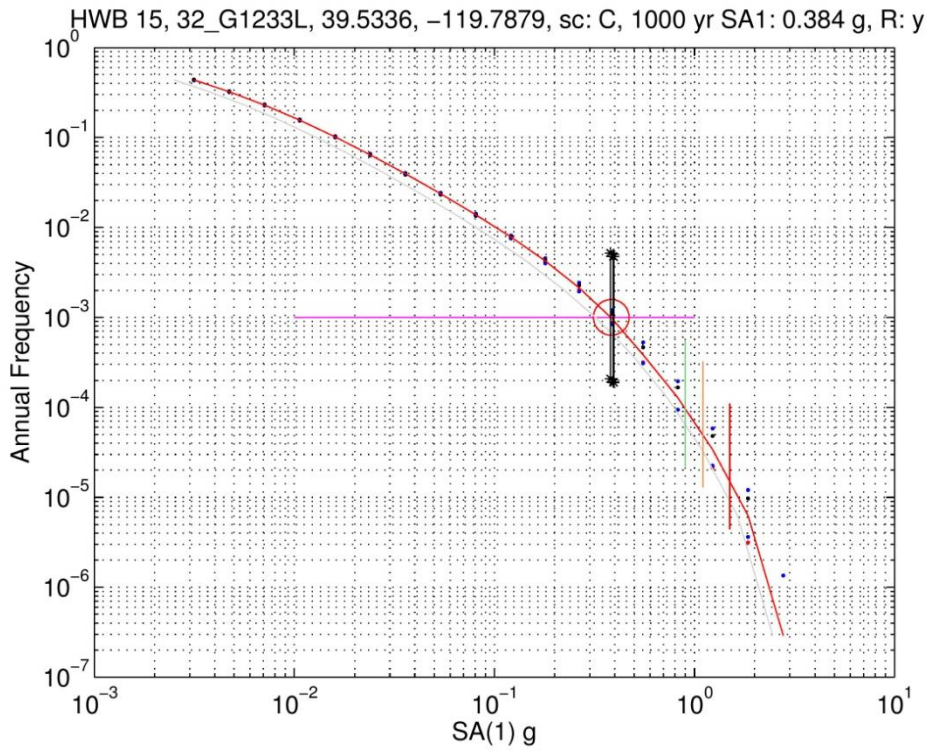


Figure B-3.16 HWB 15, 32_G1233L SA(1 Hz) hazard curve and capacity estimates.

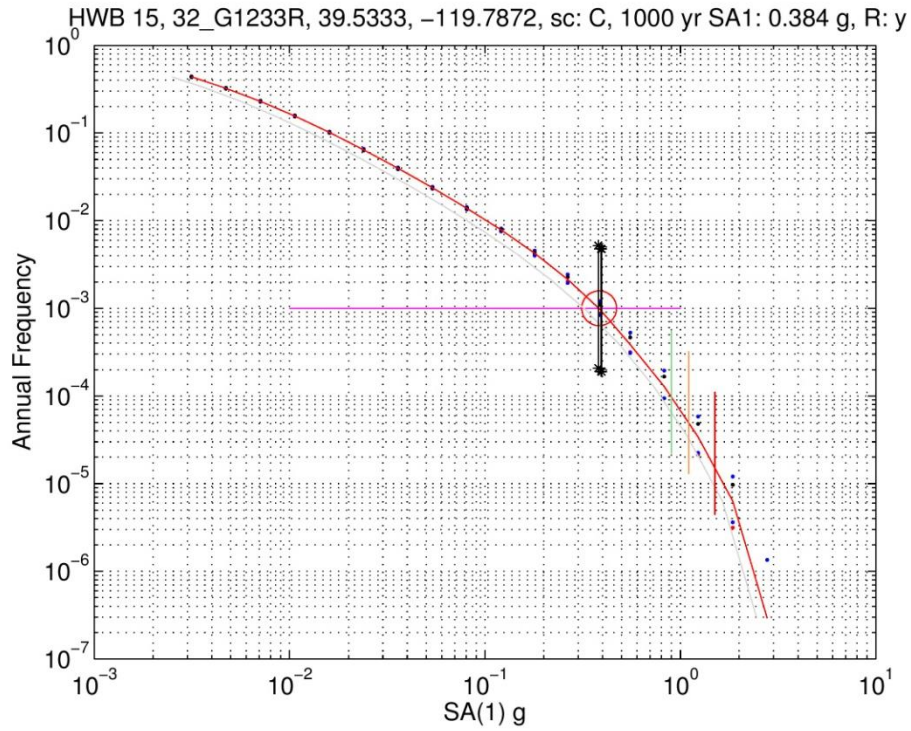


Figure B-3.17 HWB 15, 32_G1233R SA(1 Hz) hazard curve and capacity estimates.

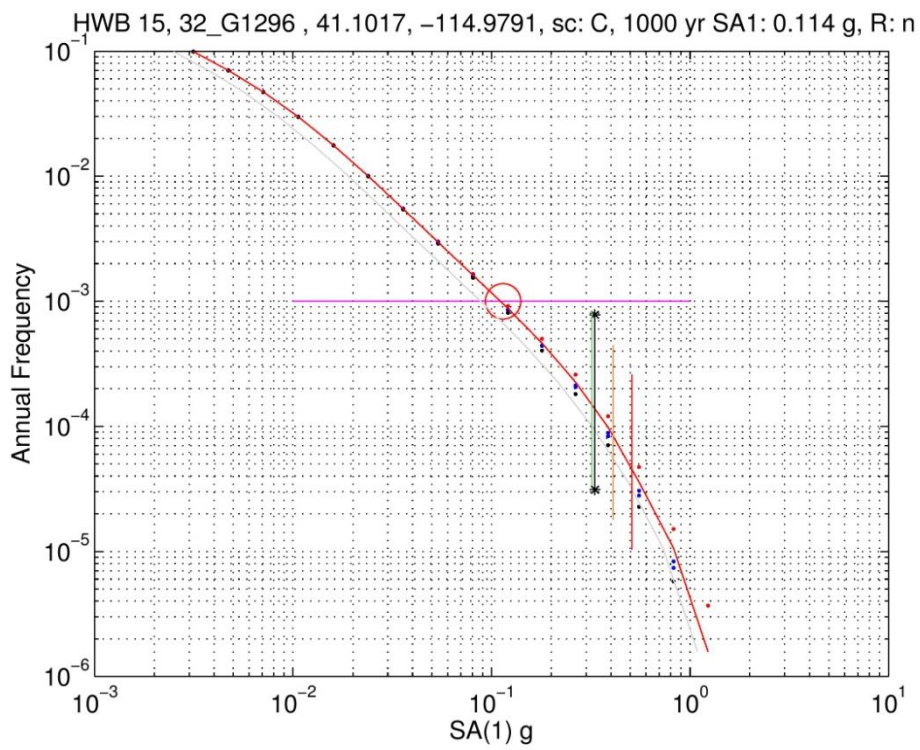


Figure B-3.18 HWB 15, 32_G1296 SA(1 Hz) hazard curve and capacity estimates.

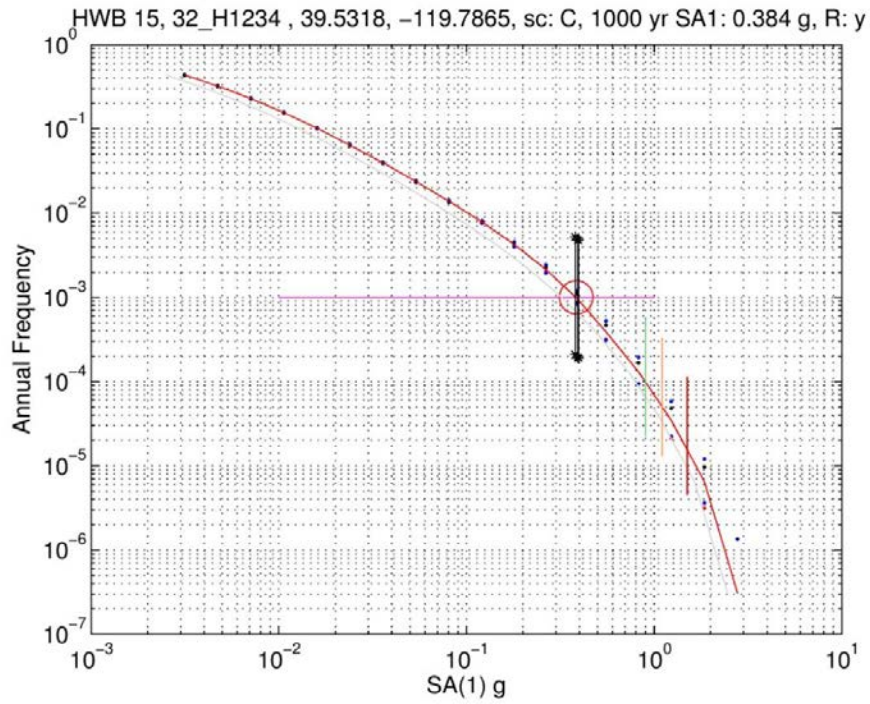


Figure B-3.19 HWB 15, 32_H1234 SA(1 Hz) hazard curve and capacity estimates.

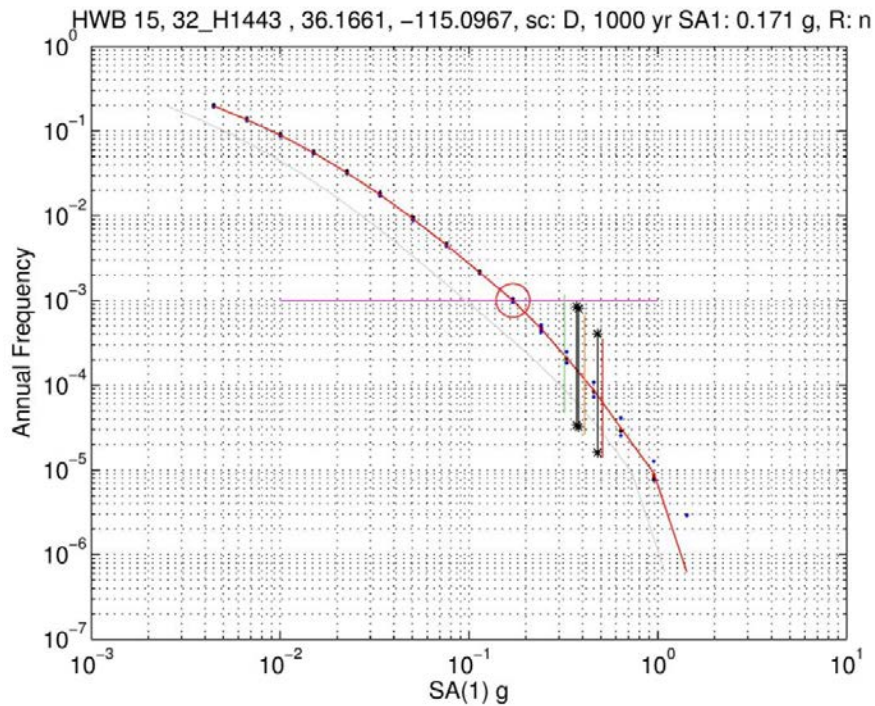


Figure B-3.20 HWB 15, 32_H1443 SA(1 Hz) hazard curve and capacity estimates.

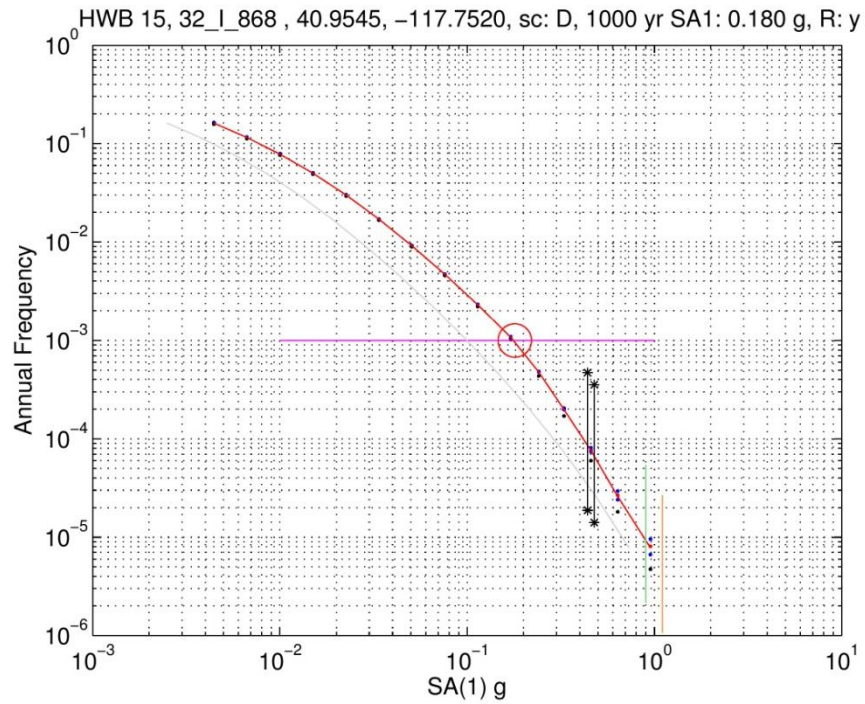


Figure B-3.21 HWB 15, 32_I_868 SA(1 Hz) hazard curve and capacity estimates.

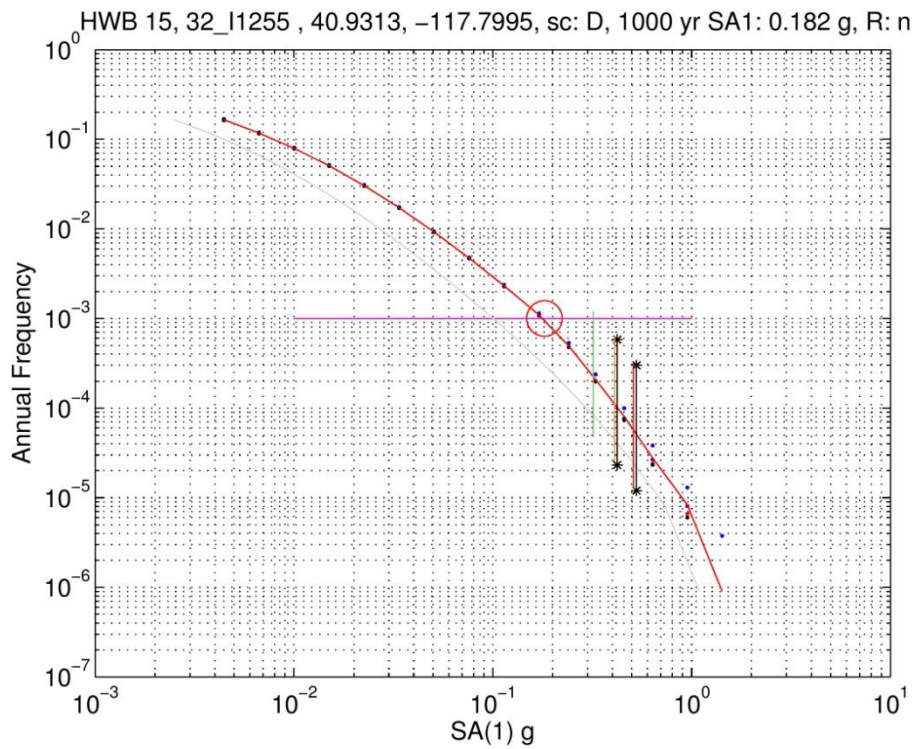


Figure B-3.22 HWB 15, 32_I1255 SA(1 Hz) hazard curve and capacity estimates.

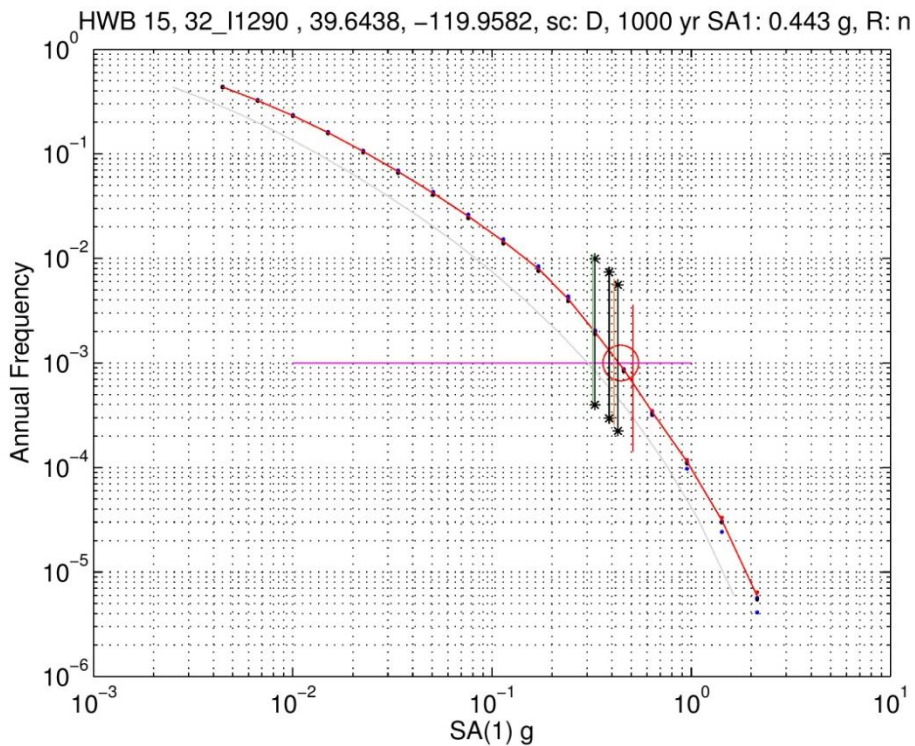


Figure B-3.23 HWB 15, 32_I1290 SA(1 Hz) hazard curve and capacity estimates.

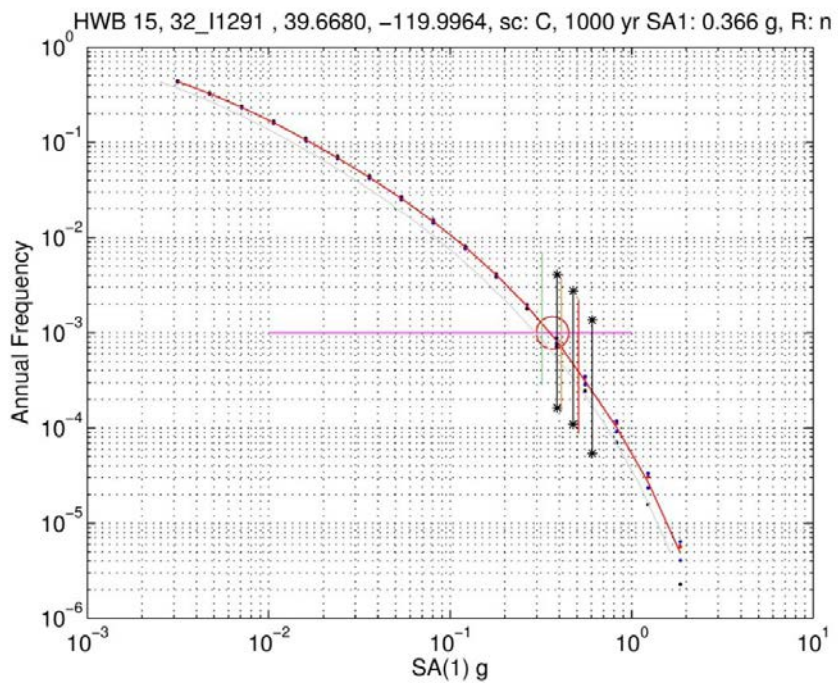


Figure B-3.24 HWB 15, 32_I1291 SA(1 Hz) hazard curve and capacity estimates

B-4 HWB22 -605 Bridges

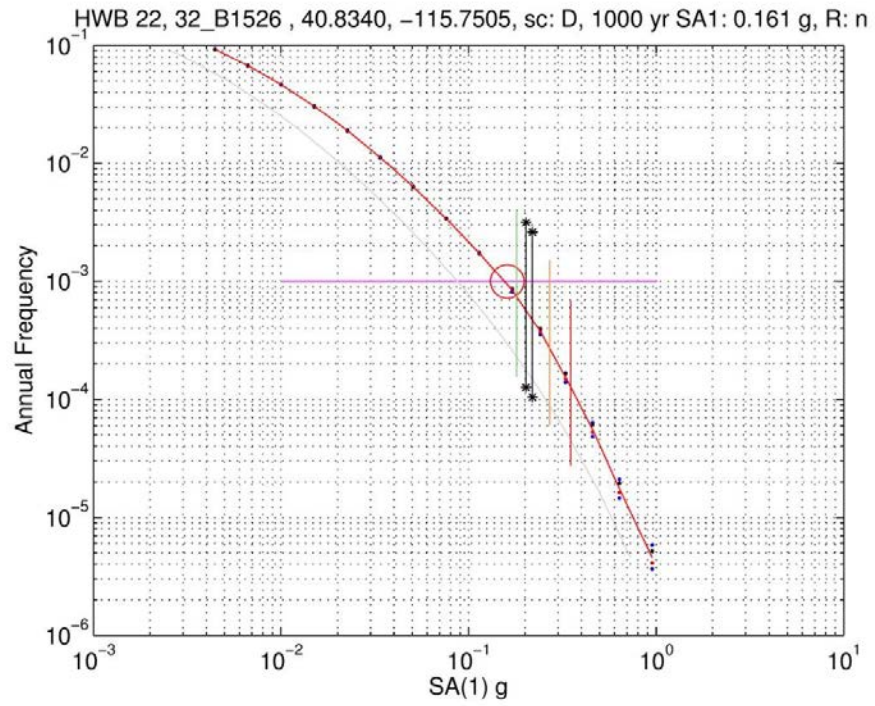


Figure B-4.1 HWB 22, 32_B1526 SA(1 Hz) hazard curve and capacity estimates.

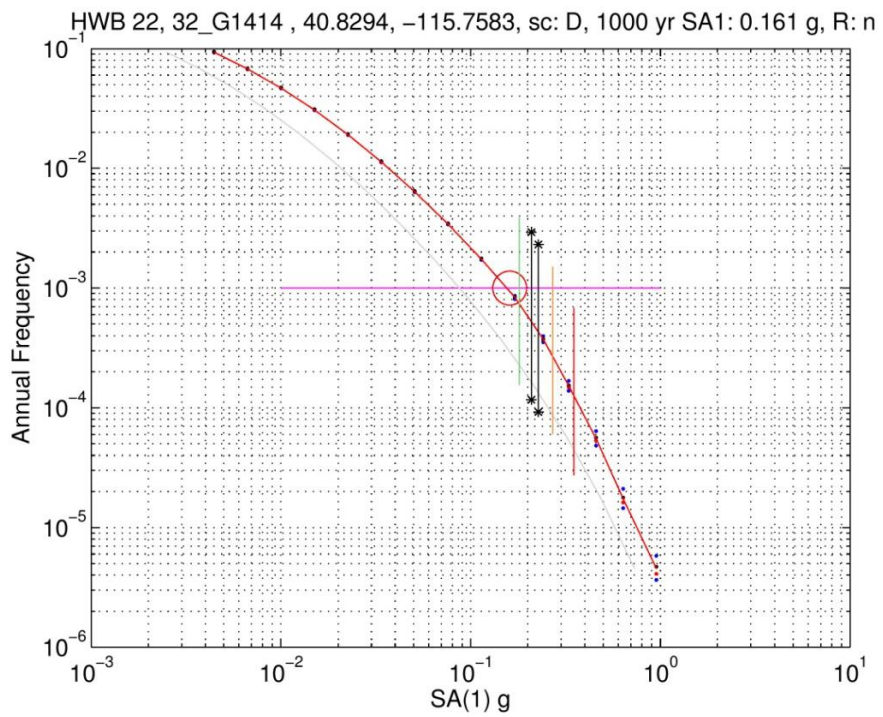


Figure B-4.2 HWB 22, 32_G1414 SA(1 Hz) hazard curve and capacity estimates.

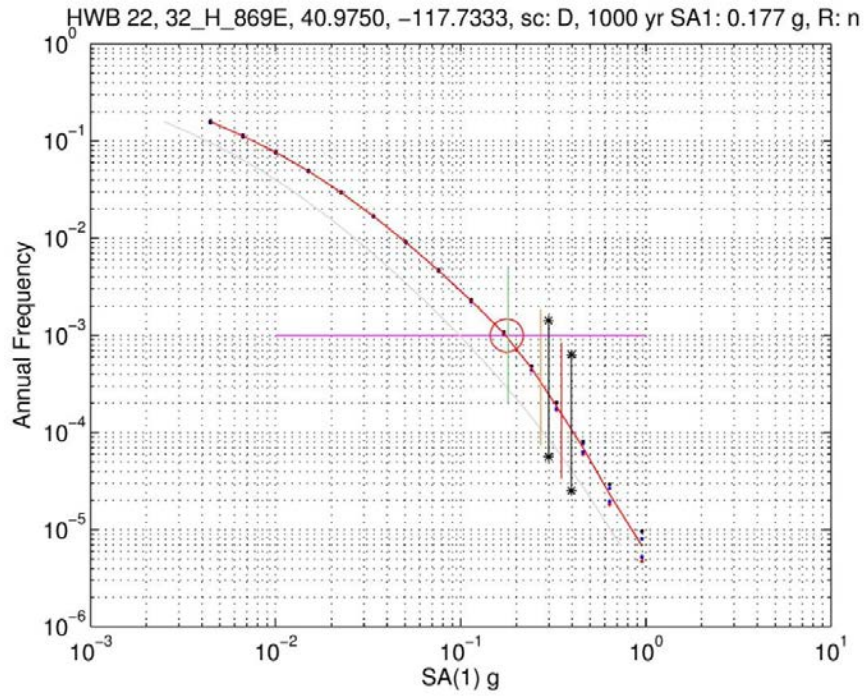


Figure B-4.3 HWB 22, 32_H_869E SA(1 Hz) hazard curve and capacity estimates.

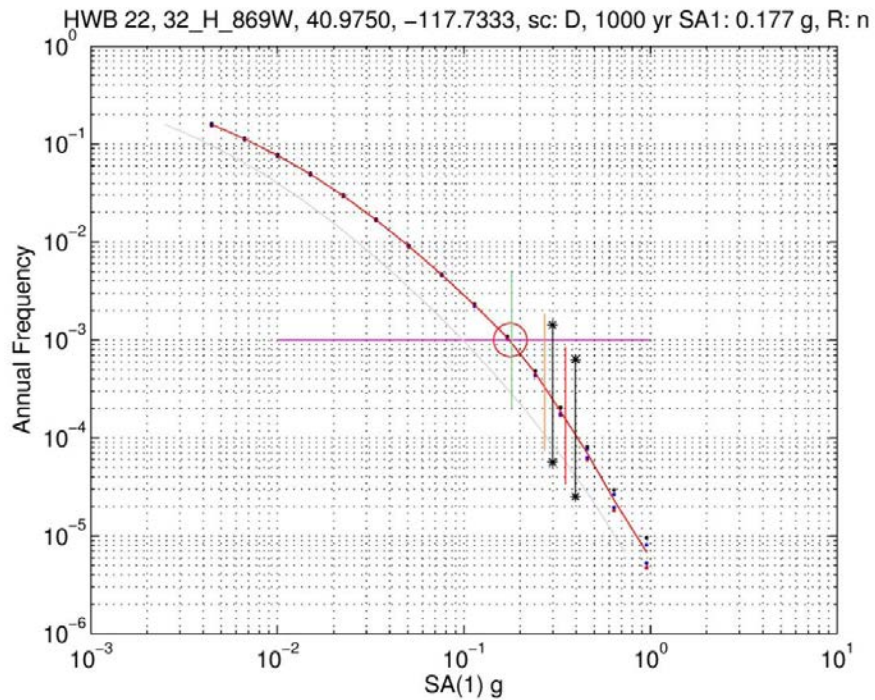


Figure B-4.4 HWB 22, 32_H_869W SA(1 Hz) hazard curve and capacity estimates.

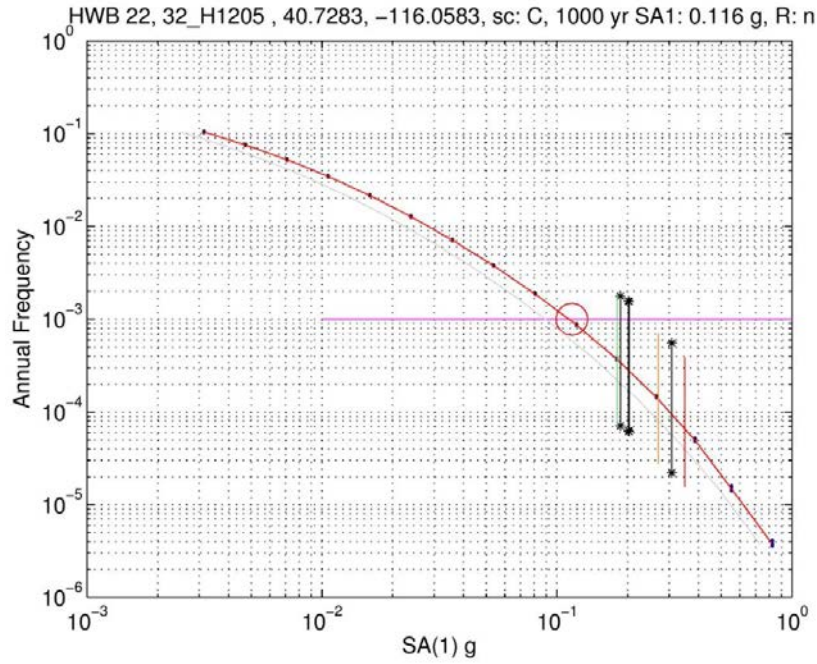


Figure B-4.5 HWB 22, 32_H1205 SA(1 Hz) hazard curve and capacity estimates.

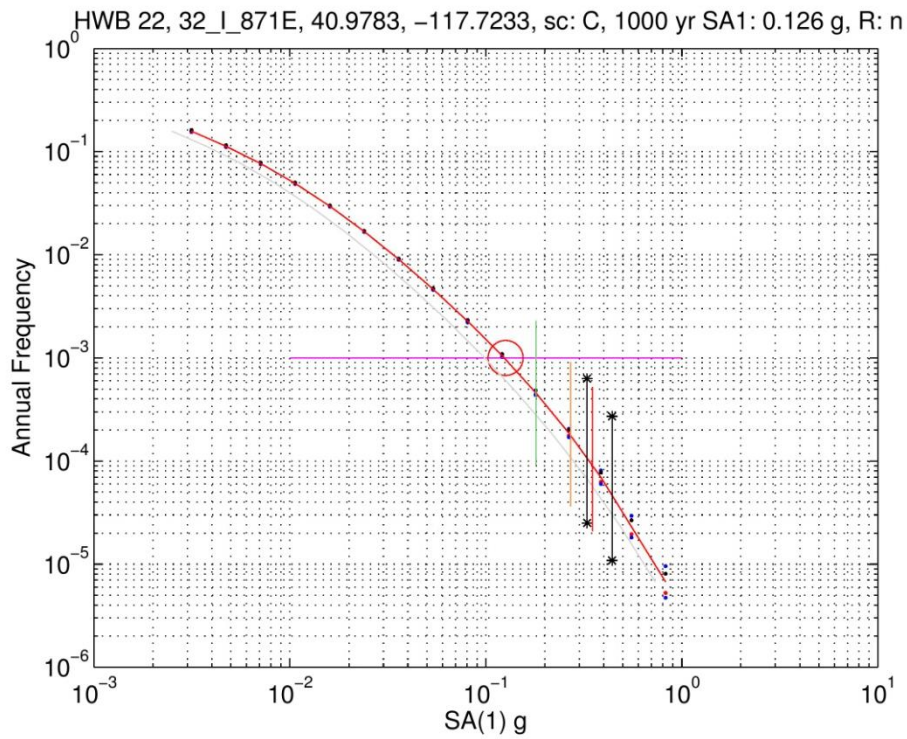


Figure B-4.6 HWB 22, 32_I_871E SA(1 Hz) hazard curve and capacity estimates.

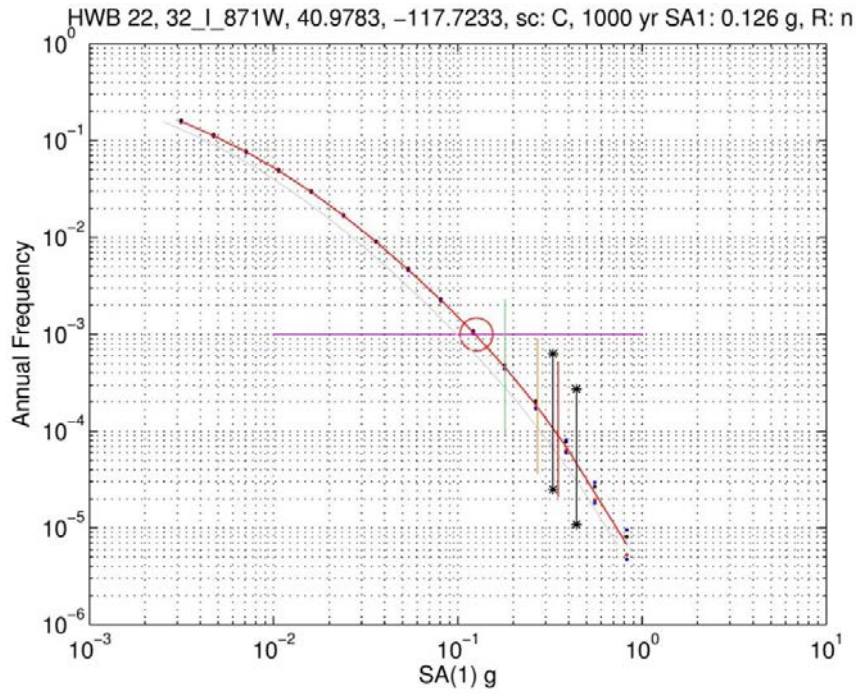


Figure B-4.7 HWB 22, 32_I_871W SA(1 Hz) hazard curve and capacity estimates.

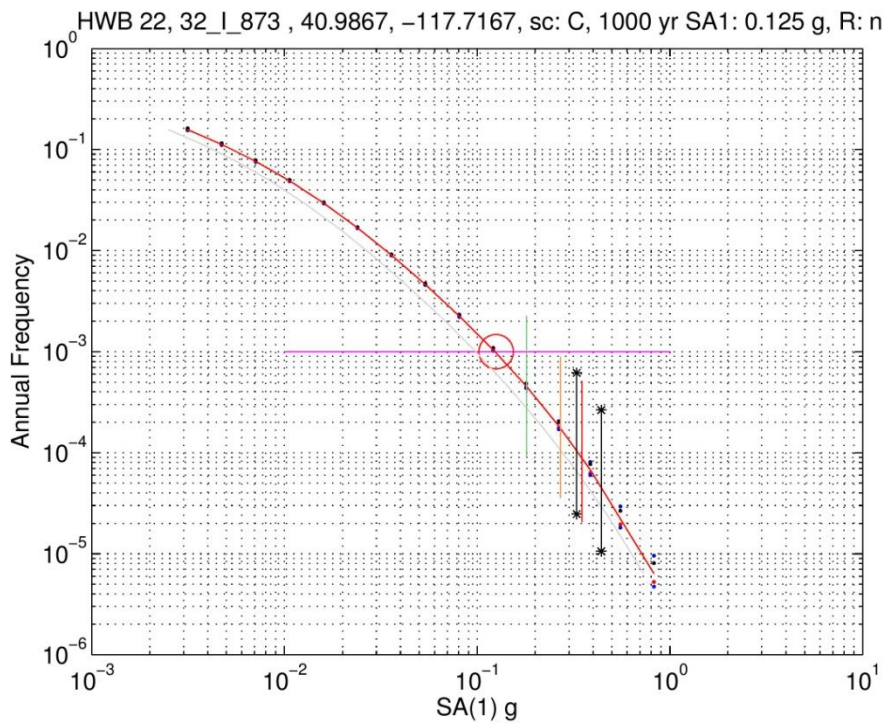


Figure B-4.8 HWB 22, 32_I_873 SA(1 Hz) hazard curve and capacity estimates.

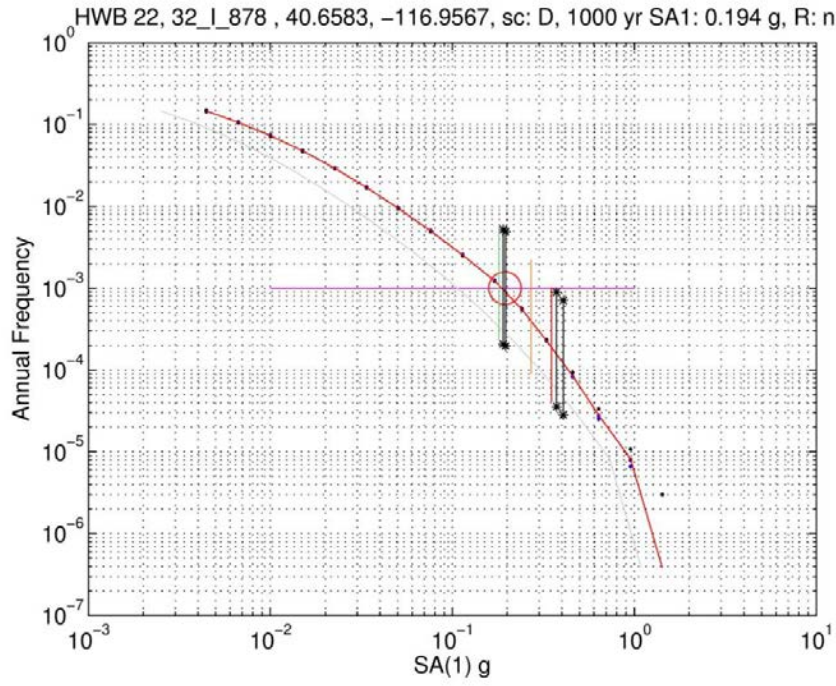


Figure B-4.9 HWB 22, 32_I_878 SA(1 Hz) hazard curve and capacity estimates.

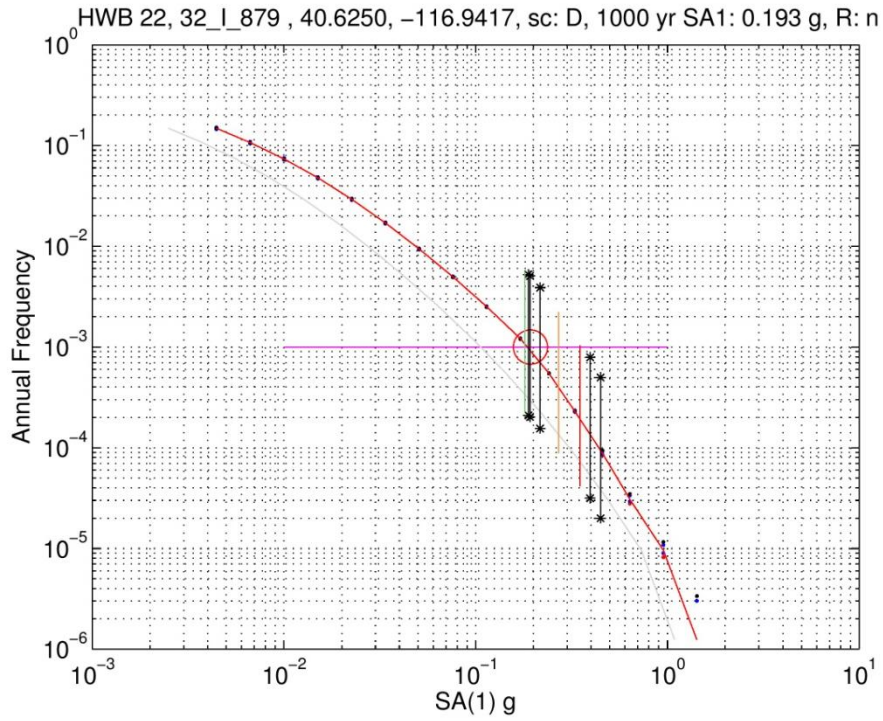


Figure B-4.10 HWB 22, 32_I_879 SA(1 Hz) hazard curve and capacity estimates.

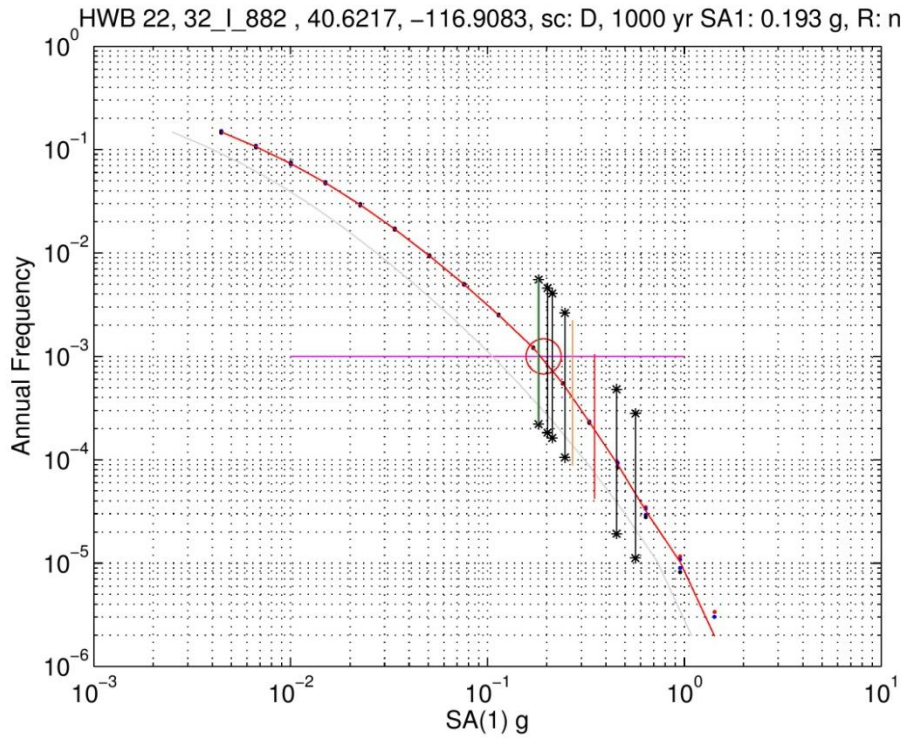


Figure B-4.11 HWB 22, 32_I_882 SA(1 Hz) hazard curve and capacity estimates.

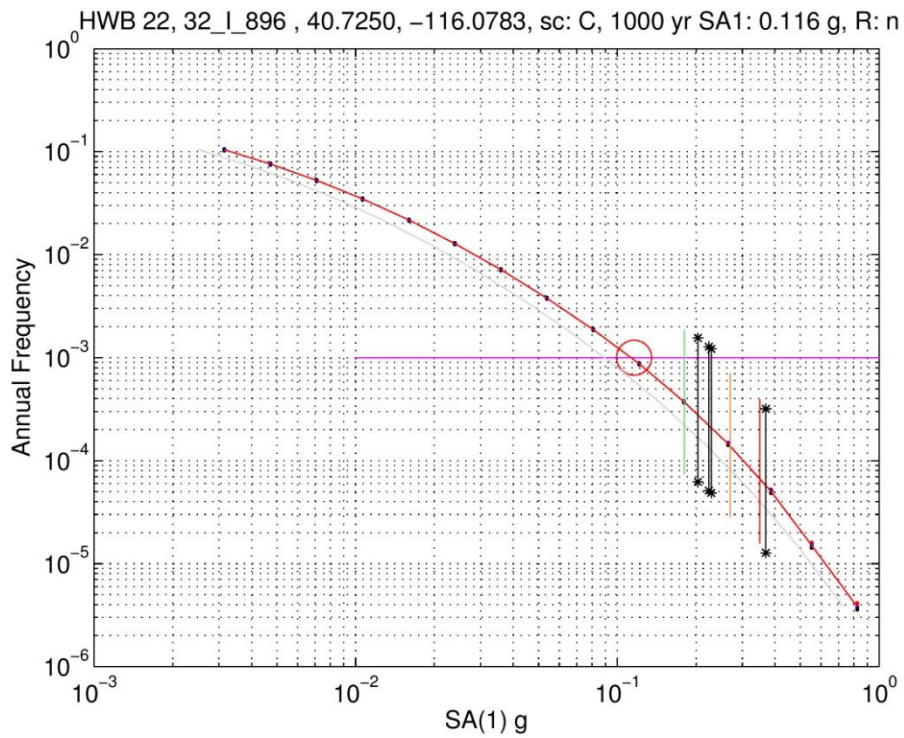


Figure B-4.12 HWB 22, 32_I_896 SA(1 Hz) hazard curve and capacity estimates.

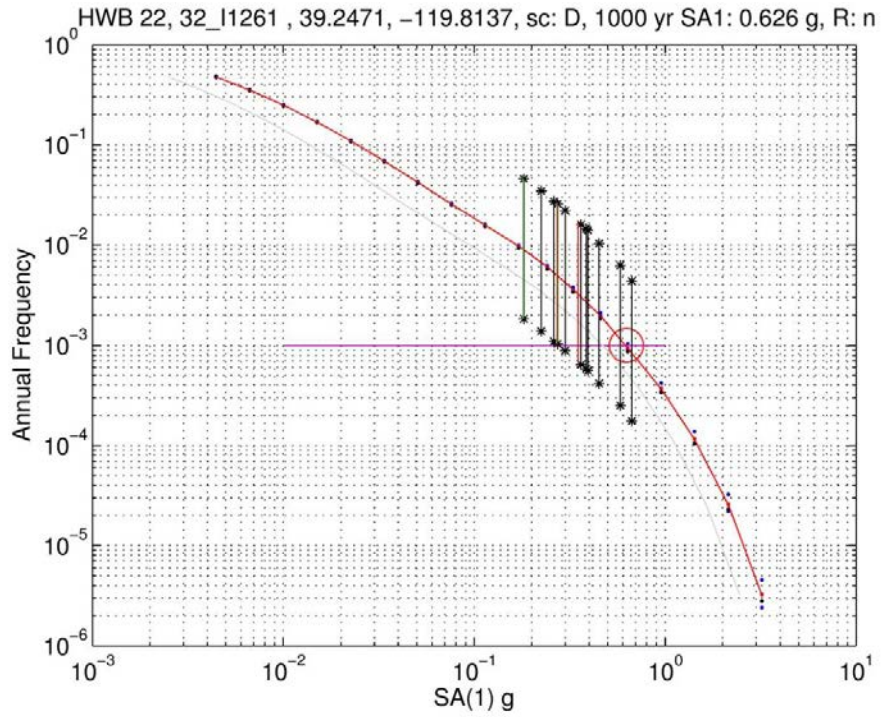


Figure B-4.13 HWB 22, 32_I1261 SA(1 Hz) hazard curve and capacity estimates.

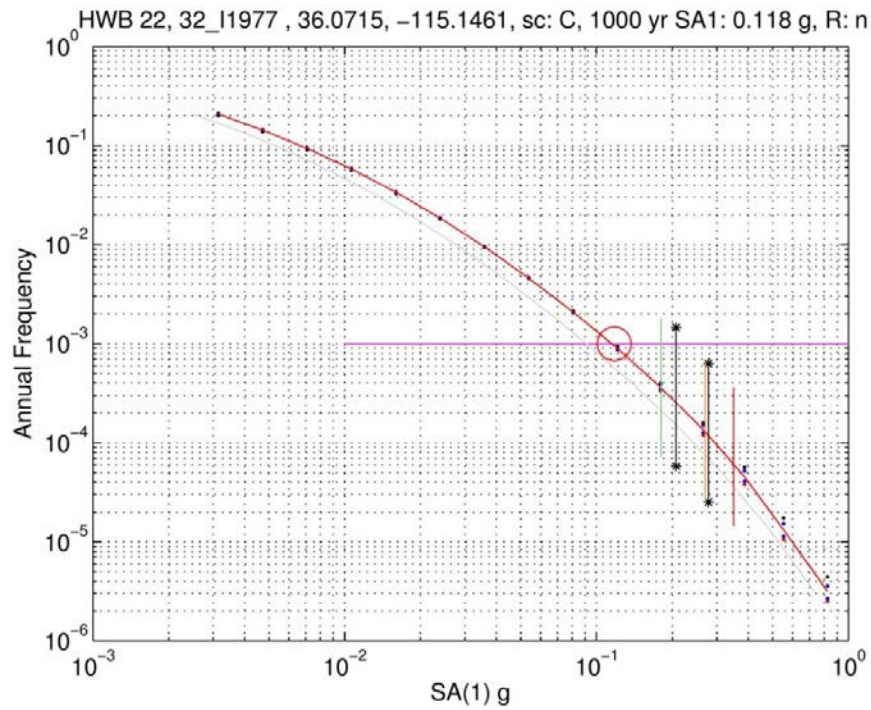


Figure B-4.14 HWB 22, 32_I1977 SA(1 Hz) hazard curve and capacity estimates.

B-5 HWB23 -605 Bridges

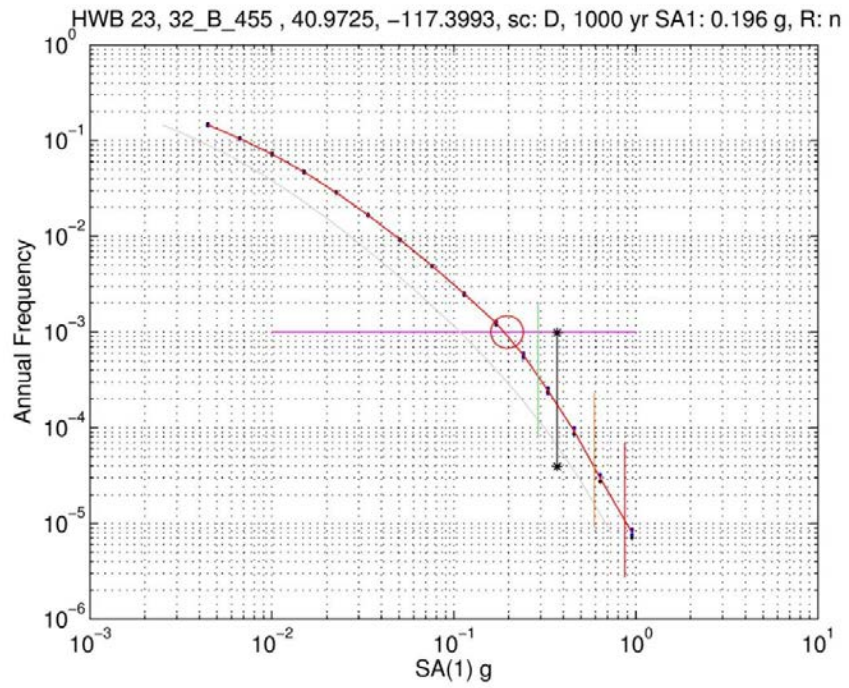


Figure B-5.1 HWB 23, 32_B_455 SA(1 Hz) hazard curve and capacity estimates.

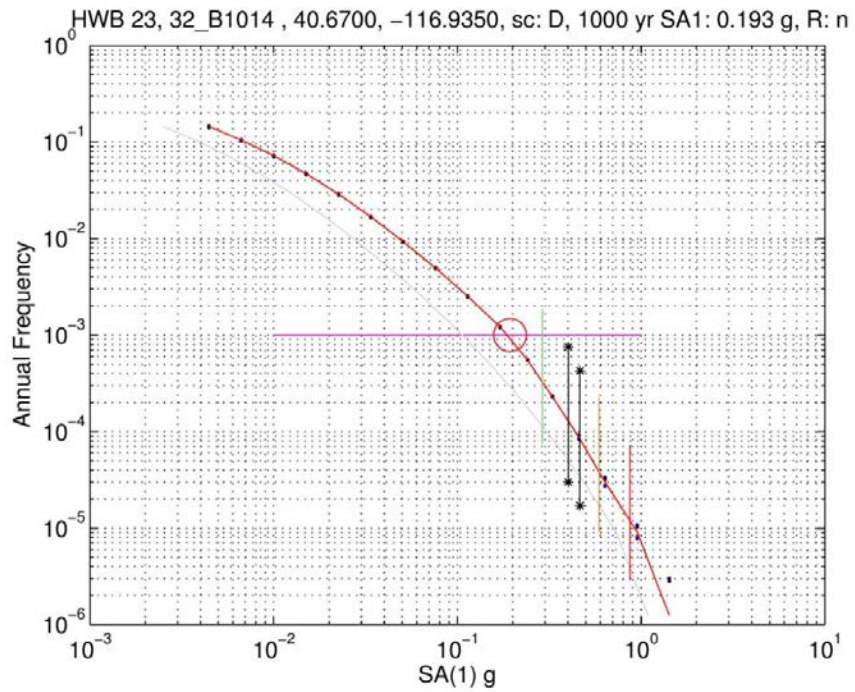


Figure B-5.2 HWB 23, 32_B1014 SA(1 Hz) hazard curve and capacity estimates.

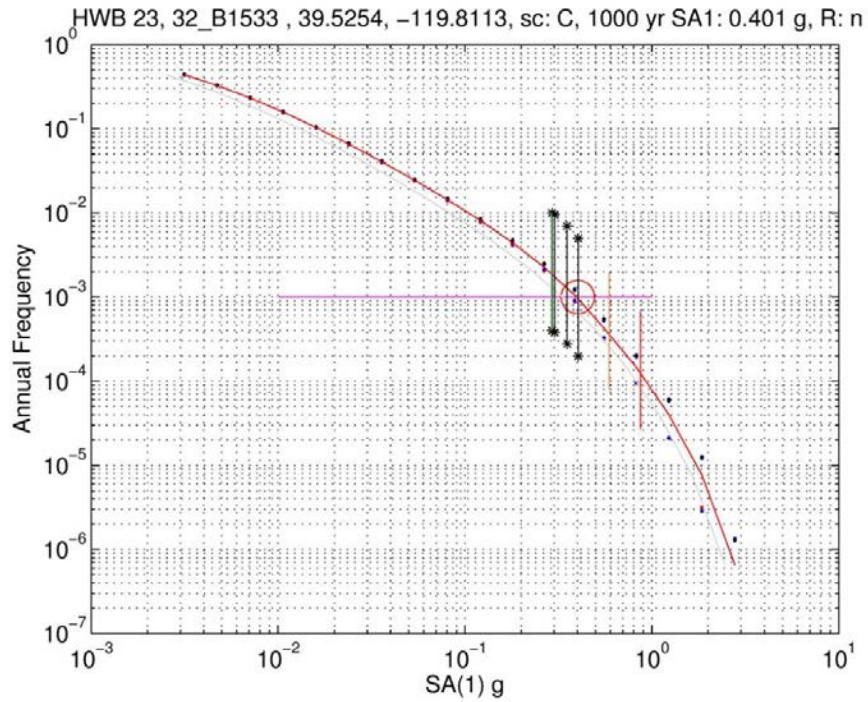


Figure B-5.3 HWB 23, 32_B1533 SA(1 Hz) hazard curve and capacity estimates.

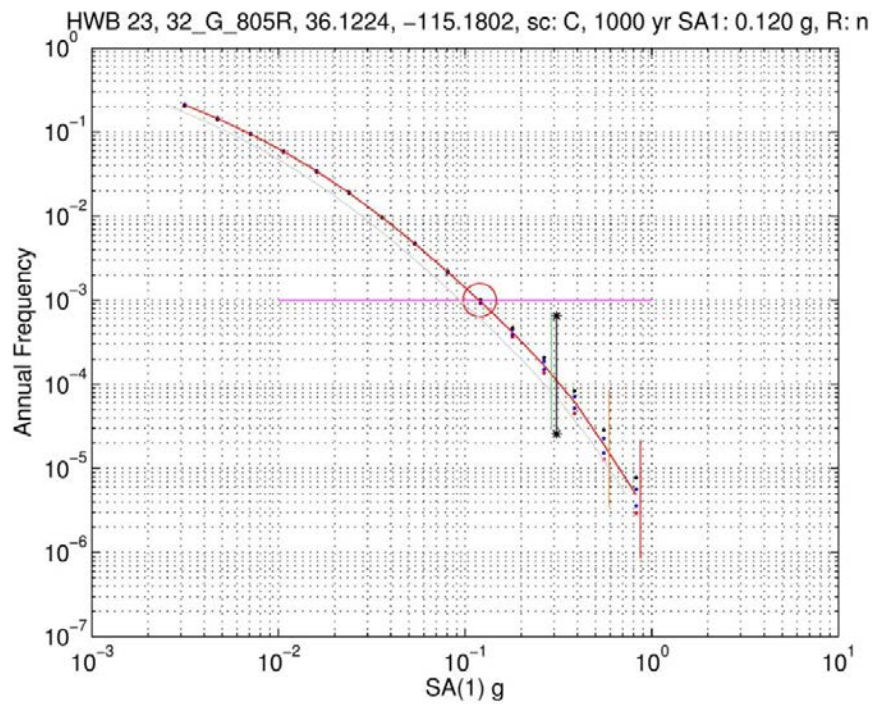


Figure B-5.4 HWB 23, 32_G_805R SA(1 Hz) hazard curve and capacity estimates.

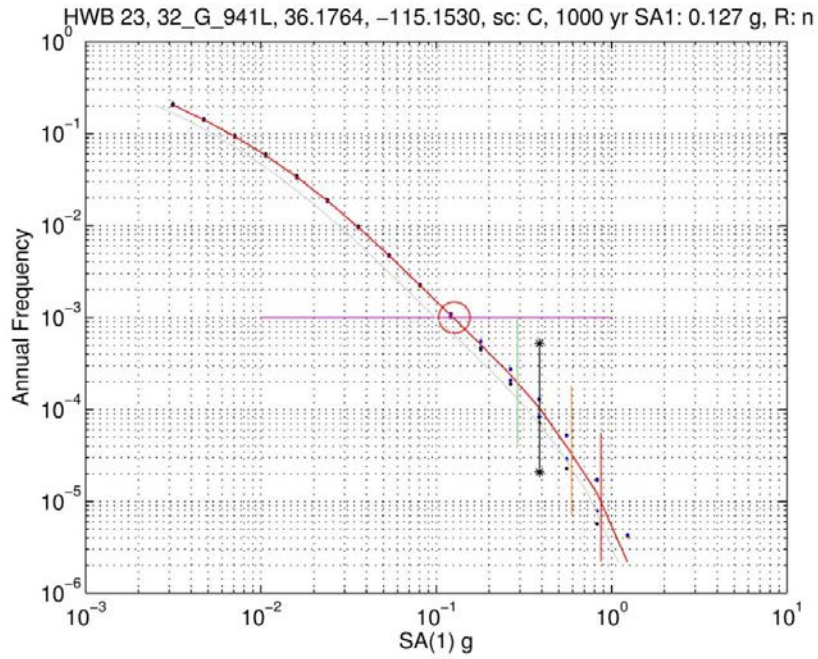


Figure B-5.5 HWB 23, 32_G_941L SA(1 Hz) hazard curve and capacity estimates.

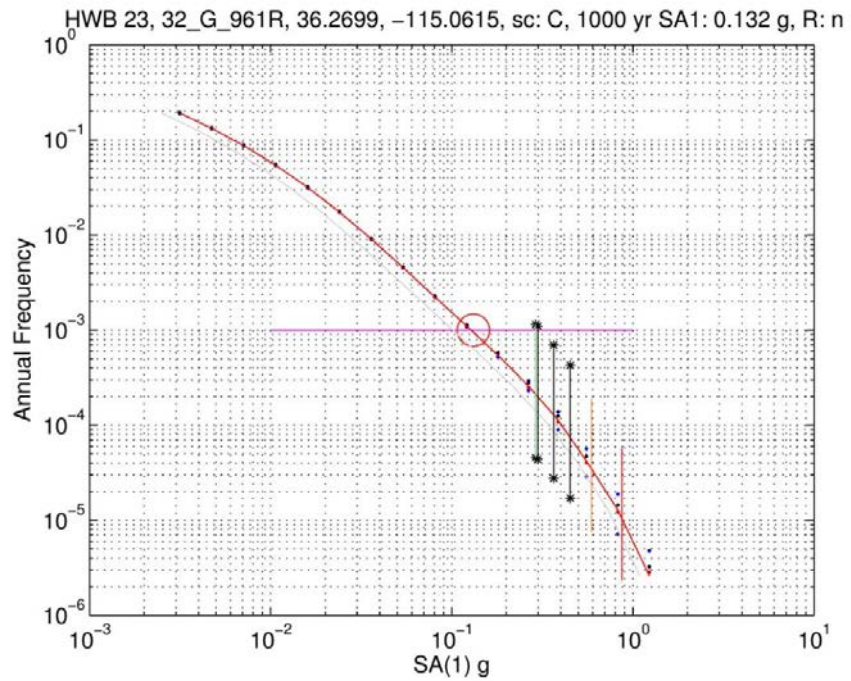


Figure B-5.6 HWB 23, 32_G_961R SA(1 Hz) hazard curve and capacity estimates.

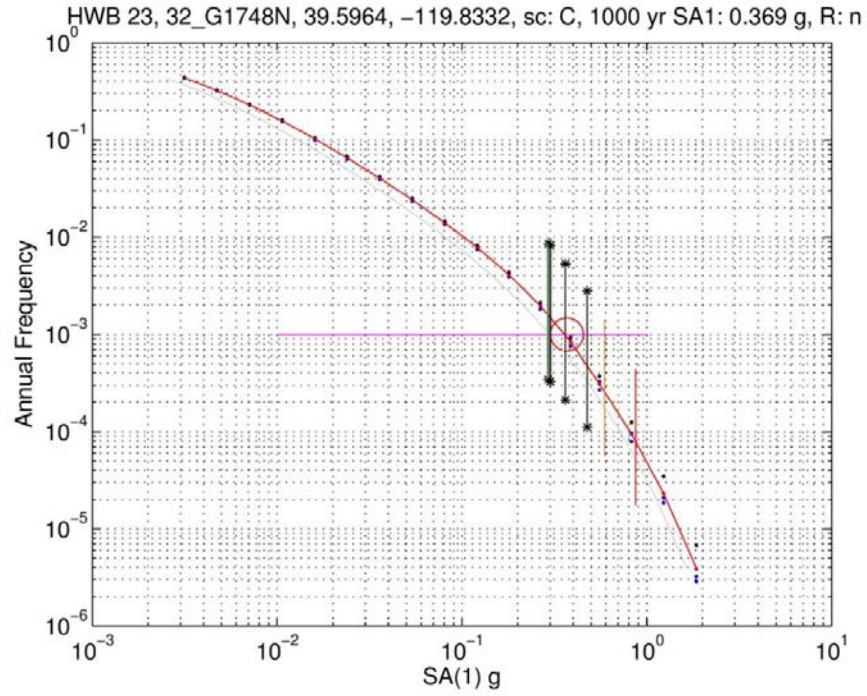


Figure B-5.7 HWB 23, 32_G1748N SA(1 Hz) hazard curve and capacity estimates.

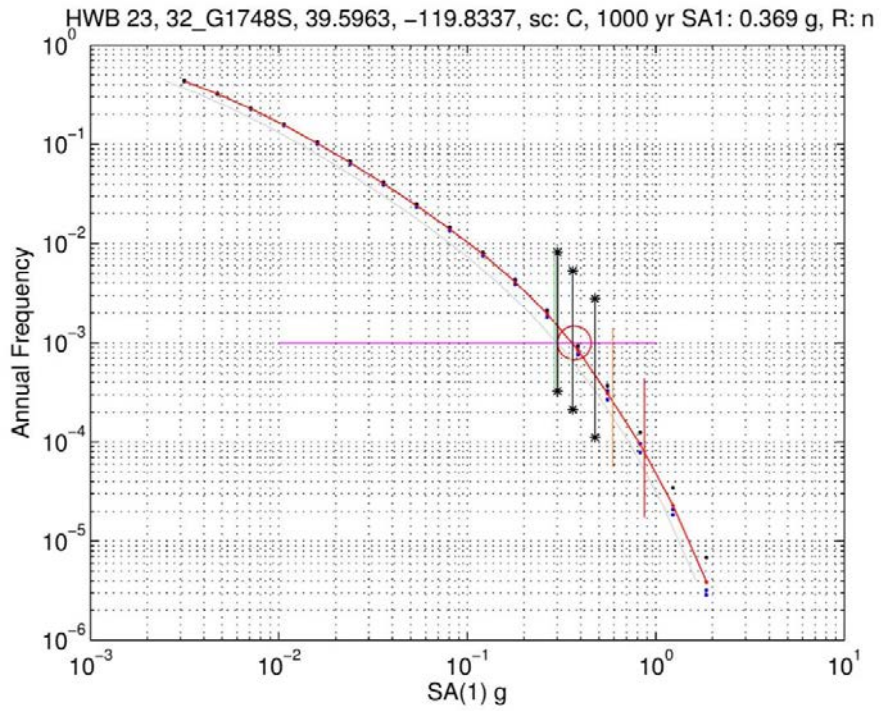


Figure B-5.8 HWB 23, 32_G1748S SA(1 Hz) hazard curve and capacity estimates.

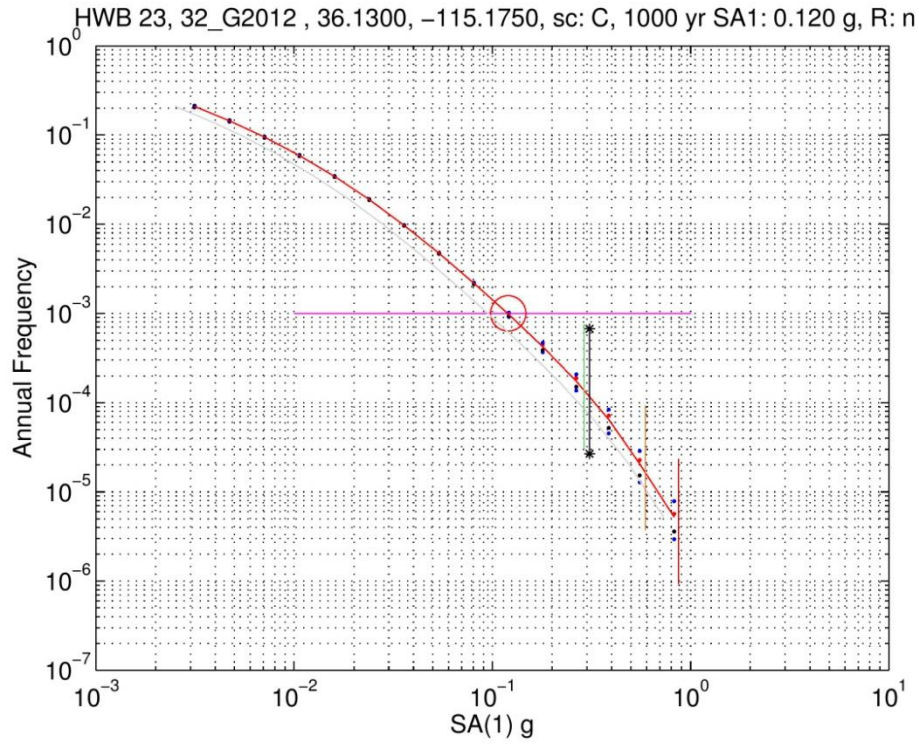


Figure B-5.9 HWB 23, 32_G2012 SA(1 Hz) hazard curve and capacity estimates.

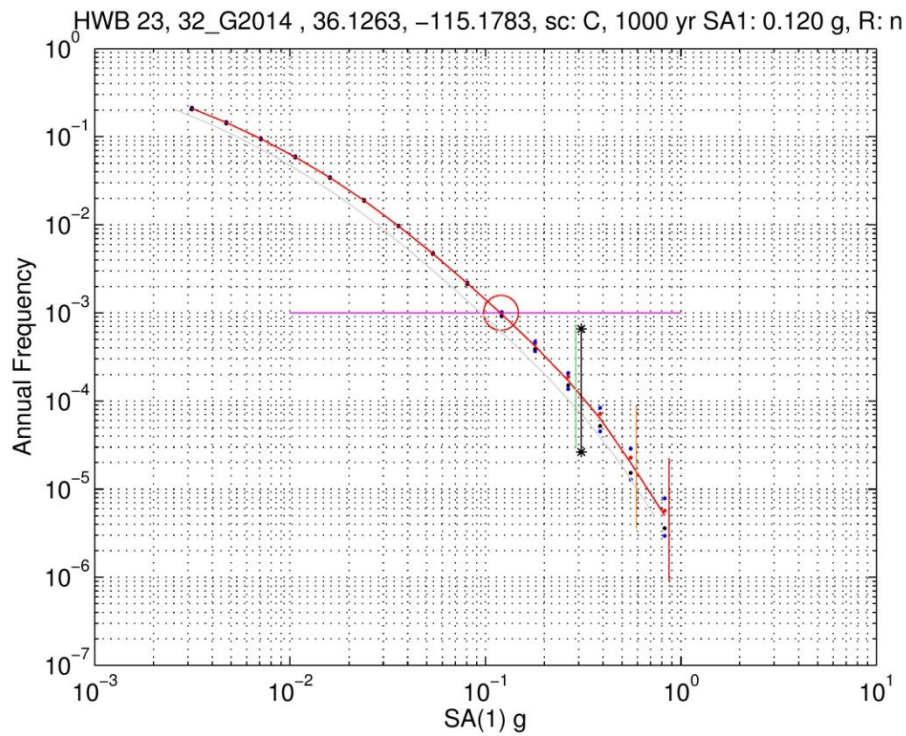


Figure B-5.10 HWB 23, 32_G2014 SA(1 Hz) hazard curve and capacity estimates.

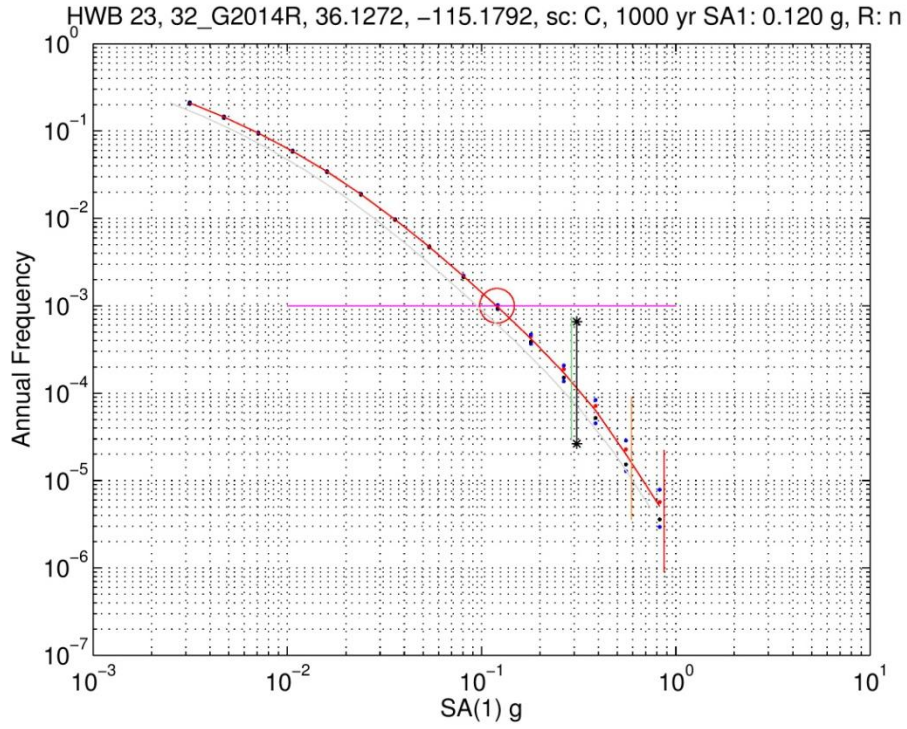


Figure B-5.11 HWB 23, 32_G2014R SA(1 Hz) hazard curve and capacity estimates.

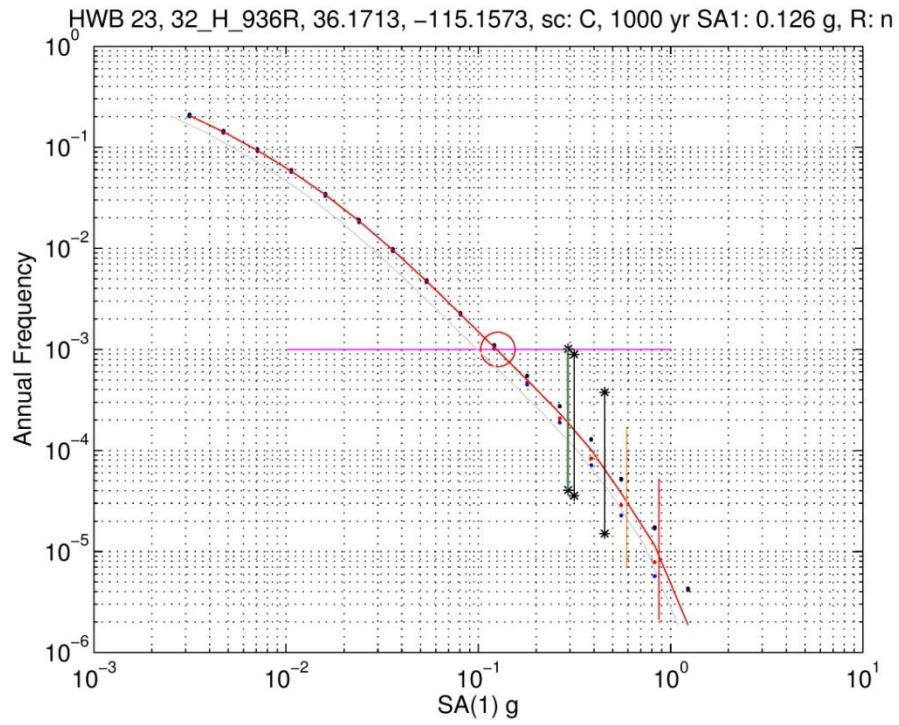


Figure B-5.12 HWB 23, 32_H_936R SA(1 Hz) hazard curve and capacity estimates.

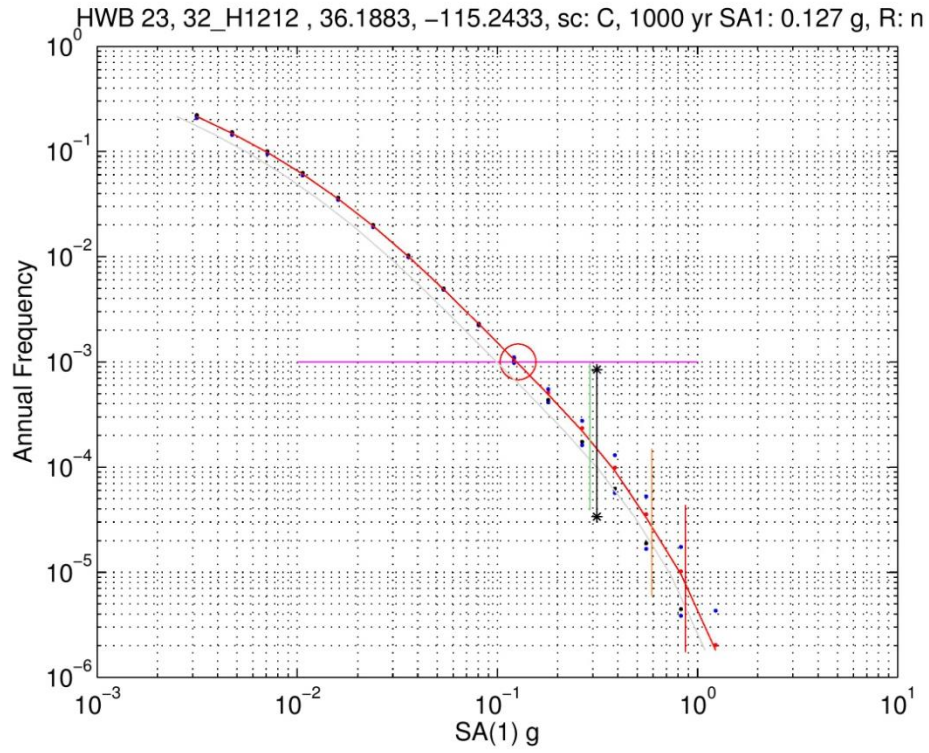


Figure B-5.13 HWB 23, 32_H1212 SA(1 Hz) hazard curve and capacity estimates.

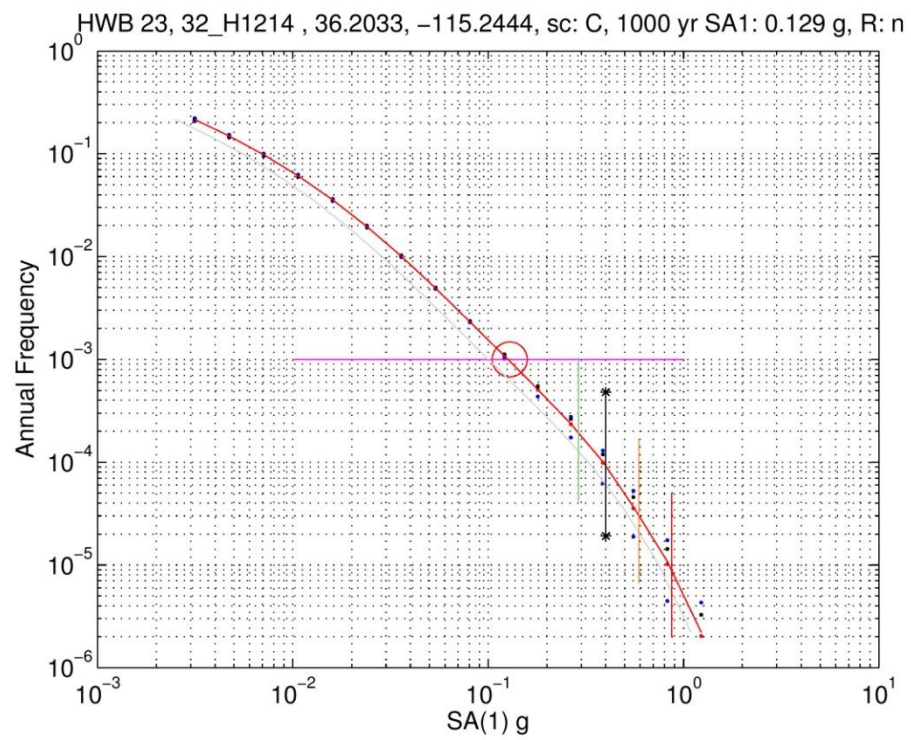


Figure B-5.14 HWB 23, 32_H1214 SA(1 Hz) hazard curve and capacity estimates.

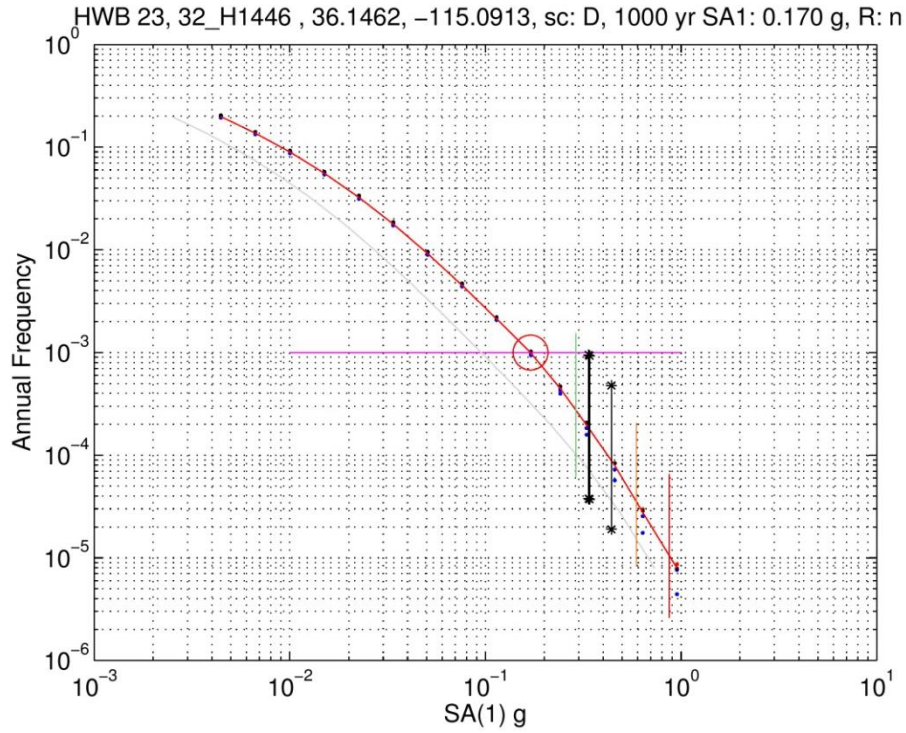


Figure B-5.15 HWB 23, 32_H1446 SA(1 Hz) hazard curve and capacity estimates.

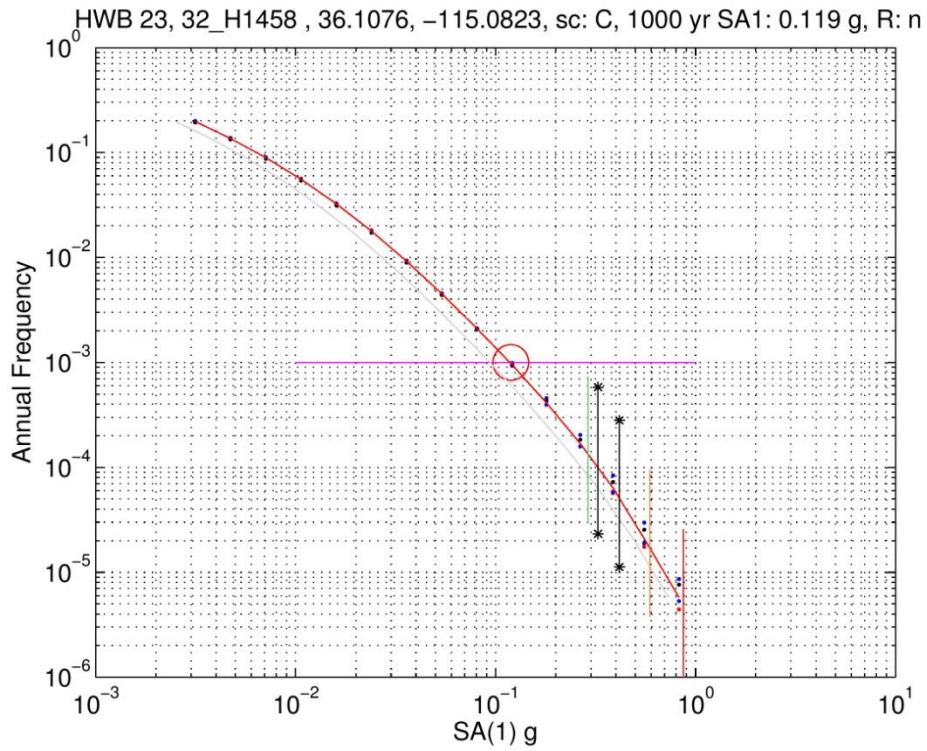


Figure B-5.16 HWB 23, 32_H1458 SA(1 Hz) hazard curve and capacity estimates.

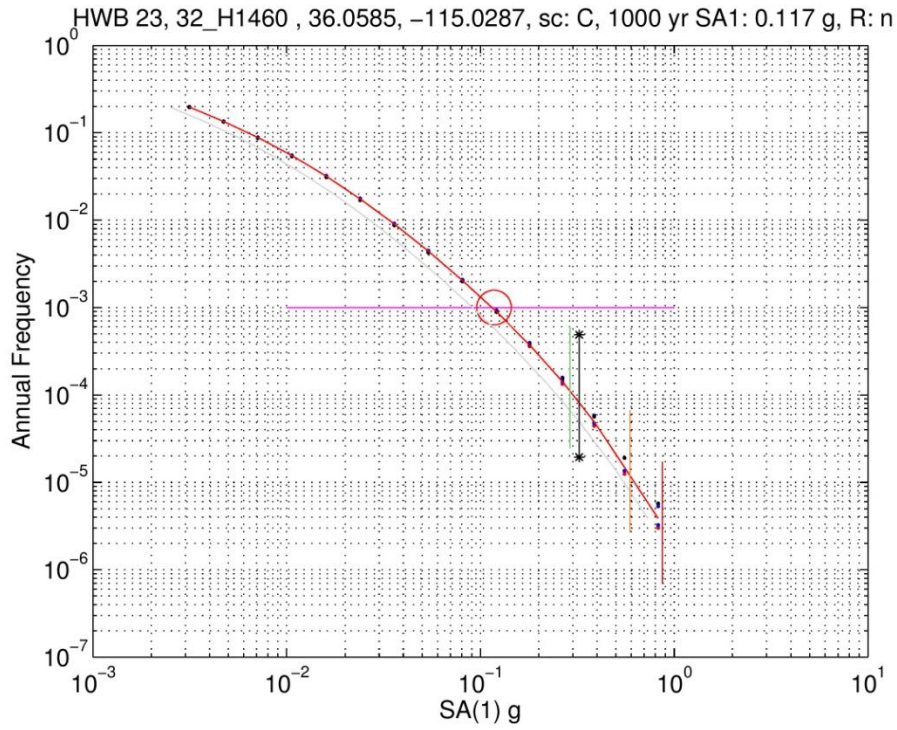


Figure B-5.17 HWB 23, 32_H1460 SA(1 Hz) hazard curve and capacity estimates.

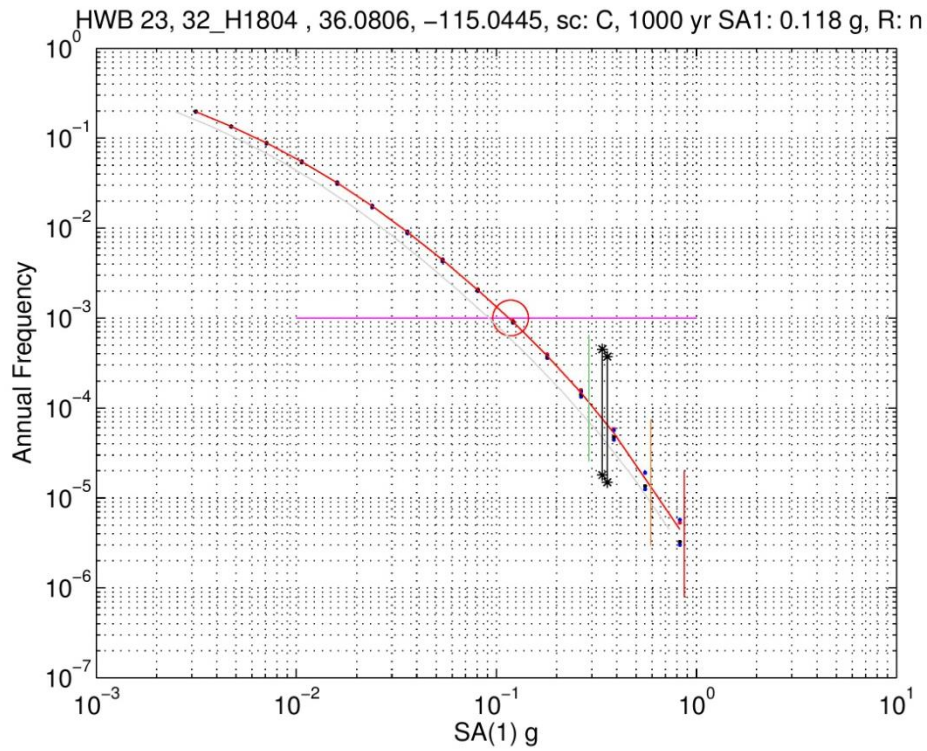


Figure B-5.18 HWB 23, 32_H1804 SA(1 Hz) hazard curve and capacity estimates.

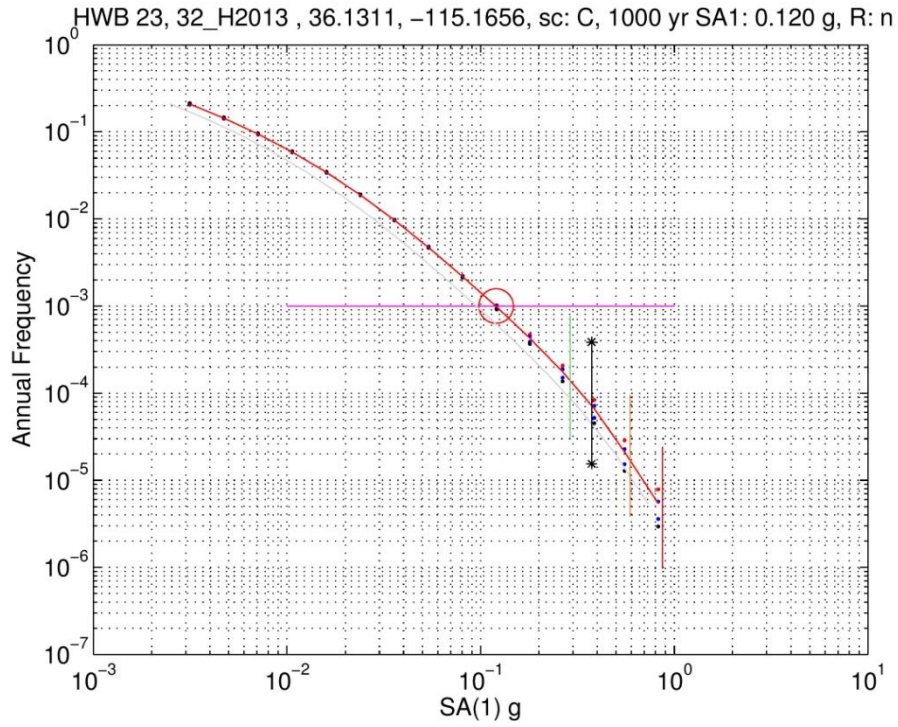


Figure B-5.19 HWB 23, 32_H2013 SA(1 Hz) hazard curve and capacity estimates.

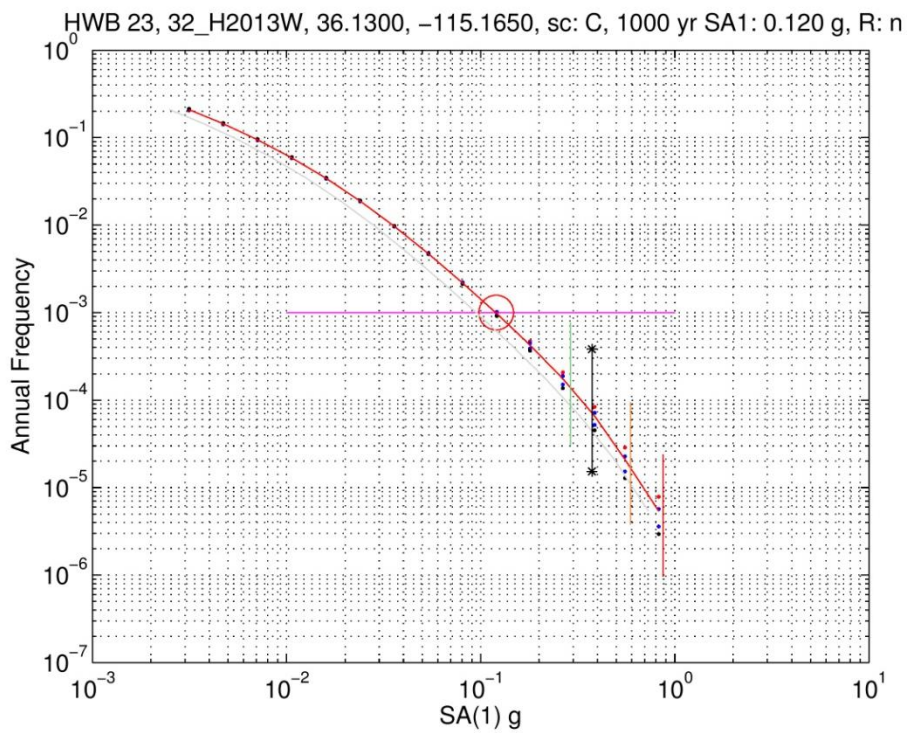


Figure B-5.20 HWB 23, 32_H2013W SA(1 Hz) hazard curve and capacity estimates.

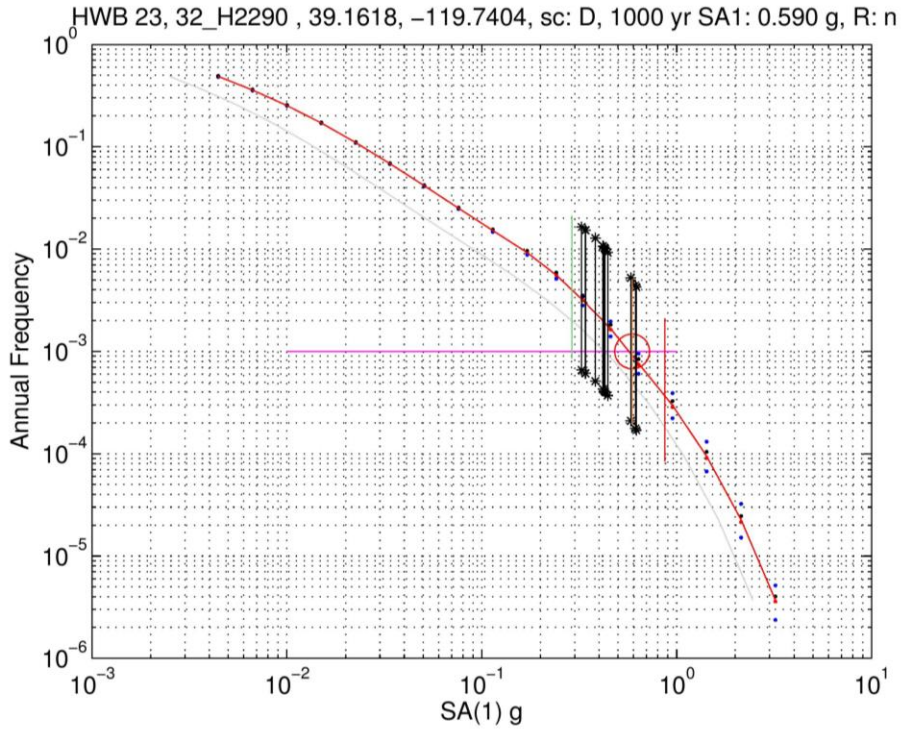


Figure B-5.21 HWB 23, 32_H2290 SA(1 Hz) hazard curve and capacity estimates.

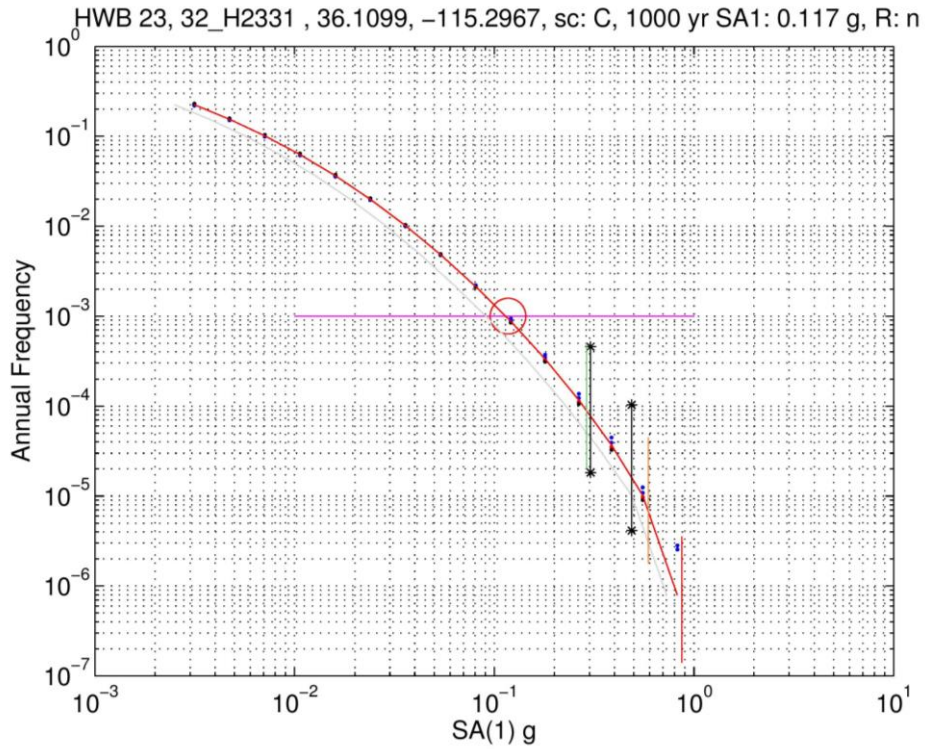


Figure B-5.22 HWB 23, 32_H2331 SA(1 Hz) hazard curve and capacity estimates.

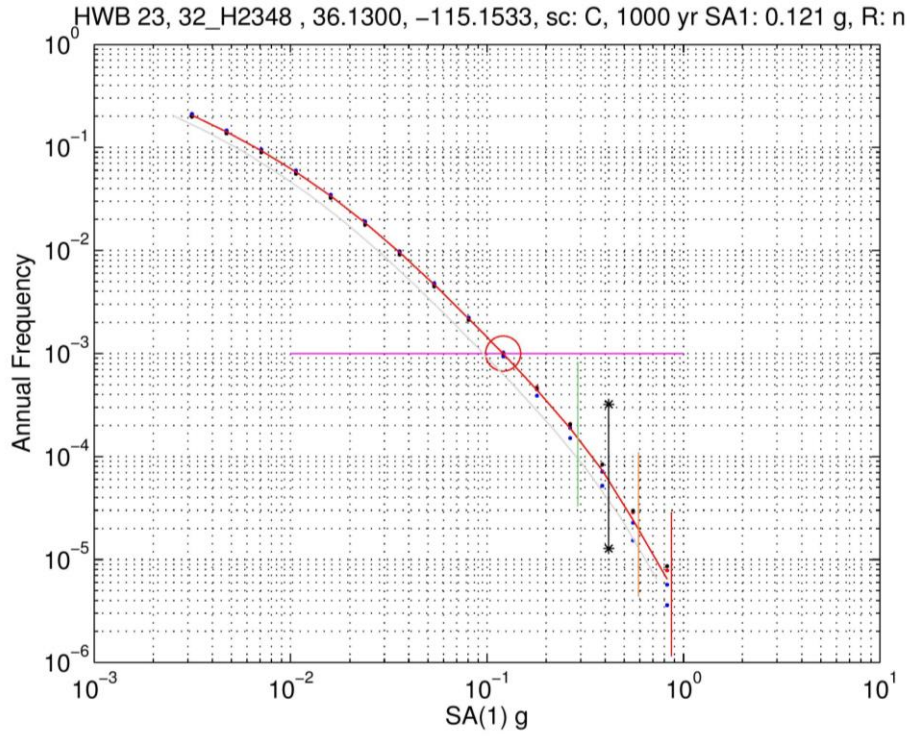


Figure B-5.23 HWB 23, 32_H2348 SA(1 Hz) hazard curve and capacity estimates.

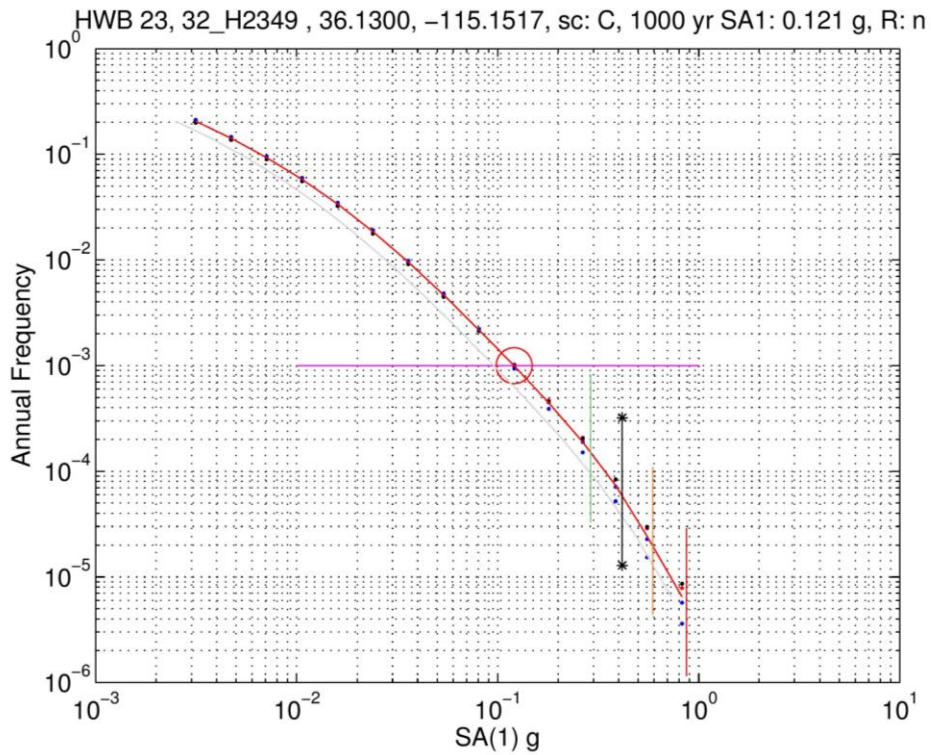


Figure B-5.24 HWB 23, 32_H2349 SA(1 Hz) hazard curve and capacity estimates.

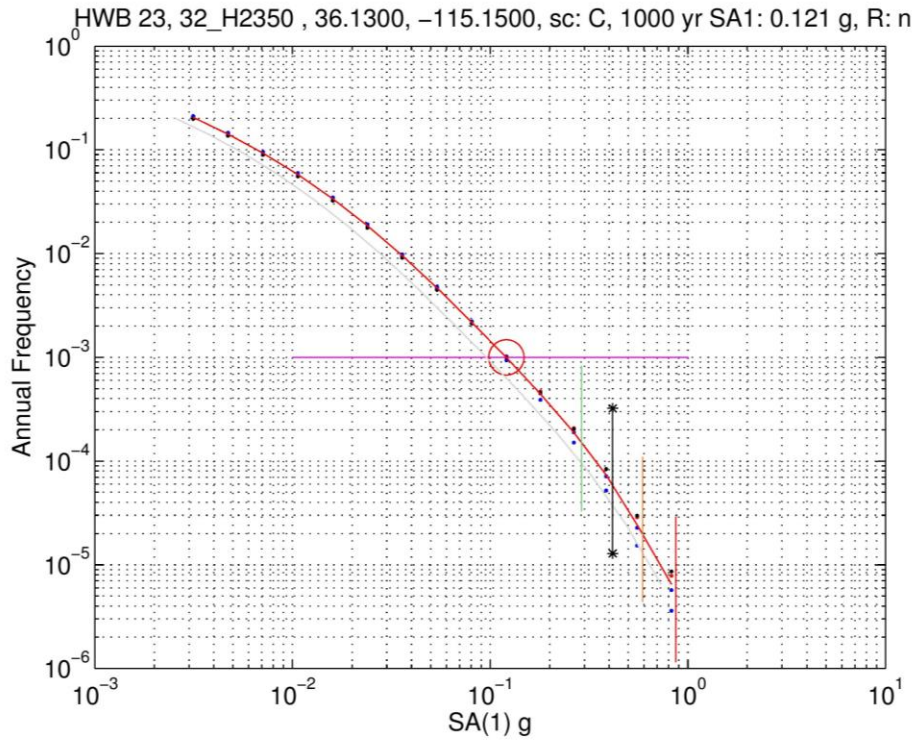


Figure B-5.25 HWB 23, 32_H2350 SA(1 Hz) hazard curve and capacity estimates.

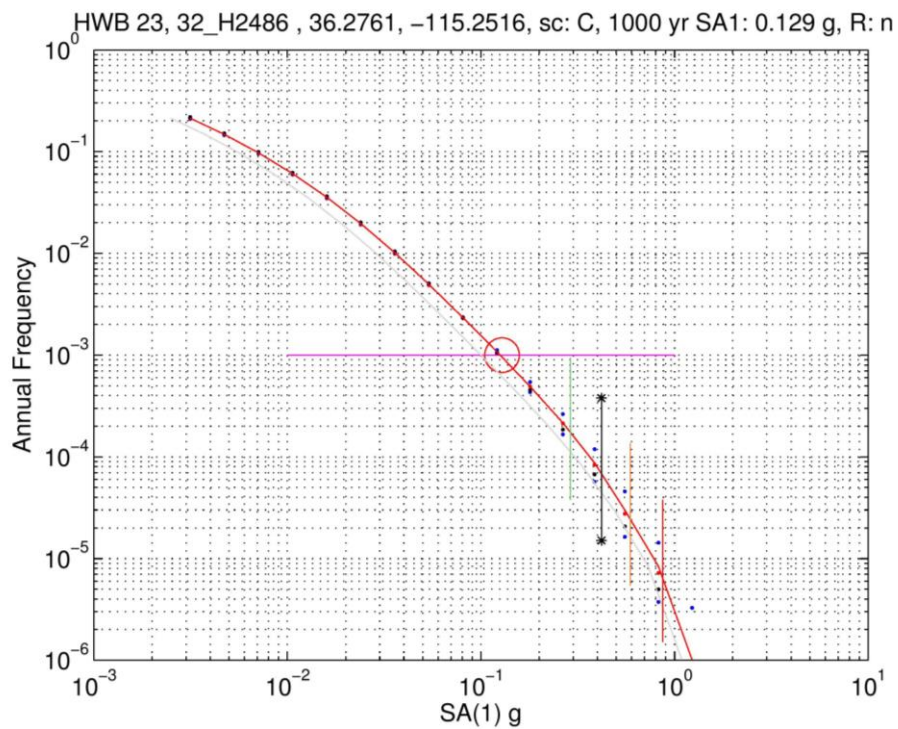


Figure B-5.26 HWB 23, 32_H2486 SA(1 Hz) hazard curve and capacity estimates.

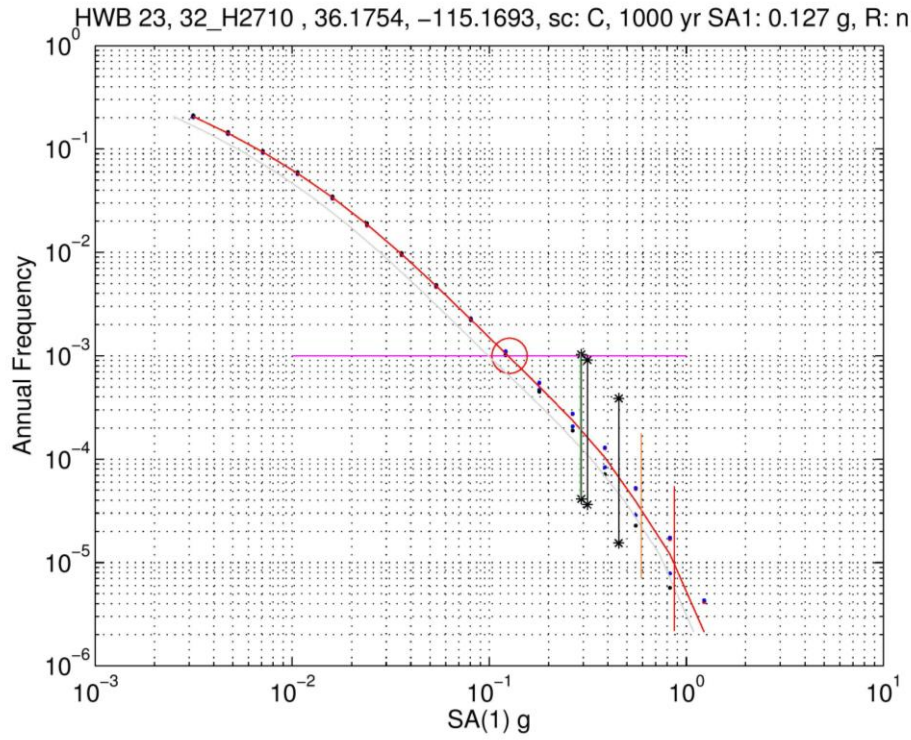


Figure B-5.27 HWB 23, 32_H2710 SA(1 Hz) hazard curve and capacity estimates.

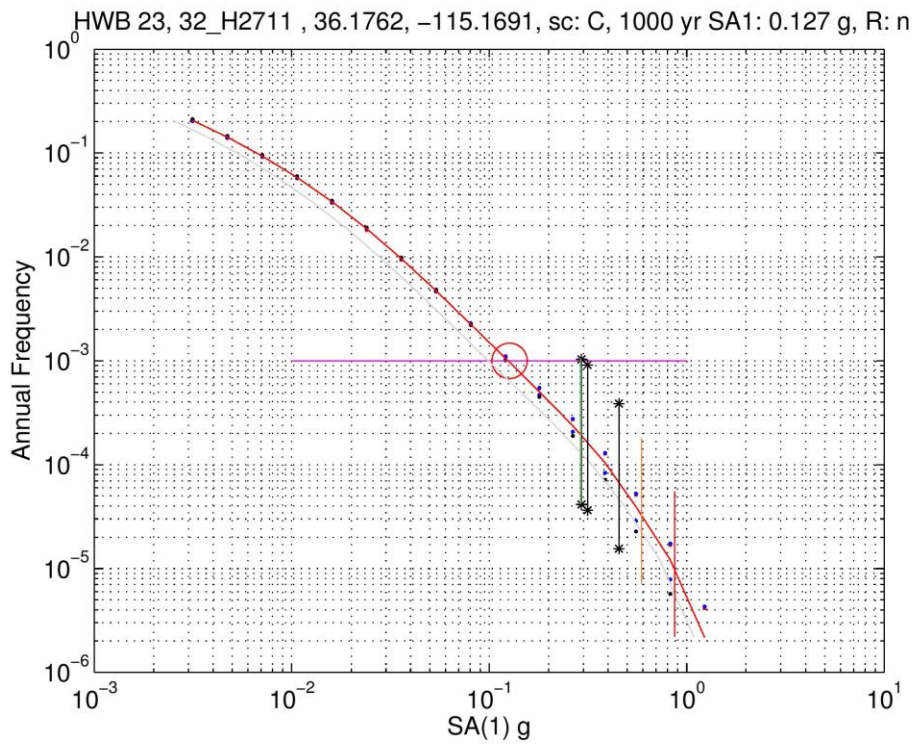


Figure B-5.28 HWB 23, 32_H2711 SA(1 Hz) hazard curve and capacity estimates.

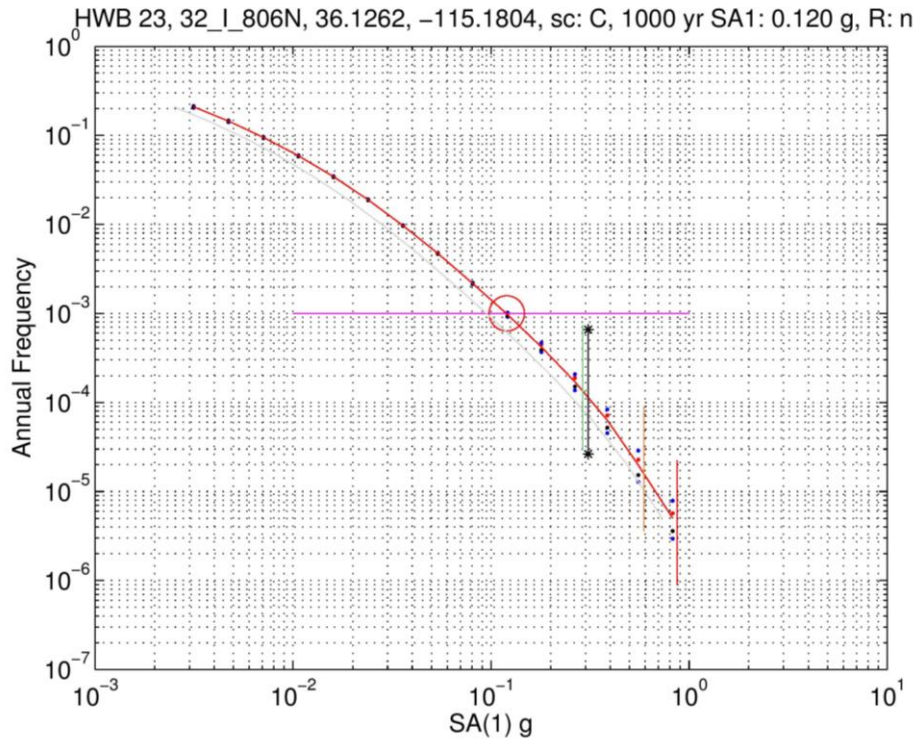


Figure B-5.29 HWB 23, 32_I_806N SA(1 Hz) hazard curve and capacity estimates.

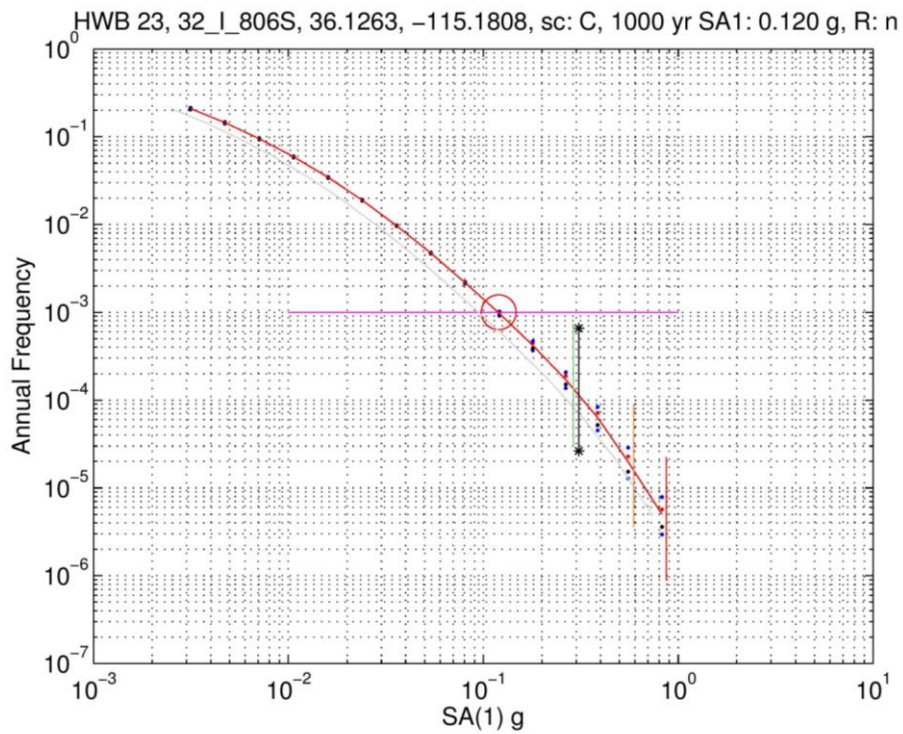


Figure B-5.30 HWB 23, 32_I_806S SA(1 Hz) hazard curve and capacity estimates.

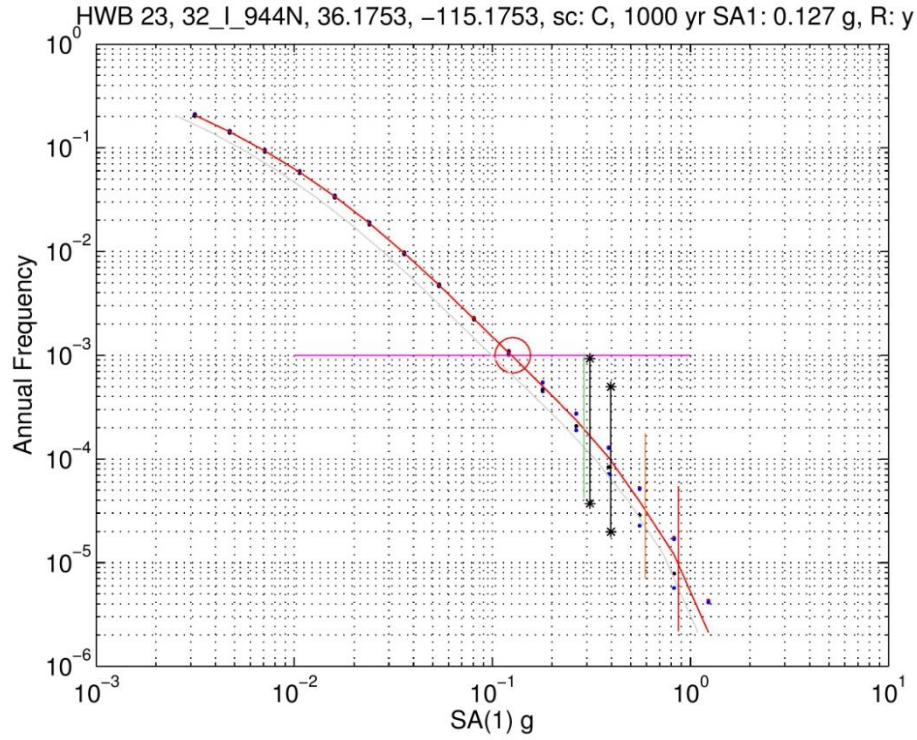


Figure B-5.31 HWB 23, 32_I_944N SA(1 Hz) hazard curve and capacity estimates.

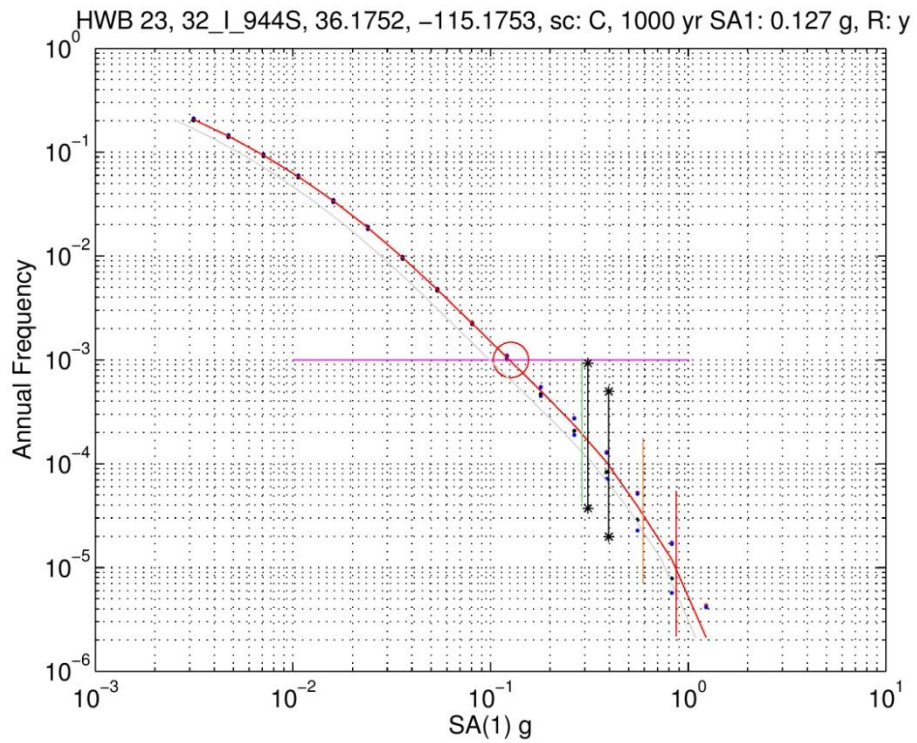


Figure B-5.32 HWB 23, 32_I_944S SA(1 Hz) hazard curve and capacity estimates.

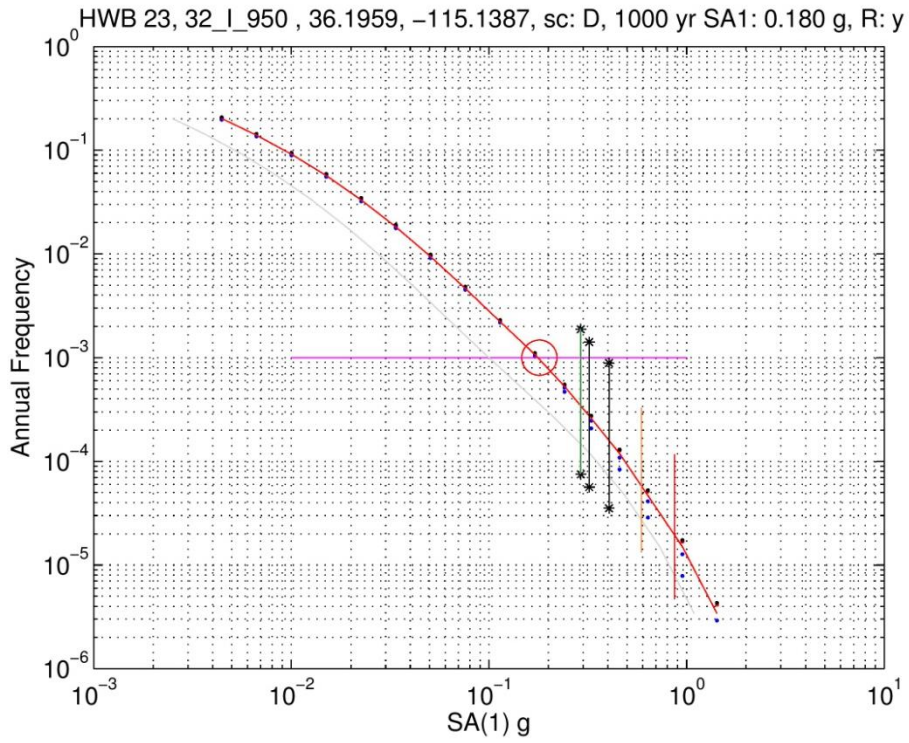


Figure B-5.33 HWB 23, 32_I_950 SA(1 Hz) hazard curve and capacity estimates.

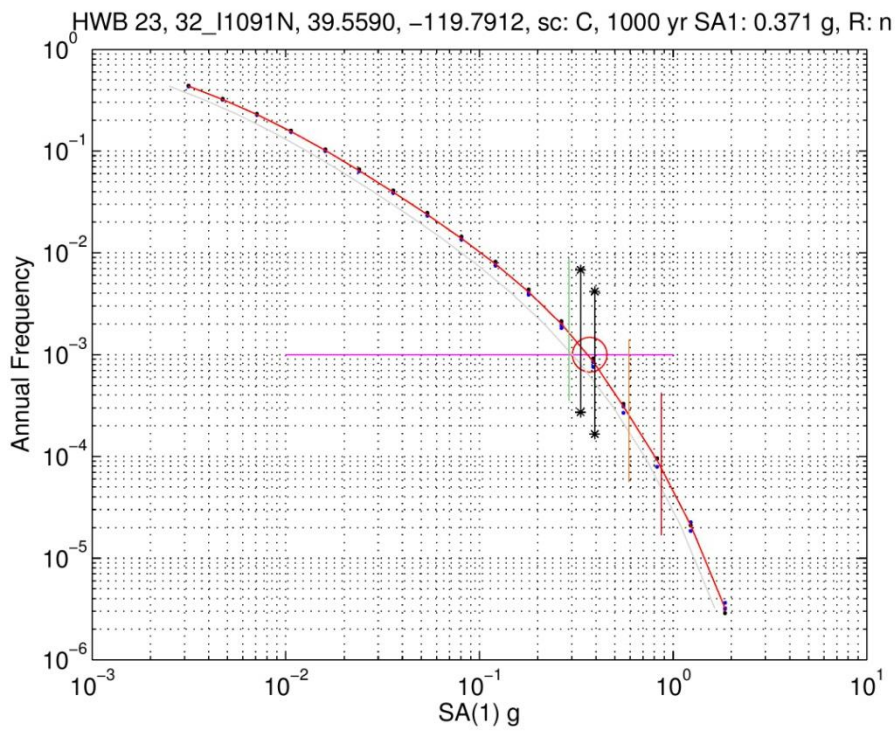


Figure B-5.34 HWB 23, 32_I1091N SA(1 Hz) hazard curve and capacity estimates.

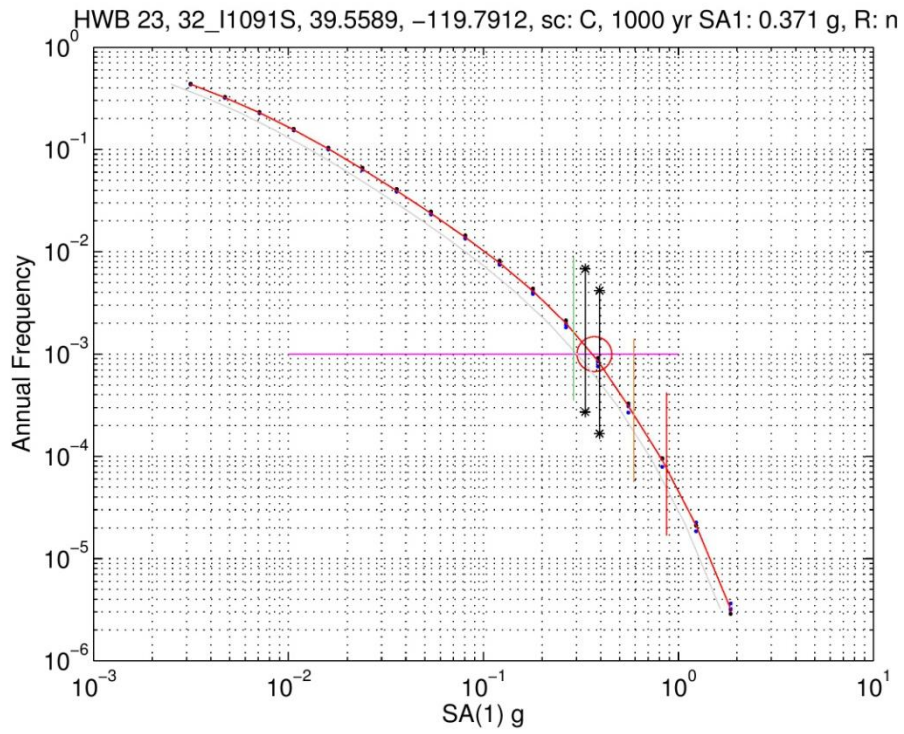


Figure B-5.35 HWB 23, 32_I1091S SA(1 Hz) hazard curve and capacity estimates.

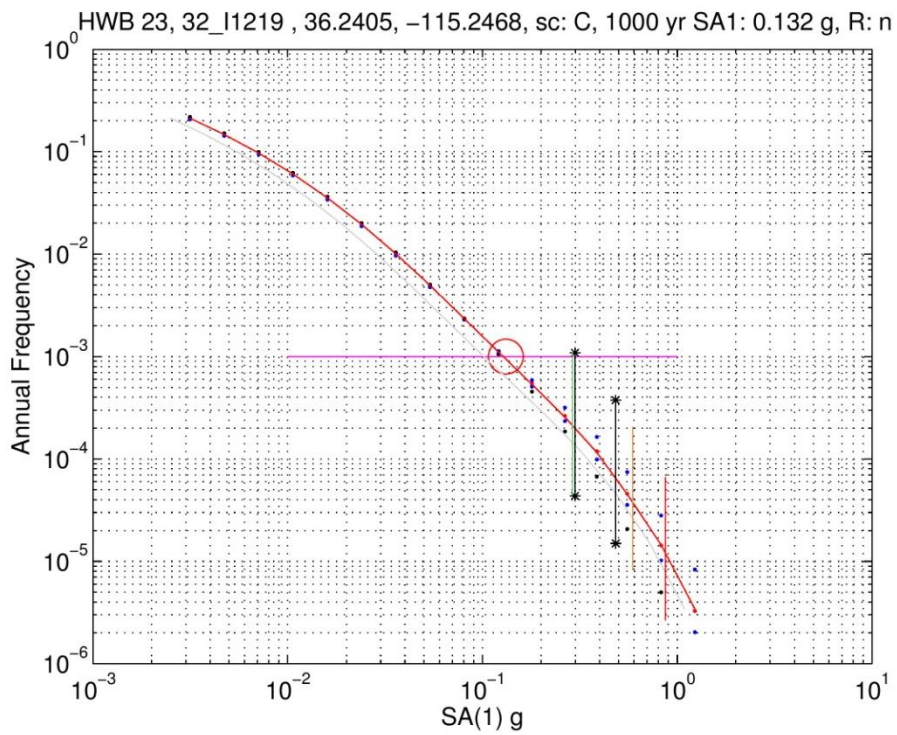


Figure B-5.36 HWB 23, 32_I1219 SA(1 Hz) hazard curve and capacity estimates.

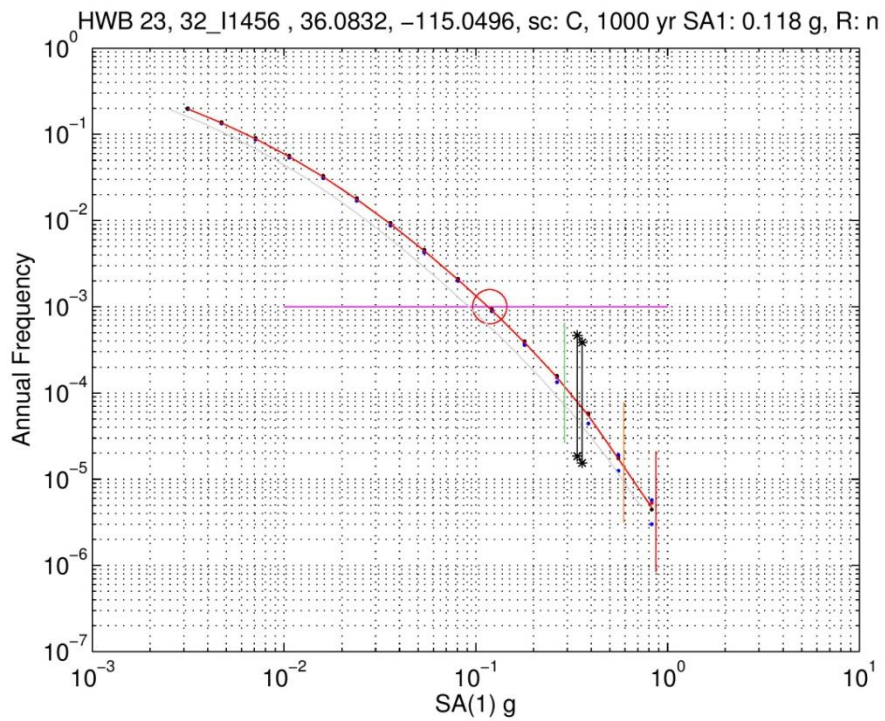


Figure B-5.37 HWB 23, 32_I1456 SA(1 Hz) hazard curve and capacity estimates.

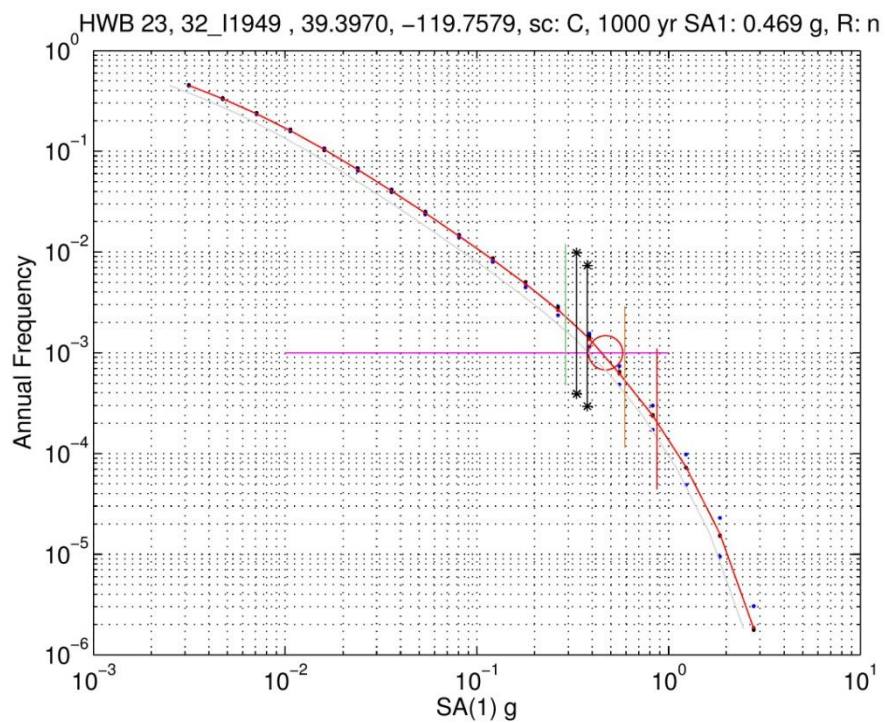


Figure B-5.38 HWB 23, 32_I1949 SA(1 Hz) hazard curve and capacity estimates.

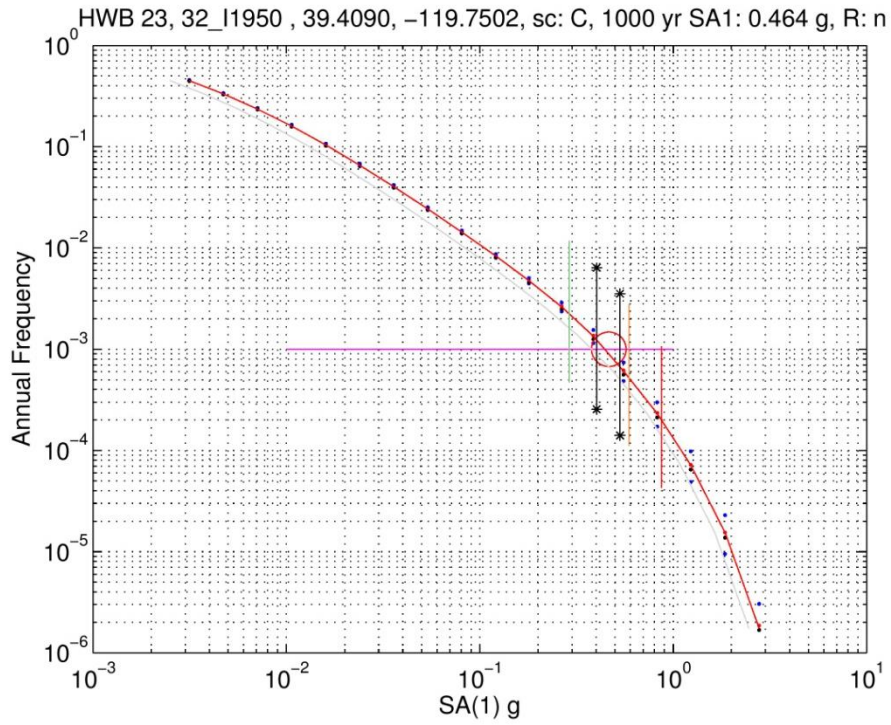


Figure B-5.39 HWB 23, 32_I1950 SA(1 Hz) hazard curve and capacity estimates.

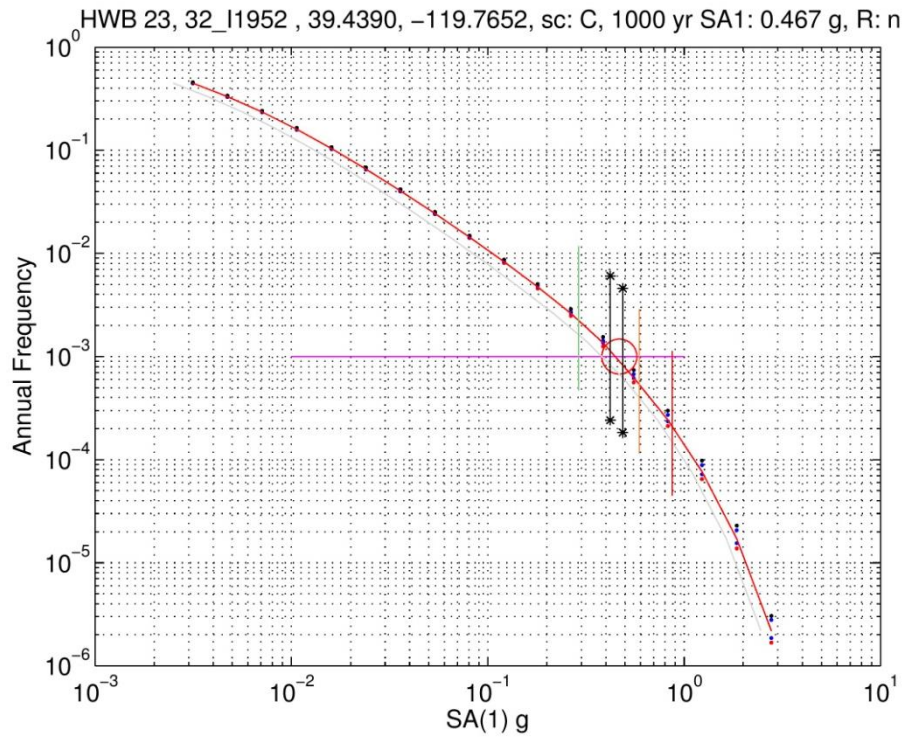


Figure B-5.40 HWB 23, 32_I1952 SA(1 Hz) hazard curve and capacity estimates.

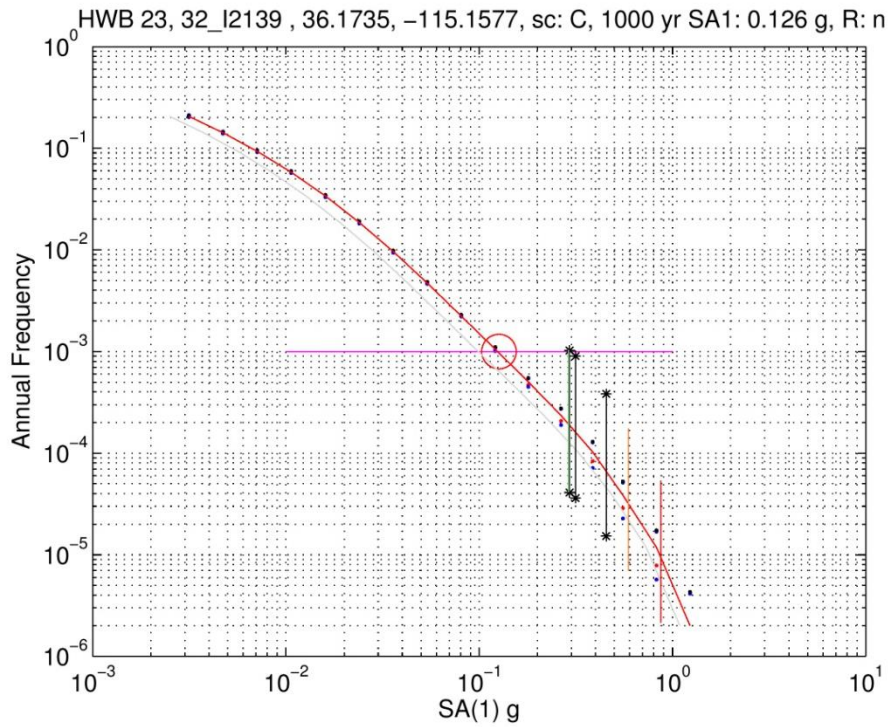


Figure B-5.41 HWB 23, 32_I2139 SA(1 Hz) hazard curve and capacity estimates.

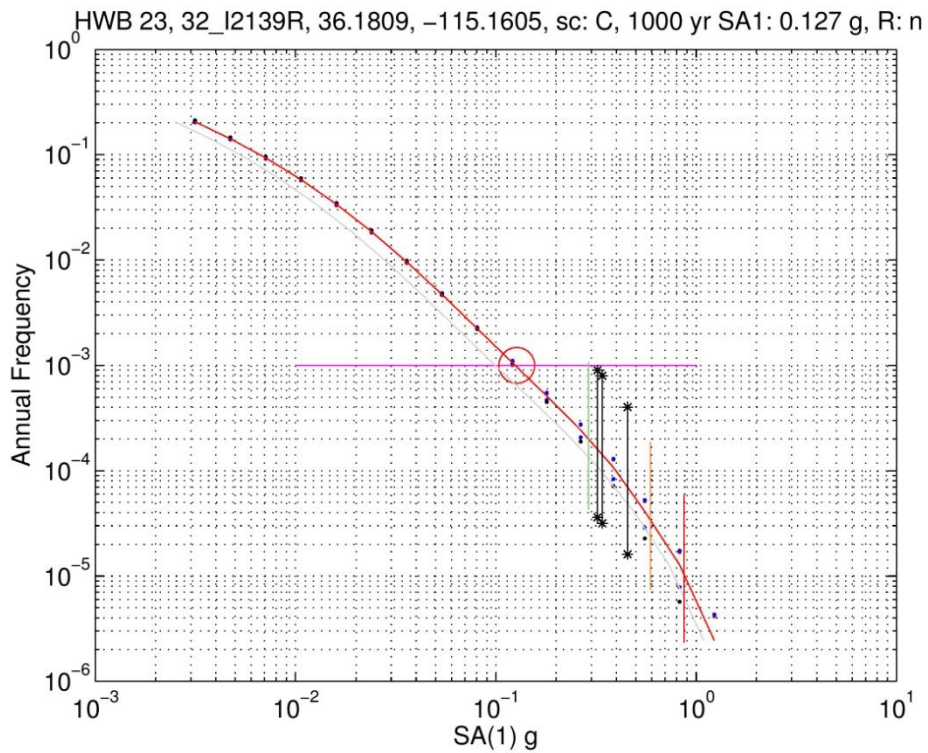


Figure B-5.42 HWB 23, 32_I2139R SA(1 Hz) hazard curve and capacity estimates.

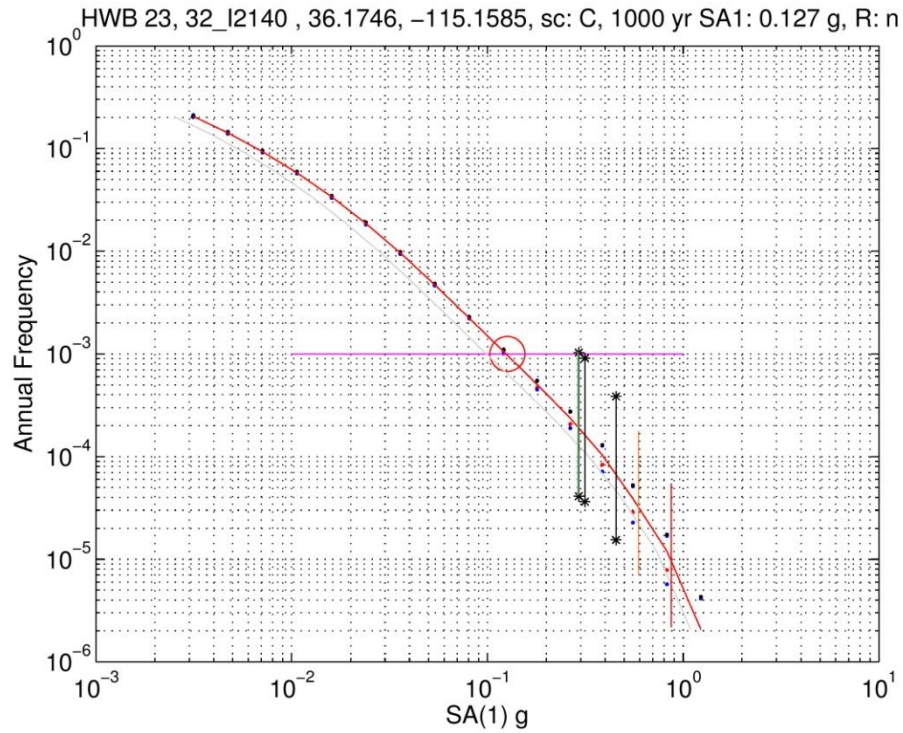


Figure B-5.43 HWB 23, 32_I2140 SA(1 Hz) hazard curve and capacity estimates.

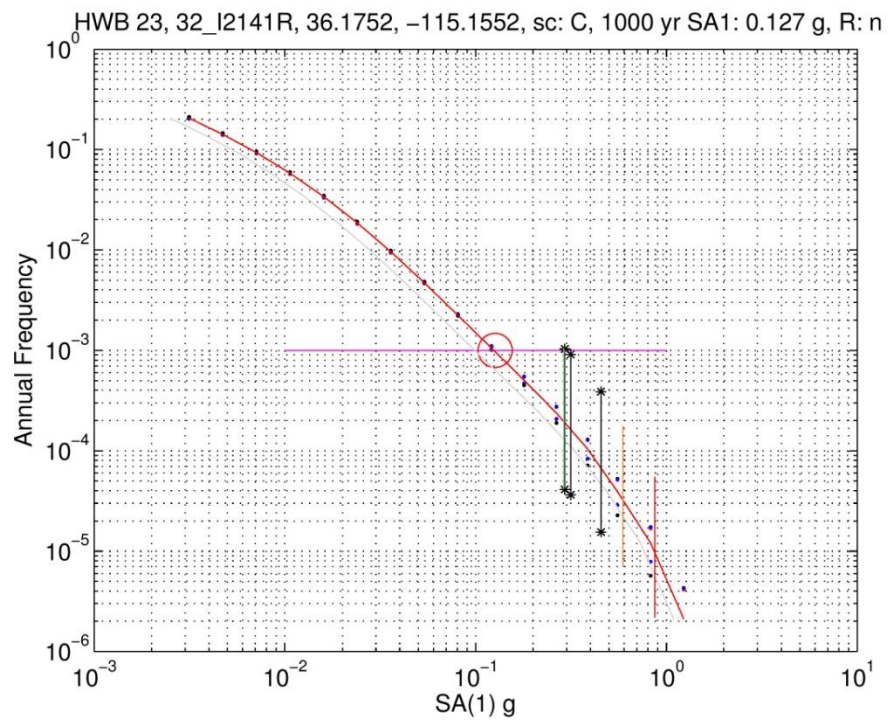


Figure B-5.44 HWB 23, 32_I2141R SA(1 Hz) hazard curve and capacity estimates.

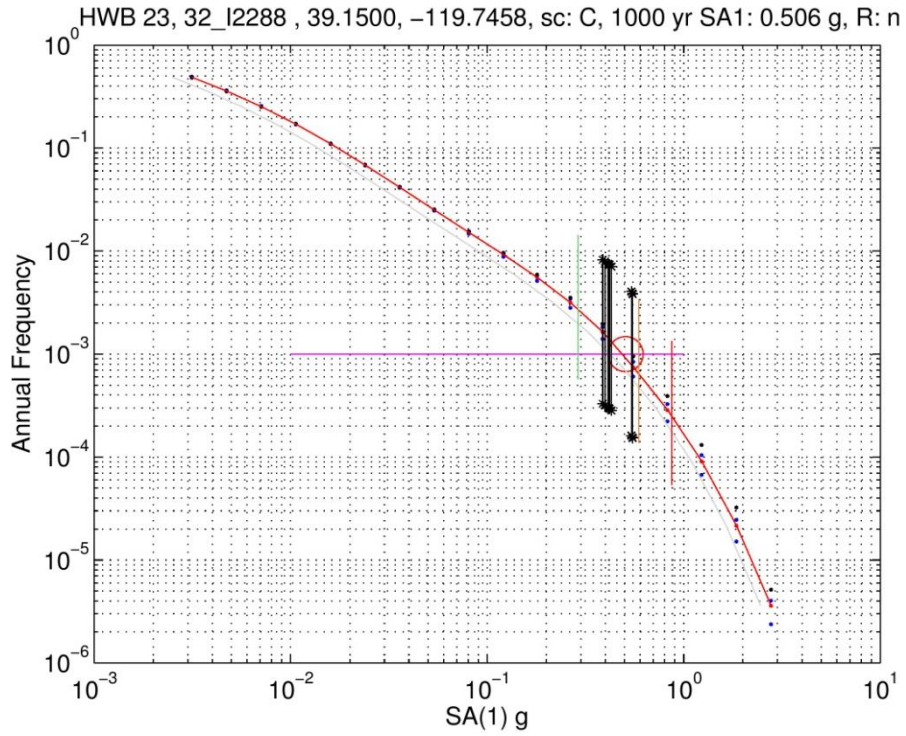


Figure B-5.45 HWB 23, 32_I2288 SA(1 Hz) hazard curve and capacity estimates.

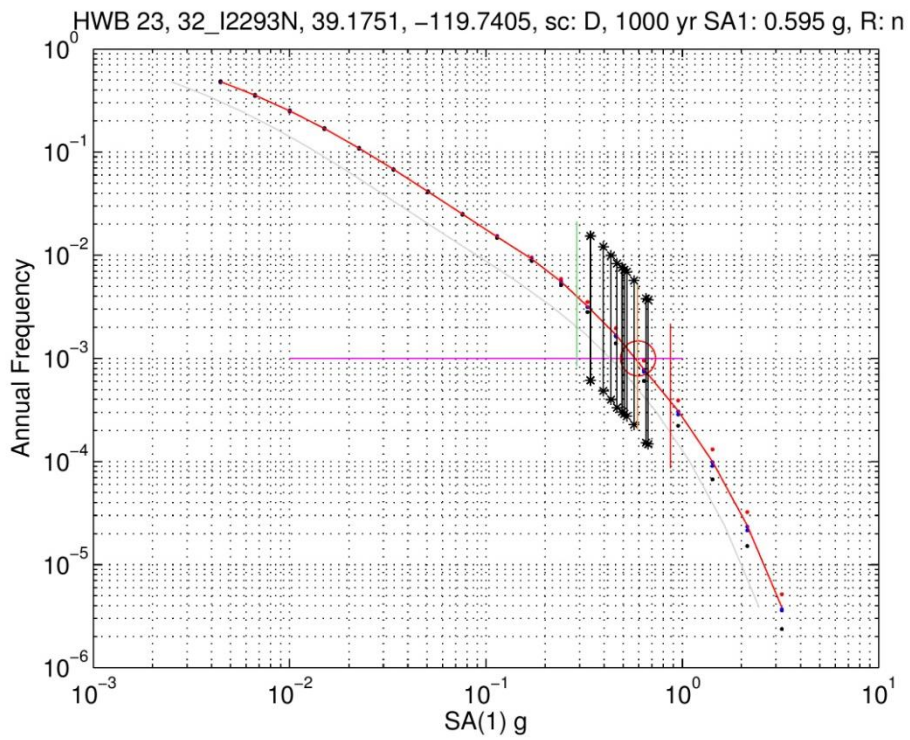


Figure B-5.46 HWB 23, 32_I2293N SA(1 Hz) hazard curve and capacity estimates.

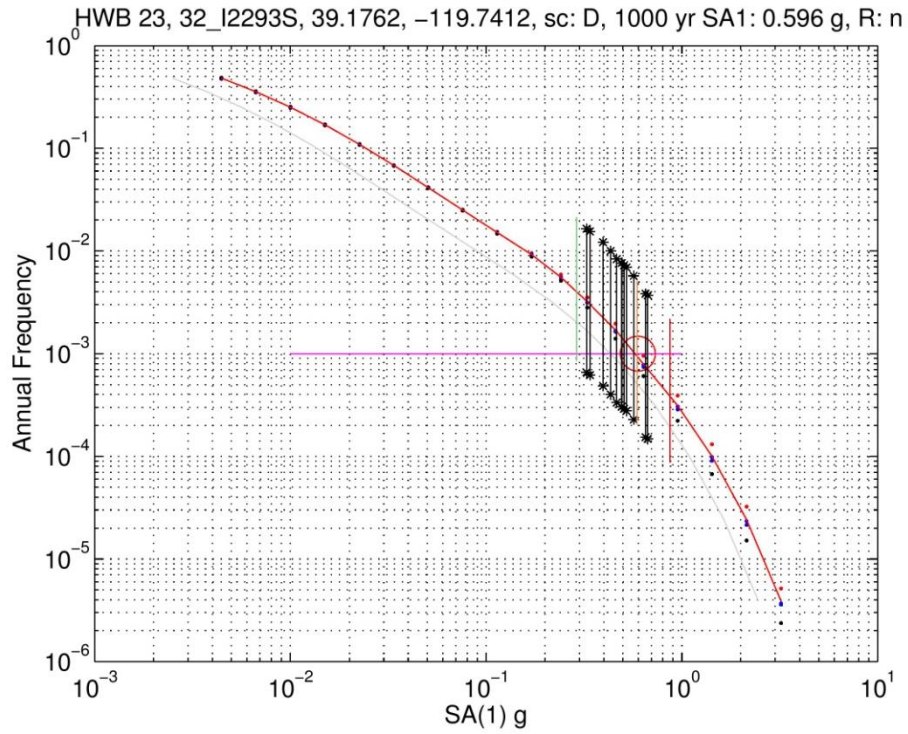


Figure B-5.47 HWB 23, 32_I2293S SA(1 Hz) hazard curve and capacity estimates.

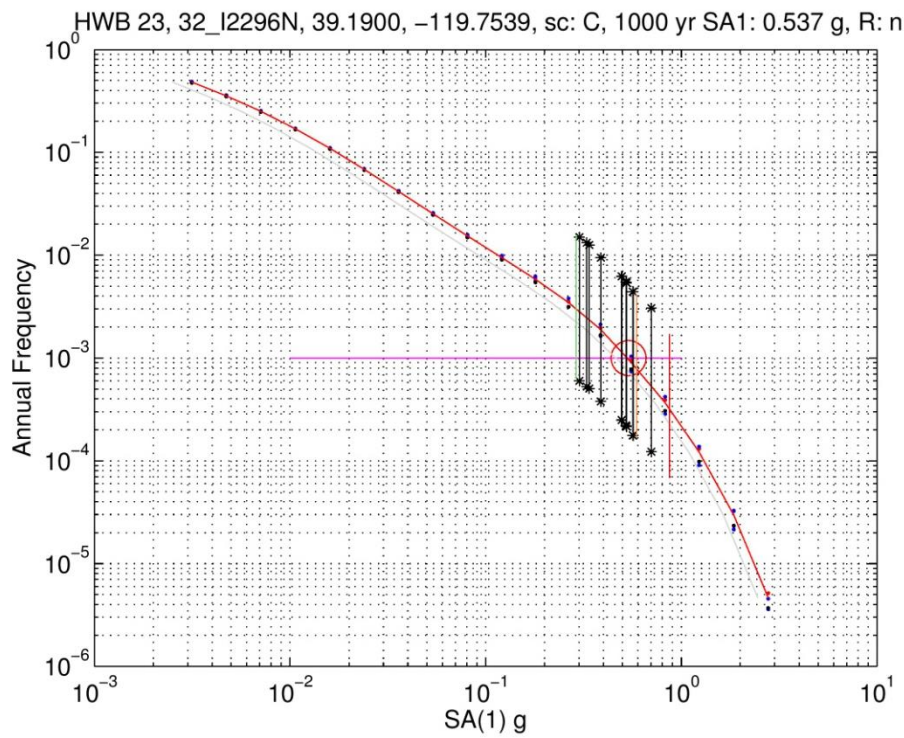


Figure B-5.48 HWB 23, 32_I2296N SA(1 Hz) hazard curve and capacity estimates.

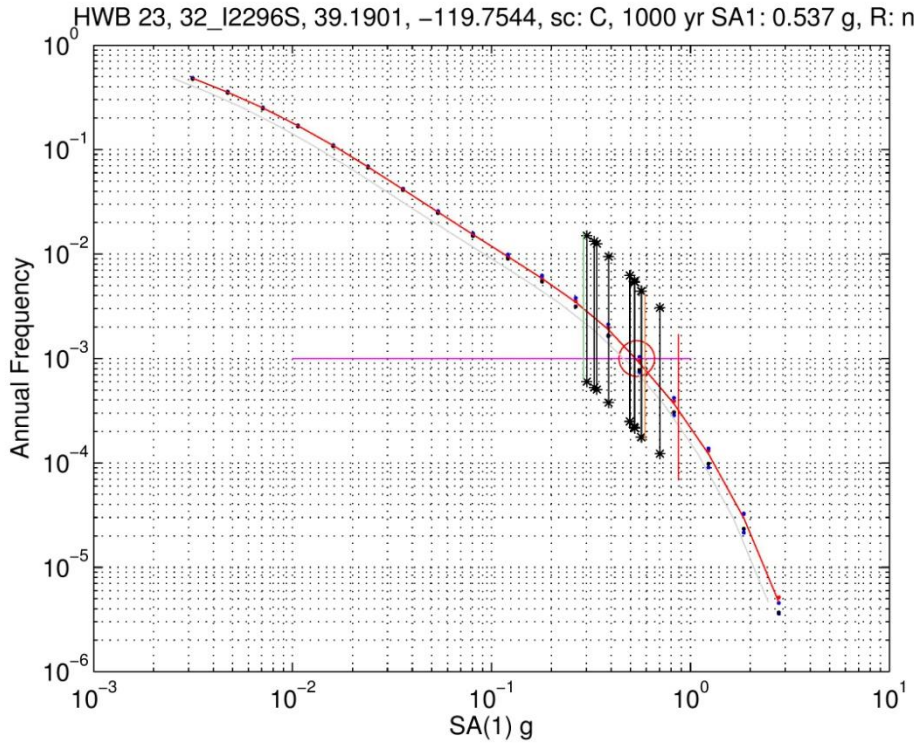


Figure B-5.49 HWB 23, 32_I2296S SA(1 Hz) hazard curve and capacity estimates.

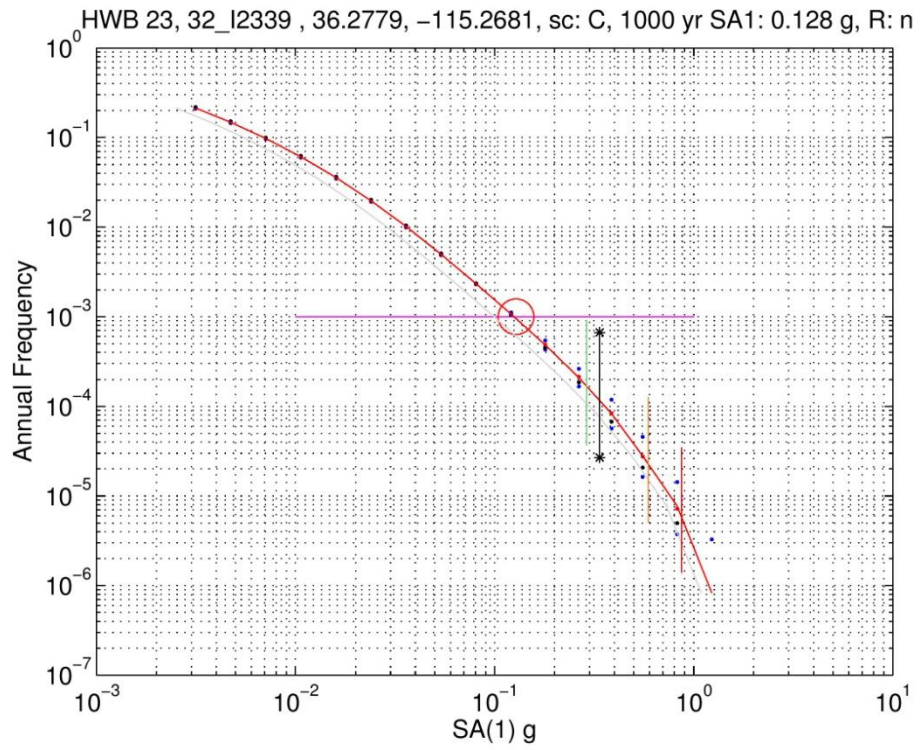


Figure B-5.50 HWB 23, 32_I2339 SA(1 Hz) hazard curve and capacity estimates.

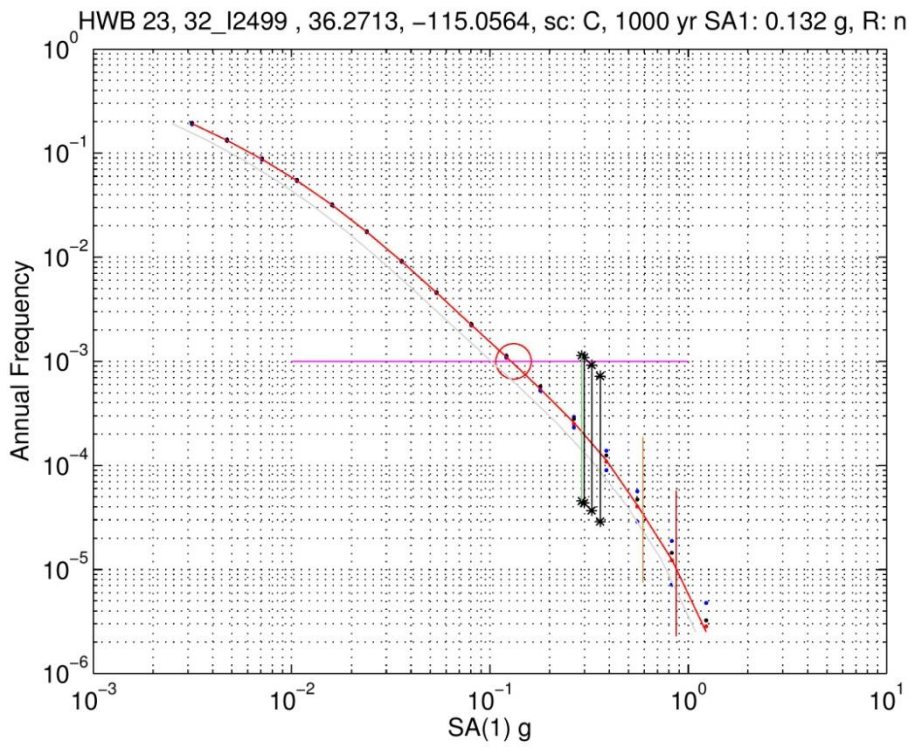


Figure B-5.51 HWB 23, 32_I2499 SA(1 Hz) hazard curve and capacity estimates.

APPENDIX C: Return Periods Corresponding to Different Damage States

This Appendix presents return periods corresponding to different damage states for all the bridges in Appendix A (Tables C.1 -C.5). They are sorted from lower to higher return periods for the extensive damage state (orange). A threshold of 1000 year return period is used to separate bridges with higher priority to be retrofitted which is consistent with the AASHTO where specifies a design return period corresponding to a seven percent probability of exceedance in 75 years and the acceptable damage is inelastic hinges in the columns. Bridges written in italic are those which are already retrofitted. The highlighted bridges are those with return periods corresponding to the extensive damage state less than or equal to 1000 years.

Table C.1 Bridges of type HWB10-205 (Return periods for different damage states)

Bridge ID	Moderate Damage State			Extensive Damage State			Complete Damage State		
	SA(1 sec)(%)	Annual Frequency	Return Period (Years)	SA(1 sec)(%)	Annual Frequency	Return Period (Years)	SA(1 sec)(%)	Annual Frequency	Return Period (Years)
32_I1172	18	7.48E-03	133.7	27	3.67E-03	272.4	36	2.08E-03	481.6
32_I1250	18	7.46E-03	134.0	27	3.66E-03	273.5	36	2.06E-03	484.9
32_H1003	18	7.34E-03	136.2	27	3.53E-03	283.2	36	1.94E-03	515.0
32_I1010	18	7.34E-03	136.3	27	3.53E-03	283.4	36	1.94E-03	515.4
32_H_866W	18	7.30E-03	137.0	27	3.50E-03	285.4	36	1.92E-03	519.8
32_H_866E	18	7.30E-03	137.0	27	3.50E-03	285.4	36	1.92E-03	519.9
32_I1007E	18	7.08E-03	141.3	27	3.37E-03	297.0	36	1.83E-03	546.4
32_I1007W	18	7.08E-03	141.3	27	3.37E-03	297.1	36	1.83E-03	546.7
32_H_767W	18	4.61E-03	217.0	27	2.27E-03	440.2	36	1.44E-03	694.0
32_H_990	18	4.40E-03	227.0	27	2.19E-03	456.1	36	1.39E-03	717.1
32_H_991	18	4.40E-03	227.4	27	2.19E-03	457.2	36	1.39E-03	719.2
32_H_993	18	4.37E-03	228.6	27	2.17E-03	461.1	36	1.38E-03	727.1
32_H_995	18	4.36E-03	229.4	27	2.16E-03	463.5	36	1.37E-03	732.1
32_I1149	18	4.22E-03	236.9	27	2.08E-03	480.7	36	1.31E-03	760.8
32_I1002	18	4.21E-03	237.4	27	2.08E-03	481.1	36	1.31E-03	760.5
32_I1086	18	4.21E-03	237.3	27	2.07E-03	482.3	36	1.31E-03	764.5
32_I1001	18	4.21E-03	237.3	27	2.07E-03	482.4	36	1.31E-03	764.7
32_I1087	18	4.21E-03	237.3	27	2.07E-03	482.4	36	1.31E-03	764.6
32_I1000	18	4.21E-03	237.3	27	2.07E-03	482.4	36	1.31E-03	764.8
32_I1088	18	4.21E-03	237.3	27	2.07E-03	482.4	36	1.31E-03	764.6
32_I1173	18	4.21E-03	237.7	27	2.07E-03	484.1	36	1.30E-03	768.4
32_H_997	18	4.24E-03	235.8	27	2.06E-03	484.7	36	1.29E-03	775.6
32_I1171	18	4.21E-03	237.4	27	2.05E-03	488.8	36	1.28E-03	782.9
32_I1089	18	4.20E-03	238.4	27	2.03E-03	493.1	36	1.26E-03	792.7
32_I_770	18	4.39E-03	227.6	27	1.96E-03	511.0	36	1.16E-03	862.1
32_I1093S	18	4.07E-03	245.7	27	1.91E-03	523.4	36	1.17E-03	855.9
32_I1093N	18	4.07E-03	245.8	27	1.91E-03	523.6	36	1.17E-03	856.3
<i>32_I1005W</i>	<i>26</i>	<i>3.04E-03</i>	<i>328.8</i>	<i>59</i>	<i>5.36E-04</i>	<i>1867.1</i>	<i>87</i>	<i>1.93E-04</i>	<i>5174.2</i>

Bridge ID	Moderate Damage State			Extensive Damage State			Complete Damage State		
	SA(1 sec)(%)	Annual Frequency	Return Period (Years)	SA(1 sec)(%)	Annual Frequency	Return Period (Years)	SA(1 sec)(%)	Annual Frequency	Return Period (Years)
32_B_954S	18	1.02E-03	977.8	27	4.62E-04	2164.5	36	2.55E-04	3926.9
32_B_954N	18	1.02E-03	977.9	27	4.62E-04	2165.1	36	2.55E-04	3928.6
32_G_953	18	1.01E-03	988.3	27	4.53E-04	2209.8	36	2.48E-04	4035.6
32_I1075S	18	1.07E-03	936.7	27	4.43E-04	2257.3	36	2.57E-04	3886.1
32_I1075N	18	1.07E-03	936.7	27	4.43E-04	2257.3	36	2.57E-04	3886.1
32_H_856	18	1.11E-03	898.2	27	3.94E-04	2540.7	36	1.81E-04	5516.1
32_I_908	18	6.39E-04	1566.1	27	3.71E-04	2696.6	36	2.57E-04	3895.8
32_I_992	26	1.97E-03	506.9	60	3.67E-04	2724.5	87	1.24E-04	8096.6
32_I_994	26	1.97E-03	508.3	60	3.65E-04	2740.2	87	1.23E-04	8159.1
32_B_839S	18	5.97E-04	1674.5	27	3.52E-04	2842.9	36	2.51E-04	3981.6
32_I1005E	26	1.88E-03	531.7	60	3.47E-04	2879.3	87	1.17E-04	8569.4
32_I_915	18	5.84E-04	1711.9	27	3.36E-04	2974.9	36	2.35E-04	4258.1
32_I_862	18	5.61E-04	1783.9	27	2.61E-04	3824.5	36	1.64E-04	6108.5
32_G_941	18	5.03E-04	1988.5	27	2.33E-04	4299.9	36	1.44E-04	6921.1
32_I_938	18	5.01E-04	1995.0	27	2.31E-04	4326.6	36	1.43E-04	6975.2
32_I_937	18	5.00E-04	1998.6	27	2.30E-04	4341.5	36	1.43E-04	7005.5
32_G_947	18	4.97E-04	2011.8	27	2.29E-04	4366.6	36	1.42E-04	7051.4
32_I_947R	18	4.97E-04	2012.1	27	2.29E-04	4367.4	36	1.42E-04	7053.0
32_I_947M	18	4.97E-04	2012.9	27	2.29E-04	4370.8	36	1.42E-04	7059.9
32_I_947L	18	4.95E-04	2020.1	27	2.27E-04	4398.7	36	1.41E-04	7116.0
32_H_935	18	4.92E-04	2034.5	27	2.23E-04	4490.4	36	1.37E-04	7311.5
32_I_754	18	5.43E-04	1842.2	27	2.17E-04	4614.1	36	1.23E-04	8151.7
32_I_934	18	4.73E-04	2113.5	27	2.08E-04	4805.5	36	1.26E-04	7964.7
32_H_933	18	4.70E-04	2126.0	27	2.06E-04	4864.2	36	1.24E-04	8092.4
32_H_970	18	4.80E-04	2082.9	27	2.01E-04	4963.2	36	1.17E-04	8581.8
32_I_969S	18	4.80E-04	2084.2	27	2.01E-04	4977.2	36	1.16E-04	8617.3
32_I_969N	18	4.80E-04	2084.6	27	2.01E-04	4980.0	36	1.16E-04	8624.0
32_G_925E	18	5.11E-04	1956.6	27	1.99E-04	5013.1	36	9.44E-05	10589.5
32_G_925W	18	5.11E-04	1956.7	27	1.99E-04	5013.4	36	9.44E-05	10590.2
32_I_889	18	4.52E-04	2210.2	27	1.87E-04	5352.9	36	1.08E-04	9221.3
32_G1153	18	4.59E-04	2177.0	27	1.83E-04	5477.4	36	1.05E-04	9514.7
32_I_892	18	3.86E-04	2588.8	27	1.49E-04	6718.3	36	8.36E-05	11960.8
32_B1544S	18	3.79E-04	2640.5	27	1.43E-04	6985.8	36	8.02E-05	12466.3
32_B1544N	18	3.79E-04	2641.0	27	1.43E-04	6988.1	36	8.02E-05	12471.3
32_H_918E	18	3.61E-04	2770.9	27	1.40E-04	7133.6	36	7.90E-05	12666.2
32_H_918W	18	3.61E-04	2771.6	27	1.40E-04	7136.3	36	7.89E-05	12672.0
32_I1159E	18	2.72E-04	3679.1	27	1.19E-04	8433.7	36	7.24E-05	13811.1
32_I1159W	18	2.71E-04	3684.1	27	1.18E-04	8452.3	36	7.22E-05	13847.9
32_I_924E	18	2.57E-04	3891.2	27	1.09E-04	9201.3	36	6.53E-05	15307.7
32_I_924W	18	2.57E-04	3892.1	27	1.09E-04	9204.3	36	6.53E-05	15313.3

Bridge ID	Moderate Damage State			Extensive Damage State			Complete Damage State		
	SA(1 sec)(%)	Annual Frequency	Return Period (Years)	SA(1 sec)(%)	Annual Frequency	Return Period (Years)	SA(1 sec)(%)	Annual Frequency	Return Period (Years)
32_G_961N	26	2.29E-04	4367.9	60	3.81E-05	26273.5	87	1.17E-05	85718.4
32_G_961S	26	2.29E-04	4368.0	60	3.80E-05	26288.9	87	1.17E-05	85806.7
32_H_946	26	2.07E-04	4834.1	60	3.47E-05	28817.1	87	1.06E-05	93944.3
32_H_936	26	2.06E-04	4860.1	60	3.43E-05	29174.7	87	1.05E-05	95413.5
32_H1042	26	1.86E-04	5370.9	60	2.78E-05	36020.5	87	7.86E-06	127302.4
32_I_796	26	1.25E-04	8029.7	60	1.29E-05	77429.9	87	2.77E-06	360596.9
32_H_788	26	1.06E-04	9429.2	60	9.97E-06	100265.7	87	1.50E-06	668413.5

Table C.2 Bridges of type HWB11-205 (Return periods for different damage states)

BridgeID	Moderate Damage State			Extensive Damage State			Complete Damage State		
	SA(1 sec)(%)	Annual Frequency	Return Period (Years)	SA(1 sec)(%)	Annual Frequency	Return Period (Years)	SA(1 sec)(%)	Annual Frequency	Return Period (Years)
32_II126	26	2.45E-04	4073.9	60	4.77E-05	20971.0	87	1.60E-05	62404.1
32_I_947W	26	2.04E-04	4890.0	60	3.40E-05	29453.3	87	1.04E-05	96598.8
32_I_947E	26	2.04E-04	4897.4	60	3.38E-05	29542.7	87	1.03E-05	96992.3
32_I_947	26	2.02E-04	4946.2	60	3.32E-05	30096.0	87	1.01E-05	99330.5
32_II452	26	2.78E-04	3592.8	60	3.31E-05	30248.8	87	1.01E-05	99163.1
32_H1815	26	1.26E-04	7921.1	60	1.32E-05	75729.5	87	3.12E-06	320837.8
32_H1816	26	1.26E-04	7948.1	60	1.32E-05	76038.1	87	3.11E-06	321695.5
32_H1817	26	1.26E-04	7965.7	60	1.31E-05	76300.3	87	3.10E-06	322811.8

Table C.3 Bridges of type HWB15-402 (Return periods for different damage states)

BridgeID	Moderate Damage State			Extensive Damage State			Complete Damage State		
	SA(1 sec)(%)	Annual Frequency	Return Period (Years)	SA(1 sec)(%)	Annual Frequency	Return Period (Years)	SA(1 sec)(%)	Annual Frequency	Return Period (Years)
32_II290	32	2.18E-03	458.2	41	1.28E-03	782.4	51	7.15E-04	1398.4
32_B_303	32	1.72E-03	581.2	41	9.70E-04	1031.1	51	5.92E-04	1688.3
32_B1327W	32	1.70E-03	588.7	41	9.52E-04	1050.7	51	5.79E-04	1728.3
32_II291	32	1.41E-03	708.3	41	7.48E-04	1337.0	51	4.43E-04	2259.0
32_B_433N	32	2.88E-04	3467.1	41	1.90E-04	5253.9	51	1.29E-04	7722.4
32_G_913W	32	2.97E-04	3366.0	41	1.90E-04	5259.5	51	1.26E-04	7954.2
32_G_913E	32	2.97E-04	3365.8	41	1.90E-04	5259.8	51	1.26E-04	7955.5
32_H1443	32	2.36E-04	4245.9	41	1.33E-04	7531.7	51	7.09E-05	14107.8
32_II255	32	2.37E-04	4217.5	41	1.28E-04	7793.4	51	6.54E-05	15295.6
32_G_387	32	2.01E-04	4974.2	41	1.10E-04	9121.6	51	6.58E-05	15187.4
32_G_863W	32	2.01E-04	4975.8	41	1.10E-04	9122.4	51	6.58E-05	15186.2
32_G_863E	32	2.01E-04	4975.6	41	1.10E-04	9122.5	51	6.58E-05	15187.3
32_G1296	32	1.68E-04	5953.0	41	8.93E-05	11192.9	51	5.19E-05	19262.4

BridgeID	Moderate Damage State			Extensive Damage State			Complete Damage State		
	SA(1 sec)(%)	Annual Frequency	Return Period (Years)	SA(1 sec)(%)	Annual Frequency	Return Period (Years)	SA(1 sec)(%)	Annual Frequency	Return Period (Years)
32_G_919E	32	1.67E-04	5984.9	41	8.87E-05	11274.6	51	5.15E-05	19428.2
32_G_919W	32	1.67E-04	5989.5	41	8.86E-05	11286.4	51	5.14E-05	19452.3
32_H1234	90	1.13E-04	8875.2	110	6.58E-05	15195.7	150	2.26E-05	44219.6
32_G1233R	90	1.11E-04	9010.1	110	6.47E-05	15452.3	150	2.21E-05	45162.2
32_G1233	90	1.11E-04	9023.0	110	6.46E-05	15477.3	150	2.21E-05	45256.2
32_G1233L	90	1.11E-04	9037.9	110	6.45E-05	15506.0	150	2.20E-05	45364.0
32_G_872E	32	1.32E-04	7559.3	41	6.21E-05	16104.3	51	3.45E-05	29019.5
32_G_872W	32	1.32E-04	7561.6	41	6.21E-05	16111.5	51	3.44E-05	29035.4
32_G_872R	32	1.32E-04	7566.1	41	6.20E-05	16125.7	51	3.44E-05	29067.2
32_B1489	32	1.25E-04	7991.2	41	5.88E-05	17001.7	51	3.24E-05	30883.8
32_I_868	90	1.08E-05	92508.6	110	5.35E-06	186889.7	150	NA	NA

Table C.4 Bridges of type HWB22-605 (Return periods for different damage states)

BridgeID	Moderate Damage State			Extensive Damage State			Complete Damage State		
	SA(1 sec)(%)	Annual Frequency	Return Period (Years)	SA(1 sec)(%)	Annual Frequency	Return Period (Years)	SA(1 sec)(%)	Annual Frequency	Return Period (Years)
32_I1261	18	9.27E-03	107.8	27	5.25E-03	190.5	36	3.35E-03	298.5
32_I_878	18	1.14E-03	878.9	27	4.45E-04	2246.7	36	2.05E-04	4886.4
32_I_882	18	1.12E-03	892.2	27	4.43E-04	2257.3	36	2.08E-04	4797.1
32_I_879	18	1.12E-03	888.9	27	4.43E-04	2259.4	36	2.07E-04	4838.6
32_H_869E	18	9.75E-04	1025.5	27	3.70E-04	2701.0	36	1.68E-04	5940.3
32_H_869W	18	9.75E-04	1025.5	27	3.70E-04	2701.0	36	1.68E-04	5940.3
32_B1526	18	7.78E-04	1286.1	27	3.03E-04	3304.2	36	1.38E-04	7264.8
32_G1414	18	7.76E-04	1288.7	27	3.01E-04	3323.8	36	1.37E-04	7322.8
32_I_871E	18	4.58E-04	2184.2	27	1.82E-04	5507.0	36	1.04E-04	9579.5
32_I_871W	18	4.58E-04	2184.2	27	1.82E-04	5507.0	36	1.04E-04	9579.5
32_I_873	18	4.54E-04	2204.3	27	1.79E-04	5591.4	36	1.02E-04	9769.4
32_I_896	18	3.73E-04	2682.9	27	1.41E-04	7085.0	36	7.86E-05	12726.9
32_H1205	18	3.71E-04	2697.4	27	1.40E-04	7137.2	36	7.79E-05	12832.1
32_I1977	18	3.62E-04	2762.6	27	1.32E-04	7575.6	36	7.25E-05	13788.2

Table C.5 Bridges of type HWB23-605 (Return periods for different damage states)

BridgeID	Moderate Damage State			Extensive Damage State			Complete Damage State		
	SA(1 sec)(%)	Annual Frequency	Return Period (Years)	SA(1 sec)(%)	Annual Frequency	Return Period (Years)	SA(1 sec)(%)	Annual Frequency	Return Period (Years)
32_I2293S	26	4.24E-03	235.9	60	1.03E-03	972.6	87	4.35E-04	2297.3
32_I2293N	26	4.23E-03	236.3	60	1.02E-03	976.9	87	4.33E-04	2310.3
32_H2290	26	4.24E-03	236.1	60	1.00E-03	998.2	87	4.18E-04	2390.9
32_I2296S	26	3.14E-03	318.9	60	8.35E-04	1197.3	87	3.41E-04	2932.5
32_I2296N	26	3.14E-03	319.0	60	8.35E-04	1197.7	87	3.41E-04	2933.5
32_I2288	26	2.85E-03	351.0	60	6.85E-04	1459.5	87	2.67E-04	3746.9
32_I1952	26	2.35E-03	424.9	60	5.72E-04	1748.3	87	2.25E-04	4452.6
32_I1949	26	2.40E-03	417.3	60	5.70E-04	1754.2	87	2.20E-04	4551.7
32_I1950	26	2.35E-03	425.3	60	5.56E-04	1797.4	87	2.14E-04	4669.4
32_B1533	26	2.01E-03	496.4	60	3.90E-04	2566.9	87	1.34E-04	7436.5
32_G1748S	26	1.73E-03	576.4	60	2.80E-04	3565.3	87	8.70E-05	11492.2
32_I1091S	26	1.76E-03	567.5	60	2.80E-04	3565.4	87	8.43E-05	11865.2
32_I1091N	26	1.76E-03	567.5	60	2.80E-04	3565.8	87	8.43E-05	11866.2
32_G1748N	26	1.73E-03	576.6	60	2.80E-04	3567.6	87	8.69E-05	11501.4
32_I_950	26	3.79E-04	2641.8	60	6.57E-05	15213.8	87	2.33E-05	42897.3
32_B_455	26	3.90E-04	2563.1	60	4.62E-05	21663.4	87	1.37E-05	73174.3
32_B1014	26	3.71E-04	2697.8	60	4.49E-05	22263.0	87	1.45E-05	68944.6
32_H1446	26	3.07E-04	3258.9	60	4.12E-05	24278.9	87	1.31E-05	76462.0
32_I1219	26	2.28E-04	4395.6	60	4.11E-05	24346.8	87	1.33E-05	75122.4
32_G_961R	26	2.29E-04	4366.1	60	3.81E-05	26269.8	87	1.17E-05	85734.6
32_I2499	26	2.28E-04	4392.9	60	3.75E-05	26676.0	87	1.14E-05	87571.0
32_I2139R	26	2.14E-04	4664.9	60	3.72E-05	26864.9	87	1.17E-05	85649.4
32_G_941L	26	2.11E-04	4748.9	60	3.59E-05	27841.7	87	1.11E-05	89740.8
32_H2711	26	2.10E-04	4772.1	60	3.56E-05	28087.3	87	1.10E-05	90665.1
32_I2141R	26	2.09E-04	4777.0	60	3.55E-05	28170.6	87	1.10E-05	91119.5
32_H2710	26	2.09E-04	4786.5	60	3.54E-05	28258.3	87	1.09E-05	91383.5
32_I2140	26	2.09E-04	4792.0	60	3.53E-05	28343.9	87	1.09E-05	91833.3
32_I_944N	26	2.08E-04	4796.3	60	3.53E-05	28361.2	87	1.09E-05	91761.6
32_I_944S	26	2.08E-04	4797.9	60	3.52E-05	28380.5	87	1.09E-05	91843.4
32_I2139	26	2.08E-04	4815.0	60	3.49E-05	28621.8	87	1.07E-05	93025.9
32_H_936R	26	2.06E-04	4860.1	60	3.43E-05	29174.7	87	1.05E-05	95413.5
32_H1214	26	2.08E-04	4815.0	60	3.33E-05	30039.4	87	9.89E-06	101104.0
32_H1212	26	1.94E-04	5155.9	60	2.99E-05	33489.6	87	8.75E-06	114309.5
32_H2486	26	1.89E-04	5292.2	60	2.71E-05	36910.0	87	7.60E-06	131642.7
32_I2339	26	1.83E-04	5469.3	60	2.53E-05	39487.8	87	6.97E-06	143567.0
32_H2350	26	1.65E-04	6074.6	60	2.19E-05	45648.8	87	5.78E-06	172881.5
32_H2349	26	1.65E-04	6077.2	60	2.19E-05	45713.2	87	5.77E-06	173254.4

BridgeID	Moderate Damage State			Extensive Damage State			Complete Damage State		
	SA(1 sec)(%)	Annual Frequency	Return Period (Years)	SA(1 sec)(%)	Annual Frequency	Return Period (Years)	SA(1 sec)(%)	Annual Frequency	Return Period (Years)
32_H2348	26	1.64E-04	6080.2	60	2.18E-05	45782.1	87	5.76E-06	173646.7
32_H2013	26	1.53E-04	6516.8	60	1.90E-05	52527.4	87	4.83E-06	206832.5
32_H1458	26	1.47E-04	6800.8	60	1.89E-05	52894.4	87	5.14E-06	194385.0
32_H2013W	26	1.53E-04	6544.1	60	1.89E-05	52919.3	87	4.79E-06	208657.2
32_G2012	26	1.51E-04	6609.8	60	1.85E-05	54089.7	87	4.66E-06	214760.5
32_G2014R	26	1.49E-04	6703.7	60	1.80E-05	55538.3	87	4.51E-06	221769.3
32_G2014	26	1.49E-04	6724.4	60	1.79E-05	55818.5	87	4.48E-06	223012.7
32_I_806N	26	1.48E-04	6737.4	60	1.78E-05	56048.2	87	4.46E-06	224203.2
32_I_806S	26	1.48E-04	6737.2	60	1.78E-05	56051.9	87	4.46E-06	224241.9
32_G_805R	26	1.46E-04	6840.4	60	1.74E-05	57553.6	87	4.33E-06	231200.0
32_I1456	26	1.31E-04	7607.1	60	1.56E-05	64038.9	87	4.20E-06	237919.1
32_H1804	26	1.28E-04	7811.0	60	1.48E-05	67344.6	87	3.98E-06	251457.8
32_H1460	26	1.23E-04	8122.6	60	1.34E-05	74570.1	87	3.45E-06	289578.1
32_H2331	26	1.00E-04	9984.4	60	8.92E-06	112084.8	87	7.06E-07	1415983.3

APPENDIX D: Damage Assessment and Repair Manual

D.1 Introduction

This manual was compiled from many sources consisting mainly of journal articles and research papers studying the response and repair of various bridge components that had sustained damage from seismic loading. It describes different damage states for different bridge components. Prior studies were compiled with their methods combined and modified to form a unified repair strategy supported by multiple corroborating sources.

The first bridge component studied was columns. This is, by far, the most widely researched of the components discussed, and as such there is a great wealth of information regarding damage and many widely varied repair schemes. This is both an advantage and a hindrance, because while there is much more possibly relevant information for analysis and repair, there is also a much greater propensity for disagreement and conflicting information. An effort has been made to provide the most widely accepted techniques for repair. It is worth noting that many other researched options are available. The second component studied was shear keys, which are less widely studied, especially with regard to repair techniques. The final component included in this report is abutments. Abutments have a similarly small pool of information regarding repair techniques, much less than is available for columns.

For each component, there is a literature review on the previous research performed, followed by a verbal and pictorial description of each damage state to be used for classification of the damaged structure.

D.2 Damage States of Columns

This section covers the identification of the relative damage states of a seismically damaged column. All damage states in this section correspond directly to the ShakeCast definitions of the damage states.

Damage State 1: Damage state 1 is characterized by minor or hairline cracking, with no measurable width. There is no loss in structural strength or stability at this point. This corresponds to DS 2 in ShakeCast, but has lowest priority for inspection or repair.

Damage State 2: Damage state 2 is characterized by clearly visible cracking ($<1\text{mm}$), minor and corner concrete spalling on the structure. This damage state is not characterized by a loss of strength. This corresponds to ShakeCast DS 2 (slight/minor damage, **FIGURE D.1**).



Figure D.1 damage state 2, spalling of corner cover concrete (Kaminosono et al, 2002)

Damage State 3: Damage State 3 is characterized by wide cracks, extensive crush of cover concrete and exposure of reinforcement bars (**Figure D.2 and D.3**). At this point, some of the structural strength provided by the concrete is lost but not enough to warrant full repair mechanism implementation. This corresponds to DS 3 (moderate) in ShakeCast.

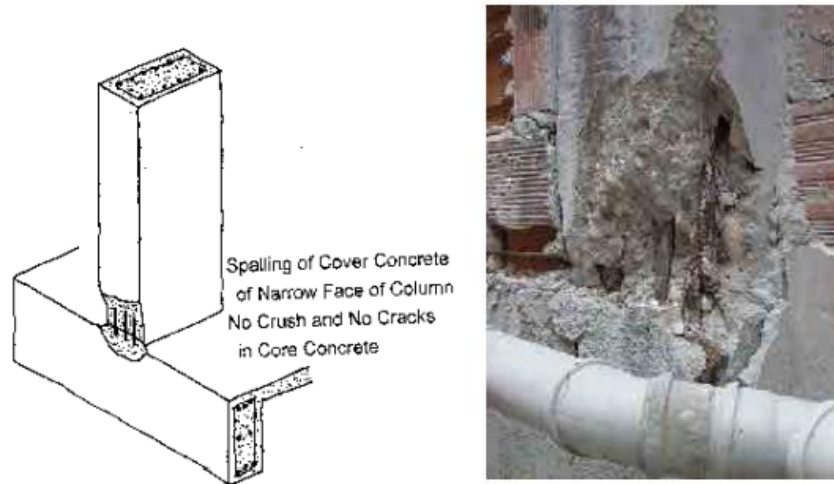


Figure D.2 Damage state 3, spalling and reinforcement exposure- no cracks in core concrete (Kaminosono et al, 2002)



Figure D.3 Damage state 3, wider shear cracking and local crush at top corner (Kaminosono et al, 2002)

Damage State 4: Damage State 4 is characterized by wide cracks (>2 mm), extensive spalling, very minor or no reinforcement buckling, and no core concrete crushing (**Figure D.4** through **D.6**). At this point, a significant amount of the strength provided by the concrete is gone, and repair to restore it is warranted. This corresponds to ShakeCast Damage state 3/4 (moderate/extensive).

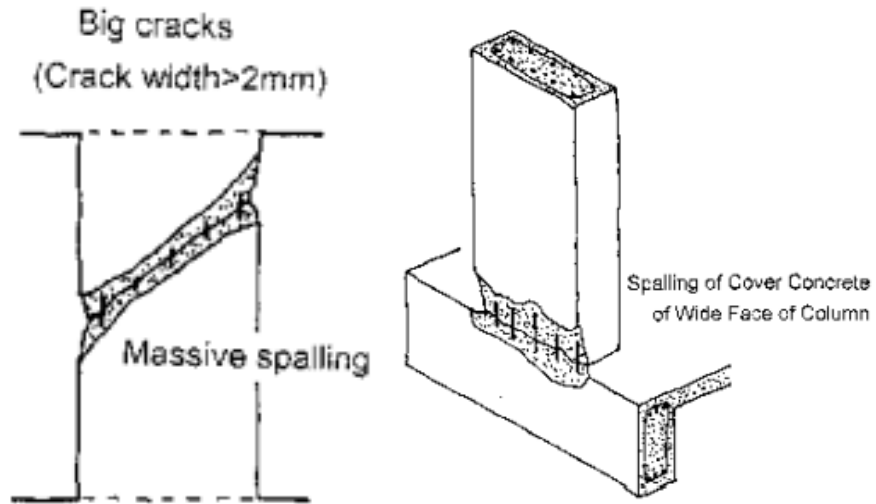


Figure D.4 Damage state 4, extensive cracking and spalling, some minor reinforcement buckling (Kaminosono et al, 2002)

Note that this is similar to **Figure D.12**, which was classified as DS 3; when the damage is on the wider column face it is treated as more severe, hence the elevated damage state.



Figure D.5 Damage state 4, extensive spalling and reinforcement exposure, but no buckling. (Kaminosono et al, 2002)



Figure D.6 Damage state 4, massive spalling and exposure of reinforcement and minor buckling (Kaminosono et al, 2002)

Damage State 5: Damage State 5 is characterized by reinforcement bars buckling or completely fracturing, core concrete crush, and total collapse or failure. This is equivalent to DS 5 in ShakeCast, or complete failure (**Figure D.7**).

Visible settlement of floor

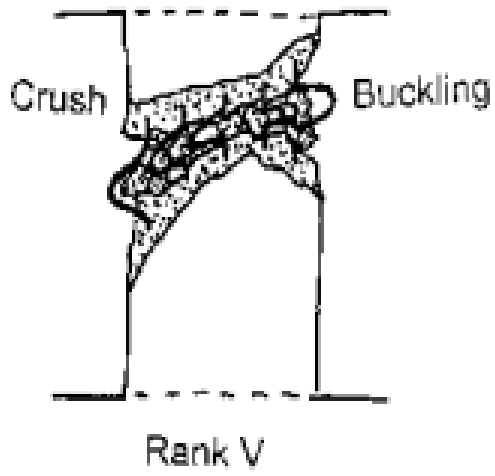


Figure D.7 Damage state 5, fracture and buckling of reinforcement and collapse (Kaminosono et al, 2002)

Damage states 1 and 2 are minor damages that have no measurable effect on structural integrity. Damage state 3, while requiring repair, will likely not require full closure of the bridge. Damage state 4 appears as the first state where closure may be warranted- this will vary based on the number of damaged elements and their importance in the structural integrity of the bridge. Damage states 5 and 6 represent significant damage and failure and, in most situations, will likely warrant bridge closure upon being observed.

D.3 Shear Keys Damage States

This section covers the research previously conducted on the seismic damage and repair of shear keys. It reviews the findings of Bozorgzadeh et. al (2004). with regard to the seismic response of shear keys in experimental settings. A total of ten test units, constructed and tested in groups of two, were studied. Groups 1, 2 and 4, each with A and B units, were constructed with variations of existing CalTrans specification, and tested. Some of them reached the CalTrans required capacity and some did not, based on construction differences. Regardless of ultimate capacity, though, all of these specimens failed at an angle along the wall, as shown in **Figure D.8**. This is undesirable because it damages the wall rather than the sacrificial shear key and is more difficult to predict and repair.



Figure D.8 Angled stem wall failure of specimen (Bozorgzadeh et. al. 2004)

Group 3 specimens were constructed with prestressing of the reinforcement structure. This precluded the possibility of diagonal shear failure into the stem wall, and produced a desirable sliding shear failure. However, units 3A and 3B both exceeded the maximum capacity defined by CalTrans specification. The final group of specimens, 5A and 5B, were constructed under specifications previously submitted to CalTrans. 5A was built with foam at the interface of the shear key and the wall; a rough construction joint surrounded the hole left for reinforcement and a smooth joint covered the remainder of the interface. 5B was constructed with a smooth construction joint between the shear key and the wall and a bond breaker at the interface to create a weak plane of failure. Specimen 5A had an ultimate lateral load of 165 kips, and 5B failed at 75.5 kips, both of which exceeded the CalTrans expected capacity by an acceptable amount. In both cases, no damage was detected in the stem walls. **Figure D.9** shows the failure patterns of the specimens.



Figure D.9 Failure of specimens 5 A and B (Bozorgzadeh et. al, 2004)

This experiment shows that the construction methods used for the specimens in Group 5 may be more useful in the practice of designing sacrificial shear keys than the existing CalTrans specification. The predictable smooth shear failure evident in the experiment is less destructive to the overall construction and allows for easier repair or replacement after failure. Additionally, the underestimation of shear key capacity would not cause damage to the stem wall with this method.

Damage State 2

The first, Damage State 2 (DS2), consists of minor cracking and spalling. This is comparable to DS2 (slight/minor damage) in the ShakeCast terminology. An example of DS2 is shown in **Figure D.10**.

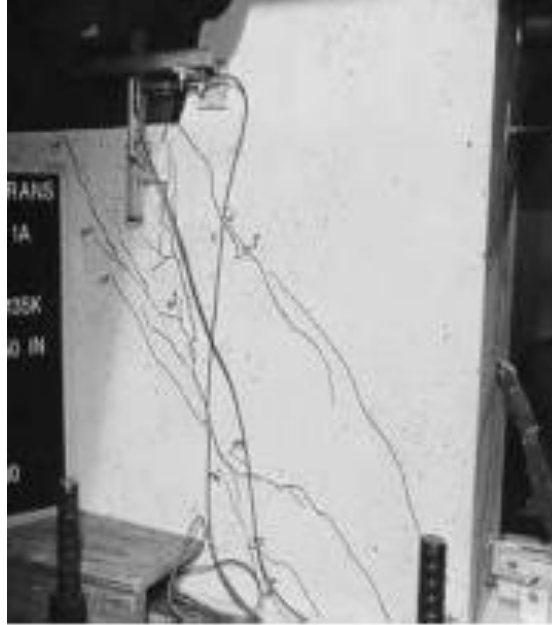


Figure D.10 Damage State 2 (Bozorgzadeh et al, 2004)

Damage State 5

This damage state in the shear key leads to imminent failure. It corresponds to DS3 (moderate damage) in the ShakeCast implementation. An example of DS5 is shown in **Figure D.11**.



Figure B.11 Damage State 5 (Saini et al, 2013)

Damage State 6

The final damage state with regard to shear keys is DS6, defined as total failure of the shear key, including reinforcement fracture and concrete failure. This corresponds to DS5 (Complete Failure) in ShakeCast terminology. An example of DS6 is shown in **Figure D.12**.



Figure D.12 Damage State 6 (Saini et al, 2013)

Damage Implications

For shear keys, the requirement for road closure is murky. While Damage state 2 is minor and will likely not require bridge closure, Damage state 5 is tenuous. Damage state 5 means imminent failure, but the road could possibly still be serviceable, at least to emergency and repair vehicles, depending on the extent of the damage to the other bridge components. In Damage state 6, the bridge will very likely require closure until repair is implemented.

D.4 Abutments Damage States

There is no notable prior research on the repair of seismically damaged abutments. This section is based on the research performed by Saini and his determined repair methods. Of the six prescribed damage states, four are relevant- DS 2, DS 3, DS 4, and DS 6. In the following report, these damage states will be described and the appropriate repair mechanisms specified.

Damage State 2

Due to the massive nature of the abutment, minor cracks are generally disregarded as structurally insignificant. Damage state 2 consists of minor cracking and spalling of cover concrete. No reduction in structural or shear strength is present at this state. An example is shown in **Figure D.13**. Damage State 2 corresponds to DS 2 (slight/minor damage) in ShakeCast terminology.



Figure D.13 Abutment Damage State 2 (Saini et al, 2013)

Damage State 3

Damage state 3 is characterized by extensive cover concrete spalling and initial loss of shear strength. An example is shown in **Figure D.14**. This corresponds to DS 3 in ShakeCast terminology, qualifying as moderate damage.



Figure D.14 Abutment Damage State 3 (Saini et al, 2013)

Damage State 4

Damage State 4 consists of further concrete spalling with the exposure of reinforcing steel. An example is shown in **Figure D.15**. At this damage state the abutment has lost approximately 50% of its shear strength and is cracking at a 45 degree angle. The repair method is designed to restore this lost 50% so the abutment will remain at full strength. This corresponds to DS 4 in ShakeCast terminology.



Figure D.15 Abutment Damage State 4 (Saini et al, 2013)

Damage State 6

Damage state 6 is characterized by fractured reinforcing bars and total abutment failure. An example of DS 6 is shown in **Figure D.16**. This corresponds to DS 5 in ShakeCast terminology, representing total failure and imminent collapse.



Figure D.16 Abutment Damage State 6 (Saini et al, 2013)

Damage Implications

For bridge abutments, the necessity of closure is especially murky. Damage state 2 requires only superficial repair, and will not require closure. Damage states 3 and 4 have similar implications, which depending on the situation may require that the road be closed. Damage state 6 indicates total failure, at which point the road should be closed at least to civilian traffic- the bridge may still be serviceable to emergency and repair vehicles.

D.5 Repair Literature Review

Columns repairs include epoxy injection into cracks, patching of spalling, and CFRP/GFRP/RC/steel jackets. Priestley, et. al. (1992) researched a column that failed under cyclic loading testing and was observed to have extensive open diagonal cracking and concrete spalling. In order to repair it, all the loose concrete was removed, voids were patched with cement and sand mortar. Then the column was wrapped in full-height with GFRP jacketing, after which epoxy was injected into cracks through the ports in the jacket. This resulted in a complete regain of initial column stiffness.

Saadatmanesh et.al. (1997) researched the repair of columns using FRP wrap. The test procedure utilized both circular and rectangular columns. The columns failed in testing to various degrees, shown in **Figure D.17**. The failure ranged from spalling and cracking to buckling and separation of the reinforcing bars. To repair these columns, they were returned to their original position at zero displacement and then loose concrete was removed and gaps filled with a patch mix. The columns were then wrapped with FRP straps and the gaps filled with pressurized epoxy. The stages of this repair are shown in **Figure D.18**. This repair process was found to restore the columns to near original strength and stiffness and increased their displacement ductility significantly.



Figure D.17 Failure of columns (Saadatmanesh et al, 1997)



Figure D.18 Repair process for columns (Saadatmanesh et al, 1997)

Li and Sung (2003) tested series of columns and enacted repair schemes based on the failure incurred. The columns failed in shear as shown in **Figure D.19**. The column was repaired by (1) removing spalling concrete and cleaning the surface, (2) inserting inlet tube at the top of area to be repaired, and preparing an outlet hole at the bottom, (3) injecting non-shrinkage mortar, and (4) high pressure epoxy injection (**Figure D.20**).



Figure D.19 Shear damaged bridge Column (Li et al, 2003)

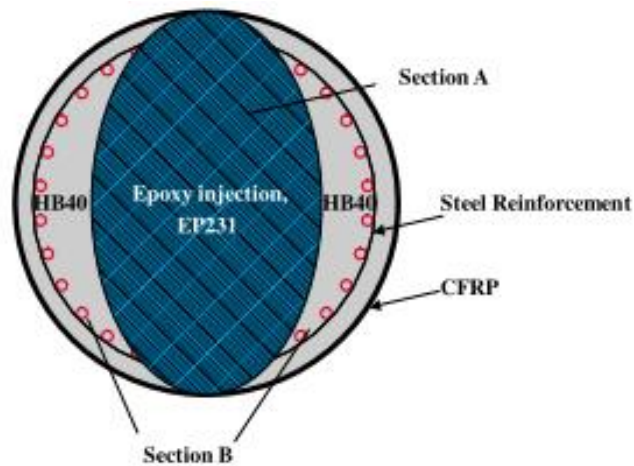


Figure D.20: Repair of damaged column (Li at al, 2003)

After the repair, the column was wrapped in CFRP to repair its shear capacity. When this repaired column was tested, the mode of failure changed from shear to flexure, indicating the success of this repair method.

Saiidi et al (2004) researched the effectiveness of composites in column repair. They repaired two columns which had already failed after being fitted with steel jackets. To repair them, they removed the steel jackets and the spalled concrete and straightened damaged bars. Broken bars were not replaced, and then new concrete was poured. Remaining cracks were injected with epoxy and the column was then wrapped in CFRP and GFRP fabrics to provide additional flexural strength and compensate for the broken bars. This repair procedure restored the columns' stiffness, strength, and displacement ductility to a "moderate level".

Lehman et. al. (2000) tested a series of four columns and categorized the damage as moderate or severe. The repair schemes varied based on the type and severity of the damage. For

the severely damaged specimens, the damaged bars were replaced by cutting and then mechanically splicing replacements. When there were too many bars to do this economically, the traditional approach of (1) Clearing spalled concrete, (2) patching damaged areas, and (3) injecting epoxy into cracks. This method proved effective for the moderately damaged specimens, fully restoring strength and deformation capacity. For severely damaged specimens, replacing the entirety of the damaged section was shown to restore the full strength, stiffness, and deformation capacity of the column.

Belarbi et.al. (2008) tested columns subjected to severe damage under several loading states. The damaged columns, with fractured and yielded bars and severely compromised concrete, were repaired with the intent to return them to full strength. The repair procedure, outlined in **Figure D.21**, consists of five main steps: (1) removal of damaged concrete, (2) restoration of the cross-section using grout, (3) longitudinal CFRP application to restore flexural strength, (4) circumferential application of CFRP to restore axial compression, and (5) mechanically anchoring the longitudinal CFRP sheets.



Figure D.21 Restoration process for damaged column (Belarbi et al, 2008)

This repair scheme was sufficient to restore column capacity, but given a failure in the anchoring of the longitudinal CFRP during testing, further testing would be appropriate.

Vosooghi et al (2011) conducted a study on column repair using CFRP. A variety of column types (standard single, two-column bent, and substandard) were tested and then repaired with CFRP. The standard columns were restored in strength and ductility, and the sub-standard columns met the current seismic standard after the repair. The stiffness of all columns was inadequately restored following material degradation during tests.

Saini et.al. (2013) repaired a set of columns with fractured bars using a combination of CFRP fabric and repairing the damaged bars. The damaged bars were replaced and the new bars connected to the undamaged section with approved couplers as shown in **Figure D.22**. Once the bars were repaired, new concrete was poured and then the column was wrapped with CFRP fabric (**Figure D.23**). This repair technique appears to have been successful in restoring the full strength of the columns.



Figure D.22 Damaged bars and coupler repair (Saini et al, 2013)



Figure D.23 CFRP wrapping (Saini et al, 2013)

He et. al. (2013) tested a series of columns subjected to various motions, recorded the respective damage states, and then applied the same repair mechanism to each. The damage states are shown in **Figure D.24**, with increasing damage corresponding to increasingly devastating motions.

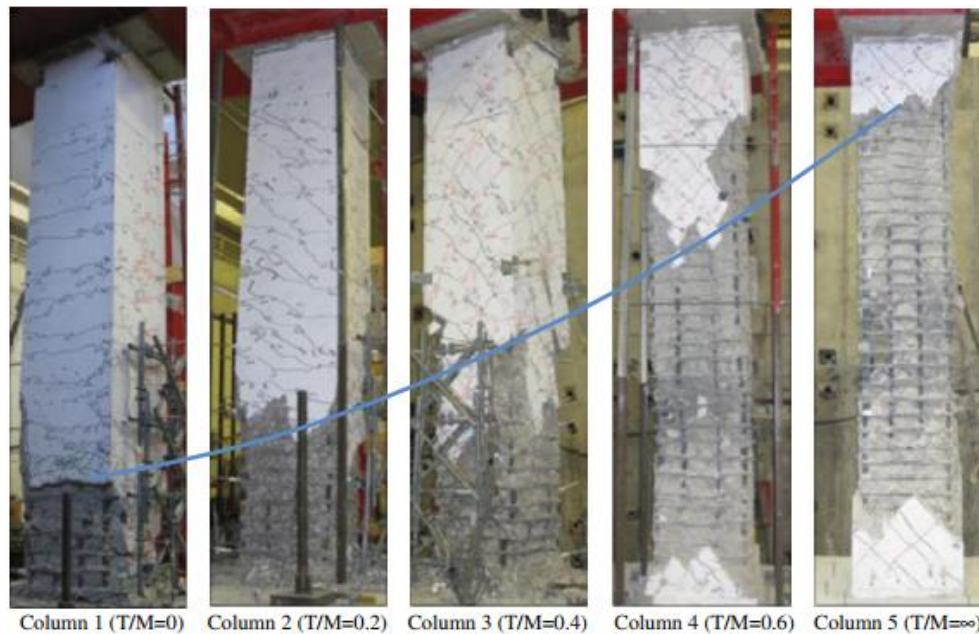


Figure D.24 Increasing damage states (He et al, 2013)

The repair sequence implemented was as follows:

1. Straightening the column
2. Removing loose concrete
3. Placing repair mortar
4. Preparing column surface
5. Installing longitudinal and transverse CFRP (different layouts for each column)

It was found that for columns without fractured bars, the repair restored them to full or even above original strength. For columns with fractured bars, the strength was restored to nearly that of the original column.

Rutledge et. al. (2013) tested three columns under intense loading with the intent to be repair relocating the plastic hinge further up the height without compromising the displacement capacity. Prior to repair, each column had buckled or fractured reinforcement (**Figure D.25**). The repair was carried out by 1) Removal of loose concrete, 2) Cross section patched, and 3) CFRP loaded with epoxy resin and then applied to column (“wet layup technique”; Longitudinally applied and anchored with carbon fiber anchors and Subsequently circumferentially applied). This procedure is shown in **Figure D.30**. This procedure restored the stiffness of the columns to the level of the original column as well as increasing displacement and force capacities.

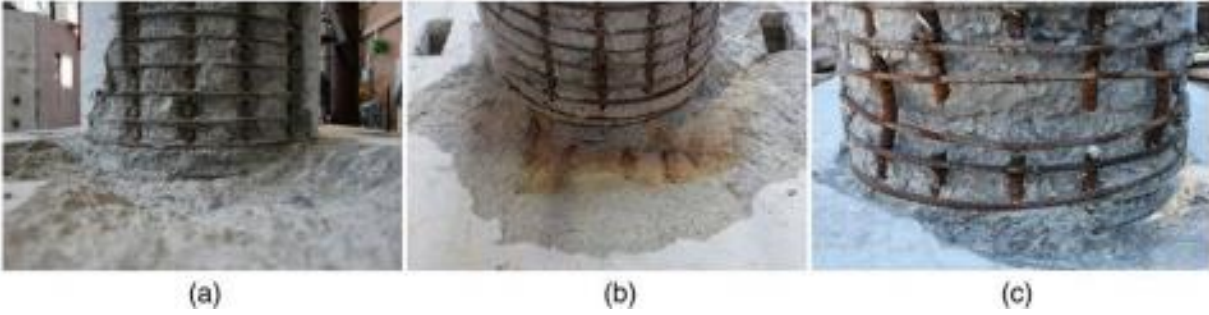


Figure D.25 Failed reinforcement prior to repair (Rutledge et al, 2013)

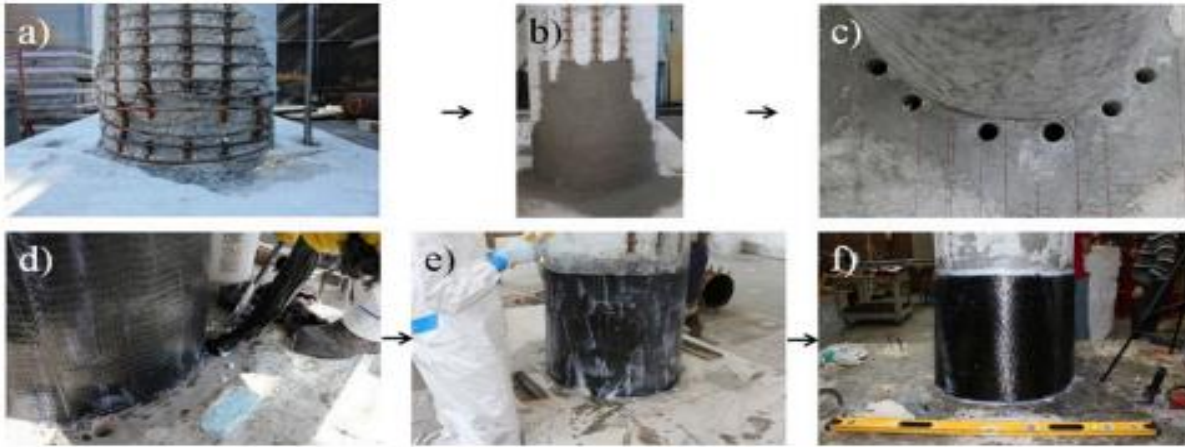


Figure D.30 Repair process (Rutledge et al, 2013)

D.6 Repair Design for Columns

This section outlines the methods for repairing seismically damaged bridge columns in the various described damage states. The equations used to calculate CFRP requirements are the same for all damage states, but with varying coefficients for the damage. These equations are shown below and should be used for all relevant damage states. Remaining strengths are provided for each DS. Equations D.1 through D.12 are provided from Saini et al (2013).

Concrete shear capacity

$$V_c = v_c \times A_e \quad \text{D.1}$$

$$A_e = 0.8 \times A_g \quad \text{D.2}$$

Inside the plastic hinge

$$v_c = \text{Factor1} \times \text{Factor2} \times \sqrt{f_c} \leq 4\sqrt{f_c} \quad (\text{psi}) \quad \text{D.3}$$

Inside the plastic hinge

$$v_c = 3 \times Factor2 \times \sqrt{f_c} \leq 4\sqrt{f_c} \quad (\text{psi}) \quad \text{D.4}$$

Where;

$$Factor1 = 0.3 \leq \frac{\rho_s \times f_{yh}}{0.15} + 3.67 - \mu_d < 1.5 \quad (f_{yh} \text{ in ksi units}) \quad \text{D.5}$$

$$Factor2 = 1 + \frac{P_c}{2000A_g} < 1.5 \quad (P_c \text{ in lbs}) \quad \text{D.6}$$

Inside the plastic hinge

$$V_s = \frac{A_v f_{yh} D'}{s} \quad \text{D.7}$$

Where;

$$A_v = n \times \frac{\pi}{2} \times A_b \quad \text{D.8}$$

$$V_n = V_c + V_s \quad \text{D.9}$$

Where; V_c is concrete shear strength, V_s is the shear reinforcement capacity, A_v is the total area of the shear reinforcement, A_b is the diameter of the spirals, n is the number of individual interlocking spiral core sections, D' is the core diameter measured from center to center of spiral, f_{yh} is the yield strength of spiral, s is the spacing between spirals, μ_d is the ductility demand (**Table D.1**), A_g is the gross area of column section, A_e is the effective area of column section, f_c' is the compressive strength of concrete, and P_c is the column axial load.

Table D.1 Ductility Demand, μ , for Damage States (Saini et al, 2013)

DS	μ
2	1.6
3	2.4
4	3.2
5	4.2

Then, to calculate the thickness of CFRP required for the column, use equations D.10 and D.11 (Saini et al, 2013).

$$t_j = \frac{V_j}{\pi/2 \times 0.004 \times E_j \times D} \quad \text{D.10}$$

$$V_j = V_n - (R_c V_c + R_s V_s) \quad \text{D.11}$$

Where V_j is the shear strength provided by jacket, D is the diameter of the column, E_j is the tensile modulus of elasticity of FRP, and R_c and R_s are the contribution of concrete and spiral at different DS's. Other parameters were defined previously.

These equations were utilized for a theoretical example column with assumed dimensions and reinforcing characteristics (steel strength, spacing, etc.). The resulting required CFRP thickness is documented in **Table B.2**, with the progression noted in **Figure B.31**.

Table D.2 Damage States v. Required CFRP Thickness- Example Column

DS	Required CFRP thickness (in)
2	.0253
3	.0521
4	.0689
5	.1041

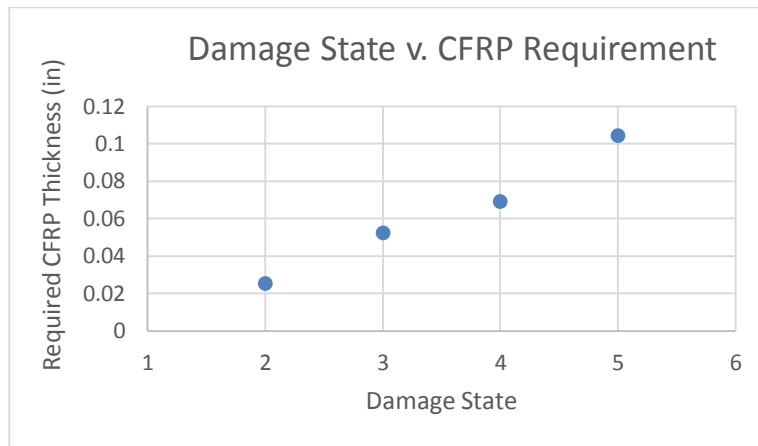


Figure D.31 Damage state v. required Cfrp thickness- Example column

D.7 Repair Design for Shear Keys

This section discusses the repair of shear keys damaged in the various states discussed in the previous section. Note that only DS 2, 5, and 6 are discussed. This is because the other damage states are not relevant for shear keys.

Damage State 2

The repair mechanism for a shear key in DS2 is meant to restore the lost shear capacity of the concrete, as it is assumed that no loss of shear strength in the steel has occurred. Unidirectional CFRP fabric is used to restore the shear strength, while limiting over strengthening to 110% of the original capacity to prevent substructure damage. An equation was developed to determine the appropriate fabric thickness to achieve desired strength. Loose concrete is removed, cracks are filled with epoxy injection, and CFRP is applied with fibers in the horizontal direction. The

equation to determine CFRP fabric thickness, with variable definitions, is shown below (Saini et al, 2013).

Step 1: Determine effective strain in CFRP:

$$\varepsilon_{fe} = 0.015 \times (t_f)^{-0.5} E_f^{-0.36} \left(\frac{f'_{ce}}{5} \right)^{0.67} \quad \text{D.12}$$

Where ε_{fe} is the effective strain in CFRP, t_f is the total thickness of CFRP layer (in.); E_f is the CFRP tensile modulus (ksi) and f'_{ce} is the expected compressive strength of concrete (ksi).

Step 2: Determine CFRP design shear force:

$$(V_f)_{Required} = \frac{1}{\psi} (V_n - (R_c V_c + V_s)) \text{ kips} \quad \text{D.13}$$

Where F_v is the shear strength provided by CFRP (kips); ψ is the additional reduction factor of .85 recommended by ACI 440.2R-08, and R_c is the contribution ratio of concrete at a given damage state.

Step 3: Determine the CFRP required thickness. The shear strength provided by the CFRP fabrics is determined by calculating the force resulting from the tensile stresses in the CFRP across the assumed 45 degree crack (Figure 2.2.1) is shown in Equation 15.

$$V_f = \varepsilon_{fe} \cdot t_f \cdot E_f \cdot d_{fv} (\sin \alpha + \cos \alpha) \quad \text{D.14}$$

Where d_{fv} is total depth (in) and α is orientation angle (degrees) of CFRP. By substituting Equation D.13 into Equation D.15, we obtain Equation D.16.

$$t_f = \left(\frac{66.67 V_f}{E_f^{0.64} d_{vf}} \right)^2 \left(\frac{5}{f'_{ce}} \right)^{1.34} \text{ inch} \quad \text{D.15}$$

The bond capacity of CFRP is developed over a critical length, l_{df} . To develop the effective CFRP stress at a section, the available anchorage length of CFRP should exceed the value given in Equation D.17 (ACI 440.2R-08).

$$l_{df} = 0.057 \cdot \sqrt{\frac{E_f t_f}{f'_{ce}}} \text{ inch} \quad \text{D.16}$$

Damage State 5

DS5 is characterized by near failure of the shear key, with heavy damage to the concrete. Representative damage includes extensive diagonal cracking and spalling. To repair a shear key in DS5, a similar approach is used to that described in DS2. This is because in DS5, the steel reinforcement is assumed to be intact and therefore the repair is still only replacing the lost capacity of the concrete to resist shear. An example of this repair is shown in **Figure D.31**.

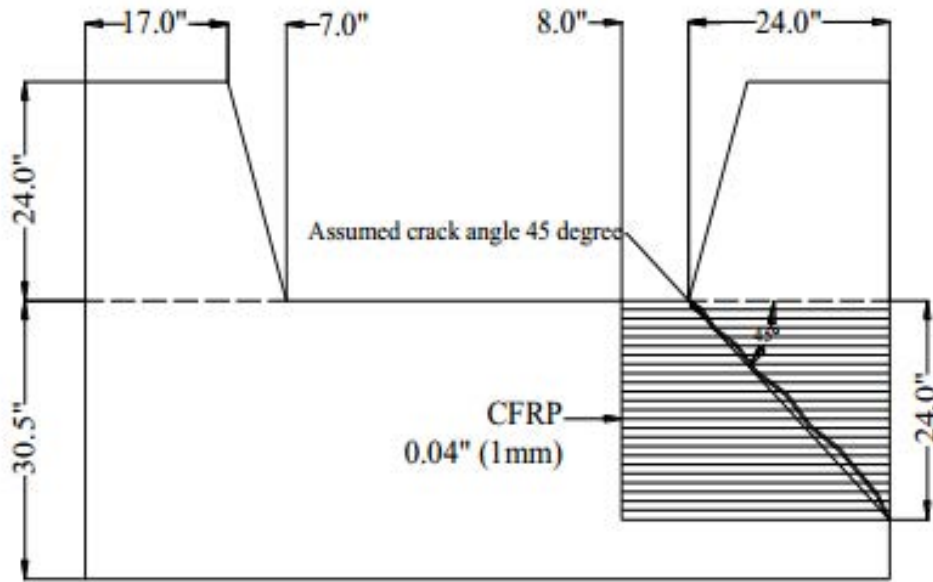


Figure D.31 Repair for DS2 and DS5 (Saini et al, 2013)

Damage State 6

DS6 is characterized by complete failure of the shear key, including reinforcement fracture and concrete failure. To repair a shear key experiencing DS6, total replacement is needed. The goals being to restore shear capacity and facilitate sliding shear friction failure, the procedure is as follows:

1. Remove concrete, exposing reinforcement
2. Remove all horizontal and inclined reinforcement
3. Straighten damaged vertical reinforcement and cut at interface level
4. Calculate required vertical reinforcement (Equation D.17) (Saiidi and Cheng, 2004).

$$A_{sk} = \frac{F_{sk}}{1.8 \times f_{ye}} \text{ in}^2 \quad \text{D.17}$$

$$A_{sk,min} = \frac{0.05 A_{cv}}{f_{ye}} \text{ in}^2 \quad \text{D.18}$$

Where; A_{sk} is the required area of shear key vertical reinforcement (in²); F_{sk} is the shear key force (kips); A_{cv} is the area of concrete considered to be engaged in interface shear transfer (in²) and f_{ye} is the expected yield strength of steel (ksi). The area of shear key vertical reinforcement calculated using Equation D.17 should be greater than or equal to the minimum (Equation D.18) recommended by Caltrans SDC 2010.

Additionally,

$$l_{dh} = 24d_b \text{ in}^2 \quad \text{D.19}$$

Where; l_{dh} is the development length, and d_b is the diameter of the reinforcement bars.

5. Drill holes in stem wall and install vertical reinforcement- fill holes with epoxy.
6. Use ACI provisions for minimum stirrups
7. Provide smooth construction joint at interface to allow use of $\mu=0.4$ as shear friction coefficient.

These steps are shown in the following series of figures from a repair report (Saini et al, 2013)

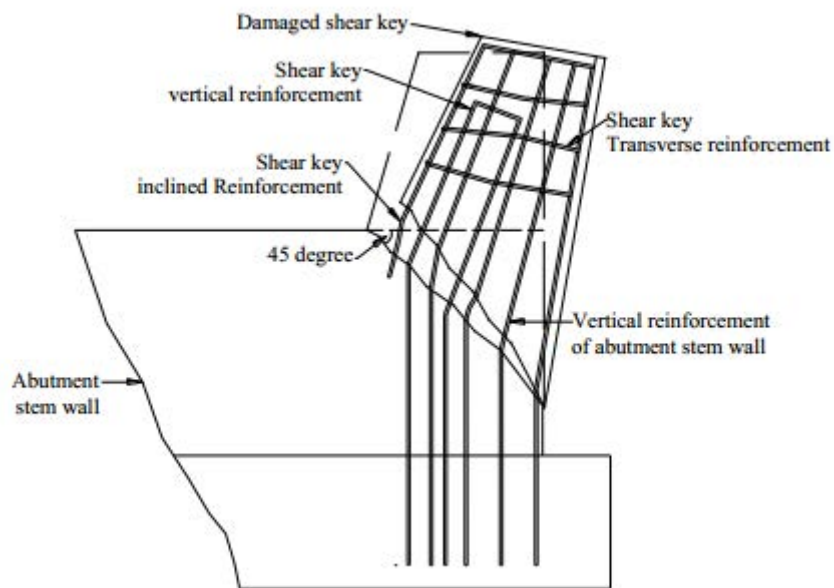


Figure D.32 DS6 repair step 1 (Saini et al, 2013)

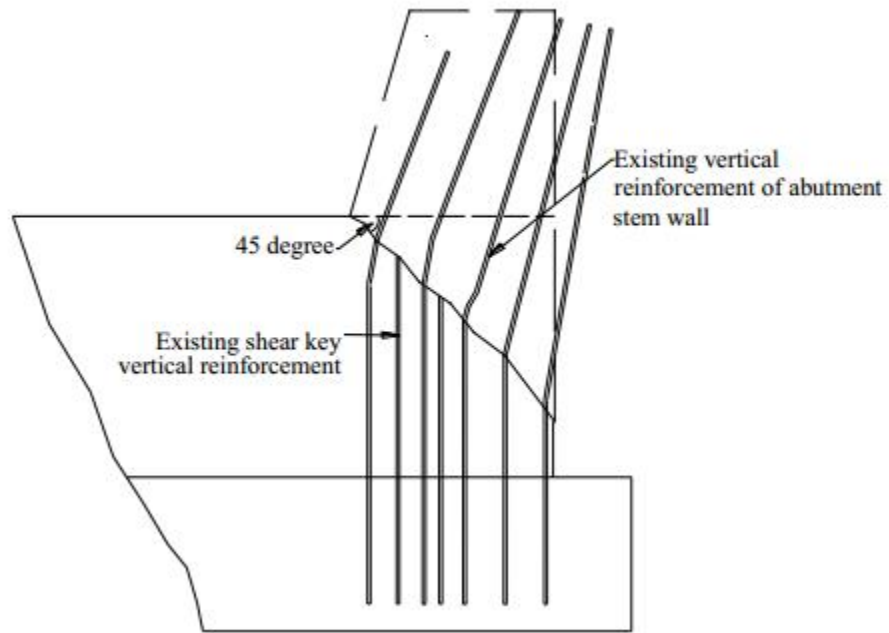


Figure D.33 DS6 repair step 2 (Saini et al, 2013)

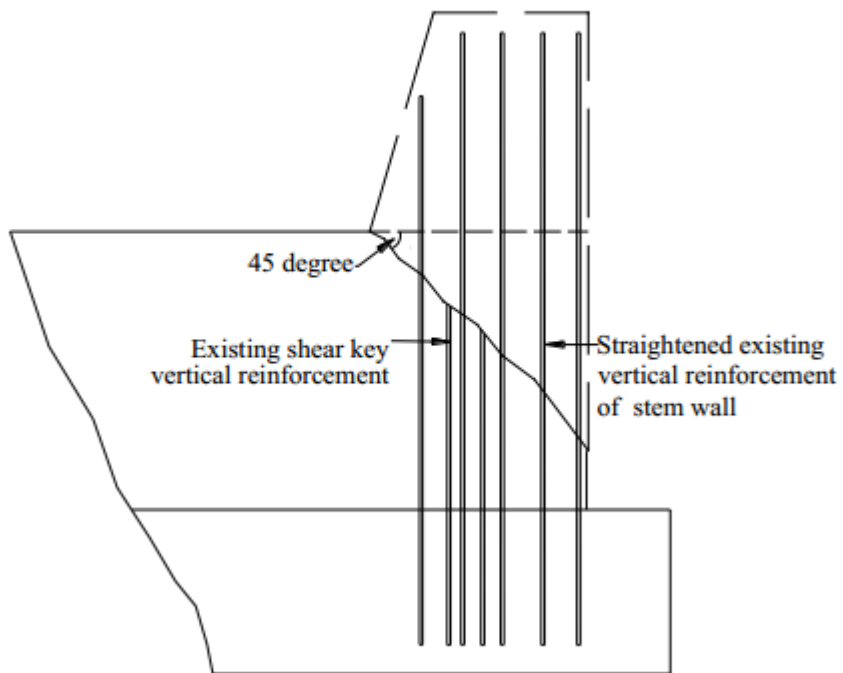


Figure D.34 DS6 repair step 3 (Saini et al, 2013)

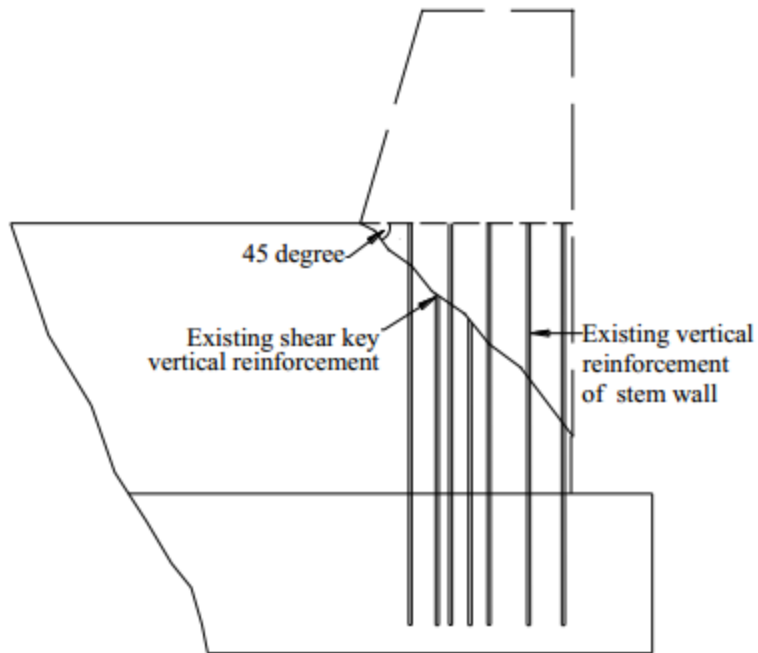


Figure D.35 DS6 repair step 4 (Saini et al, 2013)

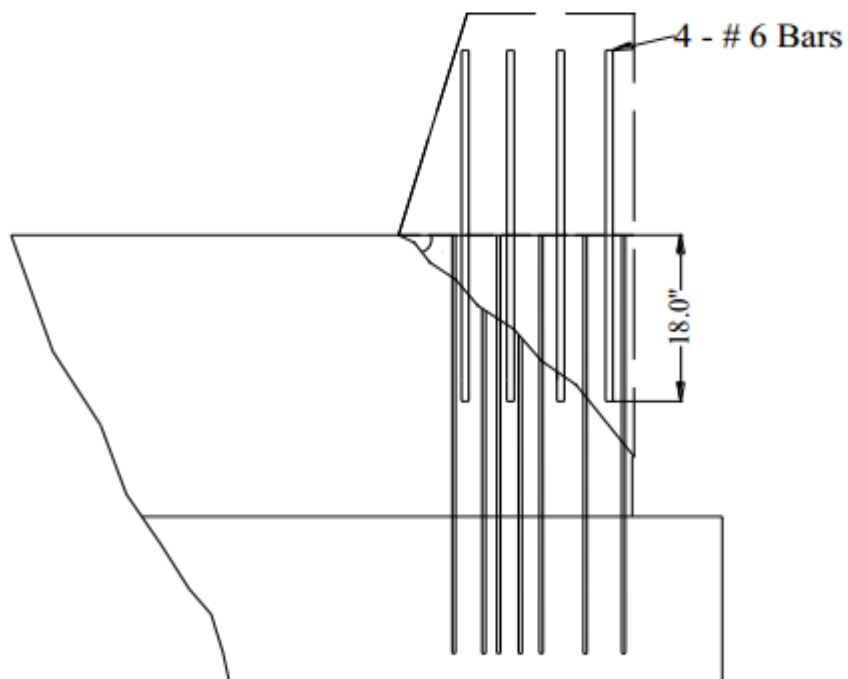


Figure D.36 DS6 repair step 5 (Saini et al, 2013)

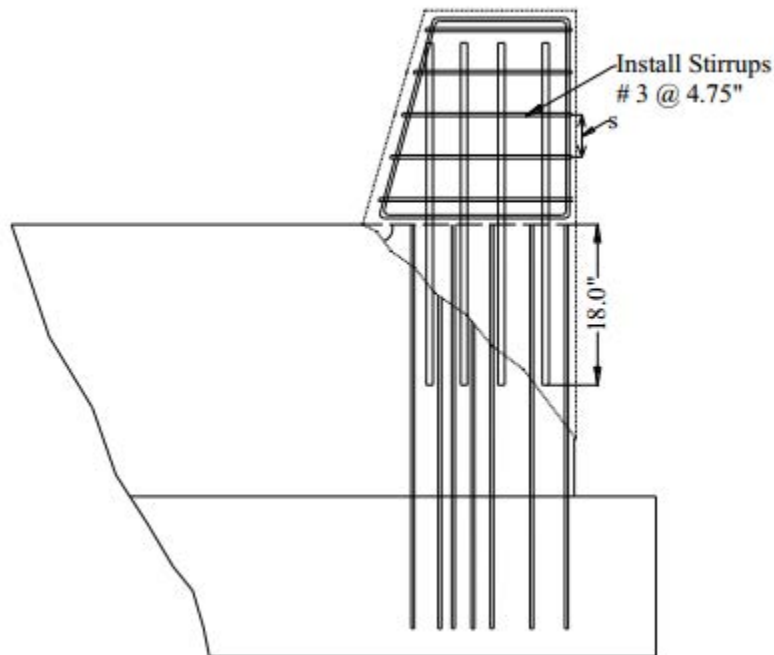


Figure D.37 DS6 repair step 6 (Saini et al, 2013)

D.8 Repair Design for Abutments

This section covers the repair of abutments in various damage states. Note that not all DSs are included, because DS1 and DS5 are not relevant to abutments and are therefore omitted.

Damage State 2

DS2 is characterized by minor cracking and spalling but with no severe structural damage. To repair an abutment in this damage state, the following steps are recommended.

1. Remove spalled and otherwise damaged concrete
2. Patch over damaged area.
3. Epoxy injection in remaining cracks.

These repairs are not structural and serve purely for aesthetics, as well as to protect the reinforcement from corrosion.

Damage State 3

DS3 is characterized by moderate cracking and spalling of concrete, with some initial failure of steel. The repair mechanism for DS 3 is the same as that for DS 4, and will be discussed in the next section.

Damage State 4

DS4 is characterized by more severe cracking and spalling of concrete, with further failure and partial exposure of steel reinforcement. At this DS, approximately 50% of shear capacity is lost, so repair attempts to recover that strength.

1. For DS 3 and DS 4, the same repairs are recommended, as follows.
2. Determine necessary CFRP strength using Equation D.20 (Saini et al, 2013), shown below.

$$(V_f)_{Required} = \frac{1}{\psi} (V_n - (R_C V_C)) \text{ kips} \quad \text{D.20}$$

3. Determine CFRP thickness using Equation D.21 (Saini et al, 2013), shown below.

$$t_f = \left(\frac{66.67V_f}{E_f^{0.64} d_{vf}} \right)^2 \left(\frac{5}{f'_{ce}} \right)^{1.34} \text{ in} \quad \text{D.21}$$

4. Remove loose concrete
5. Fill cracks with epoxy injection
6. Install CFRP in alternating horizontal and vertical directions
7. Anchor at a distance at least l from the edge of the crack, where l is determined by Equation D.22 (Saiidi and Saini, 2013), shown below.

$$l_{df} = 0.057 \cdot \sqrt{\frac{E_f t_f}{f'_{ce}}} \text{ inch} \quad \text{D.22}$$

Damage State 6

DS6 is characterized by complete failure of the abutment and near complete failure of steel. To repair an abutment in DS 6, the following steps are recommended.

1. Remove loose concrete
2. Fill cracks with epoxy injection
3. Straighten damaged reinforcing bars
4. Cast new concrete
5. Determine necessary shear strength from CFRP (EQ. 20), assuming 80% strength loss.

6. Determine necessary CFRP thickness and anchor length (EQ.s 21 and 22)
7. Place CFRP in horizontal and vertical directions to restore strength.

References

- Belarbi, Abdeldjelil, Pedro Silva, and Sang-Wook Bae. "Retrofit Using CFRP Composites of RC Bridge Columns under Combined Loads." *Fourth International Conference on FRP Composites in Civil Engineering in Zurich, Switzerland (2008)*.
- Bozorgzadeh, Azadeh, Sami Hanna Megally, Scott Ashford, and Jose Restrepo. "Seismic Response of Sacrificial Exterior Shear Keys in Bridge Abutments." *University of California, San Diego Department of Structural Engineering (2007)*.
- Bozorgzadeh, Azadeh, Sami Hanna Megally, Scott Ashford, and Jose Restrepo. "Seismic Response and Capacity Evaluation of Exterior Sacrificial Shear Keys of Bridge Abutments." *13th World Conference on Earthquake Engineering Paper No. 528 (2004)*.
- He, Ruili He, Lesley Sneed, and Abdeldjelil Belarbi. "Rapid Repair of Severely Damaged RC Columns with Different Damage Conditions: An Experimental Study." *International Journal of Concrete Structures and Materials 7.1 (2013): 35-50*.
- He, Ruili, Stephen Grelle, Lesley Sneed, and Abdeldjelil Belarbi. "Rapid Repair of a Severely Damaged RC Column Having Fractured Bars Using Externally Bonded CFRP." *Elsevier 101 (2013): 225-42. Composite Structures. Elsevier. Web. 15 Sept. 2014*.
- Kaminosono, Takashi, Fumitoshi Kumazawa, and Yoshiaki Nakano. "Quick Inspection Manual for Damaged Reinforced Concrete Buildings Due to Earthquakes." *National Institute of Land and Infrastructure Management; Ministry of Land, Infrastructure, and Transport (2002)*.
- Lehman, Dawn, and Jack Moehle. "Performance- Based Seismic Design of Reinforced Concrete Bridge Columns." *12th World Conference on Earthquake Engineering- Auckland, New Zealand (2000)*.
- Lehman, Dawn, S.J. Elkin, A.M. Nacamuli, and J.P. Moehle. "Repair of Earthquake-Damaged Bridge Columns." (2014), *ACI Structural Journal*, V. 98, No. 2, March-April 2001, January-February 2002
- Li, Yeou-Fong, and Yi-Ying Sung. "Seismic Repair and Rehabilitation of a Shear-failure Damage Circular Bridge Column Using Carbon Fiber Reinforced Plastic Jacketing." *Canadian Journal of Civil Engineering 30 (2003): 819-29. NRC Research Press*.
- Priestley, M.J., F. Seible, and E. Fyfe. "Column Seismic Retrofit Using Fiber Glass/Epoxy Jackets." *International Conference on Advanced Composite Material in Bridge and Structures; Sherbrooke, Canada (1992): 287-98*.

- Rutledge, Stephen, Mervyn Kowalsky, Rudolf Seracino, and James Nau. "Repair of Reinforced Concrete Bridge Columns Containing Buckled and Fractured Reinforcement by Plastic Hinge." *Journal of Bridge Engineering* 492 (2013).
- Saadatmanesh, Hamid, Mohammad R. Ehsani, and Limin Jin. "Repair of Earthquake-Damaged RC Columns with FRP Wraps." *ACI Structural Journal* 94.S20 (1997): 206-14.
- Saini, Amarjeet, and M. Saiid Saiidi. "Post-Earthquake Damage Repair of Various Reinforced Concrete Bridge Components." *University of Nevada, Reno Civil Engineering Department* (2013).
- Saiidi, M. Saiid, and Zhiyuan Cheng. "Effectiveness of Composites in Earthquake Damage Repair of Reinforced Concrete Flared Columns." *Journal of Composites for Construction* (2004): 306-14.
- Vosooghi, Ashkan, and M. Saiidi. "Analytical Studies of CFRP-Repaired RC Bridge Column Models Subjected to Seismic Loading." *Journal of Bridge Engineering* (2011).

LIST OF CCEER PUBLICATIONS

Report No.	Publication
CCEER-84-1	Saiidi, M., and R. Lawver, "User's Manual for LZAK-C64, A Computer Program to Implement the Q-Model on Commodore 64," Civil Engineering Department, Report No. CCEER-84-1, University of Nevada, Reno, January 1984.
CCEER-84-1 Reprint	Douglas, B., Norris, G., Saiidi, M., Dodd, L., Richardson, J. and Reid, W., "Simple Bridge Models for Earthquakes and Test Data," Civil Engineering Department, Report No. CCEER-84-1 Reprint, University of Nevada, Reno, January 1984.
CCEER-84-2	Douglas, B. and T. Iwasaki, "Proceedings of the First USA-Japan Bridge Engineering Workshop," held at the Public Works Research Institute, Tsukuba, Japan, Civil Engineering Department, Report No. CCEER-84-2, University of Nevada, Reno, April 1984.
CCEER-84-3	Saiidi, M., J. Hart, and B. Douglas, "Inelastic Static and Dynamic Analysis of Short R/C Bridges Subjected to Lateral Loads," Civil Engineering Department, Report No. CCEER-84-3, University of Nevada, Reno, July 1984.
CCEER-84-4	Douglas, B., "A Proposed Plan for a National Bridge Engineering Laboratory," Civil Engineering Department, Report No. CCEER-84-4, University of Nevada, Reno, December 1984.
CCEER-85-1	Norris, G. and P. Abdollaholizadeh, "Laterally Loaded Pile Response: Studies with the Strain Wedge Model," Civil Engineering Department, Report No. CCEER-85-1, University of Nevada, Reno, April 1985.
CCEER-86-1	Ghusn, G. and M. Saiidi, "A Simple Hysteretic Element for Biaxial Bending of R/C in NEABS-86," Civil Engineering Department, Report No. CCEER-86-1, University of Nevada, Reno, July 1986.
CCEER-86-2	Saiidi, M., R. Lawver, and J. Hart, "User's Manual of ISADAB and SIBA, Computer Programs for Nonlinear Transverse Analysis of Highway Bridges Subjected to Static and Dynamic Lateral Loads," Civil Engineering Department, Report No. CCEER-86-2, University of Nevada, Reno, September 1986.
CCEER-87-1	Siddharthan, R., "Dynamic Effective Stress Response of Surface and Embedded Footings in Sand," Civil Engineering Department, Report No. CCEER-86-2, University of Nevada, Reno, June 1987.
CCEER-87-2	Norris, G. and R. Sack, "Lateral and Rotational Stiffness of Pile Groups for Seismic Analysis of Highway Bridges," Civil Engineering Department, Report No. CCEER-87-2, University of Nevada, Reno, June 1987.
CCEER-88-1	Orie, J. and M. Saiidi, "A Preliminary Study of One-Way Reinforced Concrete Pier Hinges Subjected to Shear and Flexure," Civil Engineering Department, Report No. CCEER-88-1, University of Nevada, Reno, January 1988.
CCEER-88-2	Orie, D., M. Saiidi, and B. Douglas, "A Micro-CAD System for Seismic Design of Regular Highway Bridges," Civil Engineering Department, Report No. CCEER-88-2, University of Nevada, Reno, June 1988.
CCEER-88-3	Orie, D. and M. Saiidi, "User's Manual for Micro-SARB, a Microcomputer Program for Seismic Analysis of Regular Highway Bridges," Civil Engineering Department, Report No. CCEER-88-3, University of Nevada, Reno, October 1988.

- CCEER-89-1 Douglas, B., M. Saiidi, R. Hayes, and G. Holcomb, "A Comprehensive Study of the Loads and Pressures Exerted on Wall Forms by the Placement of Concrete," Civil Engineering Department, Report No. CCEER-89-1, University of Nevada, Reno, February 1989.
- CCEER-89-2 Richardson, J. and B. Douglas, "Dynamic Response Analysis of the Dominion Road Bridge Test Data," Civil Engineering Department, Report No. CCEER-89-2, University of Nevada, Reno, March 1989.
- CCEER-89-2 Vrontinos, S., M. Saiidi, and B. Douglas, "A Simple Model to Predict the Ultimate Response of R/C Beams with Concrete Overlays," Civil Engineering Department, Report NO. CCEER-89-2, University of Nevada, Reno, June 1989.
- CCEER-89-3 Ebrahimpour, A. and P. Jagadish, "Statistical Modeling of Bridge Traffic Loads - A Case Study," Civil Engineering Department, Report No. CCEER-89-3, University of Nevada, Reno, December 1989.
- CCEER-89-4 Shields, J. and M. Saiidi, "Direct Field Measurement of Prestress Losses in Box Girder Bridges," Civil Engineering Department, Report No. CCEER-89-4, University of Nevada, Reno, December 1989.
- CCEER-90-1 Saiidi, M., E. Maragakis, G. Ghosn, Y. Jiang, and D. Schwartz, "Survey and Evaluation of Nevada's Transportation Infrastructure, Task 7.2 - Highway Bridges, Final Report," Civil Engineering Department, Report No. CCEER 90-1, University of Nevada, Reno, October 1990.
- CCEER-90-2 Abdel-Ghaffar, S., E. Maragakis, and M. Saiidi, "Analysis of the Response of Reinforced Concrete Structures During the Whittier Earthquake 1987," Civil Engineering Department, Report No. CCEER 90-2, University of Nevada, Reno, October 1990.
- CCEER-91-1 Saiidi, M., E. Hwang, E. Maragakis, and B. Douglas, "Dynamic Testing and the Analysis of the Flamingo Road Interchange," Civil Engineering Department, Report No. CCEER-91-1, University of Nevada, Reno, February 1991.
- CCEER-91-2 Norris, G., R. Siddharthan, Z. Zafir, S. Abdel-Ghaffar, and P. Gowda, "Soil-Foundation-Structure Behavior at the Oakland Outer Harbor Wharf," Civil Engineering Department, Report No. CCEER-91-2, University of Nevada, Reno, July 1991.
- CCEER-91-3 Norris, G., "Seismic Lateral and Rotational Pile Foundation Stiffnesses at Cypress," Civil Engineering Department, Report No. CCEER-91-3, University of Nevada, Reno, August 1991.
- CCEER-91-4 O'Connor, D. and M. Saiidi, "A Study of Protective Overlays for Highway Bridge Decks in Nevada, with Emphasis on Polyester-Styrene Polymer Concrete," Civil Engineering Department, Report No. CCEER-91-4, University of Nevada, Reno, October 1991.
- CCEER-91-5 O'Connor, D.N. and M. Saiidi, "Laboratory Studies of Polyester-Styrene Polymer Concrete Engineering Properties," Civil Engineering Department, Report No. CCEER-91-5, University of Nevada, Reno, November 1991.
- CCEER-92-1 Straw, D.L. and M. Saiidi, "Scale Model Testing of One-Way Reinforced Concrete Pier Hinges Subject to Combined Axial Force, Shear and Flexure," edited by D.N. O'Connor, Civil Engineering Department, Report No. CCEER-92-1, University of Nevada, Reno, March 1992.
- CCEER-92-2 Wehbe, N., M. Saiidi, and F. Gordaninejad, "Basic Behavior of Composite Sections Made of Concrete Slabs and Graphite Epoxy Beams," Civil Engineering Department, Report No. CCEER-92-2, University of Nevada, Reno, August 1992.
- CCEER-92-3 Saiidi, M. and E. Hutchens, "A Study of Prestress Changes in A Post-Tensioned Bridge During the First 30 Months," Civil Engineering Department, Report No. CCEER-92-3, University of Nevada, Reno, April 1992.

- CCEER-92-4 Saiidi, M., B. Douglas, S. Feng, E. Hwang, and E. Maragakis, "Effects of Axial Force on Frequency of Prestressed Concrete Bridges," Civil Engineering Department, Report No. CCEER-92-4, University of Nevada, Reno, August 1992.
- CCEER-92-5 Siddharthan, R., and Z. Zafir, "Response of Layered Deposits to Traveling Surface Pressure Waves," Civil Engineering Department, Report No. CCEER-92-5, University of Nevada, Reno, September 1992.
- CCEER-92-6 Norris, G., and Z. Zafir, "Liquefaction and Residual Strength of Loose Sands from Drained Triaxial Tests," Civil Engineering Department, Report No. CCEER-92-6, University of Nevada, Reno, September 1992.
- CCEER-92-6-A Norris, G., Siddharthan, R., Zafir, Z. and Madhu, R. "Liquefaction and Residual Strength of Sands from Drained Triaxial Tests," Civil Engineering Department, Report No. CCEER-92-6-A, University of Nevada, Reno, September 1992.
- CCEER-92-7 Douglas, B., "Some Thoughts Regarding the Improvement of the University of Nevada, Reno's National Academic Standing," Civil Engineering Department, Report No. CCEER-92-7, University of Nevada, Reno, September 1992.
- CCEER-92-8 Saiidi, M., E. Maragakis, and S. Feng, "An Evaluation of the Current Caltrans Seismic Restrainer Design Method," Civil Engineering Department, Report No. CCEER-92-8, University of Nevada, Reno, October 1992.
- CCEER-92-9 O'Connor, D., M. Saiidi, and E. Maragakis, "Effect of Hinge Restrainers on the Response of the Madrone Drive Undercrossing During the Loma Prieta Earthquake," Civil Engineering Department, Report No. CCEER-92-9, University of Nevada, Reno, February 1993.
- CCEER-92-10 O'Connor, D., and M. Saiidi, "Laboratory Studies of Polyester Concrete: Compressive Strength at Elevated Temperatures and Following Temperature Cycling, Bond Strength to Portland Cement Concrete, and Modulus of Elasticity," Civil Engineering Department, Report No. CCEER-92-10, University of Nevada, Reno, February 1993.
- CCEER-92-11 Wehbe, N., M. Saiidi, and D. O'Connor, "Economic Impact of Passage of Spent Fuel Traffic on Two Bridges in Northeast Nevada," Civil Engineering Department, Report No. CCEER-92-11, University of Nevada, Reno, December 1992.
- CCEER-93-1 Jiang, Y., and M. Saiidi, "Behavior, Design, and Retrofit of Reinforced Concrete One-way Bridge Column Hinges," edited by D. O'Connor, Civil Engineering Department, Report No. CCEER-93-1, University of Nevada, Reno, March 1993.
- CCEER-93-2 Abdel-Ghaffar, S., E. Maragakis, and M. Saiidi, "Evaluation of the Response of the Aptos Creek Bridge During the 1989 Loma Prieta Earthquake," Civil Engineering Department, Report No. CCEER-93-2, University of Nevada, Reno, June 1993.
- CCEER-93-3 Sanders, D.H., B.M. Douglas, and T.L. Martin, "Seismic Retrofit Prioritization of Nevada Bridges," Civil Engineering Department, Report No. CCEER-93-3, University of Nevada, Reno, July 1993.
- CCEER-93-4 Abdel-Ghaffar, S., E. Maragakis, and M. Saiidi, "Performance of Hinge Restrainers in the Huntington Avenue Overhead During the 1989 Loma Prieta Earthquake," Civil Engineering Department, Report No. CCEER-93-4, University of Nevada, Reno, June 1993 (in final preparation).
- CCEER-93-5 Maragakis, E., M. Saiidi, S. Feng, and L. Flournoy, "Effects of Hinge Restrainers on the Response of the San Gregorio Bridge during the Loma Prieta Earthquake," (in final preparation) Civil Engineering Department, Report No. CCEER-93-5, University of Nevada, Reno.

- CCEER-93-6 Saiidi, M., E. Maragakis, S. Abdel-Ghaffar, S. Feng, and D. O'Connor, "Response of Bridge Hinge Restrainers during Earthquakes -Field Performance, Analysis, and Design," Civil Engineering Department, Report No. CCEER-93-6, University of Nevada, Reno, May 1993.
- CCEER-93-7 Wehbe, N., Saiidi, M., Maragakis, E., and Sanders, D., "Adequacy of Three Highway Structures in Southern Nevada for Spent Fuel Transportation," Civil Engineering Department, Report No. CCEER-93-7, University of Nevada, Reno, August 1993.
- CCEER-93-8 Roybal, J., Sanders, D.H., and Maragakis, E., "Vulnerability Assessment of Masonry in the Reno-Carson City Urban Corridor," Civil Engineering Department, Report No. CCEER-93-8, University of Nevada, Reno, May 1993.
- CCEER-93-9 Zafir, Z. and Siddharthan, R., "MOVLOAD: A Program to Determine the Behavior of Nonlinear Horizontally Layered Medium Under Moving Load," Civil Engineering Department, Report No. CCEER-93-9, University of Nevada, Reno, August 1993.
- CCEER-93-10 O'Connor, D.N., Saiidi, M., and Maragakis, E.A., "A Study of Bridge Column Seismic Damage Susceptibility at the Interstate 80/U.S. 395 Interchange in Reno, Nevada," Civil Engineering Department, Report No. CCEER-93-10, University of Nevada, Reno, October 1993.
- CCEER-94-1 Maragakis, E., B. Douglas, and E. Abdelwahed, "Preliminary Dynamic Analysis of a Railroad Bridge," Report CCEER-94-1, January 1994.
- CCEER-94-2 Douglas, B.M., Maragakis, E.A., and Feng, S., "Stiffness Evaluation of Pile Foundation of Cazenovia Creek Overpass," Civil Engineering Department, Report No. CCEER-94-2, University of Nevada, Reno, March 1994.
- CCEER-94-3 Douglas, B.M., Maragakis, E.A., and Feng, S., "Summary of Pretest Analysis of Cazenovia Creek Bridge," Civil Engineering Department, Report No. CCEER-94-3, University of Nevada, Reno, April 1994.
- CCEER-94-4 Norris, G.M., Madhu, R., Valceschini, R., and Ashour, M., "Liquefaction and Residual Strength of Loose Sands from Drained Triaxial Tests," Report 2, Vol. 1&2, Civil Engineering Department, Report No. CCEER-94-4, University of Nevada, Reno, August 1994.
- CCEER-94-5 Saiidi, M., Hutchens, E., and Gardella, D., "Prestress Losses in a Post-Tensioned R/C Box Girder Bridge in Southern Nevada," Civil Engineering Department, CCEER-94-5, University of Nevada, Reno, August 1994.
- CCEER-95-1 Siddharthan, R., El-Gamal, M., and Maragakis, E.A., "Nonlinear Bridge Abutment , Verification, and Design Curves," Civil Engineering Department, CCEER-95-1, University of Nevada, Reno, January 1995.
- CCEER-95-2 Ashour, M. and Norris, G., "Liquefaction and Undrained Response Evaluation of Sands from Drained Formulation," Civil Engineering Department, Report No. CCEER-95-2, University of Nevada, Reno, February 1995.
- CCEER-95-3 Wehbe, N., Saiidi, M., Sanders, D. and Douglas, B., "Ductility of Rectangular Reinforced Concrete Bridge Columns with Moderate Confinement," Civil Engineering Department, Report No. CCEER-95-3, University of Nevada, Reno, July 1995.
- CCEER-95-4 Martin, T., Saiidi, M. and Sanders, D., "Seismic Retrofit of Column-Pier Cap Connections in Bridges in Northern Nevada," Civil Engineering Department, Report No. CCEER-95-4, University of Nevada, Reno, August 1995.
- CCEER-95-5 Darwish, I., Saiidi, M. and Sanders, D., "Experimental Study of Seismic Susceptibility Column-Footing Connections in Bridges in Northern Nevada," Civil Engineering Department, Report No. CCEER-95-5, University of Nevada, Reno, September 1995.

- CCEER-95-6 Griffin, G., Saiidi, M. and Maragakis, E., "Nonlinear Seismic Response of Isolated Bridges and Effects of Pier Ductility Demand," Civil Engineering Department, Report No. CCEER-95-6, University of Nevada, Reno, November 1995.
- CCEER-95-7 Acharya, S., Saiidi, M. and Sanders, D., "Seismic Retrofit of Bridge Footings and Column-Footing Connections," Civil Engineering Department, Report No. CCEER-95-7, University of Nevada, Reno, November 1995.
- CCEER-95-8 Maragakis, E., Douglas, B., and Sandirasegaram, U., "Full-Scale Field Resonance Tests of a Railway Bridge," A Report to the Association of American Railroads, Civil Engineering Department, Report No. CCEER-95-8, University of Nevada, Reno, December 1995.
- CCEER-95-9 Douglas, B., Maragakis, E. and Feng, S., "System Identification Studies on Cazenovia Creek Overpass," Report for the National Center for Earthquake Engineering Research, Civil Engineering Department, Report No. CCEER-95-9, University of Nevada, Reno, October 1995.
- CCEER-96-1 El-Gamal, M.E. and Siddharthan, R.V., "Programs to Computer Translational Stiffness of Seat-Type Bridge Abutment," Civil Engineering Department, Report No. CCEER-96-1, University of Nevada, Reno, March 1996.
- CCEER-96-2 Labia, Y., Saiidi, M. and Douglas, B., "Evaluation and Repair of Full-Scale Prestressed Concrete Box Girders," A Report to the National Science Foundation, Research Grant CMS-9201908, Civil Engineering Department, Report No. CCEER-96-2, University of Nevada, Reno, May 1996.
- CCEER-96-3 Darwish, I., Saiidi, M. and Sanders, D., "Seismic Retrofit of R/C Oblong Tapered Bridge Columns with Inadequate Bar Anchorage in Columns and Footings," A Report to the Nevada Department of Transportation, Civil Engineering Department, Report No. CCEER-96-3, University of Nevada, Reno, May 1996.
- CCEER-96-4 Ashour, M., Pilling, R., Norris, G. and Perez, H., "The Prediction of Lateral Load Behavior of Single Piles and Pile Groups Using the Strain Wedge Model," A Report to the California Department of Transportation, Civil Engineering Department, Report No. CCEER-96-4, University of Nevada, Reno, June 1996.
- CCEER-97-1-A Rimal, P. and Itani, A. "Sensitivity Analysis of Fatigue Evaluations of Steel Bridges," Center for Earthquake Research, Department of Civil Engineering, University of Nevada, Reno, Nevada Report No. CCEER-97-1-A, September, 1997.
- CCEER-97-1-B Maragakis, E., Douglas, B., and Sandirasegaram, U. "Full-Scale Field Resonance Tests of a Railway Bridge," A Report to the Association of American Railroads, Civil Engineering Department, University of Nevada, Reno, May, 1996.
- CCEER-97-2 Wehbe, N., Saiidi, M., and D. Sanders, "Effect of Confinement and Flares on the Seismic Performance of Reinforced Concrete Bridge Columns," Civil Engineering Department, Report No. CCEER-97-2, University of Nevada, Reno, September 1997.
- CCEER-97-3 Darwish, I., M. Saiidi, G. Norris, and E. Maragakis, "Determination of In-Situ Footing Stiffness Using Full-Scale Dynamic Field Testing," A Report to the Nevada Department of Transportation, Structural Design Division, Carson City, Nevada, Report No. CCEER-97-3, University of Nevada, Reno, October 1997.
- CCEER-97-4-A Itani, A. "Cyclic Behavior of Richmond-San Rafael Tower Links," Center for Civil Engineering Earthquake Research, Department of Civil Engineering, University of Nevada, Reno, Nevada, Report No. CCEER-97-4, August 1997.

- CCEER-97-4-B Wehbe, N., and M. Saiidi, "User's Manual for RCMC v. 1.2 : A Computer Program for Moment-Curvature Analysis of Confined and Unconfined Reinforced Concrete Sections," Center for Civil Engineering Earthquake Research, Department of Civil Engineering, University of Nevada, Reno, Nevada, Report No. CCEER-97-4, November, 1997.
- CCEER-97-5 Isakovic, T., M. Saiidi, and A. Itani, "Influence of new Bridge Configurations on Seismic Performance," Department of Civil Engineering, University of Nevada, Reno, Report No. CCEER-97-5, September, 1997.
- CCEER-98-1 Itani, A., Vesco, T. and Dietrich, A., "Cyclic Behavior of "as Built" Laced Members With End Gusset Plates on the San Francisco Bay Bridge," Center for Civil Engineering Earthquake Research, Department of Civil Engineering, University of Nevada, Reno, Nevada Report No. CCEER-98-1, March, 1998.
- CCEER-98-2 G. Norris and M. Ashour, "Liquefaction and Undrained Response Evaluation of Sands from Drained Formulation," Center for Civil Engineering Earthquake Research, Department of Civil Engineering, University of Nevada, Reno, Nevada, Report No. CCEER-98-2, May, 1998.
- CCEER-98-3 Qingbin, Chen, B. M. Douglas, E. Maragakis, and I. G. Buckle, "Extraction of Nonlinear Hysteretic Properties of Seismically Isolated Bridges from Quick-Release Field Tests," Center for Civil Engineering Earthquake Research, Department of Civil Engineering, University of Nevada, Reno, Nevada, Report No. CCEER-98-3, June, 1998.
- CCEER-98-4 Maragakis, E., B. M. Douglas, and C. Qingbin, "Full-Scale Field Capacity Tests of a Railway Bridge," Center for Civil Engineering Earthquake Research, Department of Civil Engineering, University of Nevada, Reno, Nevada, Report No. CCEER-98-4, June, 1998.
- CCEER-98-5 Itani, A., Douglas, B., and Woodgate, J., "Cyclic Behavior of Richmond-San Rafael Retrofitted Tower Leg," Center for Civil Engineering Earthquake Research, Department of Civil Engineering, University of Nevada, Reno. Report No. CCEER-98-5, June 1998
- CCEER-98-6 Moore, R., Saiidi, M., and Itani, A., "Seismic Behavior of New Bridges with Skew and Curvature," Center for Civil Engineering Earthquake Research, Department of Civil Engineering, University of Nevada, Reno. Report No. CCEER-98-6, October, 1998.
- CCEER-98-7 Itani, A and Dietrich, A, "Cyclic Behavior of Double Gusset Plate Connections," Center for Civil Engineering Earthquake Research, Department of Civil Engineering, University of Nevada, Reno, Nevada, Report No. CCEER-98-5, December, 1998.
- CCEER-99-1 Caywood, C., M. Saiidi, and D. Sanders, "Seismic Retrofit of Flared Bridge Columns with Steel Jackets," Civil Engineering Department, University of Nevada, Reno, Report No. CCEER-99-1, February 1999.
- CCEER-99-2 Mangoba, N., M. Mayberry, and M. Saiidi, "Prestress Loss in Four Box Girder Bridges in Northern Nevada," Civil Engineering Department, University of Nevada, Reno, Report No. CCEER-99-2, March 1999.
- CCEER-99-3 Abo-Shadi, N., M. Saiidi, and D. Sanders, "Seismic Response of Bridge Pier Walls in the Weak Direction," Civil Engineering Department, University of Nevada, Reno, Report No. CCEER-99-3, April 1999.
- CCEER-99-4 Buzick, A., and M. Saiidi, "Shear Strength and Shear Fatigue Behavior of Full-Scale Prestressed Concrete Box Girders," Civil Engineering Department, University of Nevada, Reno, Report No. CCEER-99-4, April 1999.

- CCEER-99-5 Randall, M., M. Saiidi, E. Maragakis and T. Isakovic, "Restrainer Design Procedures For Multi-Span Simply-Supported Bridges," Civil Engineering Department, University of Nevada, Reno, Report No. CCEER-99-5, April 1999.
- CCEER-99-6 Wehbe, N. and M. Saiidi, "User's Manual for RCMC v. 1.2, A Computer Program for Moment-Curvature Analysis of Confined and Unconfined Reinforced Concrete Sections," Civil Engineering Department, University of Nevada, Reno, Report No. CCEER-99-6, May 1999.
- CCEER-99-7 Burda, J. and A. Itani, "Studies of Seismic Behavior of Steel Base Plates," Civil Engineering Department, University of Nevada, Reno, Report No. CCEER-99-7, May 1999.
- CCEER-99-8 Ashour, M. and G. Norris, "Refinement of the Strain Wedge Model Program," Civil Engineering Department, University of Nevada, Reno, Report No. CCEER-99-8, March 1999.
- CCEER-99-9 Dietrich, A., and A. Itani, "Cyclic Behavior of Laced and Perforated Steel Members on the San Francisco-Oakland Bay Bridge," Civil Engineering Department, University, Reno, Report No. CCEER-99-9, December 1999.
- CCEER 99-10 Itani, A., A. Dietrich, "Cyclic Behavior of Built Up Steel Members and their Connections," Civil Engineering Department, University of Nevada, Reno, Report No. CCEER-99-10, December 1999.
- CCEER 99-10-A Itani, A., E. Maragakis and P. He, "Fatigue Behavior of Riveted Open Deck Railroad Bridge Girders," Civil Engineering Department, University of Nevada, Reno, Report No. CCEER-99-10-A, August 1999.
- CCEER 99-11 Itani, A., J. Woodgate, "Axial and Rotational Ductility of Built Up Structural Steel Members," Civil Engineering Department, University of Nevada, Reno, Report No. CCEER-99-11, December 1999.
- CCEER-99-12 Sgambelluri, M., Sanders, D.H., and Saiidi, M.S., "Behavior of One-Way Reinforced Concrete Bridge Column Hinges in the Weak Direction," Department of Civil Engineering, University of Nevada, Reno, Report No. CCEER-99-12, December 1999.
- CCEER-99-13 Laplace, P., Sanders, D.H., Douglas, B, and Saiidi, M, "Shake Table Testing of Flexure Dominated Reinforced Concrete Bridge Columns", Department of Civil Engineering, University of Nevada, Reno, Report No. CCEER-99-13, December 1999.
- CCEER-99-14 Ahmad M. Itani, Jose A. Zepeda, and Elizabeth A. Ware "Cyclic Behavior of Steel Moment Frame Connections for the Moscone Center Expansion," Department of Civil Engineering, University of Nevada, Reno, Report No. CCEER-99-14, December 1999.
- CCEER 00-1 Ashour, M., and Norris, G. "Undrained Lateral Pile and Pile Group Response in Saturated Sand," Civil Engineering Department, University of Nevada, Reno, Report No. CCEER-00-1, May 1999. January 2000.
- CCEER 00-2 Saiidi, M. and Wehbe, N., "A Comparison of Confinement Requirements in Different Codes for Rectangular, Circular, and Double-Spiral RC Bridge Columns," Civil Engineering Department, University of Nevada, Reno, Report No. CCEER-00-2, January 2000.
- CCEER 00-3 McElhaney, B., M. Saiidi, and D. Sanders, "Shake Table Testing of Flared Bridge Columns With Steel Jacket Retrofit," Civil Engineering Department, University of Nevada, Reno, Report No. CCEER-00-3, January 2000.
- CCEER 00-4 Martinovic, F., M. Saiidi, D. Sanders, and F. Gordaninejad, "Dynamic Testing of Non-Prismatic Reinforced Concrete Bridge Columns Retrofitted with FRP Jackets," Civil Engineering Department, University of Nevada, Reno, Report No. CCEER-00-4, January 2000.

- CCEER 00-5 Itani, A., and M. Saiidi, "Seismic Evaluation of Steel Joints for UCLA Center for Health Science Westwood Replacement Hospital," Civil Engineering Department, University of Nevada, Reno, Report No. CCEER-00-5, February 2000.
- CCEER 00-6 Will, J. and D. Sanders, "High Performance Concrete Using Nevada Aggregates," Civil Engineering Department, University of Nevada, Reno, Report No. CCEER-00-6, May 2000.
- CCEER 00-7 French, C., and M. Saiidi, "A Comparison of Static and Dynamic Performance of Models of Flared Bridge Columns," Civil Engineering Department, University of Nevada, Reno, Report No. CCEER-00-7, October 2000.
- CCEER 00-8 Itani, A., H. Sedarat, "Seismic Analysis of the AISI LRFD Design Example of Steel Highway Bridges," Civil Engineering Department, University of Nevada, Reno, Report No. CCEER 00-08, November 2000.
- CCEER 00-9 Moore, J., D. Sanders, and M. Saiidi, "Shake Table Testing of 1960's Two Column Bent with Hinges Bases," Civil Engineering Department, University of Nevada, Reno, Report No. CCEER 00-09, December 2000.
- CCEER 00-10 Asthana, M., D. Sanders, and M. Saiidi, "One-Way Reinforced Concrete Bridge Column Hinges in the Weak Direction," Civil Engineering Department, University of Nevada, Reno, Report No. CCEER 00-10, April 2001.
- CCEER 01-1 Ah Sha, H., D. Sanders, M. Saiidi, "Early Age Shrinkage and Cracking of Nevada Concrete Bridge Decks," Civil Engineering Department, University of Nevada, Reno, Report No. CCEER 01-01, May 2001.
- CCEER 01-2 Ashour, M. and G. Norris, "Pile Group program for Full Material Modeling a Progressive Failure," Civil Engineering Department, University of Nevada, Reno, Report No. CCEER 01-02, July 2001.
- CCEER 01-3 Itani, A., C. Lanaud, and P. Dusicka, "Non-Linear Finite Element Analysis of Built-Up Shear Links," Civil Engineering Department, University of Nevada, Reno, Report No. CCEER 01-03, July 2001.
- CCEER 01-4 Saiidi, M., J. Mortensen, and F. Martinovic, "Analysis and Retrofit of Fixed Flared Columns with Glass Fiber-Reinforced Plastic Jacketing," Civil Engineering Department, University of Nevada, Reno, Report No. CCEER 01-4, August 2001
- CCEER 01-5 Not Published
- CCEER 01-6 Laplace, P., D. Sanders, and M. Saiidi, "Experimental Study and Analysis of Retrofitted Flexure and Shear Dominated Circular Reinforced Concrete Bridge Columns Subjected to Shake Table Excitation," Civil Engineering Department, University of Nevada, Reno, Report No. CCEER 01-6, June 2001.
- CCEER 01-7 Reppi, F., and D. Sanders, "Removal and Replacement of Cast-in-Place, Post-tensioned, Box Girder Bridge," Civil Engineering Department, University of Nevada, Reno, Report No. CCEER 01-7, December 2001.
- CCEER 02-1 Pulido, C., M. Saiidi, D. Sanders, and A. Itani, "Seismic Performance and Retrofitting of Reinforced Concrete Bridge Bents," Civil Engineering Department, University of Nevada, Reno, Report No. CCEER 02-1, January 2002.
- CCEER 02-2 Yang, Q., M. Saiidi, H. Wang, and A. Itani, "Influence of Ground Motion Incoherency on Earthquake Response of Multi-Support Structures," Civil Engineering Department, University of Nevada, Reno, Report No. CCEER 02-2, May 2002.
- CCEER 02-3 M. Saiidi, B. Gopalakrishnan, E. Reinhardt, and R. Siddharthan, "A Preliminary Study of Shake Table Response of A Two-Column Bridge Bent on Flexible Footings," Civil Engineering Department, University of Nevada, Reno, Report No. CCEER 02-03, June 2002.

- CCEER 02-4 Not Published
- CCEER 02-5 Banghart, A., Sanders, D., Saiidi, M., "Evaluation of Concrete Mixes for Filling the Steel Arches in the Galena Creek Bridge," Civil Engineering Department, University of Nevada, Reno, Report No. CCEER 02-05, June 2002.
- CCEER 02-6 Dusicka, P., Itani, A., Buckle, I. G., "Cyclic Behavior of Shear Links and Tower Shaft Assembly of San Francisco – Oakland Bay Bridge Tower," Civil Engineering Department, University of Nevada, Reno, Report No. CCEER 02-06, July 2002.
- CCEER 02-7 Mortensen, J., and M. Saiidi, "A Performance-Based Design Method for Confinement in Circular Columns," Civil Engineering Department, University of Nevada, Reno, Report No. CCEER 02-07, November 2002.
- CCEER 03-1 Wehbe, N., and M. Saiidi, "User's manual for SPMC v. 1.0 : A Computer Program for Moment-Curvature Analysis of Reinforced Concrete Sections with Interlocking Spirals," Center for Civil Engineering Earthquake Research, Department of Civil Engineering, University of Nevada, Reno, Nevada, Report No. CCEER-03-1, May, 2003.
- CCEER 03-2 Wehbe, N., and M. Saiidi, "User's manual for RCMC v. 2.0 : A Computer Program for Moment-Curvature Analysis of Confined and Unconfined Reinforced Concrete Sections," Center for Civil Engineering Earthquake Research, Department of Civil Engineering, University of Nevada, Reno, Nevada, Report No. CCEER-03-2, June, 2003.
- CCEER 03-3 Nada, H., D. Sanders, and M. Saiidi, "Seismic Performance of RC Bridge Frames with Architectural-Flared Columns," Civil Engineering Department, University of Nevada, Reno, Report No. CCEER 03-3, January 2003.
- CCEER 03-4 Reinhardt, E., M. Saiidi, and R. Siddharthan, "Seismic Performance of a CFRP/ Concrete Bridge Bent on Flexible Footings," Civil Engineering Department, University of Nevada, Reno, Report No. CCEER 03-4, August 2003.
- CCEER 03-5 Johnson, N., M. Saiidi, A. Itani, and S. Ladhany, "Seismic Retrofit of Octagonal Columns with Pedestal and One-Way Hinge at the Base," Center for Civil Engineering Earthquake Research, Department of Civil Engineering, University of Nevada, Reno, Nevada, and Report No. CCEER-03-5, August 2003.
- CCEER 03-6 Mortensen, C., M. Saiidi, and S. Ladhany, "Creep and Shrinkage Losses in Highly Variable Climates," Center for Civil Engineering Earthquake Research, Department of Civil Engineering, University of Nevada, Reno, Report No. CCEER-03-6, September 2003.
- CCEER 03-7 Ayoub, C., M. Saiidi, and A. Itani, "A Study of Shape-Memory-Alloy-Reinforced Beams and Cubes," Center for Civil Engineering Earthquake Research, Department of Civil Engineering, University of Nevada, Reno, Nevada, Report No. CCEER-03-7, October 2003.
- CCEER 03-8 Chandane, S., D. Sanders, and M. Saiidi, "Static and Dynamic Performance of RC Bridge Bents with Architectural-Flared Columns," Center for Civil Engineering Earthquake Research, Department of Civil Engineering, University of Nevada, Reno, Nevada, Report No. CCEER-03-8, November 2003.
- CCEER 04-1 Olaegbe, C., and Saiidi, M., "Effect of Loading History on Shake Table Performance of A Two-Column Bent with Infill Wall," Center for Civil Engineering Earthquake Research, Department of Civil Engineering, University of Nevada, Reno, Nevada, Report No. CCEER-04-1, January 2004.
- CCEER 04-2 Johnson, R., Maragakis, E., Saiidi, M., and DesRoches, R., "Experimental Evaluation of Seismic Performance of SMA Bridge Restrainers," Center for Civil Engineering Earthquake Research,

Department of Civil Engineering, University of Nevada, Reno, Nevada, Report No. CCEER-04-2, February 2004.

- CCEER 04-3 Moustafa, K., Sanders, D., and Saiidi, M., "Impact of Aspect Ratio on Two-Column Bent Seismic Performance," Center for Civil Engineering Earthquake Research, Department of Civil Engineering, University of Nevada, Reno, Nevada, Report No. CCEER-04-3, February 2004.
- CCEER 04-4 Maragakis, E., Saiidi, M., Sanchez-Camargo, F., and Elfass, S., "Seismic Performance of Bridge Restrainers At In-Span Hinges," Center for Civil Engineering Earthquake Research, Department of Civil Engineering, University of Nevada, Reno, Nevada, Report No. CCEER-04-4, March 2004.
- CCEER 04-5 Ashour, M., Norris, G. and Elfass, S., "Analysis of Laterally Loaded Long or Intermediate Drilled Shafts of Small or Large Diameter in Layered Soil," Center for Civil Engineering Earthquake Research, Department of Civil Engineering, University of Nevada, Reno, Nevada, Report No. CCEER-04-5, June 2004.
- CCEER 04-6 Correal, J., Saiidi, M. and Sanders, D., "Seismic Performance of RC Bridge Columns Reinforced with Two Interlocking Spirals," Center for Civil Engineering Earthquake Research, Department of Civil Engineering, University of Nevada, Reno, Nevada, Report No. CCEER-04-6, August 2004.
- CCEER 04-7 Dusicka, P., Itani, A. and Buckle, I., "Cyclic Response and Low Cycle Fatigue Characteristics of Plate Steels," Center for Civil Engineering Earthquake Research, Department of Civil Engineering, University of Nevada, Reno, Nevada, Report No. CCEER-04-7, November 2004.
- CCEER 04-8 Dusicka, P., Itani, A. and Buckle, I., "Built-up Shear Links as Energy Dissipaters for Seismic Protection of Bridges," Center for Civil Engineering Earthquake Research, Department of Civil Engineering, University of Nevada, Reno, Nevada, Report No. CCEER-04-8, November 2004.
- CCEER 04-9 Sureshkumar, K., Saiidi, S., Itani, A. and Ladhani, S., "Seismic Retrofit of Two-Column Bents with Diamond Shape Columns," Center for Civil Engineering Earthquake Research, Department of Civil Engineering, University of Nevada, Reno, Nevada, Report No. CCEER-04-9, November 2004.
- CCEER 05-1 Wang, H. and Saiidi, S., "A Study of RC Columns with Shape Memory Alloy and Engineered Cementitious Composites," Center for Civil Engineering Earthquake Research, Department of Civil Engineering, University of Nevada, Reno, Nevada, Report No. CCEER-05-1, January 2005.
- CCEER 05-2 Johnson, R., Saiidi, S. and Maragakis, E., "A Study of Fiber Reinforced Plastics for Seismic Bridge Restrainers," Center for Civil Engineering Earthquake Research, Department of Civil Engineering, University of Nevada, Reno, Nevada, Report No. CCEER-05-2, January 2005.
- CCEER 05-3 Carden, L.P., Itani, A.M., Buckle, I.G., "Seismic Load Path in Steel Girder Bridge Superstructures," Center for Civil Engineering Earthquake Research, Department of Civil Engineering, University of Nevada, Reno, Nevada, Report No. CCEER-05-3, January 2005.
- CCEER 05-4 Carden, L.P., Itani, A.M., Buckle, I.G., "Seismic Performance of Steel Girder Bridge Superstructures with Ductile End Cross Frames and Seismic Isolation," Center for Civil Engineering Earthquake Research, Department of Civil Engineering, University of Nevada, Reno, Nevada, Report No. CCEER-05-4, January 2005.
- CCEER 05-5 Goodwin, E., Maragakis, M., Itani, A. and Luo, S., "Experimental Evaluation of the Seismic Performance of Hospital Piping Subassemblies," Center for Civil Engineering Earthquake Research, Department of Civil Engineering, University of Nevada, Reno, Nevada, Report No. CCEER-05-5, February 2005.

- CCEER 05-6 Zadeh M. S., Saiidi, S, Itani, A. and Ladkany, S., “Seismic Vulnerability Evaluation and Retrofit Design of Las Vegas Downtown Viaduct,” Center for Civil Engineering Earthquake Research, Department of Civil Engineering, University of Nevada, Reno, Nevada, Report No. CCEER-05-6, February 2005.
- CCEER 05-7 Phan, V., Saiidi, S. and Anderson, J., “Near Fault (Near Field) Ground Motion Effects on Reinforced Concrete Bridge Columns,” Center for Civil Engineering Earthquake Research, Department of Civil Engineering, University of Nevada, Reno, Nevada, Report No. CCEER-05-7, August 2005.
- CCEER 05-8 Carden, L., Itani, A. and Laplace, P., “Performance of Steel Props at the UNR Fire Science Academy subjected to Repeated Fire,” Center for Civil Engineering Earthquake Research, Department of Civil Engineering, University of Nevada, Reno, Nevada, Report No. CCEER-05-8, August 2005.
- CCEER 05-9 Yamashita, R. and Sanders, D., “Shake Table Testing and an Analytical Study of Unbonded Prestressed Hollow Concrete Column Constructed with Precast Segments,” Center for Civil Engineering Earthquake Research, Department of Civil Engineering, University of Nevada, Reno, Nevada, Report No. CCEER-05-9, August 2005.
- CCEER 05-10 Not Published
- CCEER 05-11 Carden, L., Itani, A., and Peckan, G., “Recommendations for the Design of Beams and Posts in Bridge Falsework,” Center for Civil Engineering Earthquake Research, Department of Civil Engineering, University of Nevada, Reno, Nevada, Report No. CCEER-05-11, October 2005.
- CCEER 06-01 Cheng, Z., Saiidi, M., and Sanders, D., “Development of a Seismic Design Method for Reinforced Concrete Two-Way Bridge Column Hinges,” Center for Civil Engineering Earthquake Research, Department of Civil Engineering, University of Nevada, Reno, Nevada, Report No. CCEER-06-01, February 2006.
- CCEER 06-02 Johnson, N., Saiidi, M., and Sanders, D., “Large-Scale Experimental and Analytical Studies of a Two-Span Reinforced Concrete Bridge System,” Center for Civil Engineering Earthquake Research, Department of Civil Engineering, University of Nevada, Reno, Nevada, Report No. CCEER-06-02, March 2006.
- CCEER 06-03 Saiidi, M., Ghasemi, H. and Tiras, A., “Seismic Design and Retrofit of Highway Bridges,” Proceedings, Second US-Turkey Workshop, Center for Civil Engineering Earthquake Research, Department of Civil Engineering, University of Nevada, Reno, Nevada, Report No. CCEER-06-03, May 2006.
- CCEER 07-01 O'Brien, M., Saiidi, M. and Sadrossadat-Zadeh, M., “A Study of Concrete Bridge Columns Using Innovative Materials Subjected to Cyclic Loading,” Center for Civil Engineering Earthquake Research, Department of Civil Engineering, University of Nevada, Reno, Nevada, Report No. CCEER-07-01, January 2007.
- CCEER 07-02 Sadrossadat-Zadeh, M. and Saiidi, M., “Effect of Strain rate on Stress-Strain Properties and Yield Propagation in Steel Reinforcing Bars,” Center for Civil Engineering Earthquake Research, Department of Civil Engineering, University of Nevada, Reno, Nevada, Report No. CCEER-07-02, January 2007.
- CCEER 07-03 Sadrossadat-Zadeh, M. and Saiidi, M., “Analytical Study of NEESR-SG 4-Span Bridge Model Using OpenSees,” Center for Civil Engineering Earthquake Research, Department of Civil Engineering, University of Nevada, Reno, Nevada, Report No. CCEER-07-03, January 2007.
- CCEER 07-04 Nelson, R., Saiidi, M. and Zadeh, S., “Experimental Evaluation of Performance of Conventional Bridge Systems,” Center for Civil Engineering Earthquake Research, Department of Civil Engineering, University of Nevada, Reno, Nevada, Report No. CCEER-07-04, October 2007.

- CCEER 07-05 Bahen, N. and Sanders, D., "Strut-and-Tie Modeling for Disturbed Regions in Structural Concrete Members with Emphasis on Deep Beams," Center for Civil Engineering Earthquake Research, Department of Civil Engineering, University of Nevada, Reno, Nevada, Report No. CCEER-07-05, December 2007.
- CCEER 07-06 Choi, H., Saiidi, M. and Somerville, P., "Effects of Near-Fault Ground Motion and Fault-Rupture on the Seismic Response of Reinforced Concrete Bridges," Center for Civil Engineering Earthquake Research, Department of Civil Engineering, University of Nevada, Reno, Nevada, Report No. CCEER-07-06, December 2007.
- CCEER 07-07 Ashour M. and Norris, G., "Report and User Manual on Strain Wedge Model Computer Program for Files and Large Diameter Shafts with LRFD Procedure," Center for Civil Engineering Earthquake Research, Department of Civil Engineering, University of Nevada, Reno, Nevada, Report No. CCEER-07-07, October 2007.
- CCEER 08-01 Doyle, K. and Saiidi, M., "Seismic Response of Telescopic Pipe Pin Connections," Center for Civil Engineering Earthquake Research, Department of Civil Engineering, University of Nevada, Reno, Nevada, Report No. CCEER-08-01, February 2008.
- CCEER 08-02 Taylor, M. and Sanders, D., "Seismic Time History Analysis and Instrumentation of the Galena Creek Bridge," Center for Civil Engineering Earthquake Research, Department of Civil Engineering, University of Nevada, Reno, Nevada, Report No. CCEER-08-02, April 2008.
- CCEER 08-03 Abdel-Mohti, A. and Pekcan, G., "Seismic Response Assessment and Recommendations for the Design of Skewed Post-Tensioned Concrete Box-Girder Highway Bridges," Center for Civil Engineering Earthquake Research, Department of Civil and Environmental Engineering, University of Nevada, Reno, Nevada, Report No. CCEER-08-03, September 2008.
- CCEER 08-04 Saiidi, M., Ghasemi, H. and Hook, J., "Long Term Bridge Performance Monitoring, Assessment & Management," Proceedings, FHWA/NSF Workshop on Future Directions," Center for Civil Engineering Earthquake Research, Department of Civil and Environmental Engineering, University of Nevada, Reno, Nevada, Report No. CCEER 08-04, September 2008.
- CCEER 09-01 Brown, A., and Saiidi, M., "Investigation of Near-Fault Ground Motion Effects on Substandard Bridge Columns and Bents," Center for Civil Engineering Earthquake Research, Department of Civil and Environmental Engineering, University of Nevada, Reno, Nevada, Report No. CCEER-09-01, July 2009.
- CCEER 09-02 Linke, C., Pekcan, G., and Itani, A., "Detailing of Seismically Resilient Special Truss Moment Frames," Center for Civil Engineering Earthquake Research, Department of Civil and Environmental Engineering, University of Nevada, Reno, Nevada, Report No. CCEER-09-02, August 2009.
- CCEER 09-03 Hillis, D., and Saiidi, M., "Design, Construction, and Nonlinear Dynamic Analysis of Three Bridge Bents Used in a Bridge System Test," Center for Civil Engineering Earthquake Research, Department of Civil and Environmental Engineering, University of Nevada, Reno, Nevada, Report No. CCEER-09-03, August 2009.
- CCEER 09-04 Bahrami, H., Itani, A., and Buckle, I., "Guidelines for the Seismic Design of Ductile End Cross Frames in Steel Girder Bridge Superstructures," Center for Civil Engineering Earthquake Research, Department of Civil and Environmental Engineering, University of Nevada, Reno, Nevada, Report No. CCEER-09-04, September 2009.
- CCEER 10-01 Zaghi, A. E., and Saiidi, M., "Seismic Design of Pipe-Pin Connections in Concrete Bridges," Center for Civil Engineering Earthquake Research, Department of Civil and Environmental Engineering, University of Nevada, Reno, Nevada, Report No. CCEER-10-01, January 2010.

- CCEER 10-02 Pooranampillai, S., Elfass, S., and Norris, G., "Laboratory Study to Assess Load Capacity Increase of Drilled Shafts through Post Grouting," Center for Civil Engineering Earthquake Research, Department of Civil and Environmental Engineering, University of Nevada, Reno, Nevada, Report No. CCEER-10-02, January 2010.
- CCEER 10-03 Itani, A., Grubb, M., and Monzon, E., "Proposed Seismic Provisions and Commentary for Steel Plate Girder Superstructures," Center for Civil Engineering Earthquake Research, Department of Civil and Environmental Engineering, University of Nevada, Reno, Nevada, Report No. CCEER-10-03, June 2010.
- CCEER 10-04 Cruz-Noguez, C., Saiidi, M., "Experimental and Analytical Seismic Studies of a Four-Span Bridge System with Innovative Materials," Center for Civil Engineering Earthquake Research, Department of Civil and Environmental Engineering, University of Nevada, Reno, Nevada, Report No. CCEER-10-04, September 2010.
- CCEER 10-05 Vosooghi, A., Saiidi, M., "Post-Earthquake Evaluation and Emergency Repair of Damaged RC Bridge Columns Using CFRP Materials," Center for Civil Engineering Earthquake Research, Department of Civil and Environmental Engineering, University of Nevada, Reno, Nevada, Report No. CCEER-10-05, September 2010.
- CCEER 10-06 Ayoub, M., Sanders, D., "Testing of Pile Extension Connections to Slab Bridges," Center for Civil Engineering Earthquake Research, Department of Civil and Environmental Engineering, University of Nevada, Reno, Nevada, Report No. CCEER-10-06, October 2010.
- CCEER 10-07 Builes-Mejia, J. C. and Itani, A., "Stability of Bridge Column Rebar Cages during Construction," Center for Civil Engineering Earthquake Research, Department of Civil and Environmental Engineering, University of Nevada, Reno, Nevada, Report No. CCEER-10-07, November 2010.
- CCEER 10-08 Monzon, E.V., "Seismic Performance of Steel Plate Girder Bridges with Integral Abutments," Center for Civil Engineering Earthquake Research, Department of Civil and Environmental Engineering, University of Nevada, Reno, Nevada, Report No. CCEER-10-08, November 2010.
- CCEER 11-01 Motaref, S., Saiidi, M., and Sanders, D., "Seismic Response of Precast Bridge Columns with Energy Dissipating Joints," Center for Civil Engineering Earthquake Research, Department of Civil and Environmental Engineering, University of Nevada, Reno, Nevada, Report No. CCEER-11-01, May 2011.
- CCEER 11-02 Harrison, N. and Sanders, D., "Preliminary Seismic Analysis and Design of Reinforced Concrete Bridge Columns for Curved Bridge Experiments," Center for Civil Engineering Earthquake Research, Department of Civil and Environmental Engineering, University of Nevada, Reno, Nevada, Report No. CCEER-11-02, May 2011.
- CCEER 11-03 Vallejera, J. and Sanders, D., "Instrumentation and Monitoring the Galena Creek Bridge," Center for Civil Engineering Earthquake Research, Department of Civil and Environmental Engineering, University of Nevada, Reno, Nevada, Report No. CCEER-11-03, September 2011.
- CCEER 11-04 Levi, M., Sanders, D., and Buckle, I., "Seismic Response of Columns in Horizontally Curved Bridges," Center for Civil Engineering Earthquake Research, Department of Civil and Environmental Engineering, University of Nevada, Reno, Nevada, Report No. CCEER-11-04, December 2011.
- CCEER 12-01 Saiidi, M., "NSF International Workshop on Bridges of the Future – Wide Spread Implementation of Innovation," Center for Civil Engineering Earthquake Research, Department of Civil and Environmental Engineering, University of Nevada, Reno, Nevada, Report No. CCEER-12-01, January 2012.

- CCEER 12-02 Larkin, A.S., Sanders, D., and Saiidi, M., “Unbonded Prestressed Columns for Earthquake Resistance,” Center for Civil Engineering Earthquake Research, Department of Civil and Environmental Engineering, University of Nevada, Reno, Nevada, Report No. CCEER-12-02, January 2012.
- CCEER 12-03 Arias-Acosta, J. G., Sanders, D., “Seismic Performance of Circular and Interlocking Spirals RC Bridge Columns under Bidirectional Shake Table Loading Part 1,” Center for Civil Engineering Earthquake Research, Department of Civil and Environmental Engineering, University of Nevada, Reno, Nevada, Report No. CCEER-12-03, September 2012.
- CCEER 12-04 Cukrov, M.E., Sanders, D., “Seismic Performance of Prestressed Pile-To-Bent Cap Connections,” Center for Civil Engineering Earthquake Research, Department of Civil and Environmental Engineering, University of Nevada, Reno, Nevada, Report No. CCEER-12-04, September 2012.
- CCEER 13-01 Carr, T. and Sanders, D., “Instrumentation and Dynamic Characterization of the Galena Creek Bridge,” Center for Civil Engineering Earthquake Research, Department of Civil and Environmental Engineering, University of Nevada, Reno, Nevada, Report No. CCEER-13-01, January 2013.
- CCEER 13-02 Vosoghi, A. and Buckle, I., “Evaluation of the Performance of a Conventional Four-Span Bridge During Shake Table Tests,” Center for Civil Engineering Earthquake Research, Department of Civil and Environmental Engineering, University of Nevada, Reno, Nevada, Report No. CCEER-13-02, January 2013.
- CCEER 13-03 Amirhormozaki, E. and Pekcan, G., “Analytical Fragility Curves for Horizontally Curved Steel Girder Highway Bridges,” Center for Civil Engineering Earthquake Research, Department of Civil and Environmental Engineering, University of Nevada, Reno, Nevada, Report No. CCEER-13-03, February 2013.
- CCEER 13-04 Almer, K. and Sanders, D., “Longitudinal Seismic Performance of Precast Bridge Girders Integrally Connected to a Cast-in-Place Bentcap,” Center for Civil Engineering Earthquake Research, Department of Civil and Environmental Engineering, University of Nevada, Reno, Nevada, Report No. CCEER-13-04, April 2013.
- CCEER 13-05 Monzon, E.V., Itani, A.I., and Buckle, I.G., “Seismic Modeling and Analysis of Curved Steel Plate Girder Bridges,” Center for Civil Engineering Earthquake Research, Department of Civil and Environmental Engineering, University of Nevada, Reno, Nevada, Report No. CCEER-13-05, April 2013.
- CCEER 13-06 Monzon, E.V., Buckle, I.G., and Itani, A.I., “Seismic Performance of Curved Steel Plate Girder Bridges with Seismic Isolation,” Center for Civil Engineering Earthquake Research, Department of Civil and Environmental Engineering, University of Nevada, Reno, Nevada, Report No. CCEER-13-06, April 2013.
- CCEER 13-07 Monzon, E.V., Buckle, I.G., and Itani, A.I., “Seismic Response of Isolated Bridge Superstructure to Incoherent Ground Motions,” Center for Civil Engineering Earthquake Research, Department of Civil and Environmental Engineering, University of Nevada, Reno, Nevada, Report No. CCEER-13-07, April 2013.
- CCEER 13-08 Haber, Z.B., Saiidi, M.S., and Sanders, D.H., “Precast Column-Footing Connections for Accelerated Bridge Construction in Seismic Zones,” Center for Civil Engineering Earthquake Research, Department of Civil and Environmental Engineering, University of Nevada, Reno, Nevada, Report No. CCEER-13-08, April 2013.

- CCEER 13-09 Ryan, K.L., Coria, C.B., and Dao, N.D., "Large Scale Earthquake Simulation of a Hybrid Lead Rubber Isolation System Designed under Nuclear Seismicity Considerations," Center for Civil Engineering Earthquake Research, Department of Civil and Environmental Engineering, University of Nevada, Reno, Nevada, Report No. CCEER-13-09, April 2013.
- CCEER 13-10 Wibowo, H., Sanford, D.M., Buckle, I.G., and Sanders, D.H., "The Effect of Live Load on the Seismic Response of Bridges," Center for Civil Engineering Earthquake Research, Department of Civil and Environmental Engineering, University of Nevada, Reno, Nevada, Report No. CCEER-13-10, May 2013.
- CCEER 13-11 Sanford, D.M., Wibowo, H., Buckle, I.G., and Sanders, D.H., "Preliminary Experimental Study on the Effect of Live Load on the Seismic Response of Highway Bridges," Center for Civil Engineering Earthquake Research, Department of Civil and Environmental Engineering, University of Nevada, Reno, Nevada, Report No. CCEER-13-11, May 2013.
- CCEER 13-12 Saad, A.S., Sanders, D.H., and Buckle, I.G., "Assessment of Foundation Rocking Behavior in Reducing the Seismic Demand on Horizontally Curved Bridges," Center for Civil Engineering Earthquake Research, Department of Civil and Environmental Engineering, University of Nevada, Reno, Nevada, Report No. CCEER-13-12, June 2013.
- CCEER 13-13 Ardakani, S.M.S. and Saiidi, M.S., "Design of Reinforced Concrete Bridge Columns for Near-Fault Earthquakes," Center for Civil Engineering Earthquake Research, Department of Civil and Environmental Engineering, University of Nevada, Reno, Nevada, Report No. CCEER-13-13, July 2013.
- CCEER 13-14 Wei, C. and Buckle, I., "Seismic Analysis and Response of Highway Bridges with Hybrid Isolation," Center for Civil Engineering Earthquake Research, Department of Civil and Environmental Engineering, University of Nevada, Reno, Nevada, Report No. CCEER-13-14, August 2013.
- CCEER 13-15 Wibowo, H., Buckle, I.G., and Sanders, D.H., "Experimental and Analytical Investigations on the Effects of Live Load on the Seismic Performance of a Highway Bridge," Center for Civil Engineering Earthquake Research, Department of Civil and Environmental Engineering, University of Nevada, Reno, Nevada, Report No. CCEER-13-15, August 2013.
- CCEER 13-16 Itani, A.M., Monzon, E.V., Grubb, M., and Amirhormozaki, E. "Seismic Design and Nonlinear Evaluation of Steel I-Girder Bridges with Ductile End Cross-Frames," Center for Civil Engineering Earthquake Research, Department of Civil and Environmental Engineering, University of Nevada, Reno, Nevada, Report No. CCEER-13-16, September 2013.
- CCEER 13-17 Kavianipour, F. and Saiidi, M.S., "Experimental and Analytical Seismic Studies of a Four-span Bridge System with Composite Piers," Center for Civil Engineering Earthquake Research, Department of Civil and Environmental Engineering, University of Nevada, Reno, Nevada, Report No. CCEER-13-17, September 2013.
- CCEER 13-18 Mohebbsi, A., Ryan, K., and Sanders, D., "Seismic Response of a Highway Bridge with Structural Fuses for Seismic Protection of Piers," Center for Civil Engineering Earthquake Research,

Department of Civil and Environmental Engineering, University of Nevada, Reno, Nevada, Report No. CCEER-13-18, December 2013.

- CCEER 13-19 Guzman Pujols, Jean C., Ryan, K.L., “Development of Generalized Fragility Functions for Seismic Induced Content Disruption,” Center for Civil Engineering Earthquake Research, Department of Civil and Environmental Engineering, University of Nevada, Reno, Nevada, Report No. CCEER-13-19, December 2013.
- CCEER 14-01 Salem, M. M. A., Pekcan, G., and Itani, A., “Seismic Response Control Of Structures Using Semi-Active and Passive Variable Stiffness Devices,” Center for Civil Engineering Earthquake Research, Department of Civil and Environmental Engineering, University of Nevada, Reno, Nevada, Report No. CCEER-14-01, May 2014.
- CCEER 14-02 Saini, A. and Saiidi, M., “Performance-Based Probabilistic Damage Control Approach for Seismic Design of Bridge Columns,” Center For Civil Engineering Earthquake Research, Department Of Civil and Environmental Engineering, University of Nevada, Reno, Nevada, Report No. CCEER-14-02, May 2014.
- CCEER 14-03 Saini, A. and Saiidi, M., “Post Earthquake Damage Repair of Various Reinforced Concrete Bridge Components,” Center For Civil Engineering Earthquake Research, Department Of Civil and Environmental Engineering, University of Nevada, Reno, Nevada, Report No. CCEER-14-03, May 2014.
- CCEER 14-04 Monzon, E.V., Itani, A.M., and Grubb, M.A., “Nonlinear Evaluation of the Proposed Seismic Design Procedure for Steel Bridges with Ductile End Cross Frames,” Center For Civil Engineering Earthquake Research, Department Of Civil and Environmental Engineering, University of Nevada, Reno, Nevada, Report No. CCEER-14-04, July 2014.
- CCEER 14-05 Nakashoji, B. and Saiidi, M.S., “Seismic Performance of Square Nickel-Titanium Reinforced ECC Columns with Headed Couplers,” Center For Civil Engineering Earthquake Research, Department Of Civil and Environmental Engineering, University of Nevada, Reno, Nevada, Report No. CCEER-14-05, July 2014.
- CCEER 14-06 Tazarv, M. and Saiidi, M.S., “Next Generation of Bridge Columns for Accelerated Bridge Construction in High Seismic Zones,” Center For Civil Engineering Earthquake Research, Department Of Civil and Environmental Engineering, University of Nevada, Reno, Nevada, Report No. CCEER-14-06, August 2014.
- CCEER 14-07 Mehrsoroush, A. and Saiidi, M.S., “Experimental and Analytical Seismic Studies of Bridge Piers with Innovative Pipe Pin Column-Footing Connections and Precast Cap Beams,” Center For Civil Engineering Earthquake Research, Department Of Civil and Environmental Engineering, University of Nevada, Reno, Nevada, Report No. CCEER-14-07, December 2014.
- CCEER 15-01 Dao, N.D. and Ryan, K.L., “Seismic Response of a Full-scale 5-story Steel Frame Building Isolated by Triple Pendulum Bearings under 3D Excitations,” Center For Civil Engineering Earthquake Research, Department Of Civil and Environmental Engineering, University of Nevada, Reno, Nevada, Report No. CCEER-15-01, January 2015.
- CCEER 15-02 Allen, B.M. and Sanders, D.H., “Post-Tensioning Duct Air Pressure Testing Effects on Web Cracking,” Center For Civil Engineering Earthquake Research, Department Of Civil and Environmental Engineering, University of Nevada, Reno, Nevada, Report No. CCEER-15-02, January 2015.

- CCEER 15-03 Akl, A. and Saiidi, M.S., "Time-Dependent Deflection of In-Span Hinges in Prestressed Concrete Box Girder Bridges," Center For Civil Engineering Earthquake Research, Department Of Civil and Environmental Engineering, University of Nevada, Reno, Nevada, Report No. CCEER-15-03, May 2015.
- CCEER 15-04 Zargar Shotorbani, H. and Ryan, K., "Analytical and Experimental Study of Gap Damper System to Limit Seismic Isolator Displacements in Extreme Earthquakes," Center For Civil Engineering Earthquake Research, Department Of Civil and Environmental Engineering, University of Nevada, Reno, Nevada, Report No. CCEER-15-04, June 2015.
- CCEER 15-05 Wieser, J., Maragakis, E.M., and Buckle, I., "Experimental and Analytical Investigation of Seismic Bridge-Abutment Interaction in a Curved Highway Bridge," Center For Civil Engineering Earthquake Research, Department Of Civil and Environmental Engineering, University of Nevada, Reno, Nevada, Report No. CCEER-15-05, July 2015.
- CCEER 15-06 Tazarv, M. and Saiidi, M.S., "Design and Construction of Precast Bent Caps with Pocket Connections for High Seismic Regions," Center For Civil Engineering Earthquake Research, Department Of Civil and Environmental Engineering, University of Nevada, Reno, Nevada, Report No. CCEER-15-06, August 2015.
- CCEER 15-07 Tazarv, M. and Saiidi, M.S., "Design and Construction of Bridge Columns Incorporating Mechanical Bar Splices in Plastic Hinge Zones," Center For Civil Engineering Earthquake Research, Department Of Civil and Environmental Engineering, University of Nevada, Reno, Nevada, Report No. CCEER-15-07, August 2015.
- CCEER 15-08 Sarraf Shirazi, R., Pekcan, G., and Itani, A.M., "Seismic Response and Analytical Fragility Functions for Curved Concrete Box-Girder Bridges," Center For Civil Engineering Earthquake Research, Department Of Civil and Environmental Engineering, University of Nevada, Reno, Nevada, Report No. CCEER-15-08, December 2015.
- CCEER 15-09 Coria, C.B., Ryan, K.L., and Dao, N.D., "Response of Lead Rubber Bearings in a Hybrid Isolation System During a Large Scale Shaking Experiment of an Isolated Building," Center For Civil Engineering Earthquake Research, Department Of Civil and Environmental Engineering, University of Nevada, Reno, Nevada, Report No. CCEER-15-09, December 2015.
- CCEER 16-01 Mehraein, M and Saiidi, M.S., "Seismic Performance of Bridge Column-Pile-Shaft Pin Connections for Application in Accelerated Bridge Construction," Center For Civil Engineering Earthquake Research, Department Of Civil and Environmental Engineering, University of Nevada, Reno, Nevada, Report No. CCEER-16-01, May 2016.
- CCEER 16-02 Varela Fontecha, S. and Saiidi, M.S., "Resilient Earthquake-Resistant Bridges Designed For Disassembly," Center For Civil Engineering Earthquake Research, Department Of Civil and Environmental Engineering, University of Nevada, Reno, Nevada, Report No. CCEER-16-02, May 2016.
- CCEER 16-03 Mantawy, I. M, and Sanders, D. H., "Assessment of an Earthquake Resilient Bridge with Pretensioned, Rocking Columns," Center For Civil Engineering Earthquake Research, Department Of Civil and Environmental Engineering, University of Nevada, Reno, Nevada, Report No. CCEER-16-03, May 2016.
- CCEER 16-04 Mohammed, M, Biasi, G., and Sanders, D., "Post-earthquake Assessment of Nevada Bridges Using ShakeMap/ShakeCast," Center For Civil Engineering Earthquake Research, Department Of Civil and Environmental Engineering, University of Nevada, Reno, Nevada, Report No. CCEER-16-04, May 2016.



Nevada Department of Transportation
Rudy Malfabon, P.E. Director
Ken Chambers, Research Division Chief
(775) 888-7220
kchambers@dot.nv.gov
1263 South Stewart Street
Carson City, Nevada 89712